Erosion of Volatile Elemental Condensed Gases by keV Electron and Light-Ion Bombardment

Schou, Jørgen

Publication date:
1991

Document Version
Publisher's PDF, also known as Version of record

RISØ

Risø-R-591(EN)

Erosion of Volatile Elemental Condensed Gases by keV Electron and Light-Ion Bombardment

Jørgen Schou

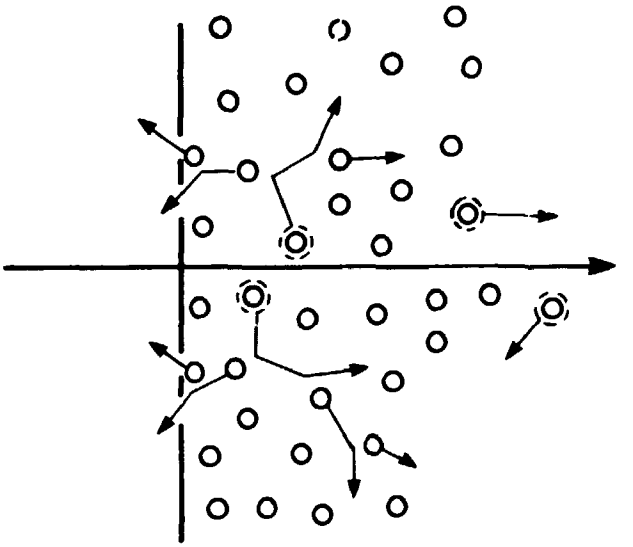

Risø National Laboratory, Roskilde, Denmark
November 1991

Erosion of Volatile Elemental Condensed Gases by keV Electron and Light-Ion Bombardment

Risø-R-591(EN)

Jørgen Schou

Risø National Laboratory, Roskilde, Denmark
November 1991

Abstract. Erosion of the most volatile elemental gases by keV electron and light-ion bombardment has been studied at the experimental setup at Risø. The present work includes frozen neon, argon, krypton, nitrogen, oxygen and three hydrogen isotopes, deuterium, hydrogen deuteride and hydrogen. The yield of these condensed gases has been measured as a function of film thickness and primary energy for almost all combinations of primary particles (1-3 keV electrons, 5-10 keV hydrogen- and helium ions) and ices. These and other existing results show that there are substantial common features for the sputtering of frozen elemental gases. Within the two groups, the solid rare gases and the solid molecular gases, the similarity is striking. The hydrogenic solids deviate in some respects from the other elements. The processes that liberate kinetic energy for the particle ejection in sputtering are characteristic of the specific gas.

To Daniel, Tobias and Margarethe

»Denne afhandling er den 13. november 1991 af Odense Universitets naturvidenskabelige fakultetsråd antaget til forsvar for den naturvidenskabelige doktorgrad.

Hans Jørgen Munkholm
h.a.dec.

Forsvaret finder sted fredag den 13. december 1991 kl. 14.00 i lokale U110, Campusvej 55, 5230 Odense M.«

ISBN 87-550-1737-1
ISSN 0106-2840

Grafisk Service, Risø, 1991

Contents

Preface

The present thesis is based mainly on results that have been obtained at the experimental setup at Risø in the period from 1981 to 1990. Most of these results have been published already in the twelve publications enclosed, but unpublished data have been included to the extent that it renews or completes the presentation. It has not been the intention of the author to add another review to the field. The main line in the survey has been to follow up the results already published and to discuss interpretations in view of the progress that has been made by other groups or by the group at Risø. One has to consider the thesis as an example of how the data would have been presented today. The articles and the survey are closely connected: The figures are usually not repeated, and references given in the articles are not necessarily included in the survey. The emphasis is on main lines and new developments in the past years. Some of the articles contain interpretations that no longer hold. This may be inevitable for work performed over such a long period. Nevertheless, it has been encouraging to reconsider the data, the models and the interpretations and to find that the overwhelming part of the previous work need be modified only slightly.

It has been an exciting time.

1 Introduction

The erosion of condensed gases by charged particles has been studied systematically for more than ten years. The field was regarded as partly exotic in the initial phase, but it turned out that the features explored extended our basic knowledge in a number of neighbor fields as well.

One of the most important points was the possibility of studying erosion of simple elemental insulators. Sputtering of frozen gases can take place as ordinary knockon sputtering and as electronic sputtering. While the knockon sputtering is the result of direct collisions between the primary and the target atoms, electronic sputtering, i.e. sputtering via electronic excitations, requires repulsive potentials during the electronic deexcitation. Usually, beam-induced evaporation of frozen gases is important at high temperatures or current densities, but at sufficiently low temperatures and current densities of the primary beam knockon or electronic sputtering is the dominant process.

Electronic sputtering takes place for insulating materials alone, since the free electrons in conductors prevent the creation of metastable repulsive potentials.

Since electronic excitations can be produced by electron and photon bombardment, it means that electronic sputtering can be performed with these two kinds of particles as well. It has turned out that sputtering by electrons usually is less efficient than that by ions, but experimentally this is partly compensated by the possibility of having much larger electron than ion currents from ordinary particle sources.

An important property of the frozen gases is the low surface binding energy which means that even a small energy release may lead to a large sputtering yield. The binding energy characterized by the sublimation energy ranges from 9 meV per hydrogen molecule up to, for example, 370 meV per molecule for sulphur dioxide. Another feature for these frozen room-temperature gases is the large variation in the magnitude of the sublimation energy. Even for such related materials as the solid rare gases the sublimation energy varies about a factor of 8 from solid neon with a value of 20 meV up to xenon with one close to 160 meV. This variation is larger than the corresponding one for related metals.

In many cases the bombardment is accompanied by a strong luminescence. The wavelengths, intensity and decay time of the emitted light give information about the electronic levels through which the system passes during the electronic deexcitation. On the other hand, it means that independent emission and absorption experiments on condensed gases have been indispensable in identifying the precise processes that lead to electronic sputtering.

Usually it has been possible to vary the film thickness of the condensed gas from thin layers up to those of thickness greater than the range of the primaries. In this way important characteristic properties of the transport mechanisms have been determined. A similar experimental procedure for varying the target thickness is much more complicated for nonvolatile materials than for frozen gases.

The elemental gases are particularly instructive because their is little chemical activity in the condensed gases. Even though the formation of ions, ion-complexes or excited-neutral complexes takes place in these materials, the elemental gases are a convenient starting point for analysising heteronuclear or mixed condensed gases.

The improved knowledge of the basic erosion processes has had a considerable impact on the field of erosion of icy surfaces in interplanetary and interstellar space. The effect of high-energy particles on hydrogenic pellets injected into plasma devices turned out occasionally to be important in refuelling studies. The erosion of cryopumping surfaces by charged particle or photon impact in ultrahigh vacuum

devices may lead to serious problems during experiments that are sensitive to impurity contamination.

The major points mentioned above will be treated in separate sections. The interplanetary or interstellar implications have been exclusively discussed by Johnson (1990). The problems concerning pellet injection into plasma devices have been treated in standard references (Chang et el. (1980), Milora (1981) and Chang (1991)). The consequences for vacuum technique is, for example, discussed by Benvenuti et al. (1987).

2 Experimental Procedure

The erosion experiments were carried out with a liquid-helium cryostat mounted on a vacuum chamber into which an electron beam and a light ion beam could be directed. For the luminescence measurements the setup was equipped with a monochromator combined with a photon detection system. Essentially, the cryostat is a modified version of the one that previously was utilized for secondary electron emission and particle range studies (Sørensen (1976), Schou and Sørensen (1978), Børgesen (1962)). The important parameters for the setup are listed in Table 1, and a survey of the setup in different modifications is shown in Figures 1-3.

Table 1. Characteristic dimensions and parameters for the setup during the present work.

Electron beam	
Distance from filament to substrate	0.3 m
Practical energy region	0.8 - 3 keV
Current	50 - 300 nA
Current density	1 - 20 μA/cm^2
Ion beam	
Distance from ion source to substrate	2.8 m
Practical energy region	4 - 10 keV
Current	1.5 - 50 nA
Current density	0.05 - 2 μA/cm^2
Target chamber	
Massive gold substrate or quartz crystal, diam.	14 mm
Opening of Faraday cup, diam.	6 mm
Aperture in front of quartz crystal, diam.	6 mm
Sweep aperture in front of crystal and cup, diam.	2 or 4 mm
Film thicknesses (10^{15} particles/cm^2)	10 - 10^4
Pressure	2 - 4 10^{-8} torr
Light detection system	
Monochromator focal length	200 mm
Accessible wavelength range (Valvo photomultip.)	200 - 600 nm
Resolution for 2 mm slits	8 nm
Monochromator aperture	f/3.5

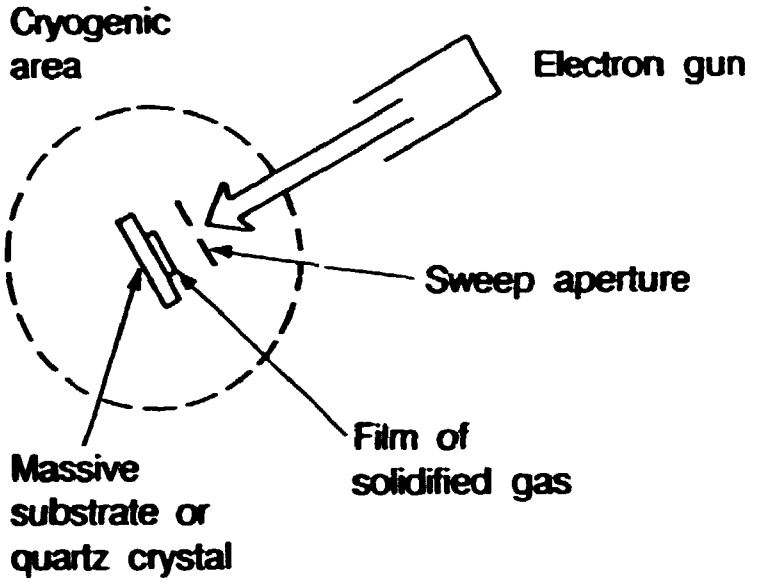

Figure 1. Schematic view of the experimental setup. View from the top. The electron gun can be replaced by the connection to the ion accelerator.

The quartz crystal microbalance has been essential for making accurate erosion measurements. Its high mass sensitivity, compact size and low cost have meant that determining the weight loss using this microbalance has been the preferential way to make the present erosion measurements.

Sputtering measurements based on this method were reported by McKeown (1961) about thirty years ago, and the method was used systematically through the seventies by for example Andersen and Bay (1972), Eernisse (1971) and others. Although the crystal occasionally was used as a thickness monitor in liquid-helium devices below 10 K (Levenson (1967)), direct beam-induced erosion of material deposited on a quartz crystal operating at liquid-helium temperatures was utilized systematically for the first time in the present work (Schou et al. (1984)).

The theory and practical applicability of the quartz crystal microbalance are relatively well known (Lu (1984) and Coburn (1989)). Basically, the deposit induces a reduction of the resonance frequency of the crystal. The subsequent erosion by the particle beam leads to an increase of the frequency relative to the film value. In the present work the area of the beam spot was always smaller than the deposition area, so that a macroscopic "crater" was formed in the film. The film thickness before exposure to the beam and the mass loss during irradiation were determined according to the specified relationship between the change of the resonance frequency and the mass area density. The problems associated with the determination of the erosion rate and the dependence on film thickness have been discussed by Schou et al. (1984) and (1986) and Ellegaard (1986).

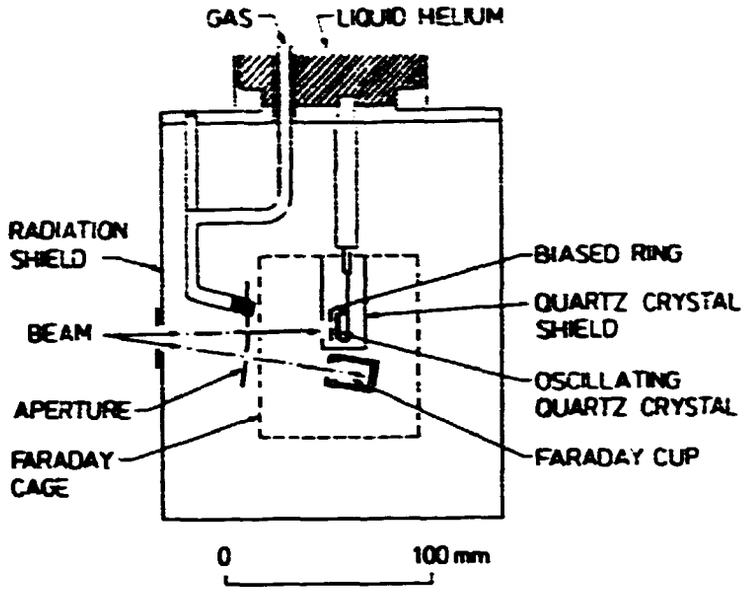

Figure 2. Schematic drawing of the target region (From Stenum et al. (1990)).

Figure 3. Schematic view of the modified setup for detection of luminescence.

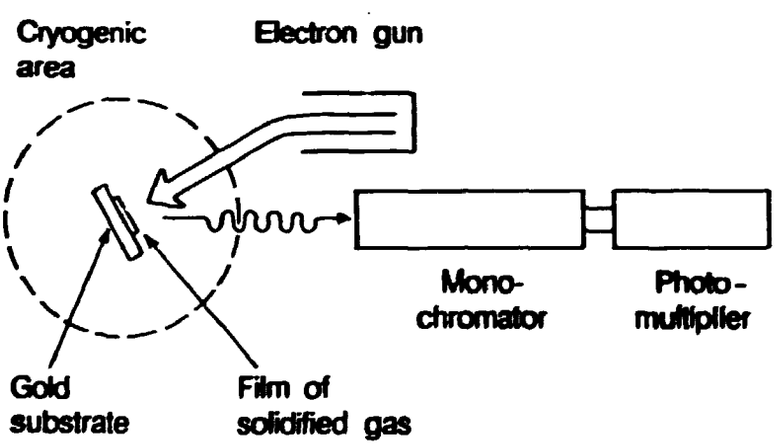

The main problem for low-temperature erosion experiments with a quartz crystal is there are two opposing demands: i) the crystal has to oscillate in a holder, and ii) the thermal conduction from the electrode, on which the film is deposited, through the holder to the cryogenic parts must be sufficiently good so that beam-induced evaporation can be avoided. It turned out that if the copper wires anchored to a flexible holder are too thick, they prevented the crystal from vibrating. The final solution was to fix the crystal in the holder with silver-epoxy glue at the edge of the electrodes, and to establish good thermal conduction with relatively thin copper wires between the contact points of the holder and the thermal coupling point on the cryostat bottom. Even then, the glue contact had to be renewed from time to time.

Recently, it turned out that it was possible to fix the crystal to the holder by making a soldering point directly on the 4000-Å thick silver electrode (Sørnum et al. (1991b)). This method improved the thermal conduction from the film to the cryogenic parts so that even solid hydrogen could be irradiated on the crystal without significant beam-induced evaporation. Results obtained in this way for proton bombardment of solid hydrogen and hydrogen deuteride are reported in Section 8.

The actual starting point for the measurements was making them on a massive substrate. The emissivity-change method is based on the idea that a the secondary electron emission coefficient of a thick film differs from that of the substrate. Usually, the reflection coefficient was used as a monitoring signal, but signals determined by other properties may also be used (Schou et al. (1984)). The important point is that the signal clearly indicates that the film is partly or completely removed from the impact area of the particle beam.

The agreement between the data set obtained by the weight loss and the emissivity-change method turned out to be satisfactory provided that the area of the beam spot was properly determined. It turned out that the real beam spot was considerably larger than the projection of the aperture on the target. This was not realized in the initial phase of the measurements (Børgesen et al. (1982) and Schou et al. (1984)). As soon as the behaviours of the quartz crystal at liquid-helium temperature and during beam irradiation were sufficiently well-known, the weight loss method was applied throughout the present work. Then the emissivity-change method was used only for measurements of the temperature dependence of the erosion yield. The determination of the precise temperature of the film on the crystal electrode was not possible, and we had to apply a massive substrate with a good thermal connection between the thermometer and film.

Recently the results obtained by Balaji et al. (1990) turned out on the whole to agree with the data from the present work. Their measurements were performed with a system of oscillating quartz crystals in a configuration different from the present one. The two sets of data are compared in Table 2.

Table 2. Comparisons Between Experimental Results at Risø and in Austin. All Points for 5 keV/ion.

(Sputtering yield given as sputtered atoms per incident atom, thicknesses in 10^{17} atoms/cm^2)

Ion	Austin Yield	Austin Thickness	Risø Yield	Risø Thickness
		Neon		
H_2^+	60[1]	2	52.4[3]	4.8
$^4He^+$	510[1]	1.8	420[4]	9
	663[2]	20		
		Argon		
H_2^+	9[1]	2	10.8[5]	4
He^+	26[1]	1.2	34[6]	3.7
	36[2]	20		
Ne^+	546[1]	3	813[7]	3.7
	596[2]	20		

1) Preliminary results by J. Michl, D. David, T. Magnera and V. Balaji. Sample preparation as in 2).

2) Balaji et al. (1990). The films were condensed at annealing temp. (Ne 9 K and Ar 33 K) and irradiated at lower temp (Ne 3.5 K and Ar 4.5 K). The estimated yield Y_0 from an undamaged surface is given.

3) Ellegaard et al. (1986). The point for 2.5 keV/atom interpolated from measured values of 3 and 2 keV/atom.

4) Ellegaard et al. (1990).

5) Schou et al. (1988). Points interpolated as in 3).

6) Schou et al. (1988).

7) J. Schou, O. Ellegaard, F. Pedrys and H. Sørensen (unpubl.)

The films produced in the present cryogenic setup are all low-temperature condensates. These films are characterized by grain sizes typically about 100 Å, accompanied by a high density of packing defects (Fugol' (1978)). Even though the dependence of the mass density on the temperature is known, the density of the films may be significantly smaller than that of perfectly grown bulk samples (Zimmerer (1987)). The films produced by almost all other groups show these characteristic features as well.

During the erosion measurement in the present setup the primary beam is swept horizontally and vertically over an aperture in front of the target. This ensures a homogeneous irradiation of the film. The determination of any thickness dependence is affected critically by the beam conditions. In particular, one may enhance the yield by beam-induced evaporation in an undesirable manner from the most volatile solids, if a well-focused beam remains at the same spot for a long period.

Table 3. Some properties of volatile solidified gases at the temperatures considered

Particle density [10^{22} part/cm^3]		Sublimation energy per particle [meV]	Structure
H_2[1]	2.65	8.65	hcp[2]
HD[1]	2.81	10.8	hcp[2]
D_2[1]	3.03	12.65	hcp[2]
Ne[3]	4.54	19.6	fcc
Ar[3]	2.67	80	fcc
Kr[3]	2.22	116	fcc
N_2	2.21[4]	78[4]	fcc[5]
O_2	2.88[4]	90[4]	monoclinic C[6]

1) Souers (1986)

2) Thin films show occasionally fcc-structure (Silvera (1980))

3) Schou (1987)

4) Ellegaard et al. (1986a)

5) Kjems and Dolling (1975)

6) Kobashi et al. (1979)

3 Erosion Processes

The low binding energy of the atoms or molecules in a condensed gas means that beam-induced evaporation as well as sputtering may take place during particle bombardment. A survey of the different possibilities is shown in Figure 4. However, for electron bombardment of these solids only electronic sputtering and beam-induced evaporation are feasible erosion processes. Direct energy transfer from an incident keV-electron to a target particle at rest may lead to sputtering (Townsend (1983)); however, for the energies used here this process may be feasible only for the two most volatile elements, solid neon and the hydrogens. Even for these two elements the cross section for energy transfer is so low that direct sputtering does not contribute significantly (Schou et al. (1986)).

3.1 Beam-Induced Evaporation

As mentioned previously, beam-induced evaporation prevails at elevated target temperatures or at sufficiently high beam current densities. Essentially, beam-induced evaporation is a consequence of the additional heating in the sample from the beam. The heating of the impact area is provided by external heating of the substrate or by the current itself. For both cases there is a threshold below which the yield is independent of the temperature and the current density. For higher temperatures or current densities the yield increases markedly.

The threshold for beam-induced evaporation by external heating depends on the particular solid. Schou (1987) has demonstrated that the threshold temperature rises generally with increasing sublimation energy. As a matter of fact, the

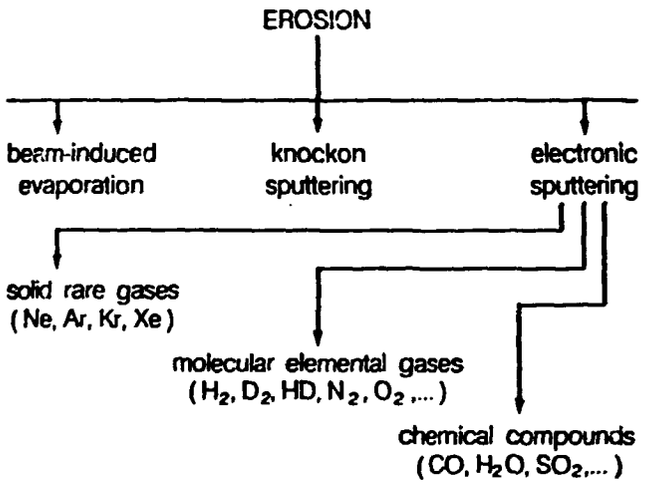

Figure 4. Schematic survey of the erosion processes.

threshold turns out to lie close to a temperature corresponding to two per cent of the sublimation energy.

An analogous case for beam-induced evaporation at high current densities was obtained by Schou et al. (1984). The total yield for electron-bombarded solid neon increased by more than two orders of magnitude mainly because of a current density increase from the threshold at 10 up to 35 $\mu A/cm^2$.

The large enhancement of the yield above the threshold is a consequence of the low binding energy and other thermal properties of these materials. According to the low-temperature spike model by Sigmund and Szymonski (1984) the total yield Y_{tot} is a sum of the ordinary low-temperature yield Y (from electronic or knockon sputtering) and a term that accounts for the yield increase by evaporation

$$Y_{tot} = Y + [\Phi(T_a + \Delta T_{eff}) - \Phi(T_a)]/J \qquad (1)$$

Φ is the evaporation rate (number of target particles evaporating per unit time and area). J is the current density, T_a the temperature of the ambient target and ΔT_{eff} the average temperature rise of the target as a result of beam heating. The evaporation rate is then enhanced drastically by the increase ΔT_{eff} from the beam because the total temperature increase $T_a + \Delta T_{eff}$ enters as an argument in an exponential.

Energy spectra from particle-bombarded solids at elevated temperatures have been investigated frequently for the alkali-halide systems. The spectra of the materials are usually quite well described by a Maxwell-Boltzmann distribution that is characterized by a temperature that corresponds to the actual macroscopic temperature of the target (Overeijnder et al. (1978), Szymonski (1980), Szymonski et al. (1980)). In one particular case, a macroscopic target temperature close to the actual one was determined from the Maxwell-Boltzmann energy distribution for one of the emitted species, F_2, during electron sputtering of sulphur hexafluoride by Pedrys et al. (1984). A later study on solid methane irradiated with light ions by Pedrys et al. (1986) showed that the spectra could be explained by Maxwell-Boltzmann distributions with a characteristic temperature ranging from the actual one of 20 K for emitted hydrogen molecules up to 200 K for the emitted methane molecules. It was shown as well that the processes were initiated by single impact rather than by macroscopic beam heating.

Unfortunately, there are no energy spectra available yet from condensed gases during conditions for which the dominant process is beam-induced evaporation.

3.2 Knockon Sputtering

As mentioned previously, knockon sputtering is well-known from ion-bombarded metals. It may be described as a sequence of events in which target particles are set in motion, from the first collision between the primary and a target atom up to eventual particle ejection resulting from collisions between slow particles. The volatility of the material plays a role only in the last stage of the cascade, when the kinetic energy of the moving atoms becomes comparable to the binding energy of the target particles. The main features of knockon sputtering at sufficiently small energy densities are well predicted by Sigmund's linear collision-cascade theory (1969, 1981).

The backsputtering yield Y from a plane surface is given by

$$Y = \Lambda F_D(E, \theta, 0) \tag{2}$$

where $F_D(E, \theta, x)$ is the spatial distribution of energy deposited into atomic collisions by the primary of initial energy E and angle of incidence θ . The constant $\Lambda = 3/(4\pi^2 N C_o U_o)$ depends only on the properties of the target material, the sublimation energy U_o and the atomic density $N(C_o = 1.18\ \text{Å}^2)$. The surface value of the deposited energy (x = 0) is often expressed by the nuclear stopping power $NS_n(E)$ for the primary and by a dimensionless parameter α:

$$F_D(E, \theta, 0) = \alpha\ NS_n(E) \tag{3}$$

α is a function of the mass ratio of the beam and target atom mass, of the angle of incidence, and a slowly varying function of the energy. The energy distribution of the sputtered particles, which explicitly enters into the evaluation of Λ, is determined by

$$dY/dE_1 = k_s\ E_1/(E_1 + U_o)^3 \tag{4}$$

where k_s is a constant (see Sigmund (1981)) and E_1 is the energy of the emitted particle. For large values of the energy E_1 the distribution exhibits the well-known E_1^{-2}-tail and for small energies a maximum at $E_1 = U_o/2$.

The results for the yields agree satisfactorily with Equation (2) as long as the (collisional) excitation density is small or the sublimation energy large. The best agreement for the materials considered in the present work is found for medium-mass ions incident on solid krypton and xenon (Stevanovic et al. (1984), Boring et al. (1987) and Brown and Johnson (1986)). For water ice Christiansen et al. (1986) and Bar-Nun et al. (1985) have reported an acceptable agreement between their results and Equation (2) as well, even though ice of ordinary and heavy water have to be regarded as complicated samples because of the temperature dependence of the yield of the different ejected species (Reimann et al. (1984a), Chrisey et al. (1986) and Benit et al. (1987)).

The data for the characteristic E_1^{-2}-behaviour of the spectrum during ion bombardment of the solid rare gases as well as of other condensed gases have been collected by Schou (1987). The behaviour does not necessarily mean that sputtering from linear collision-cascades is the dominant mechanism. However, such a mechanism is at least responsible for the particle ejection at an early stage of the sputtering process.

Usually, the maximum of the energy distribution is not at the expected value of $U_o/2$, but substantially below this value. This is a consequence of the low binding energy in the solids, which leads to a high recoil density. The nonlinear behaviour of the collision cascades enhances the number of ejected low-energy target particles. However, for low-energy ion bombardment of solid xenon Pedrys (1990) showed that the linear collision-cascade is the dominant feature, and that the maximum actually lies at one-half of the sublimation energy of xenon.

The main limitation of linear collision-cascade theory for the condensed gases is the relatively low threshold for nonlinear effects. At sufficiently high collisional excitation densities the recoils strike other target atoms that already have been set in motion. For this spike regime the existing models or their extensions for condensed gases predict a sputtering yield that is proportional to the nuclear stopping to the second or even higher powers (Sigmund and Claussen (1981), Claussen (1982a,1982b), Sigmund and Szymonski (1984), David et al. (1986), Urbassek and Michl (1987), and Balaji et al. (1990)).

A common result for these treatments and for that of Szymonski and Poradzisz (1982) as well is that the maximum in the energy distribution of the emitted particles is shifted to a lower value than that expected from linear collision-cascade theory. This is a feature that has been observed in almost all knockon sputtering experiments for condensed gases. It means that an elastic collision spike develops in the solid during the late stage of the sputtering process. The yield from an elastic collision spike may exceed the linear collision-cascade yield by more than one order of magnitude. Nevertheless, particles in the high-energy tail from the linear collision-cascades during the early stage of the sputtering process are observed clearly, since the high-energy part of the spectrum from elastic collision spikes falls off very steeply with energy.

An intermediate case between linear collision-cascades and elastic collision spikes occurs for nonoverlapping spherical elastic collision subspikes (Ellegaard et al. (1990)). The existing spike models and their extensions are based on the idea that many collisions between the primary and target atoms contribute to one common spike. In contrast, the subspikes created by the individual recoils do not interact. This mechanism may lead to a large yield, but the energy dependence shows almost the same trend as the nuclear stopping power; this contrasts with the strong nonlinearity predicted by the models mentioned previously. The predicted yield is comparatively sensitive to the binding energy of the target particles, and the yield exceeds the linear collision-cascade yield only for the most volatile materials, as for example, solid neon. For the less volatile solids as condensed argon and xenon the yield induced from nonoverlapping subspikes is comparable with that from linear collision-cascades (Ellegaard et al. (1990, 1991)).

3.3 Electronic Sputtering

Electronic sputtering is known from other materials than condensed gases (Schou (1989), Townsend (1983) and Itoh (1987)). The picture that emerges for the moment indicates clearly that there is no universal mechanism for electronic sputtering of insulating materials (Schou (1987, 1989)). Nevertheless, there are some common features for the sputtering of condensed gases, in particular for the solids within one of the groups in Figure 4.

From the model of Ellegaard et al. (1986) the electronic sputtering yield from a material without mobile electronic excitations is determined in analogy with Equation (2) :

$$Y = \Lambda \frac{1}{2} (E_s/W)\, D_e(E,\theta,0) \tag{5}$$

E_s is the nonradiative energy release from electronic deexcitation per electron-hole pair, and W the energy required for one electron-hole pair. $D_e(E,\theta,0)$ is the surface value ($x = 0$) of the distribution $D_e(E,\theta,x)$ of electronically deposited energy for a primary particle of energy E and angle of incidence θ (Schou (1980,1988)).

Let us now consider how the sputtering takes place. As a result of the slowing-down of the primary particle atoms or molecules are excited or ionized. When all these excitations deexcite, for example by dissociative recombination, the liberated

energy E_s may be so large compared with the binding energy that the repulsing atoms may initiate a low-energy cascade. Since these nonradiative transitions lead to a completely isotropic distribution of the initiating atomic pairs in contrast to the knockon case, one arrives at the factor 0.5 in Equation (5).

According to Equation (5) each material is characterized by a certain ratio E_s/W. While the energy W does not vary much from one material to another within a single group (Figure 4), the source energy E_s may vary considerably. The recent study by Pedrys et al. (1989) has shown that E_s may not emerge from one nonradiative transition alone, but that it may be regarded as a weighted sum of widely different contributions.

Ellegaard et al. (1986a) and Schou (1987) demonstrated that the yield is predicted in a satisfactory way for solid nitrogen and oxygen bombarded by keV electrons as well as MeV protons. This agreement is somewhat surprising since the target particles are ejected as molecules, but they are treated as atomic species, so that the well-known Born-Mayer cross section used in sputtering theory (Sigmund (1981)) could be applied. In a similar derivation Johnson and Brown (1982) have chosen to apply a molecular cross section. Although these authors describe the emission of nitrogen molecules rather than atoms, it involves an unknown molecular cross section at very low energies.

For mobile excitations the formula (5) was modified by Ellegaard et al. (1989) to

$$Y = \Lambda \frac{1}{2} E_s E(0) \tag{6}$$

Here $E(0)$ is the surface value of the density $E(x)$ of decaying nonradiative transitions at depth x with energy release E_s distributed equally on two repulsing particles. An additional assumption is that the surface acts as a reflecting boundary for the excitations except for solid neon.

The energy distribution, Equation (4), that explicitly enters into the evaluation of Λ, has been observed in a number of cases for which the energy deposition obviously is electronic. The low energy part of the distribution from electrons bombarding solid argon observed by Pedrys et al.(1989) agrees well with Equation (4) with a binding energy of 0.75 U_o. This binding of 60 meV is much less than the energy 0.55 eV which is imparted to each of the atoms initiating the cascades.

The characteristic E_1^{-2}-tail for large ejection energies has been observed for electron bombardment of solid nitrogen (Pedrys et al. (1989)) and oxygen (Pedrys (1991)) as well as for light keV ion bombardment of the same solids (Ellegaard et al. (unpubl.)). For the solid rare gases this behaviour was observed by Pedrys et al. (1985) for solid krypton bombarded by 6-keV He-ions. A similar trend was observed for ejected heavy water molecules from heavy water ice during 1.5-MeV He-ion bombardment by Boring et al. (1983).

Recent computer calculations by Garrison and Johnson (1984) and by Cui et al. (1988,1989a) have corroborated the use of low-energy collision-cascades in volatile condensed gases. The recoil spectrum agrees satisfactorily with that from binary cascades, and also the energy spectrum of the sputtered particles is quite well represented by the shape given by Equation (4). The development of a linear low-energy collision-cascade seems possible for low primary energies, even down to an initiating energy of about five times the sublimation energy. In fact, the general agreement between the theoretical ideas for these condensed gases and the computer calculations is very encouraging. However, there are some minor discrepancies, for example, between the angular distribution of the emitted atoms calculated from the computer codes and that predicted from linear collision-cascade theory (Garrison and Johnson (1984)).

The treatment for low-energy collision-cascades applies to cases for which the energy deposition by the primary particles is relatively small. For high eletronic

excitation densities nonlinear effects occur, predominantly because of the non-negligible interaction that takes place between two subsequent excitations. These nonlinear effects may appear from the interaction between subsequent electronic excitations before the energy release or from the interaction between two neighbor cascades after the energy release (Sigmund (1987)). This nonlinear regime is characterized by a yield that is proportional to the electronic stopping power to the second or even higher powers. A squared dependence of the yield on the electronic stopping power has been reported by Brown et al. (1986), Brown and Johnson (1986) and Gibbs et al. (1989) for solid nitrogen and oxygen.

For primary particle bombardment of volatile solids at high excitation densities one may reach the electronic spike regime. If the binding energy to the lattice site is sufficiently small, the number of atoms set in motion from each energy release process will be so large that a spike volume containing several points of energy release will be generated. The energy spectrum from such a spike may show the characteristic features known from the elastic spikes, e.g. a shift of the maximum towards lower energies.

For chemical compounds as water ice and carbon monoxide this quadratic behaviour occurs not only in the high-density regime (Brown et al. (1980) and Johnson and Brown (1983)), but has also recently turned out to be dominant for low excitation densities in solid carbon monoxide (Chrisey et al. (1990)). This behaviour indicates that excitations of a different type cooperate in the electronic release processes in these solids.

For the solid hydrogens the energy release per electronic deexcitation is so large compared with the sublimation energy that one may expect the development of subspikes (Stenum et al. (unpubl.)). The energy release may be even more than 500 times the sublimation energy, but since the deexcitation from molecular ions starts with a dissociative recombination, the subspikes may be separated in time as well as space. This leads to electronic subspikes that do not overlap, in analogy with the nonoverlapping elastic subspikes described by Ellegaard et al. (1990). However, the energy release from dissociative recombinations is so small that these deexcitations are relatively unimportant. In contrast, the energy production from direct excitations below the ionization threshold is so large, that the yield from subspike generation becomes considerable. This may happen for keV electron incidence, since these excitations are so far from each other that the subspikes do not overlap.

3.4 Similarities and Differences Between Electronic Sputtering and Desorption

One may argue that electronic sputtering is not the most appropriate term for cases in which the liberated energy is comparable to the binding energy of the target particles. One may just as well characterize this as desorption from multilayers. A typical example is the ejection of xenon atoms from solid xenon during light ion or electron bombardment reported by Pedrys et al. (1988) or O'Shaugnessy et al. (1988). In the energy distribution there is a dominant peak corresponding to ground state repulsion for the xenon atoms, whereas the contribution from low-energy cascades is small. For solid argon an overwhelming fraction of the particles are ejected at energies much below the ground state repulsion. Obviously, a straightforward criterion for electronic sputtering might be the generation of low-energy cascades.

There are even similarities between the erosion of monolayers in desorption studies and electronic sputtering of multilayers (Schou et al. (1988)). In both cases the transfer of energy from electronic excitations may occur by neutralization of

an ionized atom. The desorption of neutrals may be described by Antoniewicz's model (Menzel (1990), Steinacker and Feulner (1989)). An atom from the monolayer moves against the metal after ionization because of the image potential. Eventually, it becomes neutralized, falls onto the repulsive branch of the ground state curve, and will be reflected with a kinetic energy from the image potential attraction and the ground state repulsion.

However, in the present work the concept of electronic sputtering rather than desorption has been utilized. Even though desorption is used frequently in luminescence studies for multilayers as well, it is occasionally applied only for surface processes that lead to direct particle ejection.

4 Erosion of Thin Films

A common behaviour for the most volatile gases is the strong enhancement of the yield for thin films deposited on conductive substrates. Stenum et al. (1990) and Ellegaard et al. (1986b) showed that the yield for thin films may exceed that for thick films by more than a factor of five. An example of this behaviour is shown in Figure 5 for 8-keV H_2^+-ions incident on solid hydrogen. In general, the enhancement is characterized by the following features:

i) the effect is most pronounced for the most volatile gases,

ii) the enhancement occurs for electron as well as ion bombardment, and

iii) the choice of conductive substrate does not seem to play any role.

The effect is a clear thin-film effect since the energy of the primary particle largely is deposited in the substrate. The enhancement is clearly correlated to electronic energy deposition and has not yet been observed in a convincing manner for combinations of beam particles and film material, for which the erosion process largely is knockon sputtering. Stenum et al. (1990) pointed out that the yield-enhancement did not depend on the current density for values from 0.05 to 0.5 $\mu A/cm^2$. This observation means that the enhancement is not caused by beam-induced evaporation. On the other hand, Schou et al. (1986) estimated that the electrons backscattered from the silver substrate at most would increase the yield by a factor of two from electron-bombarded solid neon. For primary ions the increase for thin argon films on silver has been estimated to about 15 per cent (Schou et al. (1987)). Nevertheless, the contribution from backscattered primaries is easily distinguishable from the thin-film enhancement because of the linear dependence on the film thickness. This contribution appears in the most distinct manner for condensed gases without any intrinsic thickness dependence and has been observed for electron sputtering of solid oxygen by Ellegaard et al. (1986a) and for light ion sputtering of solid nitrogen by Ellegaard (1986) and Ellegaard et al. (unpubl.).

For the most volatile gases, the solid hydrogens, the yield decreases with thickness up to a value that corresponds approximately to twice the range for electrons (Børgesen et al. (unpubl.), Ellegaard (1986)). For primary ions incident on solid deuterium and hydrogen the yield increases up to film thicknesses that are slightly smaller than or comparable to the ion range (Stenum et al. (1990, unpubl.)). The enhancement effect for solid deuterium contributes to the yield even for thicknesses above 10^{16} D_2/cm^2 for ions or electrons. A similar observation was made for He^+ -ions incident on solid deuterium as well (Stenum et al. (unpubl.)). For solid neon the effect extends up to thicknesses of about 5-7 $\cdot$ 10^{16} Ne-atoms/cm^2 for 2-keV electrons (Schou et al. (1986)) as well as for ions (Ellegaard et al. (1986b)). A

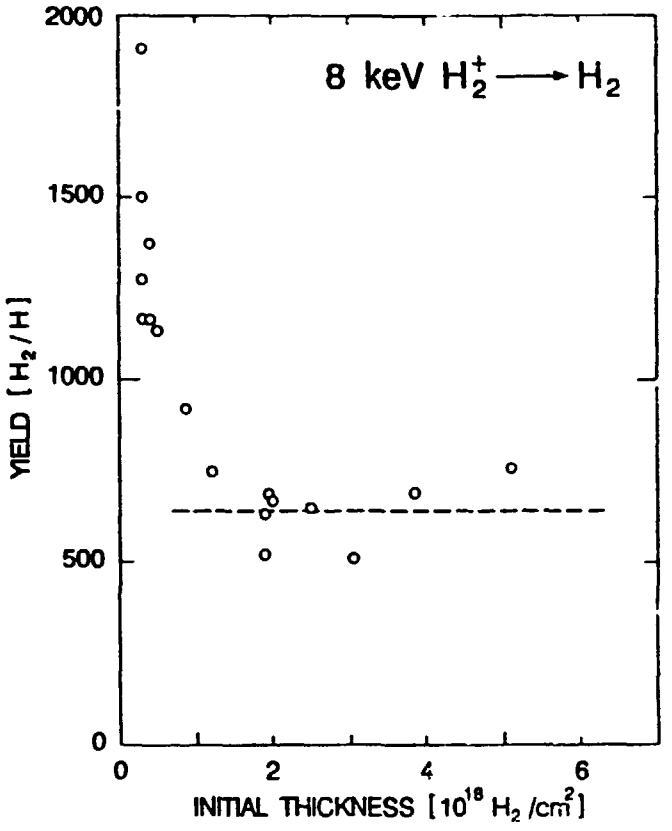

Figure 5. The yield per atom as a function of film thickness for 8 keV H_2^+-ions incident on solid hydrogen. The dashed line indicates the bulk yield (From Stenum et al. (unpubl.)).

slight enhancement may have been observed for the less volatile solid argon up to a thickness of $2 \cdot 10^{16}$ Ar/cm^2 (Schou et al. (1988)).

The yield enhancement has been observed by Erents and McCracken (1973,1975) for hydrogen, deuterium, argon, nitrogen and carbon monoxide, all solids, bombarded by keV electrons or hydrogen ions. The effect has been found only by these two groups, since their were no other groups studying erosion of the solid hydrogens or neon with these projectiles. For other materials the effect is so weak that a systematic study is difficult.

The results obtained at Risø have demonstrated that the enhancement takes place on gold, silver and carbon substrates (Børgesen and Sørensen (1982), Børgesen (1982), Schou et al. (1984)), whereas Erents and McCracken (1973,1975) utilized a copper substrate. The effect shows the same trend for all these substrates, but the absolute magnitude of the yield varies considerably from one to another (Børgesen et al. (unpubl.)). Recent measurements of the yield for thin films indicate that the enhancement depends on the purity of the substrate, and that it is less pronounced for slightly contaminated substrates.

During much of the present work the thin-film enhancement was regarded as a surface effect. However, the thicknesses for solid neon and deuterium to which the effect contributes correspond to more than 50 and 300 monolayers, respectively (Schou et al. (1986) and Stenum et al. (1990)). Then, it is hardly possible to classify the enhancement as a surface effect. In addition, it was demonstrated by Stenum et al. (1990) that the range of the effect is unambigously correlated to the

particle range. This means that the enhancement is a clear beam-induced feature rather than structural interface effect.

Even though a number of trends that characterize the thin-film enhancement have been explored, one arrives at the conclusion that the nature of the effect is far from being understood for the moment.

5 Sputtering of Solid Neon

Solid neon is the most volatile material among those which can be sputtered at liquid-helium temperature. Since reliable measurements require an efficient cryogenic setup, systematic measurements were conducted at relatively few locations, Marseille, Hamburg, Risø and Austin (Coletti and Debever (1983), Coletti et al. (1984), Kloiber et al. (1988), Kloiber and Zimmerer (1989,1990), Schou et al. (1986), Ellegaard et al. (1986b), Ellegaard et al. (1990) and Balaji et al. (1990)). In addition to these results, Coletti et al. (1985), Coletti et al. (1987), Fugol' et al. (1988), Hourmatallah et al. (1988) and Laasch et al. (1990) have reported on desorption of excited neutrals in connection with luminescence measurements.

The weak binding energy of the neon atoms in the lattice means that knockon sputtering leads to the generation of subspikes or general spikes of different geometric shape except for primary ions of very low energy. For ions in the eV range one might expect a dominant contribution from linear collision-cascades. For He-ion energies above 6 keV Ellegaard et al. (1990,1991) pointed out that the energy dependence of the yield could be explained on the basis of nonoverlapping subspikes. At these energies, the mean free distance between two subsequent collisions that initiate subspikes is so large that the subspikes do not overlap. The model combines two contradicting features: i) the large yield that is indicative of a spike behaviour, and ii) the energy dependence that resembles that of the nuclear stopping power. The energy dependence evaluated from a subspike model is partly determined by the geometry of the subspikes. The present choice of center for a spherical elastic subspike at the mean damage depth is in complete agreement with the basic model by Claussen (1982a,1982b), and leads to an energy dependence that agrees fairly well with the experimental one for $^4He^+$-ions as well as for $^3He^+$-ions.

Sputtering of solid neon by electrons is a typical example of electronic sputtering. The thickness dependence of the sputtering yield shows that solid neon behaves in a similar way as the other condensed gases except for the pronounced thin-film enhancement (Schou (1987)). The energy dependence of the yield for thick films (Figure 6) and the thickness dependence indicate that the excitations which contribute to the sputtering are able to migrate over a distance comparable to the range of an electron with an energy between 1.2 and 1.5 keV in solid neon (Schou et al. (1986)). For energies higher than that, the yield decreases with energy. The mean penetration depth of an electron with an energy in this interval is slightly above $1 \cdot 10^{17}$ Ne-atoms/cm^2 (Valkealahti et al. (1989)). Actually, this thickness corresponds to the characteristic diffusion length of 230 Å found from the diffusion model based on the treatment in Schou et al. (1986).

The existing results show evidence for **sputtering via exciton production**. Photon-stimulated desorption takes place if solid neon (and the other rare gases) are irradiated by VUV-light at the exciton levels (Kloiber and Zimmerer (1989, 1990)). About one tenth of the ejected particles are excited neutrals which have been detected in separate experiments by other methods (Kloiber et al. (1988), Kloiber and Zimmerer (1989, 1990)). Coletti showed by mass spectroscopy studies (Kloiber and Zimmerer (1989) and together with Debever by luminescence studies

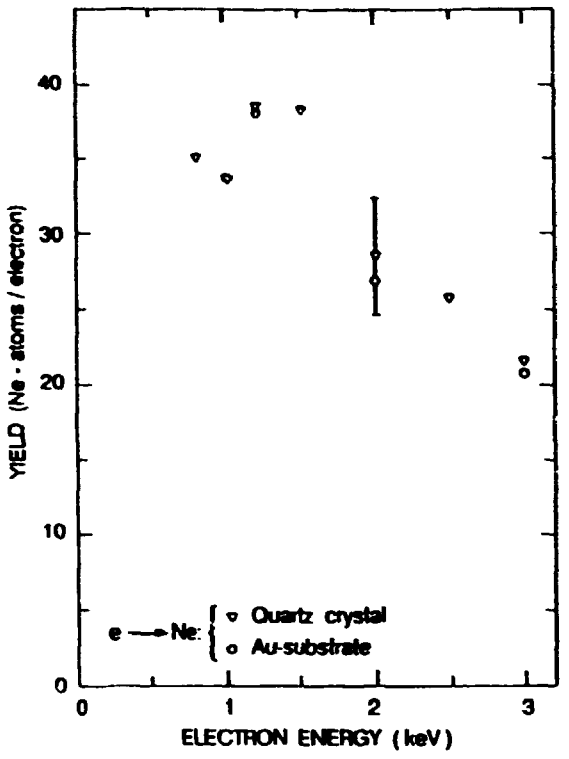

Figure 6. Sputtering yield of solid neon by keV electrons for 4.5 × 10^{17} (Ne/cm^2) thick film. Data from Schou et al. (1986).

(Coletti and Debever (1983)) that the particle ejection takes place for electron bombardment with energies below the band gap as well.

Sputtering of solid neon by both keV electrons and charged particles with comparable velocities is essentially described by a three-step process: i) production of electron-ion pairs and excitations, ii) migration of some of the excited species to the surface, and iii) a nonradiative transition so close to the surface that either the repulsing species are ejected directly or a low-energy cascade initiated in the surface layers leads to particle ejection.

In the treatment by Schou et al. (1986) the type of mobile excitations was not specified. Reimann et al. (1984b) suggested that it was either charge exchange by atomic ions or highly excited excitons for solid argon, but the arguments are reasonable for solid neon as well. From luminescence studies it is known that the free excitons are mobile (Zimmerer (1985), Fugol'(1988)), whereas the molecular excitons Ne_2^* may be regarded as almost immobile. The reason is that the equilibrium position of the atoms in this metastable molecule is too far away from the neighbor atoms so that particle exchange becomes fairly unlikely. For solid neon the molecular exciton has not been observed in the vibrational ground state, and the luminescence observed indicates a maximum in the population for $\nu = 7$ at the surface or $\nu = 4$ in the bulk (Coletti et al. (1985)). The molecular ion Ne_2^+ may be regarded as immobile at the present temperatures for the same reason (Schou et al. (1986)).

Even though the dominant carrier of the excitation, an atomic hole or a highly excited exciton, has not been identified, the results from Kloiber et al. (1988) and Kloiber and Zimmerer (1989) clearly demonstrate that the production of electron-hole pairs are important for photon-induced sputtering. However, the yield induced by direct excitation of the n,n' = 1 - excitons leads to a yield that is almost as large as that from photons just above the energy gap. Thus, these experiments do not provide us with a clear answer about the type of the mobile excitations.

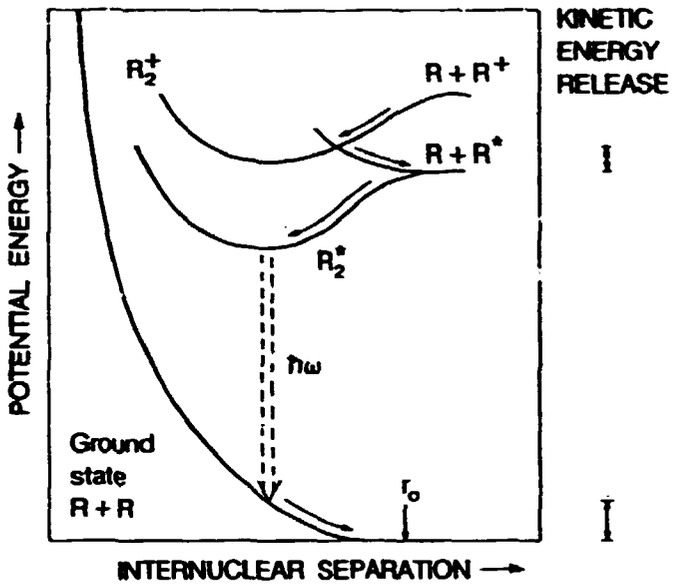

Figure 7. Schematic representation of important transitions in solid rare gases. The kinetic energy liberated is indicated at the right-hand side of the figure. r_o is the equilibrium distance in the ground state.

The characteristic diffusion length of the excitation was evaluated by Schou et al. (1986) to be about 230 Å. This number agrees well with that from Hourmatallah et al. (1988) who obtained 250 Å for mobile excitations induced by 24-eV electrons incident on solid neon of a temperature of T = 8 K. Their model is based on a number of different assumptions, and the authors claim that the excitation is a free exciton. Recently, Laasch et al. (1990) have estimated the diffusion length of the n = 1 - exciton to be of the order of 100 Å and that of the n = 2 - exciton somewhat larger. All these estimates of the diffusion length are much smaller than the value obtained by Pudewill et al. (1976) with exciton-enhanced impurity photoemission. This value was determined from a model with a number of questionable parameters. In addition, it is in striking contrast to the prediction by Fugol' (1988) that the diffusion length increases with the atomic number. A value of about 200 Å for neon fits satisfactorily into this pattern (Schou (1987)).

The processes for the energy release shown in Figure 7 are the dominant ones. The dissociative recombination

$$Ne_2^+ + e^- \rightarrow Ne_2^{**} \rightarrow Ne + Ne^*(3p) \qquad (7)$$

leads to the emission of a ground state and an excited atom if the recombination takes place close to the surface. A weak maximum at 1.1 eV of the 3p-atoms may be ascribed to this mechanism (Kloiber and Zimmerer (1990)). It means that an average energy of 2.2 eV is liberated from process (7). Since about 1.1 eV is released by from a dissociative recombination in which the molecular ion is in a vibrational ground state, the recombination has to take place from a highly vibrational state, excited extra 1.1 eV above the vibrational ground state.

The radiative transition to the repulsive ground state

$$Ne_2^* \rightarrow Ne + Ne + \hbar\omega \qquad (8)$$

terminates at an energy above the asymptotic value so that the ground state repulsion releases energy. The energy spectrum of the ejected particles has not yet been observed for solid neon. However, since the ground state repulsion or the

subsequent low-energy cascades have been observed for solid xenon, krypton and argon (Pedrys et al. (1988) and O'Shaughnessy et al. (1988)), it seems evident that this conversion process is important for solid neon as well. The liberated energy by this process is considerably less than the value $E_s = 3.7$ eV given by Schou et al. (1986). This value was estimated on the basis of gas data. However, Reimann et al. (1988) pointed out that because of the negative electron affinity one may expect a deeper well for the atoms of the metastable molecule in the solid than in the gas phase. For the solid state case one may estimate a value at most about 1 eV from Fugol' (1978), but the computations from Cohen and Schneider (1974) on gas phase molecules favour a low kinetic energy release. The transition from the vibrationally excited levels to the ground state indicated by Coletti et al. (1985) leads to a distribution of kinetic energy with a most probable value of about 200 meV and with a tail extending towards higher energies. Although 200 meV is much smaller than the value in Schou et al. (1986) of 3.7 eV, it is nevertheless one order of magnitude larger than the sublimation energy. The value of the ground state repulsion does not enter directly into the analysis of the dynamics of the mobile excitations. The result that each electron-ion pair on average leads to the ejection of 9 neon atoms is still valid (Schou et al. (1986)).

The boundary conditions introduced by Schou et al. (1986) were opposite to most of the treatments for solid argon, krypton and xenon. For these solids a model with a surface that acts as a reflecting boundary for the mobile excitations was applied (Ackermann et al. (1976), Reimann et al. (1984b)). For neon the surface was treated as an absorbing boundary, since the alternative of a reflecting surface would lead to a sputtering yield one order of magnitude too little (Schou et al. (1986)). This peculiarity of solid neon has been comfirmed by Hourmatallah et al. (1988), who found a large absorption rate of the excitations at the surface for neon as well. Their results for solid argon at this temperature indicated a highly reflective surface in agreement with other results for uncontaminated samples.

The recent results from luminescence measurements have demonstrated the rich structure of **desorped neutrals**. Coletti et al. (1984) pointed out that an atomic excitation may be trapped in a cavity as a result of the negative electron affinity. The total energy of this selftrapped atomic exciton may be minimized by the particle ejection. Coletti et al. (1985), Hourmatallah et al. (1988) and Laasch et al. (1990) have pointed out that the site at the surface or in the bulk induces a shift of energy of the excited atom relative to the free atom. The distribution of kinetic energy of emitted $^3P_2$ and $^3P_0$ atoms was measured by Kloiber and Zimmerer (1990). The most probable value of the energy of these atoms ranged from 0.16 eV up to 0.25 eV dependent on the excitation energy. The kinetic energy of these atoms is much less than the energy from the dissociative recombination. Unfortunately, no measurements of the distribution of the ground state neutrals are available for the moment.

A particular interesting case is **sputtering of neon by hydrogen ions**. Electronic sputtering is the dominant type of sputtering, and in fact, it was demonstrated by Ellegaard et al. (1986b) that the yield is proportional to the quantity $S_e^n(E)$. Here, Andersen and Zigler's stopping power tables (1977) were used, and the best agreement between the experimental curve and $S_e^n(E)$ was found for n = 0.9. In contrast to the electron results no thickness dependence was observed for solid neon during hydrogen ion bombardment. A possible explanation for this behaviour is that the ionization cross section for neon is very low at these proton energies, and that almost all excitations are below the ionization threshold. Apparently these excitations are relatively immobile compared with the atomic ions. In addition to the electronic sputtering, there is a considerable contribution from nonoverlapping subspikes. The yield from this mechanism is about 20 Ne/H^+ for almost the entire energy range under consideration (Ellegaard et al. (1991)).

6 Sputtering of Solid Argon and Krypton

Solid argon and krypton are the most extensively studied condensed gases. In particular, argon has become the standard material among the solidified gases. Electronic sputtering of solid argon by charged particles has been investigated by Reimann et al. (1984b, 1988, 1990, 1991) at A & T Bell, Besenbacher et al. (1981) in Århus, O'Shaughnessy et al. (1988) in Charlottesville, Schou et al. (1987, 1988) and Ellegaard et al. (1988) at Risø, Pedrys et al. (1988) at FOM, Amsterdam, Coletti and Debever (1983) and Coletti et al. (1984) in Marseille, Balaji et al. (1990) in Austin, Arakawa et al. (1989) in Tokyo and Leclerc et al. (1990) in Sherbrooke. Photon sputtering of neutrals from solid argon has been studied systematically by Feulner et al. (1987) and Menzel (1990) in Munich, Kloiber and Zimmerer (1989,1990) in Hamburg, and Arakawa and Sakurai (1990) in Tokyo.

The energy dependence of the electronic sputtering yield has been investigated at the present setup for primary electrons, hydrogen and helium ions in the keV-range. Only for helium ions is there a significant contribution of knockon sputtering to the total yield (see below). The electron-induced yield shows a maximum at 1.5 keV. This demonstrates that the electrons deposit their energy at a distance that is comparable to the characteristic diffusion length of the mobile excitations for 1.5 keV. The distribution of deposited energy shows a maximum at $0.5 \cdot 10^{17}$ Ar/cm^2 (190 Å) in agreement with values of the diffusion length from the literature (Ellegaard et al. (1988)). For the hydrogen ions the electronic sputtering yield turned out to be proportional to the electronic stopping power (Figure 8) (Schou et al. (1988)). The range of the ions tabulated by Andersen and Ziegler (1977) is much larger than the diffusion length except for the lowest energies. An extrapolation of the present electronic sputtering yield from these low stopping power values up to values for He-ions that correspond to the energies from Besenbacher et al. (1981) shows a fair agreement with their data. Yields obtained for energies at the high-energy side of the stopping power by Besenbacher et al. (1981) and Reimann et al. (1988) are about 0.6 less for the same stopping power than those at the low-energy side (Schou (1989)).

The characteristic diffusion length of the mobile excitations in solid argon has been determined for hydrogen ion and electron bombardment. For incident hydrogen dimers and trimers of 3 keV/atom Schou et al. (1987) estimated a diffusion length of 190 Å on the basis of a diffusion model that implies that the surface is highly reflecting for the excitations (Ellegaard et al. (1988), Reimann et al. (1988)). Furthermore, a constant stopping power for the primaries was assumed. Ellegaard et al. (1988) found that the diffusion model for 3-keV electrons gave a length of 200 Å from the thickness dependence of the sputtering yield, provided that a realistic energy-deposition profile was applied. The energy dependence indicated a length of 300 Å, but the model is relatively sensitive to variations in the source energy E_0. If the liberated energy were increased by 10 per cent the diffusion length would rather be about 200 Å, which is the value from the literature for solid argon irradiated by light ions. Reimann et al. (1988) obtained a value of 230 Å for MeV hydrogen and helium ions, and their analysis led to a somewhat larger value of about 270 Å (Reimann et al. (1984b)) for the data of Besenbacher et al. (1981). These data all show a diffusion length much larger than those obtained by photoluminescence yield spectroscopy or exciton-enhanced impurity photoemission with a value ranging from 50 to 120 Å (Zimmerer (1987)). The recent data for the electron-induced luminescence yield at considerably higher temperatures show a higher diffusion length (Hourmatallah et al. (1988)), but the trend agrees with the

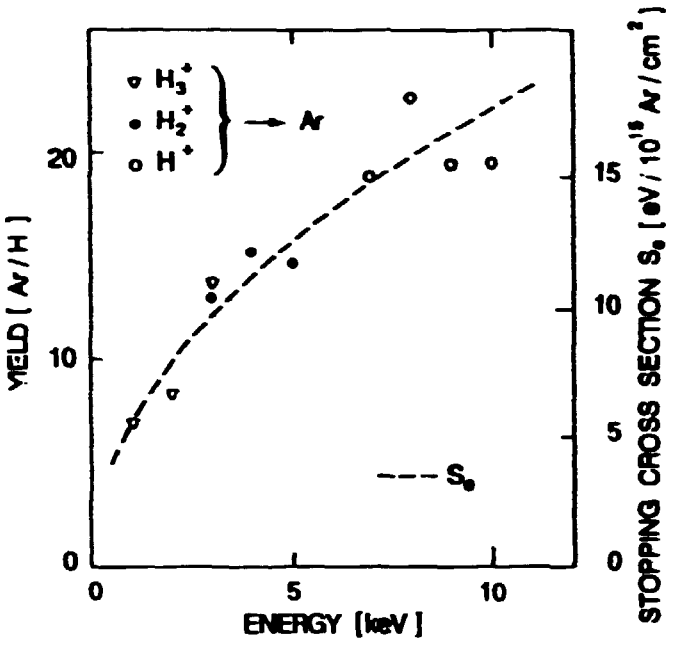

Figure 8. The sputtering yield per atom from solid argon bombarded by hydrogen ions. Film thickness: 4 · 10^{17} Ar/cm^2. Data from Schou et al. (1988). Stopping cross section from Andersen and Ziegler (1977).

data for ion or keV-electron incidence.

All data for particle-bombarded solid argon have been obtained by freezing a gas on a substrate kept at 12 K or below, except for the results of Hourmatallah et al. (1988). The results from Risø, AT & T Bell and Århus agree very well with each other (Schou (1987)). This is a clear statement about the unimportance of the type of the primary particle. In this context the dominant property is the depth profile of the electronic excitations.

For argon as well as for neon the existing results demonstrate that sputtering may take place via exciton production. For solid argon Feulner et al. (1987) and Kloiber and Zimmerer (1989, 1990) showed that selective photon irradiation at the surface and bulk exciton levels induces a considerable desorption. A strong enhancement of the yield was observed by Kloiber and Zimmerer (1989) for excitation energies above the energy gap.

The dominant mobile carrier of the excitation has not been identified yet. Reimann et al. (1988) suggest that it is an atomic hole, whereas Hourmattalah et al. (1988) consider the excitation to be a free exciton.

The energy release processes are quite similar to those for neon. The energy is liberated either from dissociative recombination or by a ground state repulsion. In addition, atoms or molecules may be ejected directly as a result of cavity formation around excited surface species. The dissociative recombination liberates about 1 eV (Reimann et al. (1988)) and the ground state repulsion 1.1 eV (Reimann et al. (1988), Ellegaard et al. (1988) and Schou et al. (1988)). The latter process has been identified in the energy distribution of neutral argon atoms by O'Shaugnessy et al. (1988) and Menzel (1990). The former authors found the peak at 0.54 eV for He-ion incidence and at 0.46 for electron incidence, and the latter author a peak around 0.49 for electron incidence. These data are corroborated by estimates

from the gas-phase interatomic potential (Pedrys et al. (1988), O'Shaughnessy et al. (1988)). The measurements by Arakawa et al. (1989) show that the energy distribution of the metastable neutrals peaks around 0.6 eV. This means that the most probable energy release from dissociative recombination is about 1.2 eV. Then, the total value of the energy liberated from these two processes is about 2.3 eV, which is considerably less than the value E_s = 2.7 eV suggested by Ellegaard et al. (1988) and larger than the value of 2.0 eV indicated by Reimann et al. (1988). All spectra show a pronounced low-energy peak that represents the sputtered particles from low-energy cascades (Pedrys et al. (1988), O'Shaughnessy et al. (1988) and Menzel (1990)). For solid argon as well as solid neon the binding energy is so small that these nonradiative deexcitation processes initiate low-energy cascades.

In almost all cases the boundary conditions for the mobile excitations in solid argon have been a highly reflective surface combined with an absorbing (metallic) substrate (Schou et al. (1987), Ellegaard et al. (1988), Reimann et al. (1984b,1988)). Only for high-temperature argon samples that were excited by low-energy electrons, have Hourmatallah et al. (1988) found a highly absorbing surface.

Since solid argon has been comparatively comprehensively investigated, a number of processes have been identified. It has been established that photon or electron bombardment produces secondary ions (Arakawa et al. (1989), Rocker et al. (1990), Dujardin et al. (1990), Hellner et al. (1990), Menzel (1990)), even though the yield is orders of magnitude smaller than that of neutrals. The metastable neutrals Ar^* $^3P_0$ and $^3P_2$ were detected by Arakawa et al. (1989), Arakawa and Sakurai (1990) and Kloiber and Zimmerer (1990). These authors found a local maximum at around 0.04 in the energy distribution. The metastable neutrals originate from cavity formation around the exciton according to the idea by Coletti et al. (1984) and further corroborated from calculations by Cui et al. (1989b) and Reimann et al. (1990). A comprehensive study on the possible sites of the atoms prior to ejection was performed by Hourmatallah et al. (1988) and Coletti et al. (1987). The excited molecular exciton that deexcites by the emission from the W-band has been observed in front of the target material by Reimann et al. (1988,1990,1991). The kinetic energy of these dimers is of the order of 1 eV, and the analysis carried out by Reimann et al. (1991) shows that the dimers are dominantly relaxed vibrationally. These dimers are probably produced by recombination between an excited argon atom, which itself originates from a dissociative recombination, and a ground state atom close to the surface.

In most of the present work on solid argon the dominant ejection mechanism is electronic sputtering. However, for He^+-ions from 2 to 10 keV knockon sputtering turned out to give a significant contribution. Schou et al. (1988) found that the electronically induced yield was 0.3 and 0.45 of the total yield for 7 keV $^4He^+$- and $^3He^+$-ion incidence, respectively. Other estimates of the relative contributions from the two types of sputtering are based on assumptions that involve theoretical calculations, e.g. Stevanovic et al. (1984) or Chrisey et al. (1986). Since the knockon yield for 7 keV He-ion incidence is about four times larger than the predicted value from linear collision-cascade theory, other mechanisms may account for a major part of the yield. The contribution from nonoverlapping subspikes accounts for about 0.40 of the total knockon yield for both light ions, and finally one may expect a significant contribution from ordinary light ion sputtering (Sigmund (1981), Schou (1989)). However, even for hydrogen ions incident on solid nitrogen that has a similar sublimation energy, the increase in yield induced by this mechanism from a "nitrogen substrate" to a silver substrate did not exceed a factor of 1.4.

Sputtering of solid krypton has been studied less comprehensively than argon. Electronic sputtering yields by charged particle bombardment have been

measured by Schou et al. (1987) and Ollerhead et al. (1980), whereas energy distributions for electronic sputtering have been measured by Pedrys et al. (1985) and O'Shaughnessy et al. (1988). Erosion studies of krypton with a significant contribution of knockon sputtering were carried out by Boring et al. (1987), Balaji et al. (1990) and Pedrys et al. (1985). The only determination of the characteristic diffusion length from charged particle bombardment was made by Schou et al. (1987). Their value $\ell_o = 300$ Å is substantially higher than most of the diffusion lengths found by photon irradiation (Schou (1987)). The energy release processes are similar to those of argon. From the ground state repulsion, 0.8 eV is liberated according to observations from Pedrys et al. (1985) and O'Shaugnessy et al. (1988). The corresponding energy release from the dissociative recombination can be estimated to 1.4 eV from the measurements of the energy distribution of the excited neutrals from Arakawa et al. (1989). An interesting aspect is that no low-energy metastable krypton atoms are emitted, since the cavity emission does not take place in materials with a positive electron affinity (Kloiber and Zimmerer (1989)). The kinetic energy distribution of the metastables obtained by Arakawa et al. (1989) does not show any low-energy neutrals, but only the feature that originates from dissociative recombination. The total yield of these metastable neutrals increases with thickness up to about 100 atomic layers and shows a saturation for higher values. This thickness dependence agrees with that obtained by Schou et al. (1987) for the total yield. This is an argument in favour of the atomic hole as the mobile carrier of the exciton. In this connection, Kloiber and Zimmerer (1989,1990) demonstrated that the photon excitation of solid krypton is very efficient above the energy gap, in particular above the threshold for inelastic electron-electron scattering.

7 Sputtering of Solid Nitrogen and Oxygen

Solid nitrogen and oxygen are in many respects the simplest molecular condensed gases. Both gases in solid form have been studied comprehensively at different laboratories. In connection with the present work, the two gases have made it possible to identify some of the properties that are determined essentially by the molecular structure. Knowledge of these properties makes it easier to distinguish between those features which are common to the molecular solids and those which are specific to the hydrogens.

Luminescence from particle-irradiated solid nitrogen has been observed by Dressler (1971), Dressler et al. (1975), Oehler et al. (1977), Coletti and Bonnot (1977), Sayer et al. (1979) and Poltorats'kiĭ and Fugol' (1979). In contrast, solid oxygen is a strongly absorbing material, and as a matter of fact, no luminescence in the visible or near-infrared regime below 900 nm has been observed from pure solid oxygen so far, (Dressler (unpubl.)). Strong absorption from solid oxygen has been reported from several groups, for example by Landau et al. (1962) and Schnepp and Dressler (1965). The major reason for this luminescent behaviour totally different from that of nitrogen is the existence of two electronically excited states only about 1 and 2 eV above the ground state in oxygen. In nitrogen the lowest electronically excited state $A^3\Sigma_u^+$ is about 6 eV above the ground state, which means that the excited atomic levels $^2D^0$ and $^2P^0$ lie below this triplet state. Therefore, the nitrogen atoms which inevitably are generated from dissociative processes, play a major role in the deexcitations as quenchers for highly excited states and as efficient photon emitters (Dressler (1971), Oehler et al. (1977)).

There are no mobile excitations that contribute to sputtering (Ellegaard et al. (1986), Ellegaard (1986), Brown et al. (1986)). On the other hand, it is known that the $A^3\Sigma_u^+$ state as well as the first vibrationally excited level in the electronic ground state are mobile (Dressler (1971)). These states deexcite by energy transfer to the trapped atoms and by multiphonon processes without any localized energy release that might lead to sputtering.

One important consequence of the virtually immobile excitations is that the electronic sputtering yield is determined primarily by the energy that is deposited at the surface. Therefore, the relationship between stopping power and electronic sputtering yield is relatively simple, and for low excitation densities Ellegaard et al. (1986a), Rook et al. (1985), Brown et al. (1986), and Gibbs et al. (1988) found a linear yield dependence on the stopping power.

Since the dissociative energy is much larger than the sublimation energy, the majority of the emitted particles during particle irradiation are the parent molecules (Pedrys et al. (1989), Brown and Johnson (1986)). However, a significant fraction of atoms was observed as well (Pedrys et al. (1989)).

An important series of yield measurements from these two solids for 0.8- to 3-keV primary electrons was performed by Ellegaard et al. (1986a). They showed that

i) the sputtering yield does not depend on the film thickness except for a contribution that is caused by electrons backscattered from the metallic substrate,

ii) the yield is almost proportional to the stopping power of the primary electrons, and

iii) the yield from solid oxygen is almost precisely a factor of two larger than that from nitrogen.

The independence on the thickness means that the constant (bulk) yield is easily identified. The contribution from backscattered electrons for the thinnest films turned out to be about 25 per cent of the bulk yield. For the two solids the bulk yield was proportional to S_e^n, where n = 1.15 for nitrogen and 1.20 for oxygen. For MeV protons incident on these two solids, Gibbs et al. (1988) observed a regime which depends linearly on the stopping cross section $S_e(E)$. In contrast, most of the yield induced by primary MeV He-ions showed a pronounced quadratic dependence on the stopping power (Gibbs et al. (1988)). Gibbs et al. (1988) found as well that the yield from oxygen was about a factor of 2.3 to 2.6 larger than that from nitrogen during light ion bombardment.

The difference in yield for nitrogen and oxygen is primarily caused by more efficient energy release processes in solid oxygen than in nitrogen. Rook et al. (1985) pointed out that the stopping power $NS_e(E)$, the sublimation energy and the energy required to produce an electron-ion pair are practically similar for these two solids. These authors suggested two substantially different values of the released energy E_s per electron-ion pair produced in nitrogen and oxygen. The yield induced by MeV protons is actually predicted within 30 per cent with Equation (5) for E_s = 3 eV for solid nitrogen and E_s = 7 eV for oxygen. The absolute magnitude for primary electrons is about a factor of two larger than the predicted value with $D_e(0) = 1.6\ NS_e(E)$ (Ellegaard et al. (1986a)). Recent Monte-Carlo calculations by Valkealahti et al. (1989) confirm that the appropriate excitation density $D_e(0)$ at the surface is somewhat larger than the stopping power because of scattering and slowing down of primary electrons. Even though Equation (5) does not lead exactly to the measured values, the energy dependence as well as the ratio of the yield from the two solids are predicted quite well from the expression. According to the discussion in Section 3.3 the sublimation energy per atom rather than per molecule has been utilized for the surface binding energy U_0. The

expression does not include any interaction between excited target particles at high excitation densities which lead to the quadratic or nonlinear dependence on the stopping power observed for MeV He-ions by Brown et al. (1986) and for keV ions by Ellegaard (1986) and Ellegaard et al. (unpubl.).

The energy release processes have been explored from energy spectra of the emitted particles by Pedrys et al. (1989) and Pedrys et al. (unpubl.). The results from electron-induced sputtering of nitrogen indicate at least two different non-radiative transitions that cause sputtering of the solid. The most energetic one of these transitions is that from highly vibrationally excited states of the molecular ground state ion or from electronically excited states of the ion down to the $N(^4S^0) + N(^2P^0)$ or $N(^4S^0) + N(^2D^0)$-level or that from the vibrational ground state to the $N(^4S^0) + N(^2D^0)$-level. A number of important electronically excited levels for nitrogen are shown in Figure 9. Transitions induced by electron impact to electronically excited ions in the $B^2\Sigma_u^+$-state (Hernandez et al. (1982)) as well as other states have been reported in the literature (Stolarski et al. (1967)). Such a dissociative recombination produces two atoms each with an initial energy of about 3 eV. The second process may be the result of relaxation and repulsion from the $N(^4S^0) + N(^2D^0)$-level. By this transition the atoms receive less than 1 eV. Even though $E_s = 3$ eV may be a feasible average, the spectrum from solid nitrogen demonstrates that the value should be regarded as a weighted sum of different contributions. For solid oxygen there are no pronounced high-energy transitions. The released energy may originate from subsequent relaxation and repulsion processes that terminate on the four lowest combinations of excited atomic levels $O(^1S)$ and $O(^1D)$, and of the ground state level $O(^3P)$. A complicating feature for the processes in solid oxygen is the ozone formation by which about 1 eV is liberated as kinetic energy. For sputtering from solid oxygen, E_s is composed by many small energy values rather than one or two specific high-energy release processes.

The data for sputtering by keV hydrogen ion bombardment are shown in Figure 10. The yield per ion is depicted as a function of the sum of the electronic stopping power $NS_e(E)$ of the individual atoms in the ion. The proton-induced as well as polyatomic ion-induced yields from solid nitrogen are proportional to S_e^n, where $n = 1.60$. Since the data points all lie on a single curve, it means that one may consider the impact of a polyatomic ion as a simultaneous impact of atoms with an equal sharing of energy. Then, the atoms are so close to each other that the excitations in those layers that contribute to sputtering correspond to those produced by one particle with an electronic stopping power equal to the sum of the stopping powers for the atoms (Stenum et al. (1991a)). This point of view is strongly corroborated by the energy spectra from proton and molecular hydrogen ion incidence. There is no indication that different processes account for the spectra of ejected particles by polyatomic hydrogen ions in the case of either solid nitrogen or oxygen (Ellegaard et al. (unpubl.)). An interesting feature is that the data points for the yield per atom as a function of the energy per atom do not lie on a single curve as they do for solid neon and argon, but on three separate branches (Ellegaard et al. (1986b)). It means that the excitations that lead to sputtering are almost immobile, as pointed out above from the thickness dependence of the sputtering yield.

For solid oxygen the yield is proportional to S_e^n, where $n = 2.0$. The proton-induced yield from oxygen is about a factor of 2.3 larger than that from nitrogen for the same electronic stopping power. For the molecular ions the yield from oxygen exceeds that from nitrogen by a factor of 4.0 for the same stopping power as well. The increase of the oxygen yield relative to that of nitrogen for comparatively high electronic stopping powers was observed by Gibbs et al. (1988) as well.

The nonlinear dependence of the ion-induced yield on the stopping power might

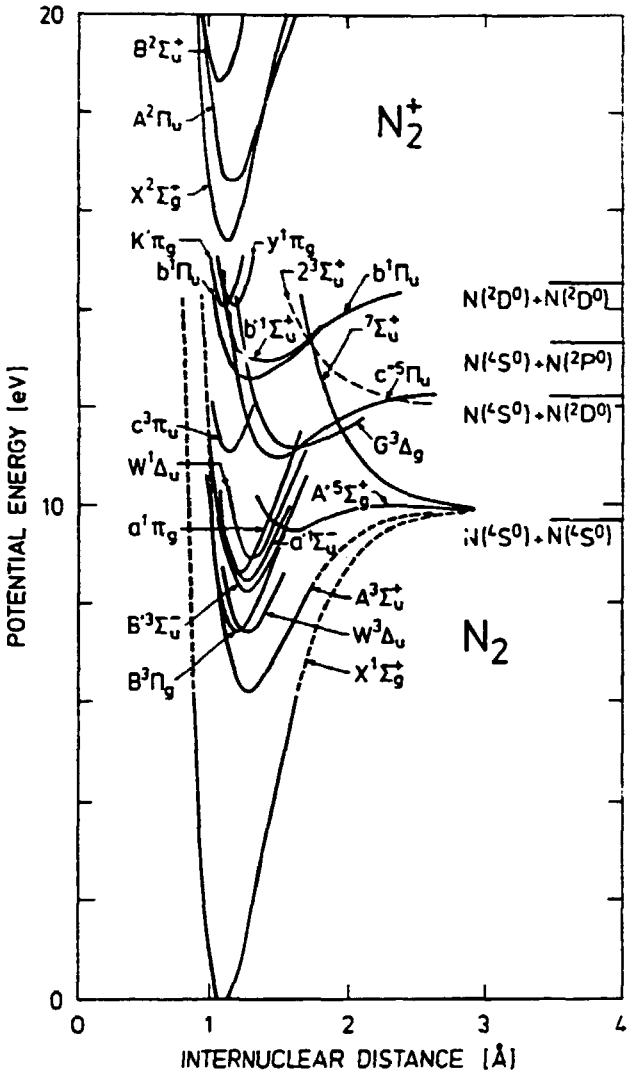

Figure 9. Potential energy diagram for gaseous nitrogen (From Ellegaard et al. (unpubl.)).

be considered to be a surprising behaviour, in particular since the yield for similar stopping powers of MeV H^+-ions does not show this nonlinearity. At present keV energies the ionization cross section is comparatively small (Rudd et al. (1985)). This means that about 60 eV is required for the first electron-ion pair, whereas the asymptotic high-energy value for W is 36.2 eV (ICRU (1979)). It follows from this that the excitations below the ionization threshold are dominant. These simultaneous excitations are so close that the average distance between two subsequent excitations may be less than 3 Å. Excited and ground state atoms that originate from different dissociated molecules may recombine and continue the relaxation so that extra energy is released. A possible additional effect is the overlapping of the cascades so that fragments of a cylindrical spike may be generated. Both effects lead to a yield dependence on the stopping power to the second or higher powers.

An interesting analysis of the important transitions to the levels below the ionization threshold during keV proton impact on gaseous nitrogen and oxygen was reported by Park (1978) and Enos et al. (1991). The authors demonstrate from high resolution translational energy spectroscopy that the dominant process for nitrogen is a transition from the ground state $X^1\Sigma_g^+$ to $a^1\Pi_g$, but also other singlet state levels as $w^1\Delta_u$ and $b^1\Pi_u$ are populated by the ion impact. For oxygen the dominant transitions are from the ground state $X^3\Sigma_g^-$ to the $B^3\Sigma_u^-$ and $A^3\Sigma_u^+$ levels. The molecules in these two excited levels dissociate in contrast to most of the excitations in nitrogen. This means that the energy from excited oxygen

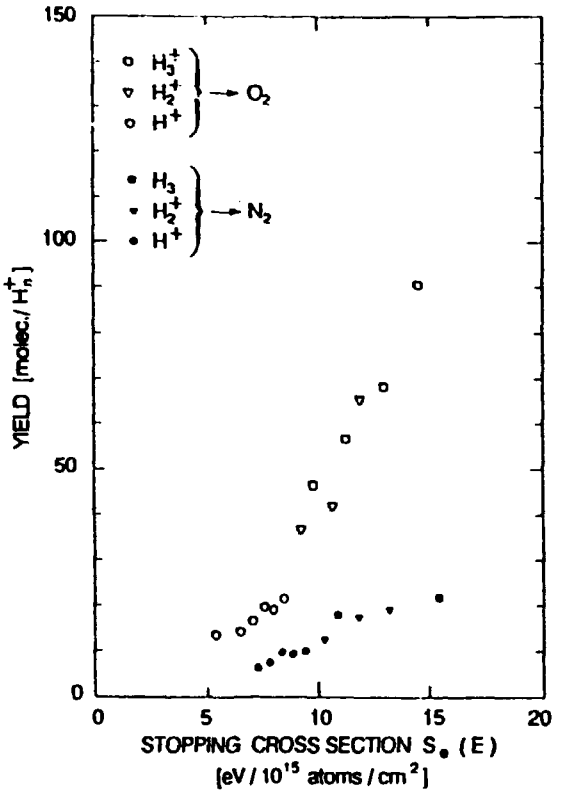

Figure 10. The total yield as a function of the sum of the total electronic stopping cross section for the primary ion. Atomic stopping cross sections from Andersen and Ziegler (1977).

molecules is much more efficiently converted to translational energy than that from electronically excited nitrogen molecules.

The linear behaviour that is shown by the electron-induced yield (Ellegaard et al. (1986a)) and for proton bombardment in the MeV range (Gibbs et al. (1988)) is primarily a result of frequent ionizations compared with excitations. The ionized molecules dissociate after electron capture, and this event may take place after relaxation of the excited atoms in the neighborhood.

8 Sputtering of Solid Hydrogen Isotopes

The solid hydrogens turned out to be the most difficult materials to study with respect to sputtering because of the high volatility. Therefore, the experiments with these solids had to be performed at temperatures below 4 K and with a comparatively low beam power. Many of the features from the sputtering results are still partly unexplained.

The properties of the solid hydrogens are remarkable in many respects. The sublimation energies are the smallest ones for all possible targets in vacuum, ranging from 8.65 for solid hydrogen up to 10.8 and 12.65 meV per molecule for hydrogen deuteride and deuterium (Souers (1986)). These values are approximately a factor of 2 smaller than that of solid neon, which is the most volatile ordinary

solid rare gas.

The mobility of the electrons in solid hydrogen is extremely low, $6 \cdot 10^{-6} cm^2/(V\ sec)^{-1}$, which is about three orders of magnitude less than that in solid nitrogen and oxygen (Le Comber et al. (1976)). The low mobiiity is primarily caused by electron trapping in lattice defects and subsequent formation of electron bubbles. These immobile electrons have been observed with absorption spectroscopical methods in solid deuterium by Brooks et al. (1983, 1985a), in solid hydrogen by Brooks et al. (1985b), and in solid hydrogen deuteride by Miller et al. (1988).

The visible luminescence from particle-bombarded solid hydrogens is weaker than from any other comparable solidified gas except solid oxygen (Stenum et al. (1989, 1991c)). The electronic structure of hydrogenic molecules differs basically from that of oxygen, since there is a gap of about 10 eV from the ground state to the lowest electronically excited states in the hydrogenic molecules. The photon emission from solid deuterium observed by Stenum et al. (1989) and by Schou et al. (1989) represents one of the less common pathways for electronic deexcitation. The majority of the electronic excitations terminate on one of the many repulsive branches above the dissociative limit or on, for example, the strongly repulsive $b^3\Sigma_g^+$ state so that the deexcitation processes release from 11 to 5.5 eV as kinetic energy. However, it is not clear if the energy is liberated in one event or shared among several events with a relatively small energy release. The formation of triatomic ions, as for example D_3^+-ions, leads probably to a subsequent generation of D_9^+-ions, which eventually may recombine. By the recombination 4-8 eV is liberated, and the observed peak around 275 nm assigned to a transition in D_3^* appears after only less than 10 per cent of the recombinations (Stenum et al. (1989, 1991c), Stenum (1991)).

Systematic measurements of the yield dependence on film thickness and primary energy have been carried out only at Risø. The work was initiated by Sørensen (1976), gradually improved by Børgesen et al. (1980), Børgesen and Sørensen (1982), Børgesen (1982), Schou et al. (1984), Ellegaard (1986), until it reached the present refinement in studies by Stenum et al. (1990,1991a,1991b) and Stenum (1991). Erents and McCracken (1973) published results for ion-bombarded solid hydrogen, which indicated a yield of similar magnitude as that from Stenum et al. (1991b), but the thickness dependence did not show a saturation behaviour for large film thicknesses in contrast to the data observed by Stenum et al. (1990).

The yield for thick films as a function of the proton energy is shown in Figure 11. For all three isotopes the energy dependence is a clear indication of electronic sputtering. The nuclear stopping power decreases significantly in this interval, and the magnitude of the knockon sputtering yield predicted from linear collision-cascade theory is typically about or below one deuterium molecule per proton. Knockon sputtering from either a cylindrical elastic spike or nonoverlapping elastic subspikes leads to an energy dependence that disagrees completely with that observed experimentally. It means that contributions from these mechanisms are relatively unimportant. For solid hydrogen deuteride and hydrogen the yield dependence on primary energy can be approximated well by the electronic stopping power squared times a constant that depends on the specific isotope. However, for solid deuterium the dependence on energy is almost proportional to the cube of the stopping power.

There is no satisfactory theory that reproduces the observed energy dependencies as well as the magnitude of the yield. The ionization cross section for protons with energies up to 10 keV incident on hydrogen gas is so small (Rudd et al. (1985)) that the average energy loss to produce an electron-ion pair varies from about 250 eV at 5 keV to 150 eV at 10 keV (Stenum et al. (unpubl.), Stenum (1991)). Since this value is far from the asymptotic high-energy value of 37.5 eV (ICRU (1979)), it means that excitations below the ionization limit are dominant.

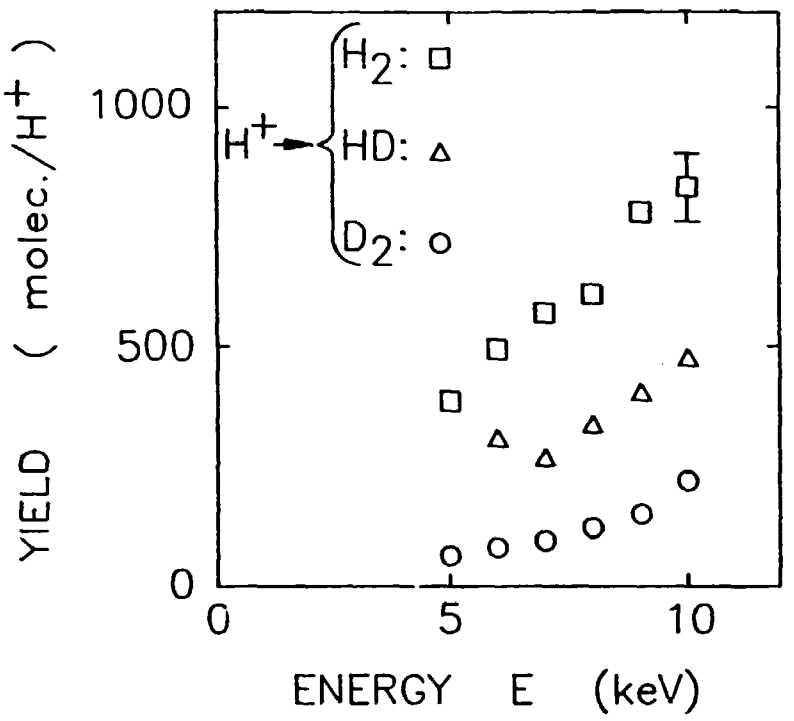

Figure 11. The sputtering yield from solid hydrogenic targets bombarded by protons. A typical standard deviation is indicated. (From Stenum et al. ((1991b)).

Collision spectrometric measurements by Park (1978) show that excitations of the $B^1\Sigma_u^+$-level or of the many close-lying molecular states just above this level from the $X^1\Sigma_g^+$ ground state prevail. The distance between two subsequent excitations, which according to the previous discussion each releases an energy ΔE_s between 5.5 and 11 eV, is so small that the recoils interact. Since the binding to the hydrogenic lattice is small, the repulsing atoms generate individual subspikes that immediately merge into a cylinder around the track. If we utilize the picture advocated by Brown et al. (1986), the number of atoms set in motion can be estimated by $\Delta E_s/U_o$. Even for the least volatile material, solid deuterium, it means that each sphere within which the molecules are set in motion contains at least several other starting points for subspikes. The resulting cylindrical spike posseses an almost perfect cylindrical geometry.

In the comparatively simple model of a cylindrical spike by Sigmund and Szymonski (1984) the yield is proportional to the square of the deposited energy per unit length. In this context the energy per unit length means the part of the electronic stopping power that ends up in electronic excitations below the ionization threshold. The energy spent in ionizations is unavailable for the cylindrical spike except the energy from the D_3^+-formation, which takes place simultaneously with the generation of the cylindrical spike. The effective stopping power $F_D'(E)$ is about 0.6 times the electronic stopping power. The remaining 40 per cent of the stopping power represent energy loss to ionization, dissociation and kinetic energy of the secondary electrons. A minor part of this energy loss leads to energy release from dissocative recombinations of D_3^+ or D_9^+-ions, which may occur on a time scale up to several seconds after the spike generation. This energy release leads to electronic sputtering as well, but the contribution is insignificant compared with the total yield from the cylindrical spike (Stenum (1991), Stenum et al (unpubl.)).

Although the yield dependence is fairly well predicted by the cylindrical electronic spike, the model cannot describe the dependence on the sublimation energy

U_s in a satisfactory way. On the basis of the model by Sigmund and Szymonski one may deduce an initial string energy $kT_s(NS_e)$ from the measured yields of the three hydrogen isotopes. However, one arrives at a temperature corresponding to a value of kT_s of approximately 4 meV, which leads to a yield that is one order of magnitude too low. A straightforward implication is that the sublimation energy may not be the most appropriate quantity for the surface binding U_s. Considering the large sputtering yields one may expect that many adjacent particles are emitted simultaneously. In that case, a constant barrier of magnitude U_s determined by fixed surface atoms becomes meaningless.

An interesting feature is that the yield from solid deuterium during molecular hydrogen ion bombardment shows the same dependence on the stopping power as that during proton bombardment. Even though we use the standard assumption that a polyatomic ion dissociates upon impact under an equal sharing of energy, the atoms from the ion are so close to the others that one may regard the impact of the molecule as one event. In this manner, it corresponds to an impact of an ion with an electronic stopping power two or three times larger than the proton stopping power. Stenum et al. (1991a) showed that the total yield as a function of the total electronic stopping power could be approximated by a single curve, independent of the number of atoms in the ion. The yield from solid deuterium turned out to be fairly well represented by a cubic dependence on the total stopping power up to S_e-values close to the maximum of the stopping cross section.

As discussed above, the dependence on the stopping power NS_e is certainly not linear. It means that the expression, Equation (5), is not feasible for hydrogen ions of energies below the stopping power maximum, and the yield predicted by this formula with $E_s/W = 0.6$ is actually less than 20 per cent of the experimental values except for deuterium, where the predicted yield approaches one-half for the lowest primary energies. Here and in the following treatment for primary electrons, we have used Equation (5) with a surface barrier for the atoms equal to one-half of the molecular sublimation energy in complete analogy with the treatment for solid nitrogen and oxygen.

For primary electrons the thickness dependence differs basically from that of ions. The dependence for 1-keV electrons incident on solid hydrogen deuteride and that for 2-keV electrons on deuterium are shown in Figure 12. It was not possible to perform any electron sputtering measurements of solid hydrogen with the quartz crystal because of a pronounced beam-induced evaporation. The thin-film enhancement is similar to that for primary protons, but the increase at large film thicknesses has no parallel in the studies with primary ions. In contrast to the ion case there is no constant yield at thicknesses that exceed the range of the primary particle. It is tempting to ascribe the behaviour at large thicknesses to a mechanism different from the ordinary electronic sputtering. It means that as a starting point one may assume that the thick-film yield comprises a significant contribution of sputtering from this mechanism and a comparatively small one from ordinary electronic sputtering. The electronic yield that should be compared to Equation (5) is the value at the minimum. However, even this value may not be the most appropriate one if the mechanisms for the thin or thick films contribute substantially to the yield at this thickness.

The deexcitation processes for primary keV electrons are somewhat different from those for protons. The distance between subsequent ionizations along the electron trajectory is typically about 200 Å for the present energies. The compilations by Miles et al. (1972) and Heaps and Green (1975) show that the cross section for ionization by keV electrons is almost a factor of two larger than that for the most probable excitation, $X^1\Sigma_g^+ \rightarrow C^1\Pi_u$, and even more for the excitation to the lowest bound electronically excited state $B^1\Sigma_u^+$. The cross section for a direct excitation of the repulsive triplet state $b^3\Sigma_u^+$ is very small for electron ener-

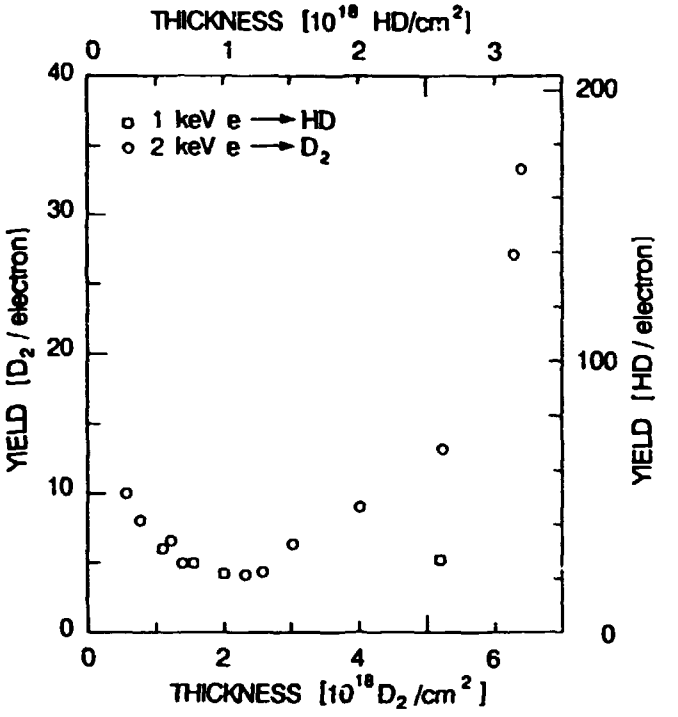

Figure 12. Sputtering yield for electron bombardment as a function of film thickness for solid deuterium and hydrogen deuteride. Note the different scales. From Ellegaard (1986) and Børgesen et al. (unpubl.).

gies above 50 eV, but most of the excitations in the system may terminate on the $b^3\Sigma_u^+$-curve after tunneling from higher electronically excited states. Only about 20 eV out of $W = 37.5$ eV per electron-ion pair are liberated as kinetic energy, whereas the other part of the deposited energy is lost to ionization, dissociation and kinetic energy of the internal secondary electrons (Stenum et al. (unpubl.)). With this choice for E_s/W and the surface value of the deposited energy from Valkealahti et al. (1989) one obtains from Equation (5) an electronic sputtering yield that is about 75 per cent of the deuterium yield, but only 30 per cent of the hydrogen deuteride yield at the minimum. The disagreement is considerable, but one has to take into account that it would be desirable to improve the treatment of how molecules pass a surface barrier in such a volatile material. The ejection effiency $Y/D_e(0)$ for hydrogen deuteride is about a factor of 2.7 larger than that for deuterium. This factor is substantially larger than the corresponding ratio 1.2 of the sublimation energies. An estimate based on the spherical subspike model with a fixed average energy release of 8 eV per deexcitation and a surface binding energy equal to the sublimation energy gives a yield that is almost three times larger than the measured value for solid deuterium and a factor of 1.15 larger than that from hydrogen deuteride. Apparently, the low-energy linear collision-cascade model gives a reasonable prediction for the least volatile material, solid deuterium, whereas the spike model seems more appropriate for hydrogen deuteride.

The behaviour of the yield for thick films is complex as demonstrated in Figure 12. Unfortunately, these two series are the only complete ones measured with the quartz crystal microbalance. The points for 2-keV electrons on deuterium show a more rapid increase than those for 1-keV electrons on hydrogen deuteride.

It is not obvious whether or not the reason is the different material or energy. However, one knows at present that

i) the thick-film enhancement is not caused by beam-induced evaporation,

ii) the enhancement has been observed for solid hydrogen as well, and

iii) the enhancement is not an artifact from the measurements on the quartz crystal microbalance, but has also been observed for a massive target.

Ellegaard (1986) showed that the magnitude of the deuterium yield was not influenced by different currents, and Børgesen et al. (unpubl.) have shown that the yield for 1 keV electrons incident on a massive gold substrate behaves in a way similar to those shown in Figure 12.

It is tempting to associate the different thickness dependencies for primary ions and electrons with the concept that the primary electrons embedded in the film build up a space charge. Børgesen (1982) saw a clear current signal from immobilized electrons during film evaporation, but there is at present no link to new sputtering mechanisms from this observation.

Extensive series of measurements on all three hydrogen isotopes were carried out with the emissivity-change method (Børgesen et al. (unpubl.)). During the initial phase the broadening of the beam spot was not taken into account (Schou et al. (1984)). Since the area of the spot almost varied 50 per cent from 1- to 3-keV electrons, it turned out to be difficult to evaluate an absolute yield from this method alone. A complicating feature was that the strong trends for thick and thin films were not studied separately. For the highest energy, it was even not possible to reach thicknesses corresponding to the thick-film regime with the emissivity-change method. On the other hand, some of these data (Børgesen et al. (unpubl.)) may now be analyzed in a satisfactory manner, because the recent data for proton bombardment of hydrogen showed that the beam spot on a hydrogen target is similar to the area on the less volatile targets, namely solid hydrogen deuteride and deuterium.

9 Status and Outlook

During the past ten years sputtering of elemental condensed gases has been explored in a systematical manner by the present author and collaborators as well as by several other groups. The features that are characteristic for the condensed gases have been largely identified. On the other hand, it has turned out that a number of phenomena known from ordinary knockon sputtering of metals occur for sputtering of condensed gases as well.

The present work has been primarily a study on erosion of some of the most volatile gases by low energy ions (1-10 keV/atom) and electrons (1-3 keV). The measurements of the yield as a function of film thickness, primary energy and other experimental parameters were not performed systematically with these primary particles for these energies at any other laboratory.

Solid neon, argon, nitrogen, oxygen and deuterium have been investigated comprehensively. Except for electron bombardment of solid deuterium the data base makes it possible to predict with fair accuracy sputtering yields of these solids outside the measured energy and thickness regime.

Some of the important results have had a considerable impact on the literature. The electron-induced yield from solid nitrogen and oxygen turned out to behave almost like a linear function of the stopping power. The thickness dependence of the yield for the condensed elemental gases appeared to be similar to that

of keV and MeV hydrogen ions. For keV hydrogen ions incident on solid argon and krypton the characteristic diffusion length of the mobile excitations was in agreement with the length obtained from bombardment by other charged particles or from recent luminescence experiments. The knowledge of the magnitude of the absolute yield has been useful in exploring which processes convert the energy in electronically excited states to kinetic energy of the target particles, and for the describing these phenomena as well. The pronounced enhancement of the yield for thin films was shown to result from the interaction between the primary particle and metallic substrate rather than from any beam-independent structural interface effect.

Nevertheless, several important problems are not satisfactorily resolved. The behaviour of the sputtering yield for primary electrons incident on thick hydrogenic films is poorly understood. Energy and mass spectra from these films will be an important step in identifying the mechanism. The thin-film enhancement is poorly understood as well. Experiments made with a combination of two ices seem to be useful, but the introduction of more than one gas leads inevitably to processes at the interface. Even systems of solid nitrogen and solid rare gases are not easy to handle. However, the prospects are probably better for successful thin-film studies of these systems than for ice combinations with too dissimilar physical properties, such as, for example, the sublimation energy.

Considerable progress has taken place at several other laboratories during this past decade. In particular, solid argon and nitrogen have been studied with MeV light-ion beams, luminescence spectroscopy and desorption, and by energy and mass analyses of the ejected particles. Although many of the features now are understood well, several beam-target combinations have been comparatively little investigated.

It is surprising that even solid argon and nitrogen have not been irradiated by MeV ions in a higher charge state than two. The effect of highly charged ions incident on these solids is a completely open field. Data of photon-stimulated neutral atomic and molecular emission from other condensed gases than the rare gas solids would yield complementary information for the sputtering studies with charged particles.

Another relatively unexplored field is sputtering from solidified gases by medium or heavy ions. At very low primary energies (below 1 keV) one may expect almost regular knockon sputtering for materials with a high surface binding energy. On the other hand, the few existing results for medium or heavy ion bombardment in the keV regime of the most volatile gases such as the solid hydrogen isotopes or neon indicate that the yields are extremely high, up to more than 10^4 target particles per primary. This material flow out of the surface represents a transition towards a hydrodynamic description.

The irradiation of even simple heteronuclear condensed gases leads to chemical reactions which complicate the sputtering studies. The deexcitation processes that lead to electronic sputtering in the chemical compounds have as yet been unidentified. In any case, one may expect that the knowledge of sputtering of elemental gases is an appropriate starting point for sputtering studies on more complex ices.

10 Acknowledgement

This work would not have been possible without the collaboration with and support from many colleagues. In particular, I thank Hans Sørensen for the close, constructive and patient collaboration through more than ten years. I appreciate greatly that the local members of my present team, Arne Nordskov and Bjarne

Stenum showed an incredible enthusiasm, also in the difficult time after the reorganization at Risø. The Ph.D. students at our setup at Risø contributed to this work as well, Peter Børgesen initiated the erosion experiment and was a stimulating and patient teacher, Ole Ellegaard was a diligent student with the courage and initiative to continue our collaboration after a short leave from science. I want to acknowledge the inventive assistance from Bjarne Sass, and the careful and versatile electronic assistance from Knud Weisberg as well as Jess Thorsen and Henryk Kossek.

My collaborators outside Risø have helped and supported me and were inspiring discussion partners. Roman Pedrys has been an active partner during many years and gave a fruitful criticism of the present thesis. Carsten Claussen pointed out to me (and others) that the condensed gases were unique materials for sputtering. Peter Gürtler convinced me about the exciting possibilities for luminescence experiments with frozen hydrogenic targets.

During these years I have had inspiring contact with Danish and foreign colleagues, even though they did not participate directly in the present work. I want to thank Peter Sigmund for having directed me into the field of electronically stimulated particle emission many years ago, and for having supported and adviced me, whenever it was necessary during these years. I appreciate discussions with Hans Henrik Andersen, R.L. Brooks, Walter L. Brown, Don David, Jean Marie Debever, Dolf de Vries, Wolfgang O. Hofer, R.E. Johnson, Josef Michl, Curt T. Reimann, Marek Szymonski, Herbert M. Urbassek, Seppo Valkealahti, Georg Zimmerer and many others.

The work was performed in the Plasma Physics Division of the Physics Department which offered me excellent conditions for the present work. I was encouraged by the colleagues here, and finally thank the head of the division, Vagn Jensen, for having prepared me to write this thesis with his numerous inquiries about when it was going to be finished.

11 Dansk sammendrag

I det foreliggende arbejde er en række flygtige frosne gasser blevet bestrålet med keV elektroner og lette ioner. Bestrålingen er foretaget ved en lavtemperatur opstilling på Forskningscenter Risø.

Hovedformålet med dette studium har været at undersøge, hvordan og hvor hurtigt denne type af faste stoffer eroderes af en partikelstråle. Ved høje temperaturer eller store partikelstrømme eroderes den frosne gas ved såkaldt beam-induceret fordampning. Ved lave temperaturer og små strømme er erosionsprocessen overvejende sputtering, d.v.s. erosion forårsaget af enkeltpartikel kollisioner. En vigtig type af sputtering, der her er studeret, er den såkaldte "elektroniske sputtering". Ved denne type erosion omdannes den energi, der afsættes af den primære partikel til excitation og ionisation af targetpartikler, til kinetisk energi ved elektroniske deexcitationer. Hvis denne energi frigøres tilstrækkeligt tæt ved overfladen, kan targetpartikler blive udsendt og overfladen dermed eroderet.

De opnåede eksperimentelle resultater viser, at sputtering af simple isolatorer som disse frosne gasser netop afviger fra normal sputtering af metaller ved, at elektronisk sputtering under mange forhold er den fremtrædende form for erosion ved partikelbestråling. Eksperimenter med frosne gasser har betydet, at det generelle kendskab til elektronisk sputtering er blevet udvidet og systematiseret. For fusionsforskningen betyder de foreliggende resultater, at en række vigtige data for erosionshastigheden af piller af faste brintisotoper i et plasma er tilvejebragt. Samtidig er disse data nyttige for problemstillinger, der vedrører erosion af iskorn

i det interplanetariske rum. Selvom det ofte er kemiske forbindelser, der eroderes, er analysen af sputteringprocessen for frosne gasser af grundstoffer hyppigt det første skridt i den videre analyse.

Målingerne er primært blevet udført med en mikrovægt, der er ophængt ved flydende-helium temperatur. Tynde film af frosne gasser er blevet deponeret på mikrovægten, en oscillerende kvartskrystal. Ved bestråling borteroderes en del af filmen, og massetabet kan direkte bestemmes. Da den indkommende partikelstrøm kan måles, kan man derved bestemme udbyttet, antallet af borteroderede partikler per indkommende artikel.

Frosne film af ædelgasserne, neon, argon og krypton har været en vigtig del af det foreliggende arbejde. I sputtering sammenhæng er fast neon for første gang blevet undersøgt systematisk, og sputtering udbyttet for primære elektroner og lette ioner bestemt. For første gang er diffusionslængden for de excitationer, der i neon producerer sputtering ved elektronbombardement, blevet bestemt. Den tilsvarende diffusionslængde er også blevet bestemt for fast argon, der blev bestrålet med elektroner så vel som med lette ioner. For fast krypton blev diffusionslængden tilnærmesvist bestemt ved bestråling med brintioner. Dette er indtil nu den eneste bestemmelse af diffusionslængden udfra partikelbestråling.

Fast kvælstof og ilt er ligeledes blevet undersøgt. I modsætning til de frosne ædelgasser er der ikke fundet mobile elektroniske excitationer, der medvirker til sputtering. Sputtering udbyttet er omkring dobbelt så stort for fast ilt som for kvælstof for både primære elektroner og og brintioner. En undtagelse er dog de polyatomare brintioner, hvor udbyttet er væsentligt større for ilt end kvælstof.

De faste brintisotoper har udgjort en væsentlig del af det foreliggende arbejde. For filmtykkelser, der er større end rækkevidden af de lette ioner, er udbyttet konstant. Dermed har det for første gang været muligt at måle udbyttet for alle stabile brintisotoper, normal brint, deuterium og hydrogen deuterid ved en række energier. Udbyttet vokser med ionenergien, hvilket er et klart tegn på, at erosionsprocessen er elektronisk sputtering. Udbyttet er langt større for det flygtige faste brint end for fast hydrogen deuterid, hvis udbytte igen er større end for det mindre flygtige faste deuterium. Afhængigheden af sublimationsenergien, der er et mål for flygtigheden, er meget kraftig. Ved bestråling med elektroner er et minimum i udbyttet blevet observeret for filmtykkelser over elektronrækkevidden. Da udbyttet imidlertid vokser med filmtykkelsen udover dette minimumspunkt, har det været vanskeligt at identificere et egentligt tykfilmsudbytte som ved de primære ioner. Der hersker stadig en del usikkerhed over hvilke processer, der frigør energi til sputtering i de faste brintisotoper. Luminescence målinger viser, at der ikke er nogen væsentlig lysudsendelse i UV-området og det synlige område fra fast deuterium under elektronbombardment, og at energien fra den primære partikel derfor i høj grad omdannes til kinetisk energi.

Et fælles træk for de mest flygtige frosne gasser er det store udbytte for tynde film både ved bestråling med elektroner og lette ioner. Med aftagende tykkelse kan udbyttet stige til en størrelsesorden over tykfilmsniveauet. Denne tyndfilmsforøgelse er observeret ved andre opstillinger og er ikke speciel for målinger med en kvartskrystal mikrovægt, som her er blevet benyttet. Selvom der for første gang er blevet foretaget systematiske undersøgelser af denne effekt, er den endnu langtfra forstået. Det er dog klart, at effekten skyldes vekselvirkningen mellem beampartikler og det underliggende metalliske substrat.

De foreliggende resultater viser, at der er store ligheder mellem de frosne gasser ved sputtering. Indenfor de to grupper, frosne ædelgasser, og flygtige frosne molekylære gasser, er lighederne markante. Kun de faste brintisotoper adskiller sig på nogle punkter fra de øvrige grundstoffer. Selve processen, der frigør energi til sputtering, er dog karakteristisk for hver enkelt gas. Der eksisterer således ikke nogen generel fælles proces til energifrigørelsen i de frosne gasser.

12 List of Enclosed Publications

1) *P. Børgesen, J. Schou, H. Sørensen* and *C. Claussen* (1982). Charged particle erosion of solid rare gases and dilute rare gas alloys. Appl. Phys. A 29, 57-61.

2) *J. Schou, H. Sørensen* and *P. Børgesen* (1984). The measurement of electron-induced erosion of condensed gases: Experimental methods. Nucl. Instr. Meth. B 5, 44-57.

3) *J. Schou, P. Børgesen, O. Ellegaard, H. Sørensen* and *C. Claussen* (1986). Erosion of solid neon by keV electrons. Phys. Rev. B 34, 93-106.

4) *O. Ellegaard, J. Schou* and *H. Sørensen* (1986). Sputtering of solid neon by keV hydrogen ions. Nucl. Instr. Meth. B 13, 567-571.

5) *O. Ellegaard, J. Schou, H. Sørensen* and *P. Børgesen* (1986). Electronic sputtering of solid nitrogen and oxygen by keV electrons. Surface Science 167, 474-492.

6) *J. Schou, R. Pedrys, O. Ellegaard* and *H. Sørensen* (1987). Electronic sputtering of solid argon and krypton by keV hydrogen ions. Nucl. Instr. Meth. B 18, 609-612.

7) *J. Schou* (1987). Sputtering of frozen gases. Nucl. Instr. Meth. B 27, 188-200.

8) *O. Ellegaard, R. Pedrys, J. Schou, H. Sørensen* and *P. Børgesen* (1988). Sputtering of solid argon by keV electrons. Appl. Phys. A 46, 305-312.

9) *J. Schou, O. Ellegaard, H. Sørensen* and *R. Pedrys* (1988). Electronic and knockon sputtering of solid rare gases by light keV ions. Nucl. Instr. Meth. B 33, 808-814.

10) *B. Stenum, J. Schou, H. Sørensen* and *P. Gürtler* (1989). Erosion and luminescence from pure and impure solid deuterium. Rad. Eff. Def. Solids 109, 235-238.

11) *B. Stenum, O. Ellegaard, J. Schou* and *H. Sørensen* (1990). Thickness dependence of the sputtering yield from solid deuterium by light keV ions. Nucl. Instr. Meth. B 48, 530-533.

12) *O. Ellegaard, J. Schou* and *H. Sørensen* (1990). Sputtering of volatile solids from nonoverlapping subspikes. Europhys. Lett. 12, 459-464.

13 Notes

NOTES TO PAPER 1

Børgesen et al. (1982)

The paper contains the first experimental results on electron-induced sputtering of solid neon. The first quantitative model that combines the production and transport of excitons with sputtering is presented as well.

p. 57. The erosion of .... UF_4 is no typical room-temperature gas. It melts at 1309 K (Griffith et al. (1980)).

.... The data point for 1.5 MeV He-ions was taken at 8 K. However, Schou et al. (1986) have demonstrated that 6 K is the upper temperature limit for sputtering without beam-induced evaporation.

We first report .... Farrell et al. (1972) suggested that excitons might play a role in desorption of solid rare gases by electrons. However, the authors did not present any quantitative model. A comprehensive analysis of the deexcitation pathways in rare gas solids was performed by Johnson and Inokuti (1983).

p. 58. The erosion yield.... The method and Eq. (2) are extensively discussed in Schou et al. (1984).

It is then found.... In Schou et al. (1986) it was confirmed that the yield for film thicknesses above 730 Å is essentially constant. The minimum of the yield for thicknesses around 140 Å could not be observed, since the method used in this paper is relatively insensitive for small thicknesses with this film-substrate combination.

p. 59. Here, a different approach .... The energy release is discussed in Sects. 5-6. The mobile excitations are either atomic holes or (highly excited) free excitons. See Sects. 5-6.

The properties of excitons... The fraction 0.35 is appropriate, but all types of excitons may contribute to the sputtering. The diffusion length was estimated to 230 Å by Schou et al. (1986), and is actually smaller than that for the heavier rare gas solids (Schou (1987)).

The observed....The experimental yield in Fig. 1 turned out to be larger than estimated from Eq. (4), since beam broadening was neglected. The energy dependence of the yield changes slightly, because the area of the beam spot decreases for energies below 1.5 keV. (See Schou et al. (1984) and (1986)).

p. 60. From (3) and (4).... This calculation does not include features, which have been taken into account by Schou et al. (1986) i) The range of the primary electrons is comparable to the diffusion length of the mobile excitation and ii) the depth distribution of the deposited energy is not constant, but relatively well approximated by a Gaussian distribution.

As discussed... This is the first example of a significant decrease of the yield in the presence of impurities. The fluence necessary for erosion is considerably less for a pure neon film than for an argon-doped or -contaminated film. The dependence on the argon concentration deviates from the expected behaviour (Claussen (1982b)). However, Brown et al. (1985) showed a convincing example of the dependence on the impurity concentration.

p.61. Ref. 14.... Børgesen et al. (unpubl.)

Ref. 15.... Schou et al. (1986).

NOTES TO PAPER 2

Schou et al. (1984)

This paper contains a comprehensive study on the two experimental methods that were used in the present work. In particular, the feasibility of utilizing a quartz crystal microbalance at liquid-helium temperature was demonstrated.

p. 44. Most of the experiments ....The high yields (about 5.10^4 molecules per ion) were published by Erents and McCracken (1973). These yields were measured for thicknesses, at which the thin-film enhancement is the dominant process.

Measurements.... In the high-energy regime nuclear reactions prevent the systematic use of light ions.

p. 46 At temperatures.... Short measurements have been performed with a frequency change of 5 Hz for the most volatile materials.

p. 47. During erosion.... In a part of the present thesis a 4-mm aperture was used as well.

An attempt.... The broadening of the beam spot relative to the projected area of the aperture is the ...ain correction to Børgesen et al. (1982) from this paper and Schou et al. (1986).

p. 48. For normal incidence.... 2d corresponds to the mean path length rather than to the mean projected range (Valkealahti et al. (1988)).

p. 49. Formula (5).... The range of a 3-keV electron is about $3.10^{18} H_2/cm^2$. Hence, the yield deduced from Fig. 6 is not a proper bulk yield, but represents the slowly decreasing yield with increasing thickness from the thin-film enhancement (Sects. 4 and 8).

p. 51. Occasionally it was possible... This example has a limited validity in view of the thickness-dependent yield for solid neon.

Finally....The current density has been estimated by the ratio of the current to the area of the sweep aperture. This density is different from, but probably of the same order of magnitude as the real current density in the stationary beam.

p. 52. The accuracy.... An important problem is not included here: The change of the sensitivity as a function of position on the quartz crystal (See Sect. 2).

p. 53. For the two.... Measurements of the electron-induced sputtering have been performed for hydrogen deuteride, but not for solid hydrogen. Even with an improved crystal holder it was only possible to measure ion-induced sputtering for solid hydrogen. The deposited power becomes too large to exclude beam-induced evaporation with primary electrons (See Sect. 8).

p. 54. The determination.... So far, no bulk value of the yield has been observed. The minimum value of the yield is 4 D_2/electron (See Sect. 8).

The slope... This argument does not hold, since it turned out that the yield from solid neon depends on the film thickness.

The hydrogen isotopes....It is not certain how the crater side influences the spectrum. The thin-film enhancement was not identified during the work for this paper.

This case... Beam-induced evaporation is discussed in Sect. 3.1, Schou et al. (1986) and Schou (1987).

p. 55. The general expressions.... This analysis does not include the varying mass sensitivity of the crystal, and may, therefore, be considered solely as an estimate.

p. 56 Ref. 22.... Schou et al. (1986)

Ref. 23.... Børgesen et al. (unpubl.)

Ref. 24.... Ellegard et al. (1986b).

NOTES TO PAPER 3

Schou et al. (1986)

In this paper, improved results for sputtering of solid neon by electrons are shown. A pronounced thickness dependence of the yield is shown. The first determination of the diffusion length of the excitations that lead to sputtering is presented.

p. 94. In many respects.... The determination of a diffusion length from optical methods is complicated and relies on a number of assumptions (See Sect. 5).

p. 97. For these measurements.... A new construction of the crystal holder on thin springs has made it possible to observe the thin-film enhancement of the yield during erosion of films with an initial thickness that exceeds that for which the enhancement occurs.

The yield of a.... The thickness of a $4.5 \cdot 10^{17}$Ne/cm^2-film corresponds to the mean projected range of 2.8 keV electrons in neon (Valkelahti et al. (1989)). The indicated range for 1.7-keV electrons is larger than that evaluated on the basis of the data from Valkealahti et al. (1989).

In these measurements.... So far, it has not been possible to reproduce these results with the frequency-change method.

p. 98. A strong dependence.... See Sect. 3.1 and Schou (1987).

A dependence.... The yield dependence on film thickness is discussed comprehensively by Schou (1987).

The magnitude.... The yield of 8 D_2/electron does not correspond to the minimum of the yield, which is 4 D_2/electron (See Sect. 8).

p. 102. Let us now estimate....The transitions from the vibrationally relaxed state have not been observed. The transitions liberate much less than the 3.7 eV suggested (Comp. Sect. 5).

Recently, Coletti et al..... Metastable atoms from this mechanism have been observed by Kloiber and Zimmerer (1990).

p. 103. Sputtering yields.... The types of excitation produced in neon by keV ions is different from those produced by keV electrons, and no clear thickness dependence was observed for ion bombardment (See Sect. 5) .

Let us now consider.... Actually Reimann et al. (1984b) includes the ground state repulsion as well.

The holes recombine.... These considerations are somewhat misleading, since Reimann et al. (1984b) and (1988) consider atomic holes.

p. 104. For solid neon.... Some results from Debever and Coletti were included by Huormatallah et al. (1988) and Kloiber and Zimmerer (1989).

The strong enhancement.... The thin-film enhancement has been observed also for the solid hydrogens (Sect. 4).

Ordinary sputtering.... A similar treatment that includes mobile excitations is presented by Ellegaard et al. (1988) The total energy release for argon is about 2.3 eV (Sect. 6).

p. 106. Ref. 35 ....Øhlenschlaeger et al. (1986).

Ref. 36.....Børgesen et al. (unpubl).

NOTES TO PAPER 4

Ellegaard et al. (1986b)

This paper shows the first example of a linear yield dependence on the electronic stopping power for light ions of energies on the low-energy side of the stopping power peak. The paper demonstrates that the thin-film enhancement for light ions is similar to that for electrons.

p. 567. In a forthcoming publication.... These comparisons were never published. Some of the results are described in Ellegaard (1986). Paper 12 contains results for solid neon bombarded by He-ions.

p. 568. As was the case.... These phenomena were not fully explored.

Thickness dependence (Fig. 2).... The present results do not show a clear increase of the yield with thickness as in the case of primary electrons. A reason for this might be that the primary ions below 10 keV produce almost exclusively excitations below the ionization threshold, whereas primary keV-electrons produce a substantial number of ionizations. The diffusion properties of the excitations above or below the ionization threshold may be fairly different.

p. 569. Nuclear collisions contribute.... This problem is discussed in paper 12. The contribution from nonoverlapping elastic subspikes is about 20 Ne/H in the entire energy range considered here. (See Sect. 5)

p. 570. For the two solid rare gases....The mobile excitation is either an atomic hole, which diffuses by electron exchange, or a highly excited free exciton. (See Sect. 5)

Model calculations.... Much less energy than 3.7 eV is liberated per ground state repulsion. (See Sect. 5)

p. 571. Ref. 7..... Schou et al. (1986).

Ref. 17.....Ellegaard et al. (1986a).

NOTES TO PAPER 5

Ellegaard et al. (1986a)

This paper showed the first example of an almost linear relation between the yield and the electronic stopping power.

p. 474. A variety of.... The list is no longer complete. See the text.

p. 475. When the density....Some considerations about the interaction between excited particles were presented by Brown et al. (1986). (See also Sect. 3.3)

The irradiation.... This list of works is extended in Sect. 7. The range of keV-ions in solid nitrogen and oxygen is commented by Børgesen (1985).

p. 483. The majority.... This survey is no longer up to date. See the text.

The yield dependence.... The decreasing yield for increasing film thickness for the solid hydrogen isotopes is caused by the thin-film enhancement, Sect. 4.

The experimental results.... The measurements and their interpretation are discussed in Sects. 3.3 and 6.

p. 484. The data of Brown....The behaviour of the electron-induced yield from carbon monoxide is recently confirmed by Chrisey et al. (1990).

We can.... The ion-explosion model was introduced primarily to explain that the yield was proportional to the electronic stopping power squared. This model is used no longer by Brown and coauthors for frozen gases.

p. 485. Another model.... This model was used for these two specific cases alone and is only occasionally quoted.

The applicability.... See Sect. 3.3.

Let us shortly.... See Sect. 3.2.

p. 486. The data for the energy.... The list of spectra is extended in Sects. 3, 6 and 7.

When the atomic motion....Eq. (3) is written in Schou (1987) for atoms, which means that 1/4 is replaced by 1/2. The material constant Λ is identical for atomic and molecular particles, as long as the surface barrier for atoms is assumed to be $U_0/2$.

p. 487. According to Rook.... The energy release is more complex than indicated here. See Pedrys et al. (1989) and Sect. 7.

p. 488. Table 2.... The atomic electronic cross section is used.

The cascade model....Strictly speaking, a thickness dependence may occur in cases, for which $D_e(0)$ changes significantly over distances that are comparable to the range of repulsing (deexciting) target particles. Usually, the range of these eV (or sub-eV) particles is small. (See p. 490).

p. 490. We have considered.... U_0 is missing in the formula for Λ.

p. 491. Ref. 15.... Brown et al. (1986).

Ref. 29.... Øhlenschlaeger et al. (1985).

Ref. 38.... Schou et al. (1986).

NOTES TO PAPER 6

Schou et al. (1987)

The paper demonstrates that the characteristic diffusion length of the mobile excitations that lead to sputtering from solid argon during keV-ion bombardment is similar to the length determined from light MeV-ions. The first estimate of the diffusion length for the mobile excitations induced by particle bombardment of solid krypton is indicated.

p. 609. In particular.... The results for MeV-ion bombardment of solid argon have been summarized in Reimann et al. (1988).

p. 611. The thickness dependence of the yield.... This is described in Zimmerer (1987) as well. The probable value of the liberated energy E_s is discussed in Sect. 6.

The precise type.... See the discussion in Sect. 6.

The contribution.... In this estimate the partial yield from backscattered hydrogen ions was assumed to be proportional to the electronic stopping power of the backscattered primaries, and the angular distribution was assumed to be a cosine-function.

The present value.... Reimann et al. (1988) consider 230 Å as their best value.

p. 612. Ref. 4.... Ellegaard et al. (1988).

Ref. 17.... Ellegaard et al. (unpubl.).

NOTES TO PAPER 7

Schou (1987)

p. 188. The solidified gases.... The sublimation energy for solid hydrogen is 8.65 meV, for solid tritium 14.8 meV (Souers (1986)).

Fig. 1..... One may incorporate the solid hydrogens in the homonuclear diatomic gases in view of the many common features. (See Sect. 8).

p. 189. Most....Films thinner than 50 Å have been irradiated as well.

The overwhelming.... Since 1987 the emission of excited neutrals have been studied in many cases (See Sects. 5 and 6).

Up to now.... Recent results have been incorporated in the text.

The energy distribution.....Recent results have been incorporated in the text.

Table 1.....The data from Salt Lake City have been improved by Balaji et al. (1990) (See Table 2).

p. 190. Particle-induced....Recent results have been incorporated in the text.

p. 192. Let us now.... The E_i^{-2}-behaviour is not observed in cases for which a strong transition is dominant, e.g. for solid krypton and xenon (Pedrys et al. (1988) and O'Shaughnessy et al. (1988)).

p. 193. Many of the results.... (See Sect. 3.2).

The class of..... In the meantime an interesting study on the room-temperature insulator sulphur has been performed by Chrisey et al. (1988).

For both.... The relaxation process described for nitrogen is simplified.

p. 194. It is regrettable....The spectra are reported in Pedrys et al. (1989).

Although most.... The ground state repulsion releases about 1.1 eV, the dissociative recombination 1.2 eV. Fig. 8 does not give the right numbers.

p. 195. Fig. 9.... The authors from AT+T recommend now a characteristic diffusion length of 230 Å (Reimann et al. (1988)).

p. 196. The similar increase.... The type of the mobile excitation(s) is not yet identified (See Sects. 5 and 6).

p. 197. The magnitude of the yield....Measurements of the energy distribution by Pedrys et al. (1988) and O'Shaughnessy et al. (1988) have confirmed that the energy release in xenon is approximately half of that in solid argon.

However,....Hourmatallah et al. (1988) found a large absorption rate at the surface for solid neon as well.

The knowledge....A number of recent experiments close to the threshold have been included in the text (Sects. 5 and 6).

Another important point.... A small peak for solid argon has been observed by O'Shaughnessy et al. (1988).

p. 198. The latter considerations....Reimann et al. (1991) demonstrate that the W-band mainly originates from ejected excited argon molecules that decay outside the surface of the solid argon.

Finally,.... Recent experiments close to the threshold are included in the text.

p. 199. Ref. 42.... Schou et al. (unpubl.).

Ref. 61.... Boring et al. (1987).

Ref. 63.... Pedrys et al. (1988) and Ellegaard et al. (unpubl.).

Ref. 64.... Schou et al. (1987).

Ref. 67.... Ellegaard et al. (1988).

p. 200. Ref. 75.... Urbassek and Michl (1987).

Ref. 90.... Børgesen et al. (unpubl.).

Ref. 92.... Reimann et al. (1988).

Ref. 94.... Will not be published.

NOTES TO PAPER 8

Ellegaard et al. (1988)

This paper contains the first systematical results for electron-induced sputtering of solid argon.

p. 305. Sputtering measurements.... Recent results are included in the text (Sects. 5-6).

The primary particles....Recent results for the composition and energy distribution are included in the text.

There are many reasons....Ref. 17 should be replaced by 18 and ref. 18 by 19.

p. 306. The release of energy....This is discussed in detail in Sect. 6.

Fig. 2....In Schou et al. (1984) it was demonstrated that the beamspot covered 25 per cent rather than 11 per cent of the electrode area. This has been incorporated in the figure.

p. 307. Fig. 3....The fact that the experimental points lie somewhat above the calculated curves may indicate that the "excess yield" is caused by electrons backscattered from the silver substrate. The reflection coefficient is slightly larger for silver than for solid argon.

p. 308. Finally....This reduction of the yield because of impurities was utilized by Schou et al. (1988).

The important quantity.... $E_s = 2.3$ eV according to the text (Sect. 6).

We have applied.....One notes that the agreement between the curve for 200 Å and the experimental points becomes better, if the surface binding energy is increased or the source energy E_s reduced.

An alternative....Reimann et al. (1988) indicate that E_s is about 2 eV.

The value....Reimann et al. (1988) recommend a diffusion length of 230 Å.

p. 311. Ref. 7. Schou et al. (1988).

NOTES TO PAPER 9

Schou et al. (1988)

This paper gives a direct example of simultaneous contributions from knockon and electronic sputtering of solid argon.

p. 809. The results agree....These spikes are discussed in Sect. 3.2

At energies....An important example is electronic sputtering of sulphur demonstrated by Chrisey et al. (1988).

The luminescence....A comprehensive report is given in Reimann et al. (1988).

The energy releasing process.... The peak in the energy distribution is observed by O'Shaughnessy et al. (1988) as well.

Reimann et al.....The energy release as well as the importance of the threshold are discussed in the text (Sect. 6).

p. 810. There are obvious....This paragraph is discussed in Sect. 3.4.

No systematic.... Error! "above" should be replaced by "below".

p. 811. The thickness dependence....Actually, Ref. 11 gives a value of 190 Å for the characteristic diffusion length. 210 Å is a representative value for several groups (Schou (1987)). The thin-film enhancement is described in Sect. 4.

p. 812. This interpretation....The influence of impurities is discussed as well by Reimann et al. (1988).

The knockon yields....The yields from nonoverlapping subspikes are a factor of two larger than those from linear collision-cascades according to the calculations by Ellegaard et al. (1990) and (1991). This contribution explains partly, why the knockon yield is so large.

The energy dependence....The magnitude of the energy release from the deexcitation process in solid neon is not yet completely clarified (Sect. 5).

Fig. 5....The energy dependence of the yield as well as the stopping power for protons incident on solid argon is shown in Fig. 8 in Sect. 6.

p. 813. Fig. 6....The efficiencies on p. 812 were determined from the stopping powers by Lindhard and coauthors. Once the efficiency is fixed at the value for 7 keV, the energy dependence is determined from the assumption that the stopping power is proportional to the energy.

p. 812. The high yield.... The stopping power for protons in argon from Andersen and Ziegler (1977) is almost twice as large as that from Lindhard and coauthors. For protons in neon the stopping power from Andersen and Ziegler (1977) is about a factor of 1.5 smaller than that from Lindhard and coauthors.

p. 813. The present experimental....The recent results from the same group (35 $Ar/^4He^+$) reported in Balaji et al. show very good agreement with the present results.

p. 814. Ref.4....Kloiber et al. (1988).

Ref.9....Ellegaard et al. (1988).

NOTES TO PAPER 10

Stenum et al. (1989)

The paper contains the first luminescence study of features from a solid hydrogen isotope in the visible and near UV range. The observations have not provided us with strong guidelines for the deexcitation channels in the solid hydrogens, but have shown us that the intensity of the luminescence in the observed range is weak compared with other frozen elemental gases except solid oxygen.

p. 235. Erosion....Brooks (1986) investigated solid deuterium and hydrogen. He observed only features in the luminescence spectrum induced by oxygen and nitrogen impurities.

The intention....A relatively strong peak from solid deuterium around 800 nm was reported by Stenum (1991) and Schou et al. (1991).

The experimental setup....In Schou et al. (1991) and Stenum et al. (1991c) the setup was modified. The photomultiplier Valvo XP2020Q was replaced by a water-cooled Hamamatsu R943-02 that extended the sensitivity range up to 800-900 nm. The setup is shown in Sect. 2 and in Schou et al. (1991).

p. 237. A luminescence....The peak around 450 nm is assigned to impurities on the substrate surface for the moment. The peak at 275 nm is definitely assigned to an intrinsic feature in solid deuterium and has been observed by Gürtler (unpubl.) as well recently. There is no complete evidence for the assignment to the D_3^*-line yet.

In fig. 1.c....This peak around 360 nm is probably the ND-transition and has been observed also by others (Dressler (unpubl.)).

In fig.2....This minimum in the yield is shown in Fig. 12 in Sect. 8.

The erosion yield....Recently, this effect on the yield from impurities has been observed also for xenon-impurities in solid deuterium (Stenum et al. (unpubl.)). The explanation based on the reduced heat capacity is not yet established.

NOTES TO PAPER 11

Stenum et al. (1990)

The paper demonstrates that it is possible to determine a "bulk" yield for solid deuterium bombarded by hydrogen ions in contrast to the yield for electron bombardment. Furthermore, it is shown that the range of the thin-film enhancement depends markedly on the ion energy.

p. 530. The major difficulty....An improved value of the sublimation energy, 8.65 meV/molecule for solid hydrogen is given in Table 3.

The analysis....Measurements of the energy dependence of the sputtering yield demonstrate that the sputtering is dominantly electronic (Stenum et al. (1991a), (1991b) and (unpubl.)). (See Sect. 8).

The present work....The measurements by Børgesen (1982) and Børgesen et al. (1980) were performed without a beam sweep arrangement, and the yield exceeded the present one by a factor of two.

Actually, the yield obtained by Erents and McCracken agrees quite well with the present yield for 2.3 keV/H (7 keV H_3^+-ions).

p. 532. The yield for thick films....The analysis is performed in Sect. 8.

The strong enhancement....See Sect. 4.

p. 533. Ref. 17....Børgesen et al. (unpubl.).

NOTES TO PAPER 12

Ellegaard et al. (1990)

This paper gives the first systematic presentation of sputtering results that are explained on the basis of a subspike mechanism.

p. 459. In the present work....Garrison and Johnson (1984) introduced a model for a mini-thermal spike, which essentially is identical to the subspike presented here. However, the authors did not derive their expressions, but the dependence on the surface binding energy U_0 is similar to that in Eq. (7).

p. 460. The present model....Strictly speaking, no fitting parameters were applied, but a number of parameters were taken from the literature. (See p. 463. The effect of heat loss...)

Fig. 2....Balaji et al. (1990) have published results for $^4He^+$-ions incident on neon as well. Their values are considerably larger than ours, but the primary energy was from 0.5 to 5 keV. In addition to the low energy, the procedure for the film deposition was somewhat different.

p. 462. Combining....The corresponding expressions for h_1 and h for the Kr-C potential are given in Ellegaard et al. (1991).

p. 464. Ref.10....Pedrys (1990)

Ref.21....Ellegaard et al. (1991).

References

Ch. Ackermann, R. Brodmann, U. Hahn, A. Suzuki and *G. Zimmerer* (1976) Phys. Stat. Sol. b 74, 579-590.

H.H. Andersen and *H. Bay* (1972) Rad. Effects 13, 67-74.

H.H. Andersen and *J.F. Ziegler* (1977) "Hydrogen stopping powers and ranges in all elements" (Pergamon) pp. 1-317.

I. Arakawa, M. Takahashi and *K. Takeuchi* (1989) J. Vac. Science Techn. A 7, 2090-2093.

I. Arakawa and *M. Sakurai* (1990) in: "Desorption by electronic transitions, DIET IV", eds. G. Betz and P. Varga (Springer) pp. 246-250.

V. Balaji, D.E. David, T.F. Magnera, J. Michl and *H.M Urbassek* (1990) Nucl. Instr. Meth. B 46, 435-440.

A. Bar-nun, G. Herman, M.L. Rappaport and *Yu. Mekler* (1985) Surface Science 150, 143-156.

J. Benit, J.-P. Bibring, S. Della-Negra, Y. le Beyec, M. Mendenhall, F. Record and K. Standing (1987) Nucl. Instr. Meth. B 19-20, 838-842.

C. Benvenuti, R. Calder and *O. Gröbner* (1987) Vacuum 37, 699-707, Erratum Vacuum 38, 145.

F. Besenbacher, J. Bøttiger, O. Graversen, J.L. Hansen and *H. Sørensen* (1981) Nucl. Instr. Meth. 188, 657-667.

J.W. Boring, R.E. Johnson, C.T. Reimann, J.W. Garret, W.L. Brown and *K.J. Marcantonio* (1983) Nucl. Instr. Meth. 218, 707-711.

J.W. Boring, D.J. O'Shaughnessy and *J.A. Phipps* (1987) Nucl. Instr. Meth. B .18, 613-617.

R.L. Brooks, M.A. Selen, J.L. Hunt, J.R. MacDonald, J.D. Poll and *J.C. Waddington* (1983) Phys. Rev. Lett. 51, 1077-1079.

R.L. Brooks, S.K. Bose, J.L. Hunt, J.R. MacDonald, J.D. Poll and *J.C. Waddington* (1985a) Phys. Rev. B 32, 2478-2488.

R.L. Brooks, J.L. Hunt, J.R. MacDonald, J.D. Poll and *J.C. Waddington* (1985b) Can. J. Phys. 63, 937-940.

R.L. Brooks (1986) J. Chem. Phys. 85, 1247-1251.

W.L. Brown, W.M. Augustyniak, L.J. Lanzerotti, R.E. Johnson and *R. Evatt* (1980) Phys. Rev. Lett. 45, 1632-1635.

W.L. Brown, C.T. Reimann and *R.E. Johnson* (1985) in: "Desorption by electronic transitions, DIET II", eds. W. Brenig and D. Menzel (Springer).

W.L. Brown and *R.E. Johnson* (1986) Nucl. Instr. Meth. B 13, 295-303.

W.L. Brown, L.J. Lanzerotti, K.J. Marcantonio, R.E. Johnson and *C.T. Reimann* (1986) Nucl. Instr. Meth. B 14, 392-402.

P. Børgesen, J. Schou and *H. Sørensen* (1980) in: "Proceedings of the symposium on sputtering, Perchtoldsdorf", eds. P. Varga, G. Betz and F.P. Viehböck (Techn. Univ., Wien, Austria) pp. 822-831.

P. Børgesen (1982) Ph.D.-Thesis, Risø-R-457, Risø National Laboratory, pp. 1-161.

P. Børgesen and *H. Sørensen* (1982) Phys. Lett. 90 A, 319-322.

P. Børgesen, J. Schou, H. Sørensen and *C. Claussen* (1982) Appl. Phys. A 29, 57-61.

P. Børgesen (1985) Nucl. Instr. Meth. B 12, 73-79.

P. Børgesen, J. Schou, O. Ellegaard and *H. Sørensen* (unpubl.) "The erosion of solid hydrogenic targets by keV electrons", in preparation.

C.T. Chang, L.W. Jørgensen, P. Nielsen and *L.L. Lengyel* (1980), Nucl. Fusion 20, 859-893.

C.T. Chang (1991) Phys. Rep. 206, 143-196.

D.B. Chrisey, J.W. Boring, J.A. Phipps, R.E. Johnson and *W.L. Brown* (1986) Nucl. Instr. Meth. B 13, 360-364.
D.B. Chrisey, J.W. Boring, R.E. Johnson and *J.A. Phipps* (1988) Surface Science 195, 594-618.
D.B. Chrisey, W.L. Brown and *J.W. Boring* (1990) Surface Science 225, 130-142.
J.W. Christiansen, D. Delli Carpini and *I.S.T. Tsong* (1986) Nucl. Instr. Meth. B 15, 218-221.
C. Claussen (1982a) Nucl. Instr. Meth. 194, 567-571.
C. Claussen (1982b) Ph.D.-Thesis, Odense University.
J.W. Coburn (1989) in: "Plasma diagnostics", Vol. 2, eds. O. Auciello and D.L. Flamm (Academic), pp. 1-18.
J.S. Cohen and *B. Schneider* (1974) J. Phys. Chem. 61, 3230-3239.
F. Coletti and *A.M. Bonnot* (1977) Chem. Phys. Lett. 45, 580-582.
F. Coletti and *J.M. Debever* (1983) Solid St. Comm. 47, 47-50.
F. Coletti, J.M. Debever and *G. Zimmerer* (1984) J. Physique Lett. 45, L 467-473.
F. Coletti, J.M. Debever and *G. Zimmerer* (1985) J. Chem. Phys. 83, 49-57.
F. Coletti, J.M. Debever and *A. Heurmatallah* (1987) Phys. Scr. 35, 168-170.
S. Cui, R.E. Johnson and *P.T. Cummings* (1988) Surface Science 207, 186-206.
S. Cui, P.T. Cummings and *R.E. Johnson* (1989a) Surface Science 222, 491-498.
S. Cui, R.E. Johnson and *P.T. Cummings* (1989b) Phys. Rev. B 39, 9580-9583.
D.E. David, T.F. Magnera, R. Tran, D. Stulik and *J. Michl* (1986) Nucl. Instr. Meth. B 14, 378-391.
D.E. David and *J. Michl* (1989) Prog. Solid St. Chem. 19, 283-328.
K. Dressler (1971) Mem. Soc. R. Sci. Liege 20, 357-374.
K. Dressler, O. Oehler and *D.A. Smith* (1975) Phys. Rev. Lett. 34, 1364-1367.
K. Dressler (unpubl.) Private communication.
G. Dujardin, L. Hellner, M.J. Besnard Ramage and *R. Azria* (1990) Phys. Rev. Lett. 64, 1289-1292.
E.P. EerNisse (1971) J. Appl. Phys. 42, 480-482.
O. Ellegaard (1986) Ph.D.-Thesis, Risø-M-2617, Risø National Laboratory, pp. 1-175.
O. Ellegaard, J. Schou, H. Sørensen and *P. Børgesen* (1986a) Surface Science 167, 474-492.
O. Ellegaard, J. Schou and *H. Sørensen* (1986b) Nucl. Instr. Meth. B 13, 567-571.
O. Ellegaard, R. Pedrys, J. Schou, H. Sørensen and *P. Børgesen* (1988) Appl. Phys. A 46, 305-312.
O. Ellegaard, J. Schou and *H. Sørensen* (1990) Europhys. Lett. 12, 459-464.
O. Ellegaard, J. Schou, B. Stenum, H. Sørensen and *R. Pedrys* (1991) "Sputtering yields and energy distributions from nonoverlapping subspikes in ion-bombarded volatile solids", to be published.
O. Ellegaard, J. Schou, B. Stenum, H. Sørensen, R. Pedrys, D.J. Oostra, A. Haring and *A.E. de Vries* (unpubl.) "Sputtering of solid nitrogen and oxygen by keV ions" to be published.
C.S. Enos, A.R. Lee and *A.G. Brenton* (1991) Int. J. Mass Spectr. Ion Proc. 104, 137-144.
S.K. Erents and *G.M. McCracken* (1973) J. Appl. Phys 44, 3139-3145.
S.K. Erents and *G.M. McCracken* (1975), in: "Atomic collisions in solids", eds. S. Datz, B.R. Appleton and C.D. Moak (Plenum, New York), pp. 625-634.
H. H. Farrell, M. Strongin and *J.M. Dickey* (1972) Phys. Rev. B 6 4703-4710.
P. Feulner, T. Müller, A. Puschmann and *D. Menzel* (1987) Phys. Rev. Lett. 59, 791-794.
I.Ya. Fugol' (1978) Adv. Phys. 27, 1-87.
I.Ya. Fugol' (1988) Adv. Phys. 37, 1-35.
I.Ya. Fugol', A.G. Belov and *V.N. Svishchev* (1988) Solid St. Comm. 66, 503-507.

B.J. Garrison and *R.E. Johnson* (1984) Surface Science **148**, 388-400.
K.M. Gibbs, W.L. Brown and *R.E. Johnson* (1988) Phys. Rev. **B 38**, 11001-11007.
P. Gürtler (unpubl.) Private communication.
J.E. Griffith, R.A. Weller, L.E. Seiberling and *T.A. Tombrello* (1980) Rad. Effects **51**, 223-232.
M.G. Heaps and *A.E.S. Green* (1975) J. Appl. Phys. **46**, 4718-4725.
L. Hellner, M.J. Besnard-Ramage, G. Dujardin and *R. Azria* (1990) in: " Desorption induced by electroninc transitions, DIET IV ", eds. G. Betz and P. Varga (Springer) pp. 240-245.
S.P. Hernandez, P.J. Dagdigian and *J.P. Doering* (1982) J. Chem. Phys. **77**, 6021-6026.
A. Hourmatallah, F. Coletti and *J.M. Debever* (1988) J. Phys. **C. 21**, 1307-1320.
ICRU (1979) Rep. 31, " Average energy required to produce an ion pair", (International Commission on Radiation Units and Measurements, 7910 Woodmont Avenue, Washington, D. C. 20014, U.S.A), pp. 1-49.
N. Itoh (1987) Nucl. Instr. Meth. **B 27**, 155-166.
R.E. Johnson and *W.L. Brown* (1982) Nucl. Instr. Meth. **198**, 103-118.
R.E. Johnson and *W.L. Brown* (1983) Nucl. Instr. Meth. **209-210**, 469-476.
R.E. Johnson and *M. Inokuti* (1983) Nucl. Instr. Meth. **206**, 289-297.
R.E. Johnson (1990) "Energetic charged-particle interactions with atmospheres and surfaces" (Springer) pp. 1-232.
J.K. Kjems and *G. Dolling* (1975) Phys. Rev. B **11**, 1639-1647.
T. Kloiber, W. Laasch, G. Zimmerer, F. Coletti and *J.M. Debever* (1988) Europh. Lett. **7**, 77-82.
T. Kloiber and *G. Zimmerer* (1989) Rad. Eff. Def. Solids **109**, 219-227.
T. Kloiber and *G. Zimmerer* (1990) Phys. Scr. **41**, 962-965.
K. Kobashi, M.L. Klein and *V. Chandrasekharan* (1979) J. Chem. Phys. **71**, 843-849.
W. Laasch, H. Hagedorn, T. Kloiber and *G. Zimmerer* (1990) Phys. Sta. Sol. b **158**, 753-767.
A. Landau, E. J. Allin and *H.L. Welsh* (1962) Spectr. Acta **18**, 1-19.
G. Leclerc, A.D. Bass, M. Michaud and *L. Sanche* (1990) J. Elec. Spec. Rel Phen. **52**, 725-734.
P.G. Le Comber, J.B. Wilson and *R.J. Loveland* (1976) Solid St. Comm. **18**, 377-380.
L.L. Levenson (1967) Nuovo Cimento, Suppl. Ser. I, **5**, 321-328.
C. Lu (1984), in: "Applications of piezoelectric quartz crystal microbalances", eds. C. Lu and A.W. Czanderna (Elsevier), pp. 19-61.
D. McKeown (1961) Rev. Sci. Instr. **32**, 133-136.
D. Menzel (1990) Appl. Phys. **A 51**, 163-171.
W.T. Miles, R. Thompson and *A.E.S. Green* (1972) J. Appl. Phys. **43**, 678-686.
J.J. Miller, R.L. Brooks, J.L. Hunt and *J.D. Poll* (1988) Can. J. Phys. **66**, 1025-1030.
S.L. Milora (1981) J. Fus. Energy **1**, 15-48.
O. Oehler, D.A. Smith and *K. Dressler* (1977) J. Chem. Phys. **66**, 2097-2107.
R.W. Ollerhead, J. Bøttiger, J.A. Davies, J. L'Ecuyer, H.K. Haugen and *N. Matsunami* (1980) Rad. Eff. **49**, 203-212.
D.J. O'Shaughnessy, J.W. Boring, S. Cui and *R.E. Johnson* (1988) Phys. Rev. Lett. **61**, 1635-1638.
H. Overeijnder, M. Szymonski, A Haring and *A.E. de Vries* (1978) Rad. Eff. **36**, 63-71.
J.T. Park (1978) in: "Collision spectroscopy", ed R.G. Cooks (Plenum) pp. 19-90.
R. Pedrys, R.A. Haring, A. Haring and *A.E. de Vries* (1984) Nucl. Instr. Meth. **B 2**, 573-577.

R. Pedrys, D.J. Oostra and *A.E. de Vries* (1985) in: "Desorption induced by electronic transitions, DIET II", eds. W. Brenig and D. Menzel (Springer) pp. 190-198.

R. Pedrys, D.J. Oostra, R.A. Haring, L. Calcagno, A. Haring and *A.E de Vries* (1986) Nucl. Instr. Meth. **B 17**, 15-21.

R. Pedrys, D.J. Oostra, A. Haring, A.E. de Vries and *J. Schou* (1988) Nucl. Instr. Meth. **B 33**, 840-843.

R. Pedrys, D.J. Oostra, A. Haring, A.E. de Vries and *J. Schou* (1989) Rad. Eff. Def. Solids **109**, 239-244.

R. Pedrys (1990) Nucl. Instr. Meth. **B 48**, 525-529.

R. Pedrys, D.J. Oostra, A. Haring, A.E. de Vries and *J. Schou* (unpubl.) "Energy distributions from electron sputtered solid oxygen and nitrogen", to be published.

Yu.B. Poltoratskii and *I.Ya Fugol'* (1979) Sov. J. Low Temp. **5**, 439-444.

D. Pudewill, F.-J. Himpsel, V. Saile, N. Schwentner, M. Skibowski, E.E. Koch and *J. Jortner* (1976) J. Phys. Chem. **65**, 5226-5238.

C.T. Reimann, J.W. Boring, R.E. Johnson, J.W. Garret, K.R. Farmer, W.L. Brown, K.J. Marcantonio and *W.M. Augustyniak* (1984a) Surface Science **147**, 227-240.

C.T. Reimann, R.E. Johnson and *W.L. Brown* (1984b) Phys. Rev. Lett. **53**, 600-603.

C.T. Reimann, W.L. Brown and *R.E. Johnson* (1988) Phys. Rev. **B 37**, 1455-1473.

C.T. Reimann, W.L. Brown, M.J. Nowakowski, S.-T. Cui and *R.E. Johnson* (1990) in: "Desorption induced by electronic transitions, DIET IV", eds. G. Betz and P. Varga (Springer) pp. 226-234.

C.T. Reimann, W.L. Brown, D.E. Grosjean, M.J. Nowakowski, W.T. Buller, S.-T. Cui and *R.E. Johnson* (1991) Nucl. Instr. Meth. **B 58**, 404-410.

G. Rocker, P. Feulner, R. Scheuerer, L. Zhu and *D. Menzel* (1990) Phys. Scr. **41**, 1014-1021.

F.L. Rook, R.E. Johnson and *W.L. Brown* (1985) Surface Science **164**, 625-639.

M.E. Rudd, Y.-K. Kim, D.H. Madison and *J.W. Gallagher* (1985) Rev. Mod. Phys. **57**, 965-994.

R.J. Sayer, R.J. Prince and *W.W. Duley* (1979) Proc. R. Soc. Lond. **A 365**, 235-251.

O. Schnepp and *K. Dressler* (1965) J. Chem. Phys. **42**, 2482-2489.

J. Schou and *H. Sørensen* (1978) J. Appl. Phys. **49**, 816-821.

J. Schou (1980) Phys. Rev. **B 22**, 2241-2174.

J. Schou, H. Sørensen and *P. Børgesen* (1984) Nucl. Instr. Meth. **B 5**, 44-57.

J. Schou, P. Børgesen, O. Ellegaard, H. Sørensen and *C. Claussen* (1986) Phys. Rev. **B 34**, 93-106.

J. Schou (1987) Nucl. Instr. Meth. **B 27**, 188-200.

J. Schou, R. Pedrys, O. Ellegaard and *H. Sørensen* (1987) Nucl. Instr. Meth. **B 18**, 609-612.

J. Schou (1988) Scan. Microsc. **2**, 607-63?.

J. Schou, O. Ellegaard, H. Sørensen and *R. Pedrys* (1988) Nucl. Instr. Meth. **B 33**, 808-814.

J. Schou (1989) in: "Structure-property relationships in surface-modified modified ceramics", eds. C.J. McHargue, R. Kossowsky and W.O. Hofer (Kluwer Academics) pp. 61-10.

J. Schou, B. Stenum, H. Sørensen, and *P. Gürtler* (1989) Phys. Rev. Lett. **63**, 969-971.

J. Schou, B. Stenum, H. Sørensen, K.-V. Weisberg and *P. Gürtler* (1991) Nucl. Fus. **31**, 589-591.

J. Schou, O. Ellegaard, R. Pedrys and *H. Sørensen* (unpubl.) "Sputtering of solid neon and argon by medium mass ions". Nucl. Instr. Meth. B (in press).
P. Sigmund (1969) Phys. Rev. **184**, 383-416.
P. Sigmund (1981) in: "Sputtering by particle bombardment, I" ed. R. Behrisch (Springer) pp. 9-71.
P. Sigmund and *C. Claussen* (1981) J. Appl. Phys. **52**, 990-993.
P. Sigmund and *M. Szymonski* (1984) Appl. Phys. **A 33**, 141-152.
P. Sigmund (1987) Nucl. Instr. Meth **B 27**, 1-20.
I.F. Silvera (1980) Rev. Mod. Phys. **52**, 393-452.
P.C. Souers (1986) "Hydrogen properties for fusion energy" (University of California Press, Berkeley) pp. 1-391.
E. Steinacker and *P. Feulner* (1989) Phys. Rev. **B 40**, 11348-11351.
P. Stenum, J. Schou, H. Sørensen and *P. Gürtler* (1989) Rad. Eff. Def. Solids **109**, 235-238.
B. Stenum, O. Ellegaard, J. Schou and *H. Sørensen* (1990) Nucl. Instr. Meth. **B 48**, 530-533.
B. Stenum (1991) Ph.D.-Thesis, "Studies on luminescence and sputtering from particle-bombarded solid hydrogens".
B. Stenum, O. Ellegaard, J. Schou, H. Sørensen and *R. Pedrys* (1991a) Nucl. Instr. Meth. **B 58**, 399-403.
B. Stenum, J. Schou, O. Ellegaard, H. Sørensen and *R. Pedrys* (1991b) Phys. Rev. Lett. **67**, 2842-2845.
B. Stenum, J. Schou, H. Sørensen and *P. Gürtler* (1991c) "UV and visible luminescence from pure and impurity-doped solid deuterium irradiated by keV electrons", to be published.
B. Stenum, J. Schou, O. Ellegaard, R. Pedrys and *H. Sørensen* (unpubl.) "Sputtering of the solid hydrogens by light ions", in preparation.
D.V. Stevanovic, D.A. Thompson and *J.A. Davies* (1984) Nucl. Instr. Meth. **B 1**, 315-320.
R.S.Stolarski, V.A. Dulock, Jr., C.E. Watson and *A.E.S. Green* (1967) J. Geoph. Res. **72**, 3953-3960.
M. Szymonski (1980) in: "Proceedings of the symposium on sputtering, Perchtoldsdorf", eds. *P. Varga, G. Betz and F.P. Viehböck* (Techn. Univ., Wien, Austria) pp. 761-772.
M. Szymonski and *Poradzisz* (1982) Appl. Phys. **A 28**, 175-178.
M. Szymonski, P. Czuba, T. Dohnalik, L. Jozefowski, A. Karawajczyk, J. Kolodziej, R. Lesniak and *Z. Postawa* (1990) Nucl. Instr. Meth. **B 48**, 534-537.
H. Sørensen (1976) Appl. Phys. **9**, 321-329.
P.C. Townsend (1983) in: "Sputtering by particle bombardment, II", ed. R. Behrisch (Springer) pp. 147-176.
H.M. Urbassek and *J. Michl* (1987) Nucl. Instr. Meth. **B 22**, 480-490.
S. Valkealahti, J. Schou, H. Sørensen and *R.M. Nieminen* (1988) Nucl. Instr. Meth. **B 34**, 321-331.
S. Valkealahti, J. Schou and *R.M. Nieminen* (1989) J. Appl. Phys. **65**, 2258-2266.
G. Zimmerer (1987), in: "Excited state spectroscopy in solids", ed. M. Manfredi (XCVI Corso, Soc. Italiana di Fisica, Bologna, Italy) and eds. U.M. Grassano and N. Terzi (North-Holland, Amsterdam, The Netherlands) pp. 37-110.
M. Øhlenschlaeger, H.H. Andersen, J. Schou and *H. Sørensen* (1985) Rad. Prot. Dos. **13**, 61-64.

Appl. Phys. A 29. 57–61 (1982)

Applied Physics A Solids and Surfaces

Charged Particle Erosion of Solid Rare Gases and Dilute Rare Gas Alloys

Experiment and Theory

P. Børgesen*, J. Schou, and H. Sørensen

Physics Department, Association Euratom-Risø National Laboratory, DK-4000 Roskilde, Denmark

C. Claussen

Fysisk Institut, Odense Universitet, DK-5230 Odense M, Denmark

Received 8 July 1982/Accepted 26 July 1982

Abstract. We present the first experimental results on electron-induced erosion of solid neon. The measurements are interpreted qualitatively within a new model invoking excitation transport by free excitons and their subsequent decay at the surface. The model accounts for the magnitude of the observed yield and the energy dependence. A theoretically predicted decrease in the erosion yield due to doping with a heavier rare gas, in casu argon, has been observed experimentally. The strong influence of very small amounts of different types of impurities makes sample purity a crucial problem in investigations of the erosion of solid rare gases.

PACS: 79.20.−m, 61.80.−x, 71.35.+z

The erosion of condensed gases by energetic charged particles has been studied intensively during the last years. In part, this is due to the importance of this effect in technological problems such as cryopumping in radiation environments and in astrophysical problems such as the shaping of planetary surfaces. Amongst the gases studied by ion-induced erosion are H_2O [1–3], UF_4 [4–5], the hydrogens [6], and the rare gases: Ar [7], Kr and Xe [8–10]. For solid neon only one data point (1.5 MeV He-ions) exists [10]. Electron-induced erosion has been studied intensively for the hydrogens [11], but little is known for the other gases [1, 8].

Various models have been put forward to explain the erosion of condensed gases, but there is at present no generally accepted mechanism for any of the gases studied. The main problem is how energy is transferred from the electronic system (i.e. from the initial excitations and ionizations and the kinetic energy of secondary electrons) to the atomic motion that is necessary to explain the erosion. One should, however, not expect that one universal mechanism may explain erosion for all condensed gases as the constituents are widely differing in, e.g., the possibility of internal excitations (vibration and rotation). The rare gases are unique in this respect as the atoms are almost unperturbed in the very lightly bound solid state.

We first report on erosion experiments for pure solid neon using 1–3 keV electrons. Measurements like these complement experiments on ion-induced erosion and may serve to illucidate the above mentioned energy transfer mechanism, since essentially all the energy of the electrons is initially deposited in the electronic system. It is found that our data for the erosion of pure neon may be explained quite well within a new model for erosion of rare gas solids. This model invokes excitation transport through the target by excitons

* Present address: Max-Planck-Institut für Plasmaphysik, D-8046 Garching bei München, Fed. Rep. Germany

(essentially bound dimers) that through their decay at the surface may allow one of the constituent atoms to escape from the target.

The model predicts quite significant effects of even very small amounts of impurities in rare gas solids. This provides us with a possibility for testing the validity of the model. The effect has been studied experimentally for electron-induced erosion of a dilute neon-argon alloy.

1. Experiments

The basic experimental set-up [12] as well as the method employed in erosion measurements [11, 13, 14] have been described in detail previously. A more thorough investigation of the application of this method to Ne erosion will be published in the near future [15]. We shall here briefly outline the principles.

A film of solid Ne is produced by letting a jet of cooled gas impinge on a gold plate cooled to ~4.2 K below a liquid helium cryostat. The gas inlet system has been carefully calibrated, and the film thicknesses are known to within 5–10% [13, 14]. In the case of doped gases we have no direct control of the composition of the actually deposited material, but it is estimated that relative dopant concentrations are known within a factor of 2–3.

Beams of 1–3 keV electrons are obtained from a small electron gun, and swept horizontally and vertically by two independent sawtooth voltages over a 2 mm aperture in front of the target, thus ensuring homogenous irradiation of the target area. The substrate is heated by the incident electron beam, but care is taken to keep the temperature well below 6 K, where the erosion is insensitive to substrate temperature.

The target plate is electrically insulated from the cryostat, and during irradiation the target current i_t will generally differ from the true beam current i_b because of emission of secondary and reflected electrons (and possible ions). A negative bias of −50 V applied to a very open grid in front of the target will suppress almost all secondary electron emission, whereas most reflected electrons still have sufficient energy to escape. Comparing the resulting target current i_t to the true beam current i_b measured in a Faraday cup we may then define an "electron reflection coefficient" η by

$$i_t = (1-\eta)\cdot i_b. \tag{1}$$

A possible ion emission [15] will not disturb our exploitation of the relation between η and film thicknesses. For normal incidence of keV electrons on pure gold the reflection coefficient η is of the order of 40%, whereas it is less than 20% for bulk Ne. For film thicknesses less than half the electron range, η decreases almost linearly with thickness, from the value for pure gold down to that of neon. Upon continuosly measuring i_t (and thus η) during irradiation, we may therefore easily determine the incident beam fluence D_0 necessary to erode away a given Ne film [13–15].

The erosion yield Y is now determined from measurements of D_0 for various initial film thicknesses x_0. Under the reasonable assumption that the instantaneous erosion yield $Y(x)$ at thickness x is independent of prior erosion, it is simple to show that

$$Y = N\frac{dx_0}{dD_0}. \tag{2}$$

where N is the number density. The film thicknesses are determined in terms of area densities (e.g., atoms/cm^2), but for consistency with optically measured lengths, they are converted to length units (e.g., Å), using the bulk density.

It is then found that for film thicknesses above ~735 Å, the erosion yield Y equals the slope of a straight line, i.e. is independent of film thickness. As this holds at least up to ~6000 Å (which is considerably above the projectile range) we interpret this as the "bulk" erosion yield for solid Ne. Because there are indications [15] that the erosion yield is larger for thin films (~100 Å) than for bulk Ne, we may not determine absolute erosion yields from measurements on only one film thickness.

The erosion of solid Ne seemed to be very sensitive to the presence of small concentrations of impurities, even well below the per cent level. Almost all contaminants are considerably less volatile than Ne, and could thus be excluded by simply cooling the gas inlet sufficiently. Contamination with H_2 and D_2, which are frequently used in our set-up, was avoided by, e.g., heating the whole system to room temperature prior to experiments with neon.

2. Exciton Decay Model

Most of the condensed-gas erosion experiments have been performed with swift charged particles (of velocity $> e^2/\hbar$) that deposit most of their energy in the electronic system of the target. However, erosion requires that part of this energy be transferred to atomic motion. Coulomb repulsion between ions created at nearby lattice sites has been invoked as a means for such energy transfers [16–18, 1]. This model requires that the electrons ejected from the track of the primary particle be trapped away from the track; this is hard to justify for the closed-shell rare gases [7, 19]. Alternative models exist [20, 5].

Here, a different approach is taken. The discussion applies to argon, krypton, and xenon and with some qualifications given later to neon. It is well known that following charged particle irradiation of a rare gas solid, luminescent light is emitted in the vacuum-uv region [21, 22]. The luminescence spectrum is very similar to the gas phase emission spectrum. Both of these are, in turn, similar to the solid and gas phase absorption spectra, except for a red-shift (Stokes shift) of some eV between absorption and emission. Because of these similarities the luminescence is ascribed to excitons [22], i.e., excited dimers, Ar_2^*, etc., trapped in microscopic cavities in the solid. The Stokes shift is due to an efficient vibrational relaxation of the excited dimer leading to the trapping of the excitation on the picosecond time scale. Subsequently, these exitons decay radiatively (with a ns-μs lifetime dependent on the relative orientation of the spins) to the *repulsive* ground state. This repulsion imparts ~ 1 eV of kinetic energy to each of the two atoms.

Close inspection of the luminescence spectrum shows emission from vibrationally excited, mobile excitons, albeit with a low intensity relative to the emission from trapped excitons ($\lesssim 10^{-2}$). From this, a characteristic trapping time $\tau \sim 1$ ps has been deduced [22] in good agreement with theoretical estimates [23]. The motion of the excitons prior to trapping is generally described as diffusive, with a diffusion constant $D \sim 1\,\mathrm{cm}^2/\mathrm{s}$ [22]. The key experimental quantity is the exciton diffusion length, $l_0 \equiv (D\tau)^{1/2}$, which from, e.g., photoemission experiments is found to lie between 100 Å and 200 Å for the heavier rare gases [24].

Excitons have been invoked previously in the explanation of electron-induced erosion af alkali halides by Townsend and collaborators [25]. Lately, Johnson and Inokuti [19] have considered excitons in rare gas solids with the main emphasis on the energetics of the energy transfer mechanism.

We suggest a new model for the erosion of condensed rare gases. Details will be given in a forthcoming and more extensive publication [26]. The key point is that enough free excitons may reach the surface prior to possible trapping to account for the observed erosion yield through their radiative decay at the surface. The model then consists of three steps:

1) production of the excitons by the primary charged particle, specified through a production cross section σ;

2) exciton transport to the surface, described by the diffusion length l_0;

3) emission of rare gas atoms from the surface through the radiative decay to the repulsive ground state, controlled by an emission probability p that depends on the available energy and the surface binding forces.

The erosion yield of a thick (bulk) target may therefore be written

$$Y_\infty = N\sigma l_0 p, \tag{3}$$

where N is the number density. The dependence of the yield on the target thickness, as observed for, e.g. Ar [7], can also be accounted for [26]. A general discussion of the pertinent cross sections and emission probabilities will be given later. We shall restrict ourselves here to an application of the basic ideas to neon erosion.

The properties of excitons in neon differ in two ways from those described above for excitons in the heavier rare gases. From luminescence experiments it is known [27] that the major fraction of excitons in neon are of an atomic type, corresponding to an excited atom Ne*, which does not contribute to the erosion in the present model. The "molecular" excitons Ne_2^* of interest here account for a minor fraction $f \sim 0.35$ of the total luminescence intensity. Furthermore, these "molecular" excitons are all essentially free as they decay radiatively before they can be trapped [28]. Consequently the exciton diffusion length in neon should be considerably larger than in the heavier rare gases.

The above model may be used to predict absolute erosion yields from independently measured data (cross sections and diffusion lengths). Furthermore, the close relation to optical experiments enables us to make a quite crucial test of the basic assumptions. From luminescence experiments on dilute alloys, it is known [29, 24, 22] that doping with a heavier rare gas causes a strong quenching of the host exciton luminescence. Instead, light characteristic of the guest is emitted. The experiments are interpreted through an efficient excitation transfer to the guest leading to a reduced exciton diffusion length for the host excitons.

3. Results and Discussion

The bulk erosion yield Y_∞ of neon was measured for 1.2–3 keV electrons (Fig. 1). The yield decreases by a factor of almost two over this energy range, scaling with the Bethe electronic stopping cross section, S_e [30]. Various erosion models predict a scaling with S_e^n, where $n \geqq 2$ [1, 5, 17, 18], and may thus be excluded in the present case.

The observed energy dependence is in quite reasonable agreement with (3), as the exciton production cross section σ is expected to have the same energy variation as the stopping cross section. For an evaluation of the absolute magnitude of the erosion yield, a simple estimate of the cross section σ for the production of "molecular excitons" is

$$\sigma = f \cdot S_e / W, \tag{4}$$

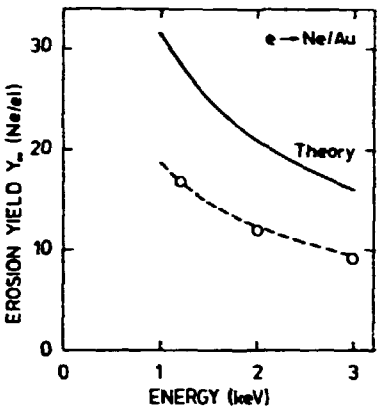

Fig. 1. The bulk erosion yield Y_x *versus* the primary electron energy: (O) experimental yield; (---) electronic stopping cross section normalized to the three experimental points; (——) theoretical yield, Eqs. (3) and (4), with $p=1$

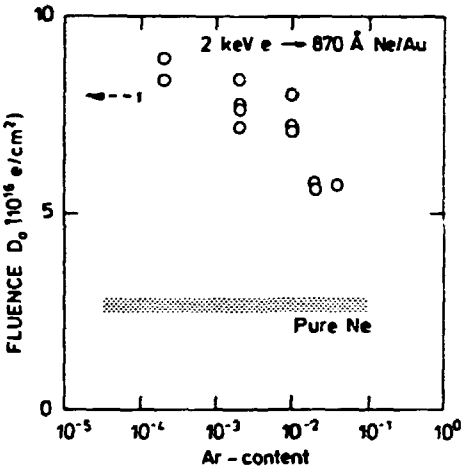

Fig. 2. The electron fluence D_0 necessary for the erosion of 870 Å argon-doped solid neon *versus* the argon content in the film. The neon film was deposited on a gold substrate. The arrow indicates the level for a very low argon content ($<10^{-4}$). The fluence for erosion of a *pure* Ne-film is shown as well

where $W(\simeq 35\,\text{eV}$ [31]) is the energy required to make an ion-pair neon. A small positive correction may enter for excitons produced through excitations rather than ionizatons but it will be ignored here.

From (3) and (4) we have calculated the theoretical erosion yields using the experimentally measured diffusion length $l_0 \simeq 2500$ Å (± 500 Å) [29]. The result is shown in Fig. 1. In the calculation, the upper limit, $p=1$, for the emission probability has been used.

In view of the large uncertainty of the experimental exciton diffusion length, the agreement between experiment and theory is surprisingly good.

As discussed in the previous section, a small concentration of impurities in the neon target will significantly reduce the excition diffusion length and thereby the erosion yield, see (3). From optical measurements [24, 29], it may be estimated [26] that the diffusion length in neon with argon added at a relative concentration of, say, $c \sim 10^{-3}$ is $l \sim 0.3 l_0$. It is therefore expected that the erosion yield will be reduced by the same factor.

This has been investigated experimentally for a few film thicknesses with various concentrations of argon. As even very small impurity concentrations were found to produce a significant effect, great care had to be taken in controlling the target. We have, therefore, not measured at sufficiently many thicknesses to be able to determine absolute values of the erosion yield for the various impurity concentrations. However, the effect is clearly demonstrated from measurements of the total beam fluence D_0 necessary to erode away a given film thickness (Fig. 2). Of course, one should expect D_0 to tend towards the value for pure neon for minute concentrations of argon. The arrow in Fig. 2 indicates the fluence D_0 determined for very small, but not well known impurity concentrations. The measurements were performed on otherwise pure neon films which were contaminated by impurities from the target chamber, e. g., argon from previous runs.

Conclusion

Experimental results have been presented for electron-induced erosion of solid neon in the energy range 1 keV – 3 keV. The energy dependence and magnitude of the erosion yield can be accounted for within a new model for the erosion of solid rare gases. From the model, one predicts a decrease in the erosion yield for films doped with a heavier rare gas. The magnitude of this effect has been confirmed experimentally for argon-doped neon.

Further details on the model and its extension to erosion by MeV ions, as well as a more complete description of the experiment will be given in forthcoming publications [26, 15].

Acknowledgements. Part of this work has been made possible through a research grant (to CC) from the Danish State Natural Science Research Council (Statens Naturvidenskabelige Forskningsråd). Fruitful discussions with our colleagues in the Danish Sputtering Club are gratefully acknowledged.

References

1. W.L. Brown, L.J. Lanzerotti, J.M. Poate, W.M. Augustyniak: Phys. Rev. Lett. **40**, 1027–1030 (1979)
2. W.L. Brown, W.M. Augustyniak, E. Brody, B. Cooper, L.J. Lanzerotti, A. Ramirez, R. Evatt, R.E. Johnson: Nucl. Instrum. Methods **170**, 321–325 (1980)
3. W.L. Brown, W.M. Augustyniak, L.J. Lanzerotti, R.E. Johnson, R. Evatt: Phys. Rev. **45**, 1632–1635 (1980)

4. J.E. Griffith, R.A. Weller, L.E. Seiberling, T.A. Tombrello: Radiat. Eff. 51, 223–232 (1980)
5. L.E. Seiberling, J.E. Griffith, T.A. Tombrello: Radiat. Eff. 52, 201–210 (1980)
6. P. Børgesen, J. Schou, H. Sørensen: In *Proceedings of the Symposium on Sputtering*, Perchtoldsdorf/Wien, Austria, April 1980, ed. by P. Varga, G. Betz, and F.P. Viehböck (Institut für Allgemeine Physik, Technische Universität Wien, Austria 1980) pp. 822–831
7. F. Besenbacher, J. Bøttiger, O. Graversen, J.L. Hansen, H. Sørensen: Nucl. Instrum. Methods **191**, 221–234 (1981)
8. J. Bøttiger, J.A. Davies, J.L. Ecuyer, N. Matsunami, R. Ollerhead: Radiat. Eff. **49**, 119–124 (1980)
9. R.W. Ollerhead, J. Bøttiger, J.A. Davies, J.L. Ecuyer, H.K. Haugen, M. Matsunami: Radiat. Eff. **49**, 203–212 (1980)
10. R.E. Johnson, L.J. Lanzerotti, W.L. Brown, W.M. Augustyniak, C. Musil: Astron. Astrophys. (1982) (in press)
11. P. Børgesen, H. Sørensen: Phys. Lett. A **90**, 319–322 (1982)
12. H. Sørensen: Appl. Phys. **9**, 321–329 (1976); H. Sørensen, J. Schou: J. Appl. Phys. **49**, 5311–5318 (1978)
13. P. Børgesen: RISØ Report R-457, Risø National Laboratory (1982)
14. P. Børgesen, H. Sørensen, J. Schou: "Erosion of solid H_2, HD, and D_2 by keV electrons" (in preparation)
15. To be published
16. R.L. Fleischer, P.B. Price, R.M. Walker: J. Appl. Phys. **36**, 3645–3652 (1965) R.L. Fleischer, P.B. Price, R.M. Walker: *Nuclear Tracks in Solids* (University of California Press, Berkeley 1975)
17. P.K. Haff: Appl. Phys. Lett. **29**, 473–475 (1976)
18. R.E. Johnson, W.L. Brown: Nucl. Instrum. Methods **198**, 103–118 (1982)
19. R.E. Johnson, M. Inokuti: Nucl. Instrum. Methods (submitted)
20. R.H. Ritchie, C. Claussen: Nucl. Instrum. Methods **198**, 133–138 (1982)
21. J. Jortner, L.M. Meyer, S.A. Rice, E.G. Wilson: J. Chem. Phys. **42**, 4250–4253 (1965)
22. N. Schwentner, E.E. Koch, J. Jortner: "Electronic Excitations in Condensed Rare Gases", in *Rare Gas Solids III*, ed. by M.L. Klein and J.A. Venables (Academic Press, London 1982)
23. M. Martin: J. Chem. Phys. **54**, 3289–3299 (1971)
24. Z. Ophir, B. Raz, J. Jortner, V. Saile, N. Schwentner, E.E. Koch, M. Skibowski, W. Steinmann: J. Chem. Phys. **62**, 650–665 (1975) N. Schwentner, G. Martens, H.W. Rudolf: Phys. Stat. Sol. (b) **106**, 183–192 (1981)
25. Y.Al Jammal, D. Pooley, P.D. Townsend: J. Phys. C **6**, 247–254 (1973) F. Agullo-Lopez, P.D. Townsend: Phys. Stat. Sol. (b) **97**, 575–580 (1980)
26. C. Claussen: Thesis, Odense University (to be submitted, fall 1982) (to be published)
27. R.E. Packard, F. Reif, C.M. Surko: Phys. Rev. Lett. **25**, 1435–1439 (1970)
28. Y. Yakhot, M. Berkowitz, R.B. Gerber: Chem. Phys. **10**, 61–66 (1975)
29. D. Pudewill, F.-J. Himpsel, V. Saile, N. Schwentner, M. Skibowski, E.E. Koch, J. Jortner: J. Chem. Phys. **65**, 5226–5238 (1977)
30. H.A. Bethe, J. Ashkin: In *Experimental Nuclear Physics*, Vol. I, ed. by E. Segrè (Wiley, New York 1953) p. 253
31. *Average Energy Required To Produce An Ion Pair*, ed. by H. Bichsel, ICRU report no. 31 (International Commision on Radiation Units and Measurements, Washington, DC 1974)

Nuclear Instruments and Methods in Physics Research B5 (1984) 44–57
North-Holland, Amsterdam

THE MEASUREMENT OF ELECTRON-INDUCED EROSION OF CONDENSED GASES: EXPERIMENTAL METHODS

J. SCHOU, H. SØRENSEN and P. BØRGESEN *

Physics Department, Association Euratom-Risø National Laboratory, DK-4000 Roskilde, Denmark

Received 14 March 1984 and in revised form 15 May 1984

Two experimental methods for measuring the erosion yield of condensed gases are described. One, the frequency-change method, utilizes a quartz-crystal microbalance operating at liquid-helium temperature. The other, the emissivity-change method is based on the strongly varying electron emission as a function of the condensed-gas film thickness. Satisfactory results have been obtained for both methods for solid Ne and D_2 at electron energies up to 3 keV, and the mutual agreement is good as well. Accurate measurements are affected critically by the beam conditions, particularly if the erosion yield depends on the film thickness. The erosion yield has been measured for dominant electron sputtering of solid Ne (≈ 28 Ne-atoms/electron) as well as for beam-induced evaporation at 2 keV. In the latter case a clear lateral broadening of the erosion spot is observed.

1. Introduction

The erosion of condensed gases by ions, predominantly light MeV ions, has been studied intensively during the past years [1–3]. The corresponding data for electron bombardment [4–9] are far less comprehensive and generally much more uncertain, because such measurements of erosion yields are somewhat inhibited by the few available methods for detecting erosion.

Erosion of surfaces of condensed gases plays an appreciable role in interstellar and planetary atmospheric problems [10,11]. In technological problems such as cryopumping in radiation environments [12] the phenomenon has also turned out to be important. A particular case is the study of the erosion of solid hydrogen isotopes by keV electrons [4,5,9] and light ions [5,13] which is aimed at understanding the behaviour of a fuel pellet in a fusion plasma [14,15]. However, the mentioned lack of electron erosion data is serious, since electron bombardment is just as frequent as ion bombardment in many of these areas.

Most of the experiments to date have been made with ions, and the results typically exceed the estimates of "standard" sputtering theory [16] by several orders of magnitude. In particular, the erosion of thin films of solid H_2 by keV light ions has resulted in yields of the order of 10^3–10^5 molecules per ion [4,5,9]. There is little doubt that the large erosion yields for the condensed gases are essentially caused by the energy initially deposited in electronic excitations. In addition, there may be a significant contribution from nuclear stopping for sufficiently low keV ions. Various models, more or less related to electron stimulated desorption [17,18], have been presented in an attempt to explain how this energy is transferred to atomic motion [1–3].

Measurements of electron sputtering complement erosion experiments with light MeV ions, since in both cases essentially all the incident energy is deposited initially in the electronic system. In fact, electron irradiation extends the regime of electronically deposited energy to low energy densities which are virtually impossible to reach with light MeV ions. Below we shall describe two methods, which we have used with success for the determination of erosion yields, e.g. electron sputtering yields as well as yields during beam-induced evaporation.

If the film to be eroded is deposited on an oscillating quartz crystal, we may observe the erosion directly in terms of the frequency change or weight loss versus irradiation time. This method has obvious advantages, but is somewhat limited in sensitivity. Furthermore, it is difficult to control the temperature of the crystal surface with accuracy during such a measurement.

Sensitive measurements are possible if the film is deposited instead on a metal substrate with a secondary electron emission coefficient unlike that of the film. The variation of the total secondary electron emission or electron reflection coefficient from the target during irradiation may then be used to indicate when the film has been eroded away. This emissivity-change method is sensitive to even very small film thicknesses, and has actually been exploited previously to indicate the sputtering of the oxide layer on an Al-target [19].

* Present address: Max-Planck-Institut für Plasmaphysik, D-8046 Garching bei München, FRG.

0168-583X/84/$03.00

These two methods have been used, at times simultaneously, for measuring the erosion of solid H_2, D_2, HD, Ne, Ar, CO, O_2, N_2 as well as various gas mixtures, by keV electrons. The erosion of solid neon was studied intensively. Apparently, there is no large effect of the film thickness on the erosion yield, and neon is particularly suited to erosion measurements on the quartz crystal. Results from solid neon were utilized to check a theoretical model for charged-particle erosion of solid rare gases as well [20]. Within this model the erosion yields are calculated on the basis of independent optical data [21], and a critical test was the observation of a predicted, significant effect of even very small amounts of impurities.

The present work supplies the first full description of a method for measuring electron-induced erosion via secondary emission (current measurements). Furthermore, we present the first results of measuring directly the erosion of condensed gas films by means of a quartz-crystal microbalance. A comprehensive presentation of the results for the different condensed gases will be communicated later [22–24].

2. The experimental set-up

The experimental set-up will be described in some detail. It is a rebuilt and extended version of the original one [25] that was used for incidence of ions and electrons on condensed gases [26,27].

A schematic drawing of the target region of the set-up is shown in fig. 1. Fig. 2 shows how the interior of the set-up is altered when the target plate is replaced by a quartz-crystal microbalance. The target region is located below the bottom of a liquid helium cryostat and limited by two shields affording protection against thermal radiation; only the shield at liquid helium temperature is shown. An electron beam from a small electron gun mounted on a tube on the side of the vacuum chamber enters the target region through small holes in these shields. The beam can either hit the target perpendicular to the surface or be deflected by a set of deflection plates placed just outside the radiation shields so that it enters a Faraday cup.

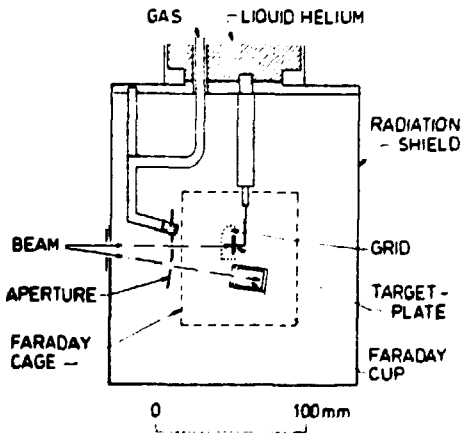

Fig. 1. Schematic drawing of the target region of the experimental set-up.

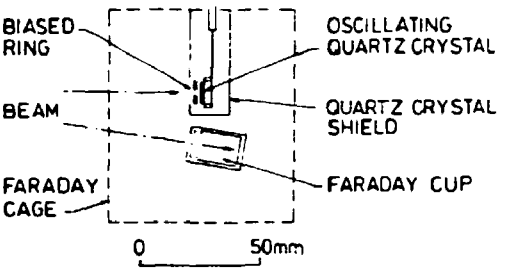

Fig. 2. The modified target region with the quartz crystal.

A film of solidified gas is produced on the target plate or on the quartz crystal when a jet of cooled gas impinges on it. The film may be rapidly removed just by heating the target plate with an electrical heater. The gas comes from a 4-liter reservoir, and it enters the target region through the gas tube shown. The gas tube is heated sufficiently at the low-temperature end to allow passage of the gas. During measurements on hydrogen isotopes the liquid helium is cooled to below 2.5 K by pumping, while it is held at the normal boiling temperature of 4.2 K for work with other gases. The gas inlet rate is determined by the setting of a needle valve and by the pressure in the reservoir.

The gas inlet system was calibrated by means of the quartz-crystal microbalance placed in a simple crystal holder at the target position. The thickness of the film deposited on the target plate (fig. 1) may then be known with an accuracy of 10%.

The vacuum pressure is measured at a tube placed on the side of the vacuum chamber. Normally it is less than 2×10^{-8} Torr with a cold cryostat, and a film will thus remain uncontaminated for a long period [25].

The target plate is electrically insulated from the cryostat so it can be used for collecting the electron beam. The current collected will depend on the number of secondary electrons and reflected electrons emitted from the target plate, and this number can be controlled by means of a grid placed in front of the target plate. The true beam current is measured by deflecting the beam into the Faraday cup. The target region and the Faraday cup are both located inside an electrically grounded Faraday cage (fig. 1). Grid, cup and cage are all heated to temperatures sufficiently high to prevent the gas from condensing on them. In this manner we attempt to minimize disturbing effects from areas that may charge up. A certain heating is needed in the target

region, depending on the gas used, and thus only a limited number of gases can be handled in the present state of the set-up. The modified set-up with the quartz crystal (fig. 2) is constructed in a similar way.

2.1. Irradiation on an ordinary target plate

A number of erosion measurements were performed with a metal substrate. In most cases a polished gold plate was used as target plate (fig. 1). However, for a few measurements a copper plate covered with a carbon layer of about 100 $\mu g/cm^2$ was utilized as a carbon substrate.

With these substrates only the emissivity-change method was applied for determination of the erosion yields.

2.2. Irradiation on the quartz crystal

The quartz-crystal is an ordinary commercial AT-cut crystal of the type used for measurements of film thickness at room temperature [25,28]. The oscillating crystal itself is a disk of 14 mm diameter and 0.3 mm thickness cut from a single crystal. Two silver electrodes of 6 mm diameter are placed in the centre on the two sides of the crystal. The resonance frequency for the crystal is around 5 MHz, and the crystal has an orientation such that the resonance frequency is nearly temperature independent around room temperature. Below 250 K the frequency will decrease with decreasing temperature and below 10 K the frequency will again be temperature independent [29]. The crystal is actually an excellent thermometer between 10 K and 250 K. The crystal should only be used for erosion studies at temperatures where the resonance frequency is temperature independent.

Here we place the crystal by means of two springs in a holder similar to a room temperature holder and mount it below the cryostat at the target plate position. The springs are attached to the holder with platelets of KCl or sapphire, both of which are good heat conductors at these low temperatures. The thermal contact between the springs and the crystal itself is improved with droplets of electrically conducting lacquer [25]. The deposit on the crystal is limited to a spot of 6 mm diameter by means of an aperture placed right in front of the crystal. A carbon thermometer and an electrical heater are placed on the crystal holder. The oscillator circuit is placed right outside the vacuum system and connected to the crystal by a doubly shielded cable, through which the target current is collected as well.

The ring aperture in front of the crystal is insulated from the shield and may be biased in order to suppress the emission of low-energy secondary electrons from the target. During erosion measurements the shield and the ring are heated to avoid gas condensation.

Thus the beam limited by means of a 2-mm diameter aperture only erodes the central part of the condensed gas, i.e. all the electrons thus hit the film.

The thickness of the silver electrodes is 4000 Å which exceeds the range of our most energetic electrons [30]. For our purpose the substrate thus corresponds to one of silver alone.

The substrate is heated when hit by an eroding beam. The heat conduction from the substrate through the quartz crystal and the crystal holder and further on to the cryostat bottom is rather poor. The quartz crystal target is therefore heated more than the normal target plate by a beam.

The effect of thermal gradients on the frequency has been reported in the literature [28], but we have at most observed a frequency shift of one-two Hz when the crystal area has been irradiated with the present current beams.

At temperatures below 10 K the frequency is normally quite stable, i.e., within one-two Hz when the crystal is unloaded. There may, of course, be a small frequency drift of a few Hz during a working day mainly because of rest gas leaking in from the vacuum space outside the radiation shields. This should be compared to a typical film deposition corresponding to a frequency increase of up to more than one thousand Hz. The subsequent erosion would then lead to a frequency change of more than several hundred Hz.

The stability of the frequency during an erosion measurement is critical for a successful determination of the frequency shift. When we remove a film or the last remnants of an eroded film by heating the crystal, we normally see that the frequency returns to a value close to that measured before the film was deposited. In this way any frequency drift is immediately observed. The stability of the frequency was good also when the crystal had been cooled to the low temperature several times.

It was controlled as well that the mass increase per frequency unit for a deposited film is the same at room temperature and at liquid helium temperature. A silver film, giving a frequency change of around 5 kHz, was deposited at room temperature, and it was then seen that the change at 4.2 K was the same within 1 Hz [9,31].

Besenbacher et al. attempted to measure ion-induced erosion yields of solid argon by using a similar crystal as a target for a light ion beam at energies from 0.1 to 3 MeV [32,33]. They observed that the thicknesses determined by Rutherford backscattering analysis were systematically about 20% larger than those determined by the frequency shift at the quartz crystal during ion bombardment. The authors suggested that the penetration of MeV ions through the electrode and into the quartz would influence the accuracy of the crystal. This phenomenon does not occur with our present electron beams because the electron range is shorter than the thickness of the electrodes.

2.3. Beam sweep and beam optics

Beams of 0.5–3 keV electrons are obtained from a small electron gun placed directly on a side tube to the target chamber. The distance from the filament to the target area is approximately 0.4 m.

During erosion measurements the electron beam was well focused and then swept horizontally and vertically by two independent saw-tooth voltages over a 2-mm aperture in front of the target. This ensures a homogeneous irradiation of a large fraction of the target area if only the sweep system is ideal and the amplitudes sufficiently large to deflect the beam totally outside the aperture [9]. The latter was easily checked by measuring the target current i_t as a function of sweep voltage. The sweep voltages were applied to the two sets of deflection plates on the gun. Then, it was possible to deflect the swept beam by means of the last deflection plates before the target chamber, so that it was swept over the Faraday cup instead. The opening of this cup was also covered by a 2-mm aperture, so that the average values of cup current and target current may be compared directly.

Typical currents used for erosion measurements were from 50 nA to 300 nA, corresponding to a current density of a few $\mu A/cm^2$.

For a precise determination of the sputtering yield the extension of the eroded area is required (cf. sect. 3.1). It has, therefore, been important to determine the area of the irradiated spot.

The area of the irradiated spot is determined essentially from the beam geometry. The beam path is shown schematically in fig. 3. We assume the beam to be ideally focused in the aperture in front of the target, and that the deflection caused by the sweep voltage takes place only in the deflection plane at the electron gun. In the plane the beam has a width a determined by the exit aperture of the gun. The aperture with diameter d in front of the target has to be placed at some distance from the target in order not to disturb the gas jet (fig. 1). This results in a beam spot consisting of a fully irradiated central zone and a partially irradiated edge zone. From this model one obtains the width D of the central zone:

$$D = (dL - al)/(L - l). \quad (1)$$

L and l are the total distances, respectively, from the deflection plane and aperture to the target. The width of the edge zone is

$$\Delta D/2 = al/(L - l). \quad (2)$$

In our geometry (a = 1.6 mm, l = 38 mm, L = 200 mm, and d = 2.08 mm) it means that D and $\Delta D/2$ are 2.2 mm and 0.4 mm, respectively, and that the area of the edge zone is almost just as large as the area of the central zone. Within this model the total beam spot covers about 25% of the film deposition area on the quartz crystal. This estimate of the beam spot is somewhat uncertain because of both the non-negligible width of the beam at the aperture and edge scattering.

An attempt to determine the beam spot directly was performed as well. A brass sample covered with a thin layer of grease was irradiated in the same geometry at several electron energies from 3 to 1.2 keV. A slightly darkened spot occurred after an irradiation period of some hours. The area was measured, and it turned out that the beam spot covered 25% of the film deposition area for the quartz crystal at 3 and 2 keV, and 22% at 1.5 and 1.2 keV. This area determination can be regarded only as approximate, since the threshold fluence for making a visible change in grease probably is larger than a measurable erosion on the volatile condensed-gas films.

According to the model for the beam optics, the relative contribution from the edge zone becomes small, if the distance from the electron gun to the target is increased substantially (see eq. (2)). However, this leads to a considerably more uncontrollable electron beam path than in the present set-up. The resulting loss of intensity might be critical for measurements on the least volatile molecular solids.

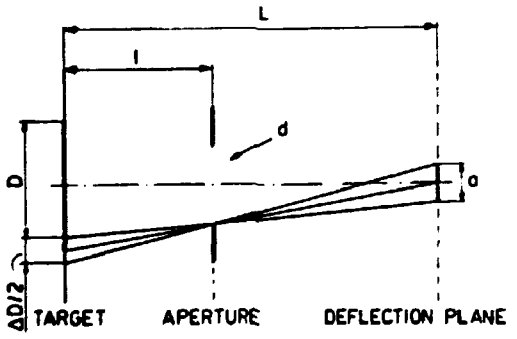

Fig. 3. Schematics of the beam geometry.

3. Performance of the measurements

Usually, the measurements were made in a three-step procedure: 1) The beam was optimized, the beam setting controlled and the current i_b was determined, 2) the erosion was followed by the emissivity-change method or by the frequency shift of the quartz-crystal microbalance, and 3) the beam current was controlled after the erosion.

The beam setting with the beam sweep turned on was controlled by measuring the ratio of the currents collected from the target with a negatively biased grid to that from the cup (cf. sect. 3.1). Since every solid has a characteristic, generally well-known electron reflection

coefficient η [34,35], this means that an uncorrect beam setting could be improved before the film deposition.

The beam current was normally fairly constant. Any beam drift was partly compensated by a numerical procedure during the data analysis.

The erosion yields were measured mostly below the temperature regime, in which the yields increase with temperature [32,36]. In the case of solid neon the average substrate temperature could be increased to about 6 K before any noticeable enhancement of the yield occurred [22]. A similar check was performed for deuterium [4] and for the other condensed gases.

In one case the erosion yield dependence on the current density was examined for current densities up to above 10 $\mu A/cm^2$. This measurement will be discussed later. Otherwise, no change in the yield was observed for several current densities below this value.

In the simple case, where the yield is independent of the film thickness x, the yield Y is determined by

$$Y = ANx/\Phi. \tag{3}$$

where A is the eroded area, N the number density of the condensed-gas film, and Φ the total number of primary electrons needed for an erosion. If the yield depends on the thickness, eq. (3) has to be modified to

$$Y(x) = N\frac{\Delta(Ax)}{\Delta\Phi}. \tag{4}$$

where $\Delta(Ax)$ is the volume sputtered by $\Delta\Phi$ electrons at the instantaneous thickness x. This expression is directly utilized for the erosion on the quartz-crystal microbalance. However, frequently it is not possible to determine the yield in the simple way indicated in eqs. (3) and (4).

In many cases one is able to determine only the total number Φ of electrons that are needed to erode the film away. Of course, the eroded area has to be estimated as well. However, even then a straightforward application of eq. (3) would lead to an average yield which may be very different from the instantaneous yield $Y(x)$ and the bulk yield (e.g. see the figures in sect. 3). Then one may evaluate the yield $Y(x)$ from

$$Y(x) = N\frac{d(Ax)}{d\Phi}c, \tag{5}$$

where c is a constant that depends on the geometry of the erosion crater, and from how Φ is estimated (see sects. 3.1 and 3.2). For a complete homogeneous erosion without a crater edge $c = 1$, but in the present work c is usually 0.7–1.0. These estimates as well as formula (5) will be discussed in the appendix.

One may use eq. (5) for the emissivity-change method as well as for a determination by means of the quartz-crystal microbalance, but more than one complete erosion is required if the instantaneous yield $Y(x)$ has to be evaluated.

3.1. Determination of the yield by the emissivity-change method

This method utilizes the fact that the electron emission coefficient of a thick condensed-gas film is different from the electron emission coefficient of the substrate. Therefore, it is generally possible to determine the time when the deposited film has been removed from the irradiated area by the beam.

Before describing the principle of the emissivity-change method we have to consider electron emission resulting from electron incidence on a solid surface. We disregard for the moment any ion emission, and may define an "electron emission coefficient" ξ by

$$i_t^- = (1 - \xi)i_b. \tag{6}$$

where i_t^- is the target current for a positively biased grid. For incidence of keV electrons we may not directly distinguish secondary from reflected electrons. Usually we expect most secondary electrons to have energies of only a few eV, whereas a considerable number of the reflected electrons will have much higher energies (particularly if reflected from Au, see below). As discussed in refs. [27,35,37] it is, therefore, an experimental convention simply to define electrons with low energies as "true" secondaries (the stringent validity of this "definition" is unimportant for the present work).

A bias of -45 V (or -90 V) applied to the grid in front of the target may thus be expected to suppress almost all secondary electron emission, leading to a current i_t^-. We define the electron reflection coefficient η as in ref. [20] by

$$i_t^- = (1 - \eta)i_b. \tag{7}$$

and note that the total emission coefficient (see above)

$$\xi = \eta + \delta. \tag{8}$$

where δ is the true secondary electron emission coefficient. Previous measurements of the ranges of 0.5–3 keV electrons in solid H_2, D_2 [37] and N_2 [27] exploited the observation that for thin films on a Au-substrate the reflection coefficient η would depend on the film thickness x (fig. 4).

For normal incidence of keV electrons on a pure gold substrate the reflection coefficient η_{Au} is about 0.4, and it is known from the literature [34,38] that the energy distribution of the reflected electrons has its maximum slightly below the primary energy. In contrast, the reflection coefficients for H_2, D_2, or N_2 are very low. Fig. 4 shows measurements of the reflection coefficient η for H_2-films on a gold substrate as a function of the film thickness x for incidence of 3 keV electrons. The coefficient is seen to fall off almost linearly. The reason is that the probability that reflected electrons from the substrate will escape through the film decreases with x. Thus $\eta(x)$ reaches the 'bulk' value

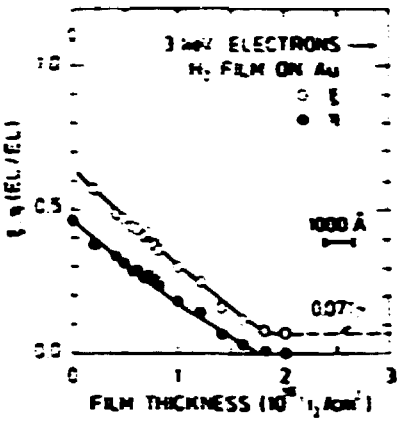

Fig. 4. The reflection coefficient η and the total electron emission coefficient ξ (eq. (8)) are plotted versus the film thickness for H_2-films on a Au-substrate. Primary electron energy: 3 keV.

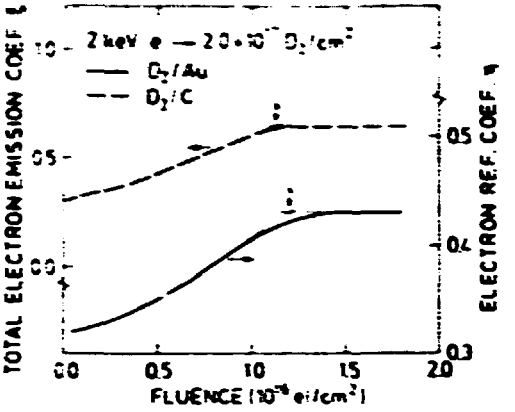

Fig. 5. The erosion of a 2×10^{17} D_2/cm² thick film on Au- or C-substrate by 2 keV electrons. The total electron emission coefficient ξ and the electron reflection η are plotted versus the electron fluence. The values for F_0 corresponding to a complete erosion are indicated by vertical arrows. (The fluence has been evaluated according to the correct area of the beam spot, cf. section 5.)

$\eta(\infty)$ at the thickness d where the electrons that have been reflected from the gold surface have no longer sufficient energy to escape through the film. The projected range was taken [27,37] as twice this thickness, $R_p = 2d$, but our present application of the relation $\eta(x)$ does not depend on this interpretation.

As we see from fig. 4, the total electron emission coefficient ξ [eq. (6)] also varies with film thickness. As the true secondary electrons often have quite a short range (escape depth), ξ will vary essentially as η for thicknesses larger than 10^{16} molecules/cm². However, for very thin films (less than 10^{16} molecules/cm²) ξ varies particularly strongly because electrons from the gold may escape as well.

We might then instead determine an unknown film thickness x by measuring the reflection coefficient η and comparing it with the known relation $\eta(x)$ (fig. 4). By measuring the target current i_t continuously during irradiation of a film we immediately obtain the reflection coefficient η versus incident beam fluence (fig. 5), and in turn the instantaneous target thickness versus eroding beam fluence (provided that the erosion is homogeneous).

The sensitivity of the measurement is limited by the slow variation of η with x. For initial film thicknesses below 10^{17} molecules/cm² the total change of η is prohibitively small, and we may measure instead the total emission coefficient ξ (fig. 5). This coefficient varies strongly at small x (fig. 4), and has been utilized for erosion measurements of relatively thin films [4].

Unfortunately, the secondary electron emission is sensitive to the structure and purity of the surface. In contrast, the reflection coefficient η will be less sensitive and be characteristic only of the average remaining target thickness. We should, therefore, tend to believe mainly in results based on measuring η, as soon as we have ensured that the applied negative bias does not influence the erosion process (see sect. 5).

Fig. 5 shows the variation of the reflection coefficient η and the total emission coefficient ξ during the erosion of 2.0×10^{17} D_2-molecules/cm² on both gold and carbon substrates. This film thickness is almost one order of magnitude less than the electron range for 2 keV electrons, which means that the initial value of η is about 0.3. This is far above the value for bulk hydrogen and deuterium of 0.01 [27]. Both coefficients increase with the fluence from the initial value up to a final value, which is determined by the substrate. In principle, both the "Au-value", η_{Au}, and the "C-value", ξ_C, are reached by the time the film is eroded away. Unfortunately, these values are approached almost asymptotically as the last remnants of the film are eroded away. Therefore, we define the erosion as completed for the total beam fluence F_0 (electrons/cm²) corresponding to the intercept of the steepest tangent (thin lines, fig. 5) to the η-curve with the "Au-level", and to the ξ-curve with the "C-level" [4]. This definition gives an experimentally convenient determination of the total fluence F_0, or the corresponding total number Φ of electrons.

A series of complete erosion data has been shown in fig. 6, where the initial thickness has been depicted as a function of the fluence F_0 that is needed to erode the film away. The yield $Y(x)$ is determined from eq. (5), and from fig. 6 one might find the tangential slope $N\mathrm{d}x/\mathrm{d}F_0$ of the "curve" which the data points compose. However, the area that determines $F_0 = \Phi/A$ must be found from another method (see section 3.2).

Formula (5) has been used in previous work [4,9] assuming a constant, estimated area. This means that a

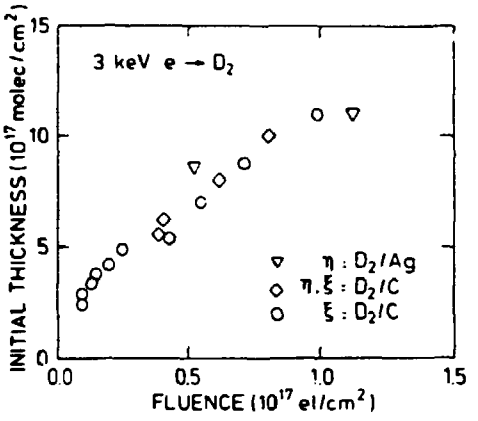

Fig. 6. The erosion of D_2-films on Ag- or C-substrate. The initial thickness is plotted as a function of the fluence necessary for a complete erosion. (η, ξ) indicates measurements in which the electron reflection coefficient η was followed in the first part, and the total electron emission coefficient ξ in the last part. Otherwise, notation as in fig. 5.

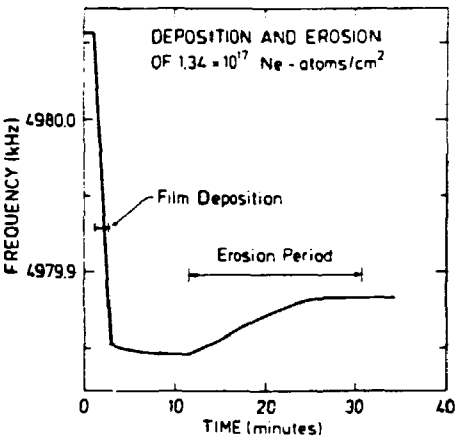

Fig. 7. The deposition and subsequent erosion of a 1.34×10^{17} Ne-atoms/cm^2 thick film on a Ag-substrate (electrode) of a quartz crystal. The frequency is plotted versus time. Electron beam energy: 2 keV.

correction of these data is necessary (cf. sect. 5). The formula is utilized also for the evaluation of the thickness-dependent yield $Y(x)$ that occurs for H_2, D_2 and HD [23]. In spite of the considerable extension of the crater side we regard eq. (5) with $c = 1$ as a fair estimate of the yield.

One notes that the slope of the 'curve' from the data points corresponds to a yield of about 10 D_2/electron, and that there is no significant difference between the three kinds of data. The trend of the data points measured by the total emission coefficient is similar to that of the reflection coefficient, which has been measured on even two different substrate materials. In only few cases has it been possible to perform measurements by means of the reflection emission coefficient η on carbon since the reflection coefficients for bulk hydrogen, deuterium and neon are very close to that of carbon. However, it was generally possible to measure erosion of hydrogen and deuterium on a carbon substrate, if the bias was changed from a negative to a positive voltage, shortly before the end of the erosion. Then the fluence was determined from the behaviour of the ξ-coefficient. The points obtained in this way are indicated by (η, ξ) in fig. 6.

3.2. Yield and area determination by the quartz-crystal microbalance

This method utilizes the possibility of measuring instantaneously the mass change on a quartz-crystal microbalance during particle bombardment [39]. In addition, the method provides a determination of the eroded area.

The principle is shown in fig. 7. A film of 1.34×10^{17} Ne-atoms/cm^2 is deposited on the silver electrode of the quartz crystal during a period of a few minutes. This film thickness leads to a decrease in the frequency of about two hundred Hz. After the gas inlet has been closed, neon corresponding to a few Hz is cryopumped onto the crystal from the gas tube and the surroundings. As soon as the electron bombardment begins, the frequency increases almost linearly. After approximately 15 min the frequency approaches a value which corresponds to a complete erosion of the film in analogy to the emissivity-change method.

The slope of the frequency curve may be applied to a direct determination of the mass loss. Then the yield is determined from eq. (4). In addition, it is possible to estimate the fluence necessary for the complete erosion by the intercept of the linear part of the curve with the asymptotical value just as described for the emissivity-change method (cf. eq. (5)).

By means of the frequency, which is asymptotically approached, one may determine the fraction of the total deposited mass that is removed by the beam. In fig. 7 approximately 20% of the deposited mass has been eroded away. However, it has turned out from similar experiments of longer duration that an even larger fraction of the condensed gas would have been removed after continued erosion.

The proper yield, determined from the emissivity-change method and from the estimate of the fluence for the complete erosion with the quartz crystal, is obtained only if the extension of the eroded area is largely known. A large number of runs at the available energies were performed on each condensed gas to determine an effective eroded area. These areas were then used to obtain the absolute values of the target

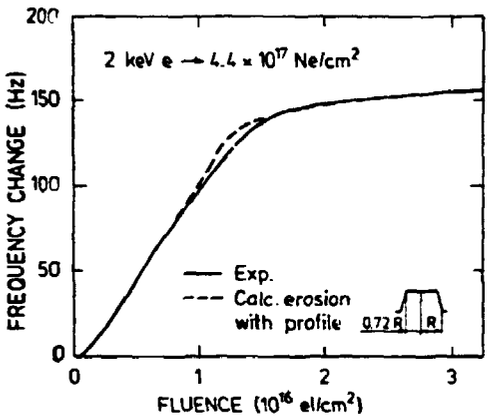

Fig. 8. The erosion of a 4.4×10^{17} Ne-atom/cm^2 thick film on a Ag-substrate (electrode) of a quartz crystal by 2 keV electrons. The frequency change is plotted versus fluence. Bias: −90 V. (— — —), calculated frequency change from eqs. (A.3)–(A.5) with $\alpha = 0.72$. (The fluence has been evaluated similarly to that in fig. 5.)

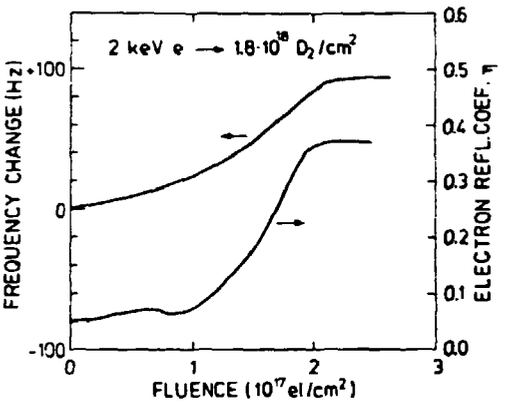

Fig. 9. The erosion of a 1.8×10^{18} D_2-molecules/cm^2 thick film on a Ag-substrate (electrode) of a quartz crystal by 2 keV electrons. The frequency change and the electron reflection coefficient are plotted versus the fluence. (The fluence has been evaluated similar to that in fig. 5.)

fluence, e.g. for the emissivity-change method (cf. eq. (5)). It turned out that the area is on the average 25% of the total film area. This area determination is feasible, since the beam geometry is almost similar for the ordinary target plate and the quartz crystal.

Occasionally it was possible to evaluate the area more accurately from a simulation of the erosion profile. This is shown in fig. 8 as a function of the target fluence for a spatial form such as a frustrum of a right circular cone. 2-keV electrons erode a neon film, the thickness of which corresponds to 3/4 of the electron range. The shape of the frequency curve is then divided into two parts: In the first part the erosion goes on until the flat plateau of the cone has reached the substrate. In the last part the erosion solely takes place in a "ring" outside the flat part. The model assumes that the erosion yield is independent of thickness, but neon has so far shown only a weak dependence on thickness (and solely for thicknesses below 3×10^{17} Ne/cm^2). The calculated curve is rather sensitive to the choice of upper and lower radius, and the curve shown gave the best overall agreement. The development of the profile with time is described in the appendix. This simulation procedure could readily be performed when the frequency were registered continuously during the measurements. This area from the simulation was then used for this specific measurement instead of the less accurate, general area calibration.

The shape of the frequency curve shown in fig. 8 is observed in almost all erosion measurements on solid neon, oxygen, nitrogen and carbon monoxide independent of the initial thickness. This similarity is a consequence of the inhomogeneous beam profile and a possible lateral extension of the erosion, and obviously not the result of a strong thickness dependence of the erosion yield.

In some cases the emissivity-change method was used simultaneously with the frequency measurement on the quartz crystal. The erosion of 1.8×10^{18} D_2-molecules/cm^2 by 2-keV electrons on the silver electrode of the quartz crystal is shown in fig. 9. This thickness corresponds to the range of the electrons. The frequency and reflection coefficient are plotted as a function of the fluence, which has been corrected according to the area calibration. One notes that the erosion is completed at almost the same fluence ($\sim 2 \times 10^{17}$ electrons/cm^2). Contrary to neon one observes a significant change in the slope of the frequency curve. This reflects a noticeable thickness dependence of the yield, which is common for solid D_2, H_2 and HD. The behaviour of the reflection coefficient during erosion shows a similar trend.

The simultaneous measurements have been performed for other gases as well, and mostly the agreement has been convincing. This mutual agreement confirms the feasibility of both methods, and in particular, it means that the emissivity-change method may be accompanied by a method which yields the instantaneous mass change.

Finally, let us consider a series of measurements in which the current density was varied from 3 to 35 μA/cm^2. In all cases a film of 4.5×10^{17} Ne-atoms/cm^2 on the quartz crystal was eroded by 2-keV electrons. The initial yield as well as the fraction of the eroded mass are plotted as a function of the current density in fig. 10. One notes that the erosion yield increases drastically above 15 μA/cm^2, and that the fraction of eroded mass rises from the usual level ($\lesssim 30\%$) up to unity.

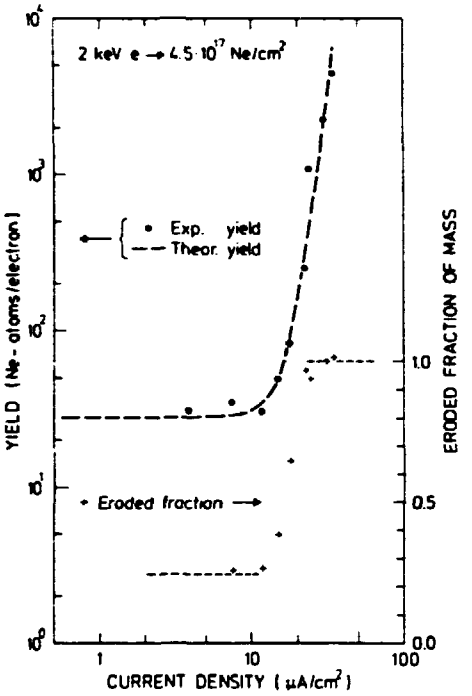

Fig. 10. The initial erosion yield for a 4.5×10^{17} Ne-atoms/cm^2 thick film is plotted versus the current density. Primary electron energy: 2 keV, bias: −90 V. (— — —), calculated curve from eqs. (9) and (10). $Y_0 = 28$ Ne/electron. The eroded fraction of mass is plotted versus current density as well. (···), initial and final fraction of mass. The values for 15 and 18 μA/cm^2 may be slightly underestimated since the erosion was not fully completed at the end of the experiment.

Since this small enhancement of current density may scarcely have any effect on the size of the beam spot, we may interpret this behaviour as a result of beam-induced evaporation of an extension much larger than the beam spot (cf. section 5). We arrive as well at the result that the eroded mass in many cases corresponds to an effective area that is substantially *larger* than any possible beam spot.

3.3. Charge-up problems

As many of the irradiated materials are electrical insulators, a problem that may arise is the simultaneous charge-up of the film: A significant charge-up might effectively influence the primary beam energy, as well as defocus the beam (changing A), and even a moderate charge-up might seriously disturb measurements based on the beam-induced emission of charged particles.

Secondary electron emission will in effect produce positive charges at the surface, while projectiles coming to rest inside the target will constitute a surplus of negative charges in depth. Furthermore, processes at the target-substrate interface may contribute. We may expect problems, as the mobility of charge carriers is quite low in diatomic molecular solids [40,41], for instance. However, it turned out that the surface potential was mostly comparable to the bias voltage. It was possible to apply the the emissivity-change method except for very thick films of deuterium [23].

Charge-up problems affect predominantly the measurements performed by the emissivity-change method. They do not influence results obtained with a quartz-crystal microbalance, as long as the surface potential does not change the primary energy noticeably. A simultaneous current and frequency measurement may then ensure a highly controllable determination of the erosion yield.

3.4. Accuracy of the methods

The accuracy of the frequency-change method is generally good. A large number of erosions of the film thickness used in figs. 8 and 10 led to a relative standard deviation of 13%. This accuracy is probably the best achievable for all of those measurements for which no strong thickness dependence of the yield occurs, and also for which no beam-induced evaporation takes place. Furthermore, this accuracy requires a stable beam current, i.e. with a variation of less than 10%.

The evaluation of the yield from eq. (5) assumes that the derivative $d(Ax)/d\Phi$ is determined. The precise estimate of $dx/d\Phi$ is hardly better than 20–30%. Finally, a considerable error may appear, dependent on how the estimate of the area of the erosion spot is done.

In the case of an ordinary target plate one has to take into account that the film thickness is calibrated only within some limits. Furthermore, the constant c in eq. (5) with our geometry may deviate up to 15% from our estimated value $c = 0.85$, unless a detailed profile calculation is made.

4. Discussion of the methods

4.1. Comparison between the methods

Of the two methods considered in the present work, the quartz-crystal microbalance has obvious advantages: i) The frequency change measured is directly related to a simultaneous mass loss, ii) contrary to the emissivity-change method one need not complete an erosion in order to obtain the yield, and iii) the effective area of the eroded spot is determined by the fraction of mass that is removed by the beam.

The principal disadvantage of the microbalance is the complicated way in which the deposited beam energy is transferred to the crystal holder. Furthermore,

there are some restrictions in choice of material and thickness of the electrodes.

The sensitivity of the method is, of course, important. For the microbalance it means that the product $Y\Phi M$ must be large. If the yield Y and the atomic/molecular mass M of the condensed gas are small, the total number Φ of the beam particles should be large, i.e. a large current or a long period of irradiation is necessary. In the first case the target may be heated too much and thermal enhancement of the yield may occur. In the second case the limit will be set by the stability of the frequency counter and the beam current. Unfortunately, a large atomic mass is found for the least volatile gases. These generally exhibit a low erosion yield for primary electrons. In this connection, *neon is extremely suitable* for electron-induced erosion because of the fortuitous combination of a large yield (~ 30 atoms/electron) and an atomic mass which is not too small. For a typical erosion of another gas at 2 keV with a beam current of 200 nA and a yield of the order of 1 (e.g. N_2), one needs an erosion period of approximately one half-hour if a frequency change of about 20 Hz is required.

The emissivity-change method is obviously advantageous under conditions at which good heat conduction from the beam impact area to the target holder is important. For example, the thermometer at the target holder registers a temperature which is much closer to that of the irradiated area if one uses a massive target plate rather than the quartz crystal. Of course, one then needs the area of the eroded spot for an absolute, accurate estimate of the yield. In particular, for thin films the emissivity-change method is superior to the microbalance. A significant change of the target current may be obtained during the erosion. The complete erosion shown in fig. 5 would correspond to a frequency change of 10 Hz, which would be difficult to register convincingly.

Finally, the emissivity-change method is feasible for any gas-substrate combination where significant changes of the total emission coefficient or of the reflection coefficient occur during erosion. The choice of substrate material is not limited by the available electrodes for the quartz crystal.

The main disadvantages of the emissivity-change method are that the erosion must continue until the substrate is reached and that one requires the area of the eroded spot. The first point means that any erosion may be performed only for thicknesses that are removed completely during a typical period of measurement, e.g. up to 5–7 hours with the present set-up (when the liquid helium in the cryostat is pumped). The second point means that the area has to be determined from an entirely different method, e.g. with the microbalance or by estimating the area from visible spots on samples.

For the two most volatile gases H_2 and HD it appeared to be difficult to determine the erosion yield precisely. There was no satisfactory agreement between the methods of emissivity-change and frequency-change for these two gases, probably because beam-induced evaporation took place at the quartz crystal. This is a consequence of the relatively poor heat conduction from the beam spot through the quartz crystal to the cryostat bottom. In addition, it means that the area calibration factor will be determined rather inaccurately, since the eroded area at the quartz crystal may be larger than the corresponding area at an ordinary target plate.

The erosion data on the quartz crystal for 1–3 keV electrons incident on deuterium films and for 2 keV electrons on solid HD agreed with the data obtained by the emissivity-change method for thick films ($\geq 10^{18}$ D_2/cm^2). The slope of the tangents from the two curves agreed satisfactorily corresponding to a well-determined yield for these films according to eq. (5). However, for thin films the erosion on the quartz crystal was up to a factor of two faster, possibly suggesting that the substrate temperature is more critical for such films. A similar trend for deuterium has previously been observed in a preliminary study of erosion by keV deuterons [13]. The reason for this is not known, but it will be investigated in future work.

In addition, it turned out that a damaged soldered joint at the crystal holder may have lead to an enhanced erosion yield because of the poor heat transport away from the beam impact area. The yield of neon for low current densities was increased by a factor of 1.5, and decreased immediately after reparation to the usual magnitude.

4.2. Comparisons with other methods

The method most applied in condensed-gas erosion has so far been Rutherford backscattering analysis [6,32,36,42–44]. With this method the area density of the condensed gas may be determined fairly accurately. As with other methods one has to ensure that the analysing beam hits the area irradiated by the eroding beam, and that the extension of the eroded area is known. These problems are, of course, common to all sputtering measurements with Rutherford backscattering analysis. The area density measurements are in principle highly accurate, but the method requires a sufficiently large number of backscattered analysing particles or an appreciable energy loss for these particles through the film. These conditions may be difficult to fulfill, and virtually impossible for thin films of hydrogen and deuterium. For these materials the emissivity-change method offers itself.

The pressure increase in the vacuum chamber during irradiation was used by McCracken and co-authors [5,45] to determine yields from solid hydrogen, deuterium, water ice and other condensed gases. The

method is simple, but apparently rather inaccurate. Comparable data on ice found by Brown et al. [43] with Rutherford backscattering turned out to be about two orders of magnitude smaller than their data.

One may mention the electron-induced erosion of thin films of solid rare gases on niobium crystals [46]. Farrell et al. utilized the change in characteristic energy-loss peaks or the intensity of a LEED first-order diffraction beam during erosion. However, they reported severe difficulties in reproducing the results, and indicated that their results should be regarded as qualitative only.

Finally, Pedrys et al. [8] have performed an estimate of the erosion yield of frozen SF_6 by 0.75 keV electrons. The fluence necessary for a complete erosion was determined approximately, and the thickness of the condensed SF_6-film was estimated roughly from a phase transition in the layer. In view of the uncertain current measurement the authors merely report that their yield is of the order of a few molecules per incident electron.

The two latter methods agree in principle with our emissivity-change method. The erosion of condensed gases is observed by measuring a signal change from the disappearing film or from the substrate. So far, our methods have been extended to a higher degree of accuracy.

5. Discussion of results

The determination of the area of the eroded spot was not made in previous work [4,20]. We assumed erroneously that the eroded area was identical to the projection of the nearest aperture. This *area correction* means that the absolute yield for 2 keV primary electrons has now been corrected from ~ 12 to ~ 28 Ne-atoms/electron. The yield of "bulk" solid deuterium [4] has been corrected to ~ 8 molecules/electron for 2 keV electrons as well.

The slope in fig. 8 leads to this latter value for neon, whereas the method using the cross-over between the linear part of the frequency curve and the asymptotic value gives a yield of 26.5 atoms/electron (provided the area correction mentioned earlier is included). This agreement between the two ways of estimating the yield means that *erosion takes place from the complete effective area* from the onset of the beam, i.e. the eroded spot is not broadened significantly during the irradiation. Of course, this comparison is possible only when the condensed gas erodes essentially linearly as neon does. Similar problems due to uneven sputtering have been discussed briefly by Lepoire et al. [42].

The hydrogen isotopes all show a pronounced *deviation from linear erosion*. It is obvious from fig. 9 that the instantaneous erosion yield increases with decreasing thickness, and the same tendency is demonstrated in ref. [4]. The decreasing steepness of the characteristic slope with increasing initial thickness, shown in this reference, originates from the decreasing contributions to the current measurement from the crater side. The steepest slope of the frequency curve in fig. 9 corresponds to a yield of 22 D_2/electron, which is considerably larger than the bulk yield.

According to the results in fig. 5, the *substrate* does not play an important role for the erosion yield of relatively thick films, even for two materials as different as carbon and gold. Fig. 6 illustrates the same trend for silver and carbon substrates. However, it should be emphasized that thin films ($< 10^{17}$ atoms/cm^2) behave very unpredictably since differences in the structure or purity of the substrate surface may conceivably influence the erosion [4].

The *sign of the bias* on the grid usually does not influence the erosion. However, for neon one finds that the erosion with positive bias is up to more than a factor of 3 slower than the erosion yield with negative bias [22]. For all other condensed gases investigated in the present set-up we have observed no significant difference in the yield with positive or negative grid voltage. This is demonstrated as well as by the data in fig. 6 for deuterium.

Let us finally return to the *dependence on the current density* shown in fig. 10. One notes that there is a flat plateau corresponding to the ordinary yield Y_0 of about 28 Ne-atoms/electron below current densities of 10 μA/cm^2. Above this temperature, increasing beam-induced evaporation takes place. Neon is so volatile that a modest enhancement in beam current density on the crystal may lead to a large increase in the erosion yield. This increase is accompanied by a clear lateral broadening of the erosion area.

This case is well described by the low-temperature spike model [47] since the average temperature rise ΔT_{eff} of the target due to the beam is considerably lower than the ambient target temperature T_a. The theoretical treatment [47] enables us to estimate these temperature quantities. The evaporation rate $\Psi(T)$ (number of evaporated atoms per unit time and area) may be estimated from experimental data on vapour pressure from solid neon [48]. The yield from the spike [47] is

$$Y_{sp} = \frac{1}{J}\left(\Psi(T_a + \Delta T_{eff}) - \Psi(T_a)\right), \tag{9}$$

where J is the current density. The total yield

$$Y = Y_0 + Y_{sp} \tag{10}$$

has been plotted in fig. 10 for $T_a = 6.6$ K and $\Delta T_{eff} = 0.13 \times J$ K, where J is given in μA/cm^2. This corresponds to a temperature rise from about 1 K at the lowest current densities up to 4.5 K at the highest current density. These temperature values give the best overall agreement with all the experimental points, and

is consistent with the theoretical prediction that the average temperature rise is proportional to J [22,47].

The behaviour of the yield in fig. 10 resembles the trend of the temperature-dependent erosion yield which have been determined in measurements with electrically heated substrates [22,32,36]. However, these data increase less than one order of magnitude from the low-temperature yield, whereas our data rise more than two orders of magnitude.

6. Conclusion

The present results show that accurate measurements of electron-induced erosion yields are affected critically by the beam conditions. In particular, one needs a beam sweep arrangement that ensures a homogeneous irradiation of the target area if the erosion yield is thickness dependent. A good determination of the beam spot area and the erosion profile is required for sufficiently accurate measurements of absolute erosion yields.

We have demonstrated that it is possible to carry out such measurements on a quartz-crystal microbalance, even at temperatures at the level of liquid helium. The emissivity-change method is applicable as well, while it requires an independent estimate of the area of the erosion spot. With large initial film thicknesses, for which the electron emission does not vary, one has to continue the erosion process, until a significant change in the emission takes place. On the other hand, the temperature of a film deposited on an ordinary target plate is far better controlled than that of a film deposited on a quartz crystal. The eroded area may be determined most accurately by the frequency-change method, which even may be supplemented by a calculation of the erosion profile.

Finally, we shall point out that the two methods, possibly with some additional precautions, offer themselves for future use in other areas, e.g. ion and neutral particle bombardment as well as synchrotron radiation of condensed gases.

The authors thank P. Sigmund, C. Claussen, O. Ellegaard and H.H. Andersen for discussions and valuable comments. We thank as well the technical staff, A. Nordskov, B. Sass and K. Borman, for competent assistance. The help of K. Weisberg in designing the electronic equipment is gratefully acknowledged.

Appendix

In the following treatment we shall consider how our particular erosion geometry affects the results. We assume that the erosion profile may be well described by a *frustrum of a right circular cone* in such a way that we can limit the discussion to the simple, rotationally symmetric case.

We discuss the general expressions for the current and frequency change with time. Then we consider the simple example of a thickness-independent yield (fig. 8), and finally we derive eq. (5).

Let us assume that the erosion takes place on an area πR^2, so that $B = N_0 \pi R^2$ is the number of particles that are eroded away asymptotically. N_0 is the initial surface density. The frustrum has an inner radius αR (see fig. 8).

The general expression for the frequency change $\Delta\nu$ is

$$\Delta\nu(t) = \mu B - \mu \int_0^R N_s(r,t) 2\pi r \, dr, \qquad (A.1)$$

where N_s is the instantaneous surface density (particles/cm^2) at the distance r from the centre of the erosion crater at the time t. μ is a constant (that relates the number of particles to Hz). The corresponding expression for the emissivity-change $\eta(t)$ of reflected electrons during erosion is more complicated:

$$\eta(t) = \frac{1}{J} \int_0^R \eta_1(N_s(r,t)) J(r) \, 2\pi r \, dr. \qquad (A.2)$$

The reasons are that the current density $J(r)$ enters into the integral, and the "local" η_1 depends on the instantaneous density, e.g. as η in fig. (4). The total current J (particles/s) is known from the current measurement with the Faraday cup.

Let us now include the reasonable assumption that the current density profile $J(r)$ has the same form as the (surface density) profile on the target. This means that any extrapolation of $\Delta\nu$ and η will lead to different periods for a complete erosion. In fact, it turns out that the fluence for an erosion determined as in sect. 3 is always less if estimated by the emissivity-change method than if estimated by the one involving frequency-change.

In the simplest case of a thickness-independent erosion yield Y_0 we obtain:

$$\Delta\nu(t)/\mu = JY_0 t: \qquad t \leqslant t_0 \qquad (A.3)$$

and

$$\Delta\nu(t)/\mu = B - (1-\alpha)B(t_0/t) + \tfrac{1}{3}(1-\alpha)^2 B(t_0/t)^2: \qquad t \geqslant t_0. \qquad (A.4)$$

$$t_0 = (1 + \alpha + \alpha^2) B/3JY_0 \qquad (A.5)$$

is the time to remove the central part of the spot. Eq. (A.3) corresponds to the linear part of the erosion, and eq. (A.4) to the subsequent erosion of the edge zone alone.

By extrapolating the linear part (A.3) to the asymptotic value B one may obtain the number Φ of beam particles necessary for an erosion as described in sect. 3.2:

$$\Phi = \frac{N_0 \pi R^2}{Y_0}. \qquad (A.6)$$

The corresponding extrapolation of eq. (A.2) results in a total number

$$\Phi = \frac{2(1+\alpha+\alpha^2)^2}{3(1+2\alpha+3\alpha^2)} \frac{N_0 \pi R^2}{Y_0}. \qquad (A.7)$$

This number, which has been determined after the procedure described in the emissivity-change method, is always smaller than the one determined from a frequency measurement. Only for the case $\alpha = 1$ (an erosion crater without edge zone) are the two numbers equal.

For both numbers (A.6) and (A.7) we obtain

$$\left(\frac{d\Phi}{dN_0}\right)^{-1} \pi R^2 = \frac{[(N_0 + \Delta N_0) - N_0]\pi R^2}{\Phi(N_0 + \Delta N_0) - \Phi(N_0)} = (1/c)\ Y_0. \qquad (A.8)$$

so that the instantaneous yield Y_0 is easily found from the derivative of $(N_0 \pi R^2)$ with respect to Φ. This expression leads immediately to eq. (5). The value of c is 1 for eq. (A.6) or equal to the fraction in eq. (A.7).

Unfortunately, it is possible to evaluate c analytically only for this simple case of a thickness-independent erosion yield Y_0. Otherwise, c has to be calculated numerically according to the specific dependence of the yield. In addition, eq. (A.8) is valid only in cases for which the thickness dependence of the yield $Y(x)$ is weak, e.g. for thicknesses comparable to the electron range. For our case ($\alpha = 0.7$) the yield is *at most* reduced by a factor $c = 0.8$. The correction has been performed in the present work, but we note that formula (5), even without the factor c, gives a satisfactory estimate of the yield $Y(x)$.

References

[1] R.E. Johnson and W.L. Brown, Nucl. Instr. and Meth. 198 (1982) 103.
[2] R.E. Johnson and W.L. Brown, Nucl. Instr. and Meth. 209/210 (1983) 469.
[3] T.A. Tombrello, in Desorption induced by electronic transitions, eds., N.H. Tolk, M.M. Traum, J.C. Tully and T.E. Madey (Springer, Berlin, 1983) p. 239.
[4] P. Børgesen and H. Sørensen, Phys. Lett. A90 (1982) 319.
[5] S.K. Erents and G.M. McCracken, J. Appl. Phys. 44 (1973) 3139.
[6] W.L. Brown, L.J. Lanzerotti, J.M. Poate and W.M. Augustyniak, Phys. Rev. Lett. 40 (1979) 1027.
[7] R. Pedrys, R.A. Haring, A. Haring, F.W. Saris and A.E. de Vries, Phys. Lett. 82A (1981) 371.
[8] R. Pedrys, R.A. Haring, A. Haring and A.E. de Vries, Nucl. Instr. and Meth. B2 (1984) 573.
[9] P. Børgesen, Risø Report, R-457, Risø National Laboratory (1982).
[10] T.A. Tombrello, Rad. Effects 65 (1982) 149.
[11] W.L. Brown, L.J. Lanzerotti and R.E. Johnson, Science 218 (1982) 525.
[12] O. Gröbner and R.S. Calder, IEEE Trans. Nucl. Sci. NS-20 (1973) 760.
[13] P. Børgesen, J. Schou and H. Sørensen, in Proc. Symp. on Sputtering, Perchtoldsdorf/Wien, Austria, (April 1980) eds., P. Varga, G. Betz and F.P. Viehbock (Institut für Allgemeine Physik, Technische Universität Wien, Austria 1980) p. 822.
[14] C.T. Chang, L.W. Jørgensen, P. Nielsen and L.L. Lengyel, Nucl. Fus. 20 (1980) 859.
[15] S.L. Milora, J. Fus. Energy 1 (1981) 15.
[16] P. Sigmund, in Sputtering by particle bombardment I, ed., R. Behrisch (Springer, Berlin, 1981) p. 9.
[17] M.L. Knotek, Phys. Scripta T6 (1983) 94.
[18] T.E. Madey, F.P. Netzer, J.E. Houston, D.M. Hanson and R. Stockbauer, in Desorption induced by electronic transitions, eds., N.H. Tolk, M.M. Traum, J.C. Tully and T.E. Madey (Springer, Berlin, 1983) p. 120.
[19] H. Schirrwitz, Beitr. Plasmaphys. 2 (1962) 188.
[20] P. Børgesen, J. Schou, H. Sørensen and C. Claussen, Appl. Phys. A29 (1982) 57.
[21] C. Claussen, Thesis, University of Odense (1982).
[22] J. Schou, P. Børgesen, O. Ellegaard, H. Sørensen and C. Claussen, to be published.
[23] P. Børgesen, J. Schou and H. Sørensen, to be published.
[24] O. Ellegaard, J. Schou, H. Sørensen and P. Børgesen, to be published.
[25] H. Sørensen, Appl. Phys. 9 (1976) 321.
[26] H. Sørensen and J. Schou, J. Appl. Phys. 49 (1978) 5311.
[27] H. Sørensen and J. Schou, J. Appl. Phys. 53 (1982) 5230.
[28] A.W. Warner, in Ultra micro weight determination in controlled environments, eds., S.P. Wolsky and E.J. Zdanuk (Wiley, New York, 1969) p. 137.
[29] L.L. Levenson, Nuovo Cimento, Suppl. Ser. I 5 (1967) 321.
[30] I.M. Bronshtein and B.S. Frayman, Rad. Eng. Electron Phys. 7 (1962) 1530 [Radiotekhn. Elektron. 7 (1962) 1643].
[31] P. Børgesen and H. Sørensen, Nucl. Instr. and Meth. 200 (1982) 571.
[32] F. Besenbacher, J. Bøttiger, O. Graversen, J.L. Hansen and H. Sørensen, Nucl. Instr. and Meth. 191 (1981) 221.
[33] F. Besenbacher, J. Bøttiger, O. Graversen, J.L. Hansen and H. Sørensen, Nucl. Instr. and Meth. 188 (1981) 657.
[34] H. Niedrig, Scanning 1 (1978) 17.
[35] J. Schou, Risø Report R-391, Risø National Laboratory (1979).
[36] W.L. Brown, W.M. Augustyniak, L.J. Lanzerotti, R.E. Johnson and R. Evatt, Phys. Rev. Lett. 45 (1980) 1632.
[37] J. Schou and H. Sørensen, J. Appl. Phys. 49 (1978) 816.
[38] I.M. Bronshtein and V.M. Stozharov, Sovjet Physics – Solid State 12 (1971) 2280 [Fiz. Tverd. Tela 12 (1970) 2824].
[39] J.W. Coburn, H.F. Winters and T.J. Chuang, J. Appl. Phys. 48 (1977) 3532.
[40] R.J. Loveland, P.G. Le Comber and W.E. Spear, Phys. Rev. B6 (1972) 3121.
[41] P.G. Le Comber, J.B. Wilson and R.J. Loveland, Solid St. Comm. 18 (1976) 377.
[42] D.J. Lepoire, B.H. Cooper, C.L. Melcher and T.A. Tombrello, Rad. Effects 71 (1983) 245.
[43] W.L. Brown, W.M. Augustyniak, E. Brody, B. Cooper, L.J. Lanzerotti, A. Ramirez, R. Evatt and R.E. Johnson,

Nucl. Instr. and Meth. 170 (1980) 321.
[44] W.L. Brown, W.M. Augustyniak, K.J. Marcantonio, E.H. Simmons, J.W. Boring, R.E. Johnson and C.T. Reimann, Nucl. Instr. and Meth. B1 (1984) 307.
[45] G.M. McCracken, Vacuum 24 (1974) 463.
[46] H.H. Farrell, M. Strongin and J.M. Dickey, Phys. Rev. B6 (1972) 4703.
[47] P. Sigmund and M. Szymonski, Appl. Phys. A33 (1984) 141.
[48] Rare gas solids, vol. 2, eds., M.L. Klein and J.A. Venables, (Academic Press, New York, 1977) pp. 687–689.

Erosion of solid neon by keV electrons

J. Schou, P. Børgesen,* O. Ellegaard, and H. Sørensen
Department of Physics, Association EURATOM–Risø National Laboratory, P.O. Box 49, DK-4000 Roskilde, Denmark

C. Claussen
Fysisk Institut, Odense Universitet, DK-5230 Odense M, Denmark

(Received 23 December 1985)

The erosion of solid neon by keV electrons has been studied experimentally and theoretically. Electronic sputtering as well as temperature-enhanced sublimation are investigated by a frequency-change measurement on a quartz crystal or in some cases by the change in intensity of reflected electrons. The erosion yield increases with increasing temperature for substrate temperatures above 7 K. Below this temperature sputtering via electronic transitions is the dominant process. The yield shows a clear minimum for film thicknesses about $(5-7)\times10^{16}$ Ne atoms/cm^2 for 2-keV electrons. The sputtering yield for thick films has a maximum at 1.2–1.5 keV. The results are explained by the diffusion of excitations to the surface with subsequent decay. From this model and the experimental results one derives a characteristic diffusion length of about 1×10^{17} Ne atoms/cm^2. The eventual particle ejection is driven by decay of surface-trapped excitons or by dissociative recombination. The magnitude of the yield indicates that deexciting neon particles at the surface induce further sputtering. Direct sputtering from electron-nucleus collisions does not contribute significantly to the yield.

I. INTRODUCTION

The erosion of condensed gases by ions or electrons plays an important role in many fields. In interstellar and planetary atmospheric problems the recent laboratory data for erosion are expected to have implications for the competition of collection and loss of volatiles by icy bodies in space.[1–3] In technological problems such as cryopumping in radiation environments,[4] the phenomenon has also turned out to be important. A particular case is the study of erosion of hydrogen pellets in a plasma.[5,6]

The erosion of condensed gases by charged particles has been investigated intensively during the past years.[2,7–12] The types of phenomena studied range from electronic sputtering alone to beam-induced evaporation at high current densities or at high temperatures. Most of the experiments have been performed for ion bombardment, and the results typically exceed the estimates of ordinary sputtering theory[13] by orders of magnitude. There is little doubt that the large erosion yields for the condensed gases are essentially caused by the energy initially deposited in electronic excitations. However, in addition, there may be a significant contribution from nuclear stopping for sufficiently low energy ions. Various models, more or less related to electron-stimulated desorption, have been presented in an attempt to explain how the energy is transferred to atomic motion.[9,10,14–18] Sputtering via electronic transitions is well known from irradiation of alkali halides,[19] for which the yield is above ten at electron bombardment below 1 keV at temperatures of about 600 K.

Measurements of the erosion of solid rare gases as a result of particle bombardment have been carried out by several groups.[2,7,9,15,16,20,21] Energy spectra of ejected particles from ion-bombarded solid argon[22] and krypton[11,22] have been reported as well. In addition, some erosion measurements have been combined with or performed by luminescence studies.[12,15,16,23] These studies complement a large number of studies on luminescence from electron-irradiated solid rare gases, e.g., Refs. 24–27.

Several of these experiments demonstrate clearly that there is a close connection between electronic sputtering and luminescence for solid neon and argon. Brown *et al.* measured the electronic sputtering of solid argon as a result of MeV light-ion bombardment, and correlated the thickness dependence of the yield with the emission of the strong 9.8-eV line from exciton decay in argon.[15,16] They indicated that the processes leading to particle ejection were primarily a generation of hole-electron pairs, diffusion of holes, and subsequent dissociative recombination close to the surface. An additional contribution to the yield was ascribed to the radiative decay of molecular argon excitons to the repulsive ground state. This latter mechanism for converting electronic excitations into atomic motion was suggested previously by the present authors,[18,20] and a significant effect was predicted for argon-doped solid neon.

The erosion yield at electron bombardment turned out to be a factor of 2 larger for pure solid neon than for neon with even very small amounts of impurities. This effect was explained by the reduced diffusion length of the free excitons in solid neon.[20] A similar decrease in the sputtering yield for argon was observed after doping with oxygen.[16] Coletti *et al.*[12] measured the correlation between luminescence intensity and the condensation rate of argon on graphite during low-energy-electron bombardment. They demonstrated that the sputtering rate was proportional to the density of vibrationally excited, molecular ex-

citons at the surface.

In many respects, neon deviates from the heavier rare gases. The band gap is considerably larger[28,29] (≈ 21.6 eV) and the bottom of the conduction band lies higher above the vacuum level in neon ($V_0 \approx 1.3$ eV) than in solid argon[28] ($V_0 \approx 0.4$ eV). Contrary to all the heavier rare gases, a large fraction of the excitons in neon are present as atomic excitons.[24,27,30,31] The magnitude of this fraction has turned out to be strongly influenced by the type of primary excitation, e.g., x-ray irradiation or bombardment by low-energy electrons.[30,32] For solid neon, vibrational relaxation of molecular excitons Ne_2^* shows up to be very inefficient compared to molecular excitons in, for example, solid argon, but the relative population of the vibrational levels also depends on the sample quality and on the location of the trapped exciton in the sample.[30] Furthermore, the diffusion lengths for optically excited free molecular excitons in solid neon have turned out to be more than 1 order of magnitude larger than for argon.[33]

In the present work we have studied the erosion of solid neon for a variety of experimental parameters. In several respects neon is one of the most appropriate materials for electron-induced erosion (and sputtering) of all: The yield is high, and the thickness dependence of the yield is weak above 2×10^{17} Ne atoms/cm^2. On the other hand, solid neon is so volatile that all experiments have to be performed close to liquid-helium temperature. Poor heat conduction from the substrate to the cooling aggregate will immediately lead to beam-induced evaporation from the solid neon.[7]

The erosion has been studied by two independent methods described previously:[7] The fo. ous combination of a large yield and an atomic mass, which is not too small, means that erosion of neon by keV electrons could be studied systematically with a quartz-crystal microbalance (the frequency-change method). In addition, a large number of measurements were performed by determining the number of electrons needed to remove the neon film from a massive gold substrate. The variation of the electron emission was used here to indicate when the film had been eroded away (the emissivity-change method). Neon is also well suited to this method, since the yield of high-energy secondaries (the reflection coefficient) varies by a factor of 2 from thick films of neon to the gold substrate.

The present work contains a short description of the experimental setup and of the two methods used. The first systematic experimental results for neon are presented and discussed in view of the existing theoretical models. In particular, we shall discuss possible deexcitation modes that may provide energy for the particle ejection.

II. EXPERIMENTAL SETUP AND METHODS

The basic experimental setup as well as the methods utilized have been described in great detail recently.[7,17] Here we shall only briefly outline the principles.

A film of solidified neon is produced by letting a jet of cooled gas impinge on a massive gold target plate or on an oscillating quartz crystal (Fig. 1). In both cases the substrate is cooled to a temperature close to that of liquid helium. For deposition on the crystal the film thickness is

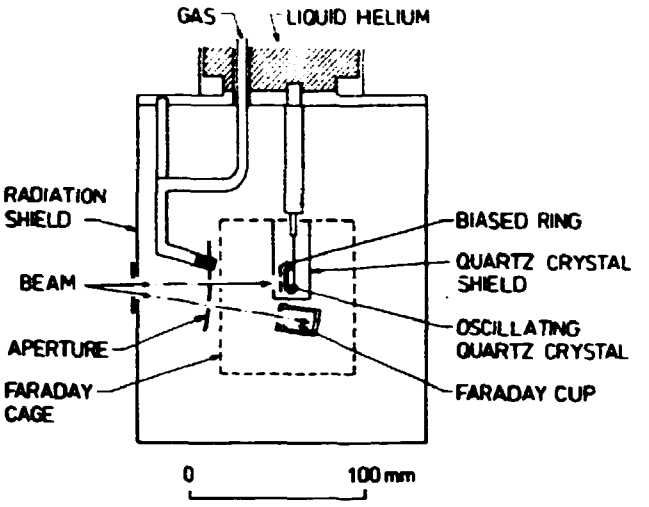

FIG. 1. Schematic drawing of the target region of the experimental setup. The quartz crystal may be replaced by a massive target plate.

determined directly from the frequency change, whereas the thickness for the massive target plate is determined by a careful calibration procedure. A typical deposition rate was 3×10^{15} Ne atoms/cm^{2}sec. A film may be removed rapidly just by heating the target area with an electric heater.

Beams of (1–3)-keV electrons are obtained from a small electron gun, and swept horizontally and vertically by two independent sawtooth voltages over a 2-mm aperture in front of the target, thus ensuring a homogeneous irradiation of a large part of the target area. It is known that the erosion profile in the film resembles a truncated frustum of a right circular cone.[7] The substrate is partially heated by the incident electron beam, but care is taken to keep the temperature about or below 6 K, where the erosion is insensitive to target temperature. The current density was usually kept below 10 μA/cm^2, where the evaporation caused by beam heating is insignificant.[7]

The target plate as well as the crystal are electrically insulated from the cryostat, and during irradiation the target current will generally differ from the true beam current because of the emission of secondary and reflected electrons (and possibly ions). A negative bias of -45 or -90 V applied to a very open grid or merely a repeller ring will suppress almost all secondary-electron emission. The true beam current is measured by deflecting the beam into a Faraday cup below the target area. The target region and the Faraday cup are both located inside an electrically grounded Faraday cage. Cup, cage, grid (or repeller ring), and quartz-crystal shield are all heated to temperatures sufficiently high to prevent the gas from condensing on them. In this manner we attempt to minimize disturbing effects from areas that may charge up.

The *frequency-change method* utilizes the possibility of measuring instantaneously the mass change on a quartz-crystal microbalance during particle bombardment. The increasing frequency is measured during erosion, and the slope of the frequency curve may then be applied to a direct determination of the erosion yield for a known

beam current. An example is shown in Fig. 2 for two different grid voltages. For both curves one notes an almost linear part which corresponds to a yield of approximately 30 Ne atoms per electron. A typical film deposition of 4×10^{17} Ne atoms/cm^2 on the silver electrode corresponds to a frequency shift of approximately 600 Hz. The subsequent erosion by the beam results in a frequency increase of about 150 Hz, which means that only a fraction of the total deposited mass is removed. In this way we obtain a satisfactory determination of the spatial extension of the erosion spot as well.

The *emissivity-change* method exploits the variation of the secondary-electron emission from the target for decreasing film thicknesses. In particular, the total number of electrons that are necessary to obtain the electron emission characteristic for the substrate (i.e., to remove the film) may be determined. We define an "electron-emission coefficient" η by

$$i_t^- = (1-\eta) i_b \,, \tag{1}$$

where i_b is the beam current measured with the cup and i_t^- the target current for a negative bias. The reflected electrons characterized by η will still have sufficient energy to escape. For thicknesses less than half the electron range, η increases almost linearly with decreasing thickness from the value of bulk neon ($\sim$0.2) to that of the gold or silver substrate ($\sim$0.4). The reflection coefficients depend slightly on the primary energy, but the method is applicable for the energies considered here.

The erosion yield Y for an initial thickness x is evaluated from

$$Y(x) \approx N \frac{d(Ax)}{d\Phi} \,, \tag{2}$$

where N is the number density, A the eroded area, and Φ the total number of electrons necessary for a complete erosion.[7] The area A must be found from another method, e.g., from the frequency-change method.

The measurements with the frequency-change method enable us to determine the erosion yield in a straightforward manner, but the thermal conduction between the cryostat and the beam-impact area on the crystal has to be sufficiently good, so that unnecessary heating of the area is avoided. This may be controlled by comparing the results to those from the emissivity-change method applied to an ordinary, massive plate with good thermal conduction to the cryostat (and thermometer). The disadvantages of the emissivity-change method are that the erosion must continue until the substrate is reached, and that one requires knowledge of the area of the eroded spot. However, the two methods supplement each other, and in many cases have been used simultaneously for erosion measurements.

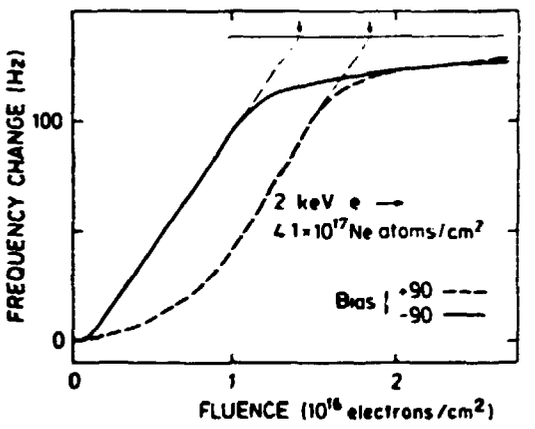

FIG. 2. Erosion of a 4.1×10^{17}-(Ne atoms/cm^2) thick film on a quartz crystal by 2-keV electrons. The frequency change is plotted versus fluence. Grid bias, + 90 V (— — —) and −90 V (——). The arrows indicate the fluence necessary for a complete erosion.

A direct comparison between the two methods is possible if the linear part of the frequency curve is prolonged as shown in Fig. 2: The intercept between the linear part and the asymptotic level determines a fluence necessary for completing the erosion. Since one evaluates the fluence for the erosion measurements with the emissivity-change method in a similar way, one may compare the fluences obtained from the two methods.[7]

Since the erosion of solid neon has appeared earlier to be sensitive to the presence of small impurities, the gas inlet tube was cooled down to temperatures for which only neon and hydrogen can pass. Contamination with hydrogen and deuterium was minimized, e.g., by heating the cryogenic system to room temperature before experiments with neon.

III. EXPERIMENTAL RESULTS

In the following subsections we shall describe the dependence of the yield on several experimental parameters, as well as the agreement between the results obtained by the two different methods.

A. Dependence on grid voltage

Practically all erosion measurements on the present setup have been performed with a negatively biased grid (−45 or −90 V). Apart from neon and argon all materials investigated so far show no dependence on the grid voltage. Since many of the solidified gases are insulating materials with high secondary-electron emission coefficients, charge-up problems during erosion may be substantially reduced by such a negative bias.

In Fig. 2 the erosion of a Ne film with positive and negative grid bias is shown. One notes that the yield during the linear part of the erosion is essentially identical for both voltages, but since the erosion with positive bias increases much more slowly than the one with negative bias, the necessary fluence for an erosion becomes more than 30% larger with positive bias.

This result has been confirmed through a number of measurements with the emissivity-change method for other film thicknesses and electron energies. The fluence with positive bias is usually larger, occasionally by more than a factor of 3.

The fluence is influenced by the magnitude of the positive grid bias as well. Measurements with the emissivity-change method have demonstrated that the fluence does

not vary for grid voltages from −100 up to about +10 V. Then the fluence increases drastically in the interval from 10 to 30 V. For voltages larger than 30 V no further enhancement of the fluence takes place.

We have chosen mainly to consider the erosion yield obtained with negative bias. Since the maximum yields during an erosion are similar, one then avoids the complex behavior with a "delay" in the erosion for positive bias. Results obtained with the frequency-change method are then compared with those with the emissivity-change method. One notes that the curve in Fig. 2 measured with negative bias is almost linear during most of the erosion.

B. Comparison between the two methods

Results obtained by the two methods—frequency and emissivity change—are shown in Fig. 3. The initial thickness has been depicted as a function of the fluence necessary to complete the erosion. Only points obtained for an erosion on a quartz crystal are directly indicated. Fluences measured for a gold as well as a silver electrode are shown, and in some cases simultaneous results obtained with the emissivity-change method are included. The average erosion yield from previous emissivity-change measurements on a massive gold target is indicated as well. One notes the convincing agreement for all thicknesses.

The agreement between the results obtained by the two methods on a massive gold target and on a quartz crystal demonstrates that the surface of the quartz crystal apparently is so cold that essentially no beam-induced evaporation takes place.

According to Eq. (1), one may estimate the yield for 2-keV electrons on neon from the slope of the curve produced by the data points. The slope shown in Fig. 3 corresponds to a yield of ~28 Ne atoms/electron.

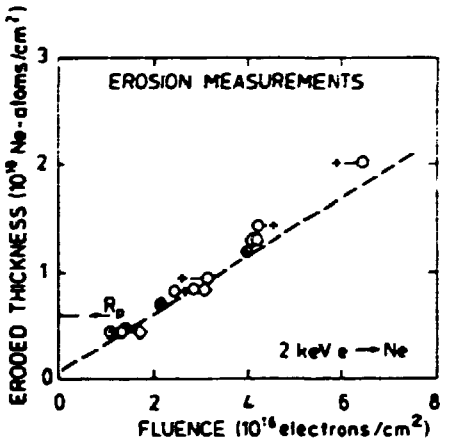

FIG. 3. Sputtering measurements by the emissivity-change and the frequency-change method for 2-keV electrons incident on neon. The eroded thickness is plotted versus the fluence necessary for an erosion (cf. Fig. 2). +, frequency change for a Ag electrode as substrate; ◇, frequency change for a Au substrate; ○, simultaneous emissivity-change measurements; – – –, previous results on a massive Au substrate by the emissivity-change method. (The beam-spot area for the two latter ones is taken from the frequency-change method.) R_p is the estimated range of 2-keV electrons in neon.

C. Dependence on temperature

As described in the previous subsection, one has to ensure that the erosion is performed below the temperature regime in which the erosion yield increases with temperature. This is conveniently done by the emissivity-change method using a massive gold substrate that is heated by an electrical heater. Because of the good heat conduction from the heater (and the thermometer) to the interface, we are able to determine the substrate temperature. The precise temperature at the beam spot on the film is, of course, known only approximately. The thermometer was approximately calibrated, so temperatures are uncertain (on an absolute scale) by ±0.2 K.

In Fig. 4 the yield has been depicted as a function of the average substrate temperature. The results have been obtained by the emissivity-change method for a film thickness of 3.2×10^{17} Ne atoms/cm^2, corresponding to a value not too far from the thickness-independent region (cf. Sec. III D). The yield is seen to increase with substrate temperature above about 6 K.

The sublimation flux from an isothermal surface as estimated from Eq. (5) (Sec. IV B) is included in Fig. 4. For the primary current used, one may estimate the sputtered flux to about 5×10^{13} Ne atoms/sec. The sublimation flux from the irradiated area (≃7 mm^2) then exceeds the sputtered flux at temperatures above 8 K. One notes the similar increase for the sublimation flux and the flux of eroded particles.

D. Dependence on film thickness

Results for 2-keV electrons incident on neon films deposited on the quartz crystal are shown in Fig. 5. These points have all been determined by the frequency-change method, since the variation of η with film thickness below 1×10^{17} Ne atoms/cm^2 is insufficient.

One notes the clear minimum slightly below 1×10^{17} Ne

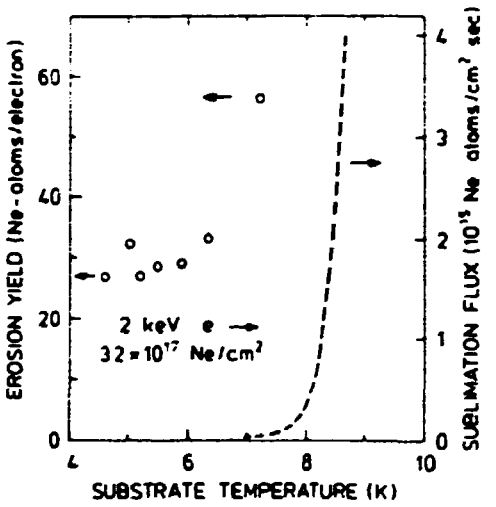

FIG. 4. Erosion of a 3.2×10^{17}-(Ne atoms/cm^2)-thick film on a massive gold plate by 2-keV electrons. The yield [Eq. (2)] is plotted versus the substrate temperature. The beam-spot area has been normalized as in Fig. 3. – – –, sublimation flux [Eq. (5)].

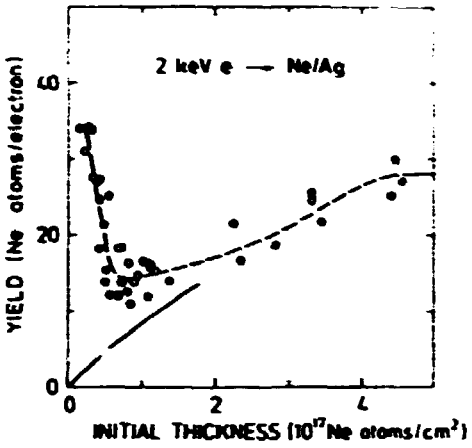

FIG. 5. Sputtering yield of solid neon resulting from bombardment of 2-keV electrons measured by the frequency-change method. The yield is plotted versus the initial thickness. The silver electrode of the crystal serves as a substrate. – – –, curve drawn to guide the eye. ——, Eq. (20) with $ff_e = 3$ and $I_0 = 1 \times 10^{17}$ Ne atoms/cm^2.

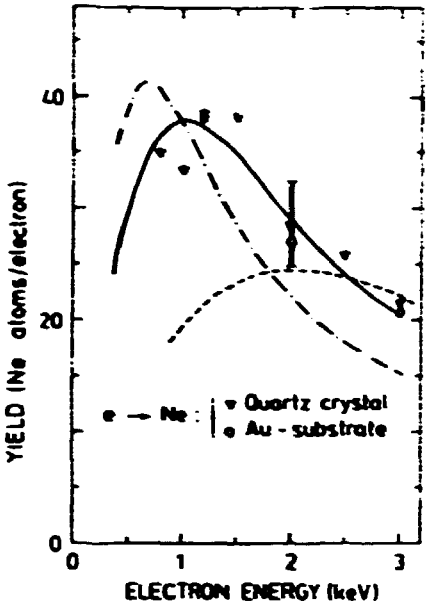

FIG. 6. Sputtering of 4.5×10^{17}-(Ne atoms. cm^{-2})-thick films by keV electrons. The yield is plotted versus the primary electron energy. Only the average value is indicated at each energy. V, the frequency-change method with the standard deviation indicated at 2 keV. O, the emissivity-change method with the beam-spot area as in Fig. 3. – – –, calculated yield from Eq. (16), $I_0 = 3 \times 10^{17}$ Ne atoms/cm^2 and $ff_e = 1$; ——, $I_0 = 1 \times 10^{17}$ Ne atoms/cm^2 and $ff_e = 3$; –·–, $I_0 = 0.5 \times 10^{17}$ Ne atoms/cm^2 and $ff_e = 5$.

atoms/cm^2, and the slowly increasing yield from this minimum up to approximately 4.5×10^{17} Ne atoms/cm^2. Above this thickness almost no further enhancement takes place. The strong increase for decreasing thicknesses below the minimum leads to a thin-film yield that exceeds the "bulk" yield of ~28 Ne atoms/electron substantially. For practical reasons the measurements were carried out on several crystal holders of slightly different construction, but the data show the same trend. A similar behavior with a minimum positioned at about the same thickness was observed for 3-keV electrons.

For these measurements we have utilized only the initial yield, as the cone profile of the eroded film makes it difficult to deduce a proper thickness dependence during the later stages of an erosion. For example, the high yield for small film thicknesses may easily be hidden in statistical fluctuations in the frequency during the erosion of thick films.

E. Energy dependence

The yield of a 4.5×10^{17}-(Ne atoms/cm^2) film is shown in Fig. 6 as a function of primary energy. The data have been obtained either by the frequency-change method on a quartz crystal with a silver electrode or by the emissivity-change method with a massive gold substrate.[20] The thickness investigated is close to the thickness-independent regime, and comparable to the range of 1.7-keV electrons in materials of similar atomic number, e.g., nitrogen and oxygen.[34,35]

The yield curve has a maximum approximately at 1.2–1.5 keV, and decreases with increasing energy almost proportionally to the stopping power. The general trend is similar for the two different kinds of data points. The previous data[20] were underestimated by a constant factor of about 2.5 that accounts for the actual magnitude of the eroded area.[7] These measurements were carried out only down to the primary energy 1.2 keV because of insufficient beam intensity. Unfortunately, it was not possible to carry out reliable measurements at energies below 0.8 keV because of beam-adjustment problems.

F. Influence of impurities

Recent measurements with the emissivity-change method on an ordinary gold substrate demonstrated that a small amount of impurities may increase the fluence necessary for an erosion by more than a factor of 2.[20]

Examples of such sputtering measurements are shown in Fig. 7. The reference measurement with pure neon was performed before any argon was let in. The other two measurements were carried out with films contaminated with argon. The contaminant was either regularly added to the neon gas in the gas container or merely present in the cryostat from previous runs with doped neon films. The sputtering is apparently much slower for the contaminated neon film.

A sequence of sputtering measurements on argon-doped neon films were performed in this way for concentrations that varied from 0.05 to 5 at.% argon (in the gas container before inlet to the cryostat). The results indicated no clear dependence on the argon content, except for large concentrations. Apparently, the fluence decreased with the concentration above an argon content of 1 at.%.[20]

In these measurements the gas tube in the cryostat has to be heated to a temperature that allows the less volatile argon to enter into the target region as well. In the reference measurements with pure neon the tube was also heated in order to keep the experimental parameters practical-

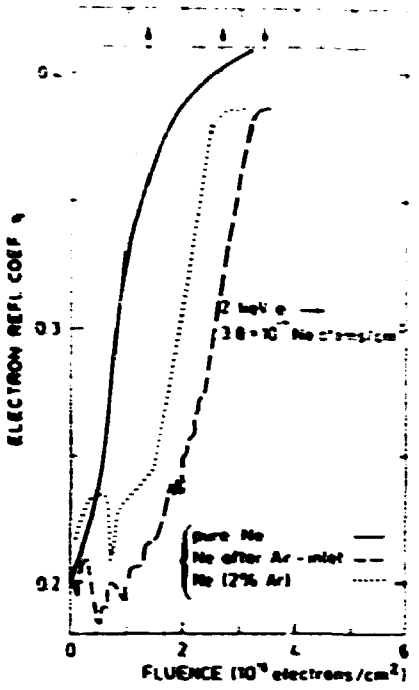

FIG. 7. Sputtering of 3.8×10^{17}-(Ne atoms/cm^2)-thick films by 2-keV electrons. The electron-reflection coefficient is plotted versus the fluence. The measurements have been performed by the emissivity-change method on a massive Au substrate. ——, for a pure neon film; – –, for a neon film deposited after a previous argon inlet; · · ·, for a neon film doped with 2 at.% argon.

ly identical. These measurements were difficult to reproduce with the frequency-change method. The film deposition on a massive gold substrate at elevated gas-tube temperature is probably largely different from that on a silver electrode of a quartz crystal because of the different surface conditions.

G. Comparison with other measurements on condensed gases

The slow sputtering of solid neon with a positive *bias* compared to a negative one has no parallel in erosion of other condensed gases.[7]

A strong dependence of the yield on the *temperature* has been observed for the solid rare gases argon and xenon.[9,21] Although the enhancement of the yield occurs at much higher temperatures for these much less volatile gases, the general trend is similar for all these targets.

The effect of an increasing *current density* on the erosion yield has also been considered by several groups.[9,21]

A dependence on the film *thickness* has been observed for solid rare gases at MeV-ion bombardment.[9,15,16,21] In all cases the yield reaches the "bulk" value between 2×10^{17} and 4×10^{17} atoms/cm^2. In particular, for xenon on a beryllium substrate the yield is found to increase, as is also seen for neon above 1×10^{17} atoms/cm^2 (Fig. 5). The sputtering of xenon on a 2000-Å layer of frozen SF_6, on the other hand, resulted in a clearly decreasing yield with increasing film thickness. For nitrogen and oxygen bombarded by electrons, the yield only decreases slightly with thickness.[7]

The *energy dependence* of the yield for light MeV ions on solid argon was previously asserted to be proportional to the square of the stopping power,[9] but recent measurements on argon show a linear dependence rather than a quadratic dependence on the stopping power.[16] With the present setup, not only the yield of solid neon for energies above 1.5 keV, but also the yield of nitrogen and oxygen, seems to be almost proportional to the stopping power for the primary electrons.[17]

The *magnitude of the yield* for neon at 2 keV is significantly larger than the corresponding electron-induced yield of 8 D_2-molecules/electron for solid deuterium[7] in spite of the much larger sublimation energy for the former (20 meV/Ne-atom) compared to 12 meV/D_2-molecule. The yield is even comparable to that for solid hydrogen.[36]

IV. THEORY I: DIRECT SPUTTERING AND BEAM-INDUCED EVAPORATION

The solid rare gases are all characterized by the weak interatomic van der Waals binding, corresponding to sublimation energies from 0.17 eV/atom for xenon down to 0.02 eV/atom for neon.[29] This low-energy value means that any electronic excitation or initiated atomic motion in neon may lead to a *high* sputtering yield, even if the mechanism involved has a low efficiency. In addition, the maximum energy transfer to a neon atom in an electron-nucleus collision for a keV electron is an order of magnitude larger than the surface binding energy. Furthermore, beam-induced sublimation may, of course, also easily contribute to the erosion yield because of this low binding energy.

In the present section we shall consider two possible mechanisms for erosion: (A) sputtering resulting from electron-nucleus collisions, and (B) erosion caused by beam heating or external heating. Sputtering via electronic transitions will be treated in Sec. V.

A. Direct electron sputtering

It is well known that sputtering resulting from direct electron-nucleus collisions may occur.[37] Since most metals have a surface binding energy of a few eV, beam energies in the MeV regime are usually necessary for a significant sputtering yield. This process is, of course, analogous to ordinary ion-induced sputtering, in which the kinetic energy is transferred directly from the primary atom to target atoms.

A 2-keV electron may transfer up to 0.2 eV to a neon nucleus at rest. With an efficiency of 1 (which, of course, is strongly overestimated) this would lead to a yield of 10 Ne atoms per such an event. The actual total yield from direct sputtering obviously depends strongly on the scattering cross section. In order to estimate the cross section we shall adopt the nonrelativistic expression from Berger *et al.*[38] for the differential cross section for elastic scattering:

$$\frac{d\sigma}{d\Omega}=\frac{Z^2e^4}{4E^2(1-\cos\theta+2\eta_s)^2}K_{rel}(\theta)\,, \tag{3}$$

where θ is the deflection angle and K_{rel} a factor (≈ 1) that includes spin and relativistic effects. As usual, Z is the atomic number and e the elementary charge. The screening parameter η_s has been evaluated to

$$\eta_s = 1.7\times 10^{-5} Z^{2/3}/[\tau(\tau+2)] , \quad (4)$$

where τ is the kinetic energy in units of the electron rest energy. A scattering in which a 2-keV electron transfers energy greater than $U_0 = 20$ meV to a neon nucleus corresponds to a scattering process in which the deflection angle exceeds $\theta \approx 10°$. Even though the angle is comparatively small, the cross section for this is about 2×10^{-17} cm^2. This means that such a collision happens on the average solely 8 times within the thickness 4×10^{17} Ne atoms/cm^2, from which the processes obviously contribute the yield, following Fig. 5. Since small scattering angles are dominant, and since any sequence of recoiling nuclei initiated by the struck nucleus is unable to transfer energy over thicknesses comparable to the electron range, at most a minor fraction of the yield may originate from this direct process. Although we have ignored the slowing down of primaries (and the subsequent enhancement of the scattering cross section), we may definitely consider sputtering via electronic transitions to be far more important.

B. Erosion by heating

Evaporation as a result of beam heating or external heating has been reported in several experiments.[7,9,21,39–41] Such a mechanism has even occasionally been asserted to be the dominant process.[21,42] In any case, it is clear that evaporation may contribute to the total yield, and even exceed the nonthermal component from beam-induced electronic transitions by more than several orders of magnitude.

The yield increase caused by substrate heating was estimated from the sublimation flux from an isothermal surface in Sec. III C. This estimate was used for solid argon to explain the temperature dependence of the yield as well.[9] The evaporation flux Ψ is given by

$$\Psi(T) = \gamma P(T)(2\pi M k_B T)^{-1/2} , \quad (5)$$

where γ is the condensation efficiency ($\gamma \approx 1$), $P(T)$ the sublimation pressure at the temperature T, k_B Boltzmann's constant, and M the mass of an neon atom.

We note that any reliable erosion on solid neon without substantial sublimation has to be performed on a substrate below 7 K.

The yield increase Y_{sp} (where sp denotes spike) as a result of high current density is well described by the late-stage component of a low-temperature spike:[43]

$$Y_{sp} = \frac{1}{J}[\Psi(T_a + \Delta T_{eff}) - \Psi(T_a)] , \quad (6)$$

where J is the current density, T_a the ambient target temperature, and ΔT_{eff} the average temperature rise of the target. The evaporation rate $\Psi(T)$ (number of evaporated atoms per unit time and area) may be estimated from experimental data on vapor pressure from the solidified gases, e.g., by use of Eq. (5).

The starting point for the spike treatment is a variation of a well-known problem in the mathematical theory of heat transfer. An initial heat pulse along a track perpendicular to the surface results in a temperature increment of cylindrical geometry in the semi-infinite medium. The temperature rise at the surface leads then to an enhanced evaporation.

The solution to the problem reduces to Eq. (6) if the initial heat input is sufficiently low, e.g., a stopping power of the order of 1 eV per 10^{15} atoms/cm^2. In addition, the temperature rise ΔT_{eff} due to the beam has to be considerably lower than the ambient temperature T_a.

The best agreement to the yield increase Y_{sp} was obtained for $T_a = 6.6$ K and $\Delta T_{eff} = 0.13J$ K (J in μA/cm^2). This corresponds to a temperature rise of about 1 K up to 4.5 K at the highest current density. Then, the temperature in the beam spot for low current densities is estimated to be about 7 K, which agrees well with the data from the massive gold substrate. In the cylindrical spike model this invokes a characteristical duration of the evaporation of the order of

$$t_{max} = \frac{\Delta T_{eff} C}{J(dE/dx)} , \quad (7)$$

where C is the heat capacity per unit volume and dE/dx the stopping power. t_{max} is about 100 μsec. The alternative case of a hemispherical spike, however, leads to a time of the order of 1 sec.

Later, the theoretical treatment[43] was extended to include heat loss through the boundary by evaporation,[44] but this does not change the previous results for low-temperature cylindrical spikes. The crater form is predicted to be very flat, i.e., the depth should be small compared to the lateral extension. A large lateral expansion of the beam spot up to an area 3–4 times larger than the usual beam spot has indeed been observed at the highest current densities.[7]

It should be noted that the erosion that takes place in our case at elevated current densities is fundamentally different from the laser-induced sputtering of oxides and compound semiconductors, where a similar energy-density dependence of the sputtering yield was observed.[45] This enhancement is definitely ascribed to the effect of dense electronic excitations.

V. THEORY II: SPUTTERING BY ELECTRONIC TRANSITIONS

The major problem in the sputtering of insulating materials is how the energy expended in electronic excitations and ionizations becomes available for atoms as kinetic energy.

A. Sputtering from electronic excitations: Constant density

Let us now regard sputtering from noble gases in terms of diffusion of excitations and subsequent *decay*[14,15,18,20] (Fig. 8). Electronic excitation and ionization by fast-charged particles in solid rare gases are known to produce luminescence from exciton decay.[26,28] However, a consid-

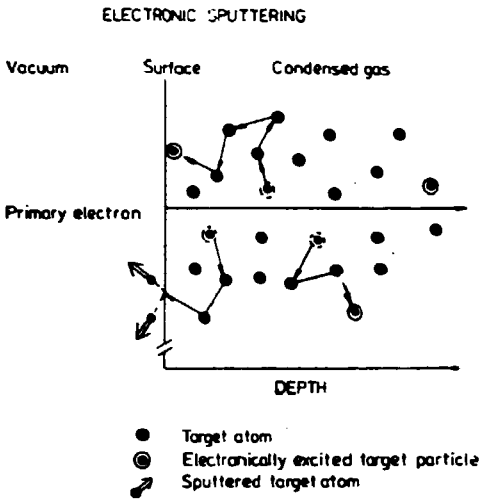

FIG. 8. Schematic drawing of electronic sputtering from electron incidence. The density of excited target particles is greatly exaggerated.

erable part of the total energy of excitons is not released as radiation, but transferred to the lattice through electronic deexcitations to repulsive states and multiphonon processes. The excitons in solid rare gases are highly mobile prior to self-trapping,[28] and a similar mobility has recently been asserted for the holes.[15]

In Ref. 20 we regarded the vibrationally excited molecular exciton R_2^* as the main "carrier" of electronic energy In the following treatment we shall derive results for sputtering originating from diffusion of excitations in a more general manner.

Let us consider an unspecified electronic excitation, e.g., a molecular exciton or a hole-electron pair, generated by charged-particle irradiation. We assume that this excitation may diffuse in a way similar to that of the lowest-lying excitons.[46] The concentration $C(\mathbf{r},t)$ of the free excitations must satisfy the diffusion equation

$$D\nabla^2 C=\frac{\partial}{\partial t}C+\frac{1}{\tau}C\ . \tag{8}$$

We further assume the initial condition

$$C(\mathbf{r},0)=n_0\delta(y)\delta(z)\quad \text{for } x>0\ , \tag{9}$$

i.e., constant depth density n_0 of excitations along the track at the time $t=0$. The latter term on the right-hand side of Eq. (8) represents the drain from the population, e.g., for mobile excitons or holes because of trapping or deexcitation. The diffusion constant D and the characteristic lifetime τ of the excitations in the mobile state are as usual related to the diffusion length $l_0=(D\tau)^{1/2}$. The δ functions $\delta(y)$ and $\delta(z)$ fix the impact of the primary in (0,0,0). The initial condition (9) corresponds to a uniform excitation density along the track of a charged particle as expected for a projectile with constant stopping power, e.g., a MeV proton up to quite large depths.

Equation (8) is solved by standard methods[18] for a semi-infinite medium, for which the plane $x=0$ corresponds to the surface. As a boundary condition, the surface is considered to be absorbing, i.e., C vanishes here:

$$C(0,y,z,t)=0\quad \text{for } t>0\ . \tag{10}$$

This boundary condition has been used in previous analyses of exciton diffusion.[46] The flux

$$j=-\left[-D\frac{\partial C}{\partial x}\right]_{x=0} \tag{11}$$

of excitations arriving at the surface then leads immediately to a total number of excitations,

$$\int_0^\infty dt\int dy\int dz\, j=n_0 l_0\ , \tag{12}$$

all of which originate from the single-particle track described by Eq. (9).

The diffusion equation utilized here is completely equivalent to the treatment given by Ophir *et al.*[46] and Reimann *et al.*,[15] although these authors predominantly considered steady-state excitation. Reimann *et al.* applied a reflecting surface as a boundary condition similar to that suggested by Schwentner *et al.*[47] from photoelectron-emission experiments. In our case the use of a reflecting surface leads to a yield that is much too small (cf. Sec. VI C).

In the case of a film of finite thickness, the system of equations has to be extended by an additional boundary condition for the film-substrate interface at $x=d$. As in all related work,[15,46,47] we regard the interface between the film and the metal substrate as absorbing in a manner analogous to Eq. (10). This leads to a modification of Eq. (12) by a factor $\tanh(d/2l_0)$.[18]

The number of excitations per depth, n_0, may be estimated by

$$n_0=fNS_e/W\ , \tag{13}$$

where N is the number density, S_e the electronic stopping cross section, and W the average energy expended to make a hole-electron pair. f is the number of this specific excitation per hole-electron pair, i.e., $f=1$ for diffusion of holes. (Note that the meaning of f is more general than that of Ref. 20.)

The total yield from an infinitely thick film then becomes

$$Y=(fNS_e/W)l_0 p f_e\ , \tag{14}$$

where p is the emission probability for an atom through a surface with a planar barrier about equal to the sublimation energy.[18] f_e indicates the average number of *ejected* atoms per deexcited molecule or atom at the surface, e.g., by a low-energy cascade as in the treatment suggested by Reimann *et al.*[15] Since the energy release at the surface from deexcitation is generally much larger than the sublimation energy, p is very close to unity for neon and argon.[18] Therefore, in the following treatment we usually neglect the factor p. We note that the bulk yield is proportional to the stopping power NS_e and to the diffusion length l_0. This result was presented in Ref. 20 as well.

The possible processes that lead to particle ejection at the surface will be considered in Sec. V C.

B. Diffusion of excitations for electron incidence

The simple approach, for which the excitation density has the constant value fNS_e/W along the track, is not applicable for electron bombardment. It is well known that the distribution of energy deposited in excitation and ionization varies considerably as a function of depth.[38,48] Furthermore, it is clear that the finite range of the electrons has to be included in the calculation. These two restrictions were not included in Ref. 20.

We approximate the distribution of electronic excitations by a Gaussian density for an electron of primary energy E:

$$n^*(\mathbf{r})=(fE/W)G(x)\delta(y)\delta(z)\,, \tag{15a}$$

where

$$G(x)=(2\pi\sigma_D^2)^{-1/2}\exp[-(x-r_D)^2/(2\sigma_D^2)]\,. \tag{15b}$$

fE/W is the number of excitations produced by the primary, and $r_D(E)$ and $\sigma_D(E)$ the mean range and standard deviation of the distribution. The latter two quantities are determined primarily by the atomic number of the target. As a good approximation both quantities may be regarded as proportional to the range. The reason for this is that the distribution of electronically deposited energy is very insensitive to variations of the primary energy, once the distribution is depicted in units of the stopping power $NS_e(E)$ versus the range $R_e(E)$ (cf. Ref. 48). Then the yield for an infinitely thick film becomes

$$Y=\tfrac{1}{2}(f_e fE/W)\exp(\sigma_D^2/2l_0^2-r_D/l_0)\times\operatorname{erfc}[\sigma_D/(\sqrt{2}l_0)-r_D/(\sqrt{2}\sigma_D)]\,, \tag{16}$$

where erfc is the complementary error function. This expression is depicted in Fig. 6 for several values of l_0 and the product ff_e.

We note that the ratios σ_D/l_0 and r_D/l_0 enter as arguments for the exponential function. For a fixed l_0 it means as expected that a broad distribution or a small mean range will lead to a large yield. The mean range r_D and the standard deviation σ_D for neon may be estimated from data for materials of similar atomic numbers.

From close inspection of the distribution of deposited energy for 2-keV electrons in atmospheric air in Ref. 38, we may then determine the proportionality constants

$$r_D=0.375R_e(E) \tag{17a}$$

and

$$\sigma_D=0.34R_e(E)\,. \tag{17b}$$

$R_e(E)$ is the extrapolated practical range in Ref. 38, which is in good agreement with the experimentally determined range in solid nitrogen[34] or oxygen.[35]

This relatively simple approach for large film thicknesses is unsuitable for small thicknesses, for which two modifications become necessary. The first important point is the additional boundary condition for an interface in the plane $x=d$, similar to the case of constant excitation density. If the atomic numbers of the condensed-gas film and the substrate are similar, the distribution of deposited energy becomes only slightly distorted relative to the distribution in a bulk film. Then, the Gaussian distribution (15) is still appropriate, and the yield becomes[49]

$$Y=(ff_eE/W)\left[\int_0^d G(x)\exp(-x/l_0)dx-\exp(-d/l_0)[\sinh(d/l_0)]^{-1}\times\int_0^d G(x)\sinh(x/l_0)dx\right]\,. \tag{18}$$

For the case of thin films on a widely different substrate, e.g., neon on a silver electrode, one has to use a completely different estimate for the excitation density in the film. We ignore the slowing down of primaries in the film, and let $r(E_0)\cos\theta_0 dE_0 d\cos\theta_0$ be the number of electrons reflected from the substrate with energy E_0 and polar angle θ_0 per primary. In this approximation we have utilized the knowledge that the reflected electrons exhibit a cosine distribution.[50] The total energy deposited by the primary and the backscattered electrons in the film then becomes

$$d\left[NS_e(E)+\int_0^E r(E_0)NS_e(E_0)dE_0\right]\,. \tag{19}$$

The first term in the large parentheses is the energy loss of the primary, and in the integral every reflected electron contributes with the energy $dNS_e(E_0)/\cos\theta_0$. Then, we obtain, for the total yield,

$$Y=(ff_e/W)\left[NS_e(E)+\int_0^E r(E_0)NS_e(E_0)dE_0\right]\times l_0\tanh(d/2l_0)\,. \tag{20}$$

For small thicknesses the yield increases with increasing film thickness d, and one notes that the yield for very thin films ($d/l_0\ll 1$) is independent of the diffusion length l_0. The approximation behind Eq. (20) is at least valid up to thicknesses of more than 1×10^{17} Ne atoms/cm^2 at the primary energy 2 keV. For larger thicknesses the excitation density increases considerably as a result of the slowing down and scattering of the primaries. The sum in the large parentheses has been evaluated on the basis of a known electron spectrum, $r(E_0)$,[51] and a semiempirical compilation of the stopping power $NS_e(E_0)$ for neon.[52] The result for 2 keV is $1.5NS_e(E)$, which means that the backscattered electrons on the average deposit half as much energy as the incident ones at the surface.

C. Energy-release processes

The fundamental channels of deexcitation of hole-electron pairs and excitons in solid neon[30,53–55] may end up in lattice distortions or sputtering. These processes occur even for transitions with an energy release of about or below 100 meV, since the sublimation energy for neon (and for argon) is comparatively low. Below we shall consider some of the possible processes which provide energy for atomic motion. The mobility of the excitations is discussed in Sec. VI.

The energy loss from keV electrons to electronic excitations is caused mainly by ionization processes of atoms and molecules,[56,57] i.e., for condensed gases by the

creation of hole-electron pairs. A hole will be localized as the molecular state Ne_2^+:[53,55]

$$Ne^+ + Ne \rightarrow Ne_2^+ . \quad (21)$$

By capturing an electron the molecular hole $A\,^2\Sigma_u^+$ forms a highly excited molecule Ne_2^{**}, which instantaneously decays nonradiatively to the free $3p$ exciton[55] or to the $3p$ self-trapped atomic exciton[53] (Fig. 9):

$$Ne_2^+ + e^- \rightarrow Ne_2^{**} \rightarrow Ne + Ne^*(3p) . \quad (22)$$

The decay sequence indicated by Inoue *et al.*[55] is shown in Fig. 9 as I, whereas the sequence suggested by Belov *et al.* is shown as II. About 1.1 eV is liberated by the decay of Ne_2^{**} after electron capture to the vibrationally relaxed state of Ne_2^+. Of course, more energy is released if the electron capture takes place for a vibrationally excited Ne_2^+, i.e., up to the dissociative energy for Ne_2^+ 1.3 eV extra.[58]

The luminescence spectrum from particle- or photon-irradiated solid neon is characterized by the lines from self-trapped atomic or molecular excitons, whereas the decay of free $3s$ excitons so far has not been observed.[28] The atomic self-trapped excitons occur both in the bulk and at the surface.[27] Fugol' *et al.*[26,59] estimate that the shift induced by the transition from $4s$ to the ground state $3p^6\,^1S$ in argon is about 0.2 eV, which is available for sputtering. An estimate for solid neon based on their tables leads to a shift of about 0.05 eV resulting from the radiative transition $3s$ to $2p^6\,^1S$ (IV in Fig. 9).

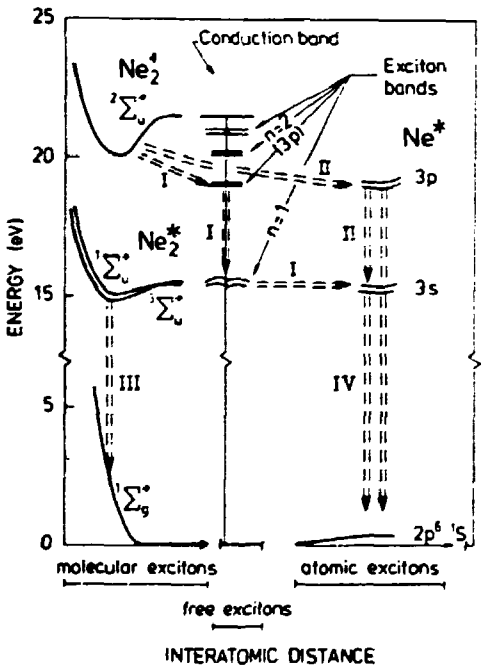

FIG. 9. Schematic representation of the important potential-energy curves. The arrows on the X axis indicate increasing interatomic distance. The bands in the middle between the molecular excitations and the atomic excitons show the position of the *free*-exciton bands and the conduction band in solid neon. The transitions indicated by dashed arrows are explained in the text. The design of the figure is taken from Ref. 53.

Let us now estimate the energy release from molecular self-trapped excitons. In solid neon these excitons occur predominantly in highly vibrationally excited states.[30,60] The relaxation to low-lying states by multiphonon processes is inefficient because of the large energy difference between the vibrational states compared with the phonon energies.[28,30] Furthermore, the transition rate is reduced substantially for molecular excitons at the surface or in small crystallites in the bulk of layers deposited by evaporation.[30] The radiative transition from the vibrationally relaxed $^{1,3}\Sigma_u^+$ molecular states to the ground state imparts about 3.7 eV of kinetic energy on the average to the two atoms[18] (see process III in Fig. 9). The decay from the *excited* levels transfers up to 0.5 eV extra energy to the atoms.[28]

The ratio of the number of atomic to molecular self-trapped excitons depends heavily on the type of the primary excitation.[30] Surface-sensitive excitation leads to an enhancement of the number of the atomic excitons relative to the molecular ones. In our previous work on solid neon[20] we utilized the ratio of intensities $[I(Ne_2^*)/[I(Ne^*)+I(Ne_2^*)] \approx 0.35)$ determined by Packard *et al.*[24] Their sample was irradiated by electrons from a tritiated external source. From the recent work by Coletti *et al.*,[27] we find a similar ratio for bombardment by 2.5-keV electrons. We note that the decay channel via these molecular self-trapped excitons is efficient for sputtering because of the comparatively large energy release.

Recently, Coletti *et al.*[12] suggested that the ejection was a result of a relaxation of a cavity with a self-trapped exciton. The minimizing of the elastic strain of the crystal and of the surface energy of the cavity at the sample surface will liberate sufficient energy for atomic motion, e.g., about 1 eV for Ar_2^*.[12]

VI. DISCUSSION: ELECTRONIC SPUTTERING

The thickness dependence of the yield in Fig. 5 indicates that two mechanisms may operate during electronic sputtering. The large yield at small thicknesses would then have another origin than the yield for thicknesses larger than 2×10^{17} Ne atoms/cm^2. The yield from thick films shows the characteristic sputtering behavior for solid rare gases deposited on a metal substrate,[9,15,16,21] if one extrapolates the yield curve to zero for a bare substrate. The yield below 2×10^{17} Ne atoms/cm^2 may then be composed of contributions from both mechanisms.

A. Yields for thick films

The continuous increase in yield with increasing film thickness above 10^{17} Ne atoms/cm^2 corroborates the idea that a single type of mobile excitation is responsible for the energy transport. (The apparent scattering in individual points reflects different series of measurements rather than actual scattering.) In the following, we shall discuss how the mechanisms in Sec. V C may lead to a yield comparable to the experimental data.

Let us first consider the possibility that the sputtering from solid neon is caused by the formation of mobile molecular excitons and their subsequent diffusion to the surface.[20] We have calculated the energy dependence of

the yield for several values of the diffusion length l_0 on the basis of Eq. (16). The shape of the yield curve is determined by l_0, whereas the absolute magnitude of the calculated yield is adjusted by the value of the product ff_e.

One notes that the curve with $l_0=1\times10^{17}$ Ne atoms/cm^2 (Fig. 6) represents a fair approximation to the experimental data. The positions of the maximum and the shape of the other two curves disagree clearly with the data, however.

The magnitude of l_0 is much less than the length of 1×10^{18} Ne atoms/cm^2 (2500 Å) reported by Pudewill *et al.*,[33] but the discrepancy is acceptable in view of the possible influence of imperfections in our sample. However, the yield evaluated from Eqs. (16) and (17) with $l_0=1\times10^{17}$ Ne atoms/cm^2 and $f=0.35$ and $f_e=1$ becomes about 3.4 Ne atoms/electron for the primary energy $E=2$ keV. This value of f corresponds to mechanism III in Fig. 9 with the ejection of one Ne atom. In this case the yield is approximately a factor of 8 lower than the measured bulk yield. If we use the diffusion length from Pudewill *et al.*,[33] $f=0.35$ and $f_e=1$, the calculated yield for 2 keV is close to the experimental value, but the yield then increases clearly with energy, in complete disagreement with the experimentally determined behavior. In contrast, a calculation with $l_0=1\times10^{17}$ Ne atoms/cm^2 (230 Å) will reproduce the shape of the curve and the position of the maximum fairly well with $ff_e=3$. Thus, our diffusion length is consistent with the overall behavior of the yield, but the suggested mechanism alone cannot explain the magnitude.

The value of $ff_e=3$ is surprisingly large. However, by inserting this value in Eq. (20), one obtains a yield-versus-thickness curve which gradually approaches the curve in Fig. 5. The slope at the origin of the calculated curve is fixed by this choice of ff_e, since all other parameters are known (except l_0, which does not enter the expression in the limit of $d=0$). The agreement between the value of ff_e from the two independent curves, the energy dependence and the thickness dependence of the yield, is very encouraging.

The product ff_e is determined partly by the type of the mobile excitation (f), and partly by the ejection efficiency per deexcitation (f_e). The largest feasible value of f is unity since we have assumed that only one excitation is mobile according to the previous discussion. Then, f_e has to be at least 3.

By the decay of the molecular excitons, we have assumed in Ref. 20 that only one neon atom is ejected, i.e., $f_e=1$. However, the other atom moving into the film may cause sputtering as well. The energy of this atom is sufficient to create a low-energy cascade (cf. Sec. VI C), and the total number of emitted atoms may very well be about the magnitude of the measured yield. In fact, one obtains agreement with the experimental yield if the impact of this atom leads to sputtering of 7–8 atoms from the neon surface. Then $f\approx0.35$ and $f_e\approx8.5$.

Sputtering yields from recent measurements for keV hydrogen-ion bombardment of solid neon demonstrate that the diffusion model is applicable for ion-induced electronic sputtering as well.[61] The energy dependence is fairly well predicted, and as in the case of electrons we obtain satisfactory agreement between the experimental yield and the calculated yield with $ff_e=3$.

Let us now consider the possibility that recombination of molecular holes is the dominant mechanism similar to that reported by Reimann *et al.*[15] for electronic sputtering of solid argon. According to these authors the radiative decay of the molecular excitons to the repulsive ground state (III in Fig. 9) leads to an additional contribution to the sputtering yield.

The holes recombine with prompt or delayed electrons from the substrate. Obviously, the recombination has to take place at or close to the surface in order to provide sufficient energy to the sputtering process. From hole-drift experiments in solid neon it is known that the holes may traverse specimens of more than a few hundreds of micrometers thick.[62] There are apparently no indications in the literature of the characteristic diffusion length of the holes in the absence of any external fields, and of the influence of sample preparation. Le Comber *et al.* point out that the tunneling of a hole Ne_2^+ to a neighboring site is a probable process,[62] which eventually leads to an ordinary diffusion behavior of the holes. However, this particular type of diffusion is not probable in our case. An extrapolation of the hole mobility in neon down to 6 K on the basis of the data and the treatment by Le Comber *et al.*[62] leads to a completely immobile hole.

Nevertheless, let us consider the possibility that recombination might be the dominant process ($f=1$) with a diffusion mechanism different from the one considered by Le Comber *et al.* With $l_0=1\times10^{17}$ atoms/cm^2 as the diffusion length for a hole, we obtain a yield of 10 Ne atoms/electron for incidence of 2-keV electrons from Eqs. (16) and (17). The dependence on energy is, of course, similar to that calculated with $f=0.35$. As in the case of molecular excitons, the dissociative recombination will lead to a yield of about 30 only if one of the atoms causes further sputtering from the neon surface (corresponding to $f_e=3$). The result is based on a complete trapping of the holes at the surface corresponding to the absorbing boundary condition. The use of a highly reflecting boundary as suggested by Reimann *et al.*[15] for the diffusing holes combined with a low-energy cascade model leads to a yield for Ne of about 2 Ne atoms/electron at 2 keV. We shall treat this case in Sec. VI C. We note that although recombination apparently is an important step in the degradation of electronically deposited energy, it does not necessarily mean that dissociative recombination is the dominant source of kinetic energy for sputtering. The energy might as well arise from a combination of transitions from self-trapped molecular and atomic excitons at the surface as the *last step* in the relaxation process initiated by the recombination. We note that the energy supply in both cases is adequate (cf. Sec. V C), but that the use of Eq. (16) without modification means that the excitons have to remain close to the surface where the recombination took place.

The importance of recombination is illustrated by Fig. 2. The effect of a positive bias is primarily that all internal low-energy secondary electrons disappear from the neon film because of the negative affinity of solid neon,

before they may recombine. This means that the sample may charge up positively relative to the metal substrate. When the potential of the film is sufficiently high, the internal secondaries do not leave the film or electrons from the substrate are attracted by the positive region in the film. The sputtering begins when the electrons start to recombine. This explanation would be consistent with the apparent delay in erosion with a positive bias.

We do not consider the contribution from deexciting atomic excitons to be substantial. The reason is primarily the low-energy release from this transition estimated by the considerations in Sec. V C.

For solid neon recent measurements[63] indicate that the sputtering by eV electrons starts close to the threshold for exciton production ($\simeq 17$ eV), whereas no strong enhancement is observed for energies close to the band gap. This observation supports the suggestion that decaying excitons are the dominant energy source for the particle ejection.

Although so far we have considered one dominant mobile excitation, one cannot exclude that two types of mobile excitations with different diffusion length contribute to the sputtering. For example, hole diffusion prior to recombination may broaden the initial Gaussian distribution of excitations. The resulting distribution of mobile excitons leads to a second diffusion of excitations, which may behave similarly to the assumptions in Sec. V. Then, the necessary energy for the sputtering is essentially provided by decaying, surface-trapped molecular, or atomic 3*s* excitons, i.e., via mechanism IV + III in Fig. 9 or by strain minimization as suggested by Coletti *et al.*[12]

B. Yields for thin films

The strong enhancement of the yield for thicknesses below 5×10^{16} Ne atoms/cm^2 has not been observed for other condensed gases at present. Recent measurements indicate that this thin-film behavior is found for incidence of keV hydrogen ions as well.[61] Thus, we are led to the conclusion that the strong enhancement for small thicknesses is primarily a property of the neon film on a metal substrate, but is not influenced much by the type of the primary particle or the spectrum of backscattered particles. In this connection, we note that the contribution from backscattered electrons for irradiation of solid oxygen was significant up to one-half of the electron range.[17] For neon, the contribution from these electrons are hidden in the complex depth dependence.

The possibility exists that the high yield for these small thicknesses is caused by a violent process with a small effective range from the substrate. A yield of about 100 Ne atoms/electron has even been observed for these thin films. In view of the sublimation energy of 20 meV, it means that the resulting process has to liberate at least approximately 2 eV, unless emission of clusters takes place.

Cluster formation for thin neon films might be another reason for the high yield. The films are more or less uniform for thicknesses above 5×10^{16} Ne atoms/cm^2, whereas films below this thickness show a strong tendency to form clusters.[64] We may not exclude that kinetic energy, e.g., released from a dissociative recombination, is consumed very effectively for erosion of clusters.

C. Comparisons with models for a reflecting surface

Let us compare the present results with two models in which the surface acts as a reflecting boundary, sputtering from low-energy cascades or spherical spikes. The energy-releasing processes may be dissociative recombination or decay of molecular excitons as described above.

Ordinary sputtering theory was extended to electronic sputtering for electron irradiation of solid oxygen and nitrogen by Ellegaard *et al.*[17] It turned out that this *low-energy cascade* model explained the energy dependence of the yield as well as its approximate magnitude for primary electrons. The yield is essentially determined by the surface value $D_e(0)$ of the distribution $D_e(x)$ of energy deposited in electronic excitations. The derivation in Refs. 17 and 49 gave the important result that the yield caused by particle bombardment for medium and low excitation densities is

$$\tfrac{1}{2}[D_e(0)/W]E_s\Lambda \text{ (atoms/primary)} . \tag{23}$$

E_s is the energy release for example by an electronic deexcitation. The constant Λ is determined by properties of the target material alone, e.g., the sublimation energy U_0 and the low-energy stopping power for atoms.[13] A similar expression involving a treatment based on low-energy cascades has been presented by Johnson and Brown,[65] and Garrison and Johnson.[66] Equation (23) is determined by the distribution of isotropic sources of released energy for these low-energy cascades. The surface density for nonmobile sources is $D_e(0)/W$, e.g., as in solid nitrogen, but for solid neon the source distribution is different from the distribution of electronically deposited energy due to the mobility of the excitations. However, if the excitations are reflected at the surface, one may estimate the simple case of a primary with constant stopping power. The two distributions are identical apart from a constant factor up to quite large depths, provided that the diffusion length is much smaller than the range of the particle. One may evaluate the yield from Eq. (23) for 1.5-MeV protons incident on solid argon to $Y=1.5$ Ar atoms/H$^+$ compared to the experimental yield $Y=2.2$ Ar atoms/H$^+$.[15,16] Here we applied $D_e(x)=NS_e(E)$ and an energy release $E_s=2$ eV, which is a typical value for argon.[15]

Let us shortly estimate the yield for 2-keV electrons incident on solid neon on the basis of this low-energy cascade model. The spatial distribution of deexciting states is broadened from the original Gaussian distribution $G(x)$, Eq. (15b), corresponding to a diffusion with the characteristic length $l_0=1\times10^{17}$ Ne atoms/cm^2. We approximate this distribution of internal sources by a constant excitation density of $2NS_e(E)$. Then, we obtain, for example, for mechanisms III ($f=0.35$) in Fig. 9, $\Lambda=49$ Å/eV and the yield $Y=1.6$ Ne atoms/electron. This yield is almost 1 order of magnitude too small, although we have used relatively high values as input parameters, e.g., an energy release of $E_s=3.7$ eV and an excitation density of $2NS_e$. As usual, the energy W required to produce an ion-electron pair has been set equal to 35 eV,[18,20] and for Λ the usual power approximation[13] has been used.

Rather than treating the deexciting particles as a center for a low-energy cascade we may consider the possibility

for *low-energy spherical spikes*[18,67] around such a center. The contribution from these elastic collision spikes may be appreciable for large values of the energy release E_t compared with the sublimation energy U_0. However, the yield from this model does not exceed 3.5 Ne atoms/electron even for the high input parameters used in the previous case for low-energy cascades.

The yield evaluation may lead only to values close to the experimental yield, if the cross section in A and in the corresponding evaluation of the spherical collision spike is replaced by a cross section 1 order of magnitude lower than its given value. Although the interaction between low-energy neon nuclei is comparatively weak, one may hardly expect such a pronounced deviation from the standard cross section.

D. Influence of impurities

The apparent delay of the erosion for the doped films (Fig. 6) is probably caused by a less efficient diffusion of the mobile excitation. The measurement of the pure film leads, as usual, to a yield of about 30 Ne atoms/electron, whereas the contaminated films apparently have a small erosion rate during the initial stage of the irradiation. However, one should note that we do not observe a clear correlation between increasing impurity concentration and decreasing sputtering yield, as Brown *et al.* did for oxygen impurities in solid argon.[16]

VII. CONCLUSION

Films of solid neon with thicknesses of 2×10^{16} up to 2×10^{18} Ne atoms/cm^2 have been irradiated by primary electrons at energies from 0.8 to 3 keV. Measurements of erosion yields, particularly of the yield for electronic sputtering, have been carried out by the frequency-change method and the emissivity-change method. The agreement between these two methods was fairly good. The yield for 2-keV electrons incident on thick films is about 30 Ne atoms/electron. The yield decreases with decreasing film thickness to about 10 Ne atoms/electron at the thickness 5×10^{16} Ne atoms/cm^2. This indicates the existence of a long-range diffusion of excitations which provide atoms close to the surface with the necessary energy for the sputtering process. The characteristic diffusion length is approximately 1×10^{17} Ne atoms/cm^2 ($\approx$230 Å). For very thin films a strong enhancement of the yield was observed.

The energy dependence of the bulk yield is consistent with the suggested diffusion length. There is a maximum in the yield at energies for which the primary electrons have a range comparable to the diffusion length. Above 1.5 keV the bulk yield is proportional to the stopping power for the primary electrons.

All measurements of the electronic sputtering yield have been performed at temperatures below about 6 K. A significant evaporation occurs for elevated temperatures. These latter measurements were performed on a massive gold substrate in order to obtain a satisfactory temperature determination. Doping of neon films with argon leads to a clear delay in the erosion.

The model presented previously for diffusion and decay of excitons has been extended to a general transport model of excitations to the surface with subsequent trapping and energy release for sputtering. The treatment for constant excitation density has been modified to include the distribution of electronically deposited energy for primary keV electrons. The electronic deexcitation is probably initiated by dissociative recombination, which may or may not be the dominant energy-releasing process. On the other hand, the important process might just as well be the radiative decay of self-trapped atomic or molecular excitons to a repulsive ground state. However, the suggested decay may hardly be responsible alone for such a large bulk yield without contributions from low-energy cascades initiated at the surface. This subsequent sputtering by surface-trapped deexciting particles with yields from about 10 to 3 Ne atoms/neon-atom may account for the observed yield of 20–40 Ne atoms/electron in our energy regime. The model is based on an absorbing surface as a boundary condition. The use of a highly reflecting surface as a boundary condition does not lead to satisfactory agreement with the experimental results in contrast to the case of MeV protons incident on solid argon.

Direct sputtering from electron-nucleus collisions in solid neon does not contribute significantly to the thick-film yield because of the very low cross section. Beam-induced evaporation may be neglected for current densities below $10\,\mu$A/cm^2.

ACKNOWLEDGMENTS

The authors have appreciated discussions with P. Sigmund, G. Zimmerer, W. L. Brown, R. Pedrys, R. E. Johnson, J. M. Debever, and F. Coletti. We thank as well J. M. Debever and F. Coletti for giving us the opportunity to include their unpublished work in our discussion. We acknowledge the technical staff, A. Nordskov and B. Sass, for competent assistance. We have appreciated the help of K. Weisberg in designing the electronic equipment. The work of one of us (C.C.) has been made possible by a research grant from the Danish Natural Science Research Council.

---

*Present address: Max-Planck-Institut für Plasmaphysik, D-8046 Garching bei München, Federal Republic of Germany.

[1]T. A. Tombrello, Radiat. Eff. 65, 149 (1982).

[2]R. E. Johnson, L. J. Lanzerotti, W. L. Brown, W. M. Augustyniak, and C. Mussil, Astr. Astrophys. 123, 343 (1983).

[3]R. A. Haring, A. W. Kolfschoten, and A. E. de Vries, Nucl. Instrum. Methods B 2, 544 (1984).

[4]O. Gröbner and R. S. Calder, IEEE Trans. Nucl. Sci. NS-20, 760 (1973).

[5]S. L. Milora, J. Fus. Energy 1, 15 (1981).

[6]C. T. Chang, L. W. Jørgensen, P. Nielsen, and L. L. Lengyel,

Nucl. Fus. 20, 859 (1980).
[7]J. Schou, H. Sørensen, and P. Børgesen, Nucl. Instrum. Methods B 5, 44 (1984).
[8]T. A. Tombrello, in *Desorption Induced by Electronic Transitions*, edited by N. H. Tolk, M. M. Traum, J. C. Tully, and T. E. Madey (Springer, Berlin, 1983), p. 239.
[9]F. Besenbacher, J. Bøttiger, O. Graversen, J. L. Hansen, and H. Sørensen, Nucl. Instrum. Methods 191, 221 (1981).
[10]W. L. Brown, W. M. Augustyniak, K. J. Marcantonio, E. H. Simmons, J. W. Boring, R. E. Johnson, and C. T. Reimann, Nucl. Instrum. Methods B 1, 307 (1984).
[11]R. Pedrys, R. A. Haring, A. Haring, F. W. Saris, and A. E. de Vries, Phys. Lett. 82A, 371 (1981).
[12]F. Coletti, J. M. Debever, and G. Zimmerer, J. Phys. (Paris) Lett. 45, L467 (1984).
[13]P. Sigmund, in *Sputtering by Particle Bombardment I*, edited by R. Behrisch (Springer, Berlin, 1981), p. 9.
[14]R. E. Johnson and M. Inokuti, Nucl. Instrum. Methods 209, 289 (1983).
[15]C. T. Reimann, R. E. Johnson, and W. L. Brown, Phys. Rev. Lett. 53, 600 (1984).
[16]W. L. Brown, C. T. Reimann, and R. E. Johnson, in *Desorption Induced by Electronic Transitions, DIET II*, edited by W. Brenig and D. Menzel (Springer, Berlin, 1985), p. 199.
[17]O. Ellegaard, J. Schou, H. Sørensen, and P. Børgesen, Surf. Sci. 167, 474 (1986).
[18]C. Claussen, Ph.D. thesis, University of Odense, 1982 (unpublished).
[19]M. Szymonski, J. Ruthowski, A. Poradzisz, Z. Postawa, and B. Jørgensen, in *Desorption Induced by Electronic Transitions, DIET II*, Ref. 16, p. 160.
[20]P. Børgesen, J. Schou, H. Sørensen, and C. Claussen, Appl. Phys. A 29, 57 (1982).
[21]R. W. Ollerhead, J. Bøttiger, J. A. Davies, J. l'Ecuyer, H. K. Haugen, and N. Matsunami, Radiat. Eff. 49, 203 (1980).
[22]R. Pedrys, D. J. Oostra, and A. E. de Vries, in *Desorption Induced by Electronic Transitions, DIET II*, Ref. 16, p. 190.
[23]F. Coletti and J. M. Debever, Solid State Commun. 47, 47 (1983).
[24]R. E. Packard, F. Reif, and C. M. Surko, Phys. Rev. Lett. 25, 1435 (1970).
[25]F. Coletti and A. M. Bonnot, Chem. Phys. Lett. 55, 92 (1978).
[26]I. Ya. Fugol', Adv. Phys. 27, 1 (1978).
[27]F. Coletti, J. M. Debever, and G. Zimmerer, J. Chem. Phys. 83, 49 (1985).
[28]N. Schwentner, E.-E. Koch, and J. Jortner, *Electronic Excitations in Condensed Rare Gases* (Springer, Berlin, 1985).
[29]V. Saile and E.-E. Koch, Phys. Rev. B 20, 784 (1979).
[30]R. Gaethke, P. Gürtler, R. Kink, E. Roick, and G. Zimmerer, Phys. Status Solidi B 124, 335 (1984).
[31]E. Schuberth and M. Creuzburg, Phys. Status Solidi B 71, 797 (1975).
[32]E. Roick, R. Gaethke, P. Gürtler, T. O. Woodruff, and G. Zimmerer, J. Phys. C 17, 945 (1984).
[33]D. Pudewill, F.-J. Himpsel, V. Saile, N. Schwentner, M. Skibowski, E.-E. Koch, and J. Jortner, J. Chem. Phys. 65, 5226 (1976).
[34]H. Sørensen and J. Schou, J. Appl. Phys. 49, 5311 (1978).
[35]M. Ghlenschlaeger, H. H. Andersen, J. Schou, and H. Sørensen, Radiat. Prot. Dosim (to be published).
[36]P. Børgesen, J. Schou, H. Sørensen, and O. Ellegaard (unpublished).
[37]D. Cherns, Surf. Sci. 90, 339 (1979).
[38]M. J. Berger, S. M. Seltzer, and K. Maeda, J. Atm. Terr. Phys. 32, 1015 (1970).
[39]W. L. Brown, W. M. Augustyniak, L. J. Lanzerotti, R. E. Johnson, and R. Evatt, Phys. Rev. Lett. 45, 1632 (1980).
[40]J. W. Boring, R. E. Johnson, C. T. Reimann, J. W. Garrett, W. L. Brown, and K. J. Marcantonio, Nucl. Instrum. Methods 218, 707 (1983).
[41]J. W. Boring, J. W. Garrett, T. A. Cummings, R. E. Johnson, and W. L. Brown, Nucl. Instrum. Methods B 1, 321 (1984).
[42]S. K. Erents and G. M. McCracken, J. Appl. Phys. 44, 3139 (1973).
[43]P. Sigmund and M. Szymonski, Appl. Phys. A 33, 141 (1984).
[44]M. Urbassek and P. Sigmund, Appl. Phys. A 35, 19 (1984).
[45]T. Nakayama, M. Okigawa, and N. Itoh, Nucl. Instrum. Methods B 1, 301 (1984).
[46]Z. Ophir, B. Raz, J. Jortner, V. Saile, N. Schwentner, E.-E. Koch, M. Skibowski, and W. Steinmann, J. Chem. Phys. 62, 650 (1975).
[47]N. Schwentner, G. Martens, and H. W. Rudolf, Phys. Status Solidi B 106, 183 (1981).
[48]J. Schou, Phys. Rev. B 22, 2141 (1980).
[49]O. Ellegaard, Ph.D. thesis, Risø National Laboratory, 1986 (unpublished).
[50]H. Niedrig, Scanning 1, 17 (1978).
[51]S. Valkealahti and R. Nieminen (private communication).
[52]A. E. S. Green and L. R. Peterson, J. Geoph. Res. 73, 233 (1968).
[53]A. G. Belov, E. M. Yurtaeva, and V. N. Svishchev, Fiz. Nizk. Temp. 7, 350 (1981) [Sov. J. Low Temp. Phys. 7, 172 (1981)].
[54]K. Inoue, H. Sakamoto, and H. Kanzaki, Solid State Commun. 44, 1007 (1982).
[55]K. Inoue, H. Sakamoto, and H. Kanzaki, Solid State Commun. 49, 191 (1984).
[56]T. Doke, A. Hitachi, S. Kobota, A. Nakamoto, and T. Takahashi, Nucl. Instrum. Methods 134, 353 (1976).
[57]L. R. Peterson and A. E. S. Green, J. Phys. B 1, 1131 (1968).
[58]L. Frommhold and M. A. Biondi, Phys. Rev. 185, 244 (1969).
[59]I. Ya. Fugol' and E. I. Tarasova, Fiz. Nizk. Temp. 3, 366 (1977) [Sov. J. Low Temp. Phys. 3, 176 (1977)].
[60]M. Selg, Phys. Status Solidi B 129, 775 (1985).
[61]O. Ellegaard, J. Schou, and H. Sørensen, Nucl. Instrum. Methods B 13, 567 (1986).
[62]P. G. Le Comber, R. J. Loveland, and W. E. Spear, Phys. Rev. B 11, 3124 (1975).
[63]J. M. Debever and F. Coletti (private communication).
[64]J. Krim (private communication); J. Krim, J. G. Dash, and J. Suzanne, Phys. Rev. Lett. 52, 640 (1984).
[65]R. E. Johnson and W. Brown, Nucl. Instrum. Methods 198, 103 (1982).
[66]B. J. Garrison and R. E. Johnson, Surf. Sci. 148, 388 (1984).
[67]C. Claussen, Nucl. Instrum. Methods 194, 567 (1982).

Nuclear Instruments and Methods in Physics Research B13 (1986) 567–571
North-Holland, Amsterdam

SPUTTERING OF SOLID NEON BY keV HYDROGEN IONS

O. ELLEGAARD, J. SCHOU and H. SØRENSEN

Physics Department, Association Euratom–Risø National Laboratory, DK-4000 Roskilde, Denmark

Sputtering of solid Ne with the hydrogen ions H_1^+, H_2^+ and H_3^+ in the energy range 1–10 keV/atom has been studied by means of a quartz microbalance technique. No enhancement in the yield per atom for molecular ions was found. The results for hydrogen ions are compared with data for keV electrons. The thickness dependence of the yield is almost the same for the two types of bombarding particles. The energy dependence as well as the absolute magnitude of the yield are discussed on the basis of mobile electronic excitations.

1. Introduction

Sputtering of condensed gases by charged particles has been investigated by a number of groups. Special attention has been paid to the solid rare gases [1–6]. These atomic solids constitute an interesting class of target materials due to the extremely weak Van der Waals' binding between the atoms in the solid. Solidified Ne has been studied using keV electrons as the bombarding particle [4, 7], while sputtering of solid Ar, Kr, and Xe was performed with MeV light ions [1–3, 5].

Only very few data are available for sputtering with ions in the low keV regime. The slowing down of the primary in the solid is caused by both nuclear and electronic stopping. Sputtering measurements of frozen Xe have been made by Stevanovic et al. [6] using 20–80 keV heavy ions (N, Ar, Sb and Bi), i.e. in a regime where nuclear stopping is the dominant process. This group atempted to separate the nuclear and electronic contribution to the yield. The agreement between the yield ascribed to nuclear collisions and the estimated yield from ordinary sputtering theory [8] was satisfactory.

Pedrys et al. [9, 10] investigated the energy distribution of sputtered krypton and argon ions by bombardment of 3 keV Xe, 6 keV Ar ions and 6 keV protons. In the case of the heavy ions, where nuclear losses dominate, they found an indication of a collision-cascade mechanism. The energy spectrum of Kr atoms in the case of proton incidence could be interpreted as the result of non-radiative deexcitations. In this case, the energy deposition for protons is due mainly to electronic stopping. The large sputtering yield for solid rare gases is caused in many cases by energy deposited in electronic excitations, while the contribution from nuclear collisions has not been studied to the same extent.

A close connection between luminescence and sputtering has been observed for the solid rare gases Ne and Ar [2–4, 11]. This feature has been studied in particular for the case of MeV light-ion bombardment of argon [2, 3]. The process leading to sputtering for Ar is primarily a generation of electron–hole pairs or excitons, diffusion of these excitations and subsequent deexcitation close to the surface.

Solid neon is the most volatile of the solid rare gases, and the sputtering by charged particles is in general an efficient process. Moreover, for sputtering by electronic transitions, processes that take place even far from the surface contribute to the particle sputtering. This is corroborated by the large diffusion length for excitons that has been observed in solid neon [4, 12].

Here, we report on the first measurement with ions bombarding a condensed gas using the quartz microbalance method. Solid neon is well suited to any sputtering measurement based on mass loss because of the large yield and the atomic mass, which is not too small. In a forthcoming publication we will compare the results for both protons and medium light bombarding ions with the existing theories for sputtering of solid Ne. For these ions we expect a significant contribution from both nuclear and electronic stopping in the material.

2. Experimental

The basic experimental set-up as well as the quartz microbalance method have been described elsewhere [13].

Films from 2×10^{16} Ne/cm^2 up to 2×10^{18} Ne/cm^2 of solidified neon are produced by letting a jet of cooled gas impinge on an oscillating quartz crystal (fig. 1). The substrate is cooled to a temperature close to that of liquid helium.

Beams of 1–10 keV H_1^+, H_2^+ and H_3^+ are extracted from a duoplasmatron ion source and selected by a 45° magnet. The energy spread in the detected beam is of

0168-583X/86/$03.50

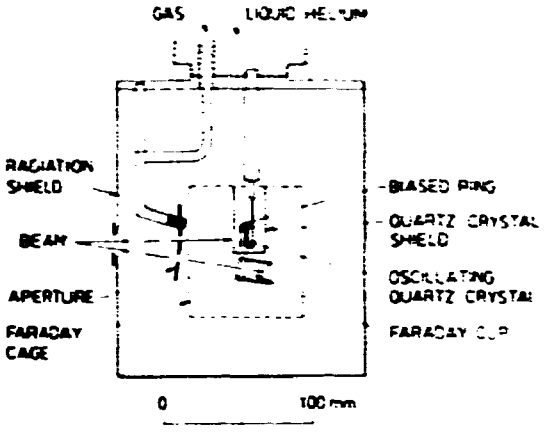

Fig. 1. Experimental set up. The target region.

the order of 10 eV or less and under good vacuum conditions ~99% of the beam consists of positive ions. Also the dissociation of H_2^+ and H_3^+ ions in the beam is negligible under good vacuum conditions. The current is measured by deflecting the beam into a Faraday cup. The beam is swept horizontally and vertically over an aperature in front of the target, thus ensuring a homogeneous irradiation of a large part of the target area. As in the case of electron-induced sputtering [7] we apply a negative bias (−90 V) to an open repeller ring in front of the target. In this way secondary electron emission is suppressed, and charge-up problems are reduced substantially.

The current density was below 1 $\mu A/cm^2$, where evaporation caused by beam heating turned out to be insignificant [13]. This current density causes no drift in the oscillator frequency. The stability of the beam was checked during the sputtering experiment. 900 frequency and target current measurements were performed during one sputtering experiment. The sputtering yield was determined from the frequency shift of the microbalance. In a typical sputtering experiment the frequency change was about 200 Hz. After each run the eroded film was thrown away by heating the quartz crystal.

3. Results

3.1. Dependence on temperature, current density and grid bias

Measurements were performed in order to study if sputtering was partly due to beam-induced evaporation. A reduction in temperature compared with the level at which the measurements were normally performed could be obtained by pumping on the helium reservoir. This did not lead to any change in the sputtering yield for film thicknesses above 1×10^{17} Ne/cm^2, while some reduction in yield was observed for the smaller thicknesses. A crucial test is the dependence on current density. Variation of the current density between 0.5 and 0.05 $\mu A/cm^2$ did not influence the sputtering yield.

As was the case for electron incidence [7] the application of a positive bias (+90 V) leads to a delay in the sputtering or a significantly lower sputtering yield.

3.2. Thickness dependence of the yield

In fig. 2 we show the thickness dependence for 8 keV H_3^+ compared with the results for electrons. The yield is almost constant for thicknesses above 1×10^{17} Ne/cm^2, and the "bulk" yield is about 60 Ne atom. This value should be compared with the "bulk" value for 2 keV electron incidence, 28 Ne/electron. The yield increases drastically for small thicknesses in both cases. The minimum in the yield for electrons below about the thickness of 1×10^{17} Ne/cm^2 is not so pronounced in the case of protons (see fig. 3) and is probably sometimes hidden in statistical fluctuations of the measured yield.

3.3. Ac[illegible] effect

As a fair approximation one may assume that the molecular ions H_2^+ and H_3^+ will dissociate upon impact under an equal sharing of energy. Such a multiple impact could locally increase the density of excitations

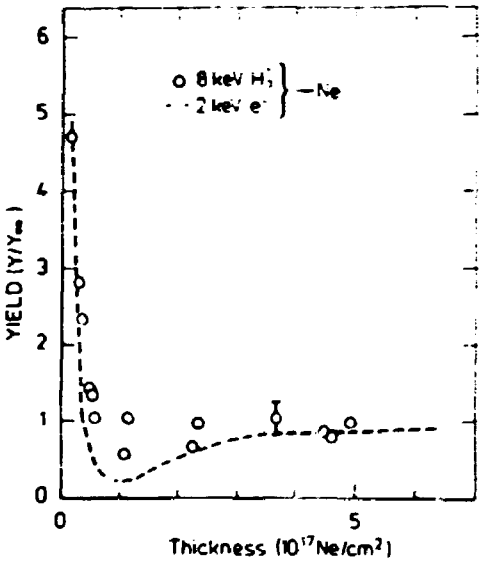

Fig. 2. Thickness dependence of the yield for 8 keV H_3^+ incident on solid Ne. The dashed curve indicates the thickness dependence for 2 keV electrons.

near the region of impact compared with the incidence of H^+ with equal energy per atom. If the sputtering were not caused by mutually independent excitation events, molecular effects could then be expected, and the yield would probably be enhanced. As shown in fig. 3 we found full agreement between the sputtering yields of 6 keV H_2^+ and 9 keV H_3^+ over the thickness range 0.2–5 × 10^{17} Ne/cm^2. Also 10 keV H_2^+ and 5 keV H^+ gave full agreement for the thickness of 4.8 × 10^{17} Ne/cm^2. This demonstrates that no molecular effect is found for such low-energy protons. In contrast, Stevanovic et al. [6] found a clear effect for solid Xe bombarded by Sb_2^+-ions with energy in the nuclear collision regime.

3.4. Energy dependence

In fig. 4 we show the energy dependence of the yield over the whole energy range 1–10 keV/atom. The yield increases with energy, and in the figure a least squares fit to the relation $Y = AS_e^q$ is shown as well. S_e is the electronic stopping cross section given by Andersen and Ziegler [14]. As the power turns out to be $q = 0.9$ the yield is almost proportional to the initial stopping power of the protons. A similar proportionality is also found for electrons with energies above 1.5 keV [7].

Nuclear collisions contribute significantly at the lowest proton energies. The amount of energy spent in nuclear collisions as calculated from the tables of Winterbon [15] changes from −20% at 1 keV to −5% at 10 keV. The yield could possibly be enhanced due to this nuclear energy loss. The importance of this mechanism in our energy range is at present unknown for

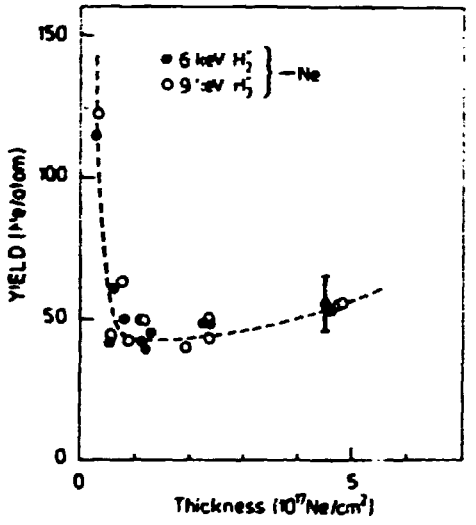

Fig. 3. The absence of molecular effects in solid Ne. The absolute values of the sputtering yield are compared for the two ions 6 keV H_2^+ and 9 keV H_3^+ which give the same amount of energy per atom after dissociation.

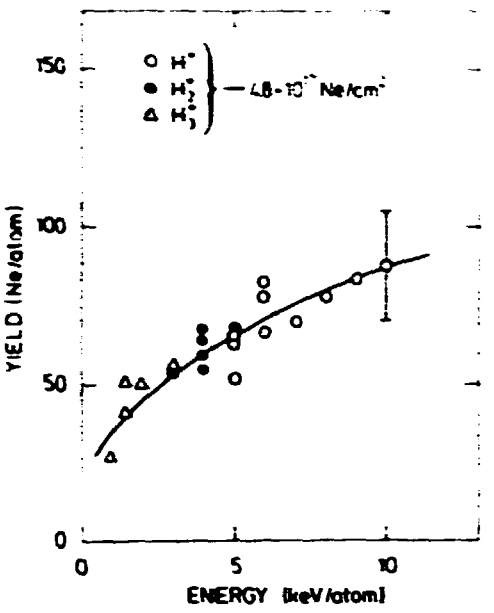

Fig. 4. Energy dependence of the sputtering yield over the energy range 1–10 keV/atom. The solid line indicates a fit to the relation $Y = S_e^q$ with $q = 0.9$.

condensed solid gases, but the use of heavier low energy ions, depositing more energy in the nuclear collision regime, may possibly give new answers.

4. Discussion

The major question arising in sputtering of condensed gases by electrons and protons is: How is the energy expended in electronic excitations and ionizations converted to the kinetic energy of the sputtered atoms? As we almost can neglect nuclear losses for protons except for the lowest energies, the interpretation of the data is supported by the results for electron bombardment. From the thickness dependence of the yield for 2 keV electrons (fig. 2) it is clear that excitations and ionizations up to a depth comparable to 5 × 10^{17} Ne/cm^2 [7] contribute to the yield. This is obvious from the observation that the yield increases up to a film thickness around 4 × 10^{17} Ne/cm^2. Then the situation for solid Ne is clearly different from that of the electron-induced sputtering of solid N_2 and O_2 [17], where we have to take only surface processes into account. For these molecular gases the thickness dependence of the yield is then ascribed to the varying excitation density due to electrons back-scattered from the substrate.

The strong enhancement of the yield for thicknesses below 5 × 10^{16} Ne/cm^2 has no parallel to other condensed gases investigated so far. As the enhancement is observed both in the case of electron and proton bombardment, we suggest the effect to be a property of the neon film itself. It has been observed for films

thinner than 5×10^{16} Ne/cm^2 that Ne-atoms show a tendency to form clusters [16]. Then the sputtering of these clusters should apparently be a rather efficient process.

Concerning the energy dependence of the yield for electrons, we observe a maximum at around 1.2–1.5 keV, and the yield decreases with energy almost in proportion to the stopping power. This behaviour can be understood if the sputtering is caused by excitation events in widely distant atoms, so the interaction between ionization centers is negligible. The decrease in yield below 1.2 keV is caused by the low range of the electrons compared to the diffusion length of the excitations. In the case of electron bombardment of N_2 and O_2, the yield was almost proportional to the stopping power over the whole energy range 0.8–3.0 keV [17]. It is also clear that for solid Ne, the total distribution of electronically deposited energy must be taken into account. For keV electrons this distribution is approximated with a Gaussian function [7]. In the case of protons a distribution has to be constructed on the basis of well-known slowing-down parameters.

For the two solid rare gases, Ne and Ar, sputtering explained in terms of diffusion and decay of excitations seems to be the most promising model. Excitations, e.g. excitons or hole–electron pairs, are produced in the solid rare gas by the charged particles. The mobile excitation in neon is a molecular exciton Ne_2^*, an atomic exciton Ne^* or a molecular hole Ne_2^+. The precise nature of the diffusion is not known, but the decay of the excitons as well as the dissociative recombination provide the neon atoms with translational energy. An initial hole recombines dissociatively into a 3p-free exciton, which in turn decays radiatively into a (n = 1)-exciton. This decay-sequence was suggested by Inoue et al. [18]. The final branching in atomic and molecular (n = 1)-excitons is unique for neon [4, 7, 12].

The decay sequence proposed is supported by our observations of sputtering measurements with a positive bias. Since all low-energy internal secondaries are expelled [12], none or relatively few recombinations take place.

Model calculations for electron bombardment indicate that each non-radiative deexcitation at the surface is accompanied by additional sputtering [7]. For example, about 3.7 eV is released as kinetic energy by the decay of a molecular exciton. Then one of the atoms has to sputter about ten more atoms off the surface. This number is essentially determined by the diffusion length which is estimated to be 1×10^{17} atoms/cm^2 (≈230 Å). The input numbers used for electron bombardment also give a satisfactory agreement with the energy dependence of the yield for incident protons.

The sputtering of neon shows some similarities to that of argon. Reimann et al. [2] related sputtering of argon to luminescence of the strong 9.8 eV-line from exciton-decay. They proposed a model where the release of kinetic energy takes place in three steps: A molecular hole Ar_2^+ makes a dissociative recombination forming a highly excited atomic exciton. This exciton then combines with a neighbour to form a vibrationally excited Ar_2^* excimer. After vibrational relaxation this excimer decays under emission of the 9.8 eV photon and with a further release of kinetic energy. On the basis of the thickness dependence of the luminescence yield the authors estimated that the diffusing species is the molecular hole or a highly excited atomic exciton with a diffusion length $l \approx 190$ Å [2]. The authors suggest for Ar as well that additional sputtering takes place by non-radiative deexcitation at the surface.

5. Conclusion

We have measured the sputtering of solid Ne with hydrogen atoms in the energy regime 1–10 keV. The dependence of the yield on a number of parameters such as primary energy, film thickness, current density and grid bias was investigated. The main purpose of our investigation was to compare protons and electrons as primary particles. In this energy regime the energy deposition by these two particles is mainly electronic.

The thickness dependence of the yield shows no major difference for the two particles, and the yield increased drastically below the film thickness $\approx 1 \times 10^{17}$ Ne/cm^2 in both cases. There is no difference in the yield per atom for the atomic, diatomic or triatomic hydrogen ions. The yield increases with increasing energy per atom almost proportionally to the electronic stopping power.

The energy dependence of the yield may be explained by the existence of a mobile excitation that deexcites at the surface. Since the diffusion length 1×10^{17} Ne/cm^2 is comparable to the range of the ions, excitations created over the whole excitation volume may contribute to the yield. This can probably also explain why no molecular effect is observed in the case of solid Ne. As sputtering is not caused by excitations close to the surface, no enhancement of the yield is seen when the molecules dissociate at the surface.

We acknowledge R.E. Johnson for discussions and valuable comments. We thank as well A. Nordskov and B. Sass of the technical staff for their competent assistance.

References

[1] F. Besenbacher, J. Bøttiger, O. Graversen, J.L. Hansen and H. Sørensen, Nucl. Instr. and Meth. 191 (1981) 221.

[2] C.T. Reimann, R.E. Johnson and W.L. Brown, Phys. Rev. Lett. 53 (1984) 600.
[3] W.L. Brown, C.T. Reimann and R.E. Johnson, in: Desorption Induced by Electronic Transitions DIET II, eds., W. Brenig and D. Menzel (Springer, Berlin, 1985) p. 199.
[4] P. Børgesen, J. Schou, H. Sørensen and C. Claussen, Appl. Phys. A29 (1982) 57.
[5] R.W. Ollerhead, J. Bottiger, J.A. Davies, J.L'Ecuyer, H.K. Haugen and N. Matsunami, Radiat. Effects 49 (1980) 203.
[6] D.V. Stevanovic, D.A. Thompson and J.A. Davies, Nucl. Instr. and Meth. B1 (1984) 315.
[7] J. Schou, P. Børgesen, O. Ellegaard, H. Sørensen and C. Claussen, to be published.
[8] P. Sigmund, Phys. Rev. 184 (1969) 383; 187 (1969) 768.
[9] R. Pedrys, D.J. Oostra and A.E. de Vries, in: Desorption Induced by Electronic Transitions DIET II, eds., W. Brenig and D. Menzel (Springer, Berlin, 1985) p. 190.
[10] R. Pedrys, R.A. Haring, A. Haring, F.W. Saris and A.E. de Vries, Phys. Lett. 82A (1981) 371.
[11] F. Coletti, J.M. Debever and G. Zimmerer, J. Phys. Lett. 45 (1984) L-467.
[12] N. Schwentner, E.-E. Koch and J. Jortner, Electronic Excitations in Condensed Rare Gases (Springer, Heidelberg) in press.
[13] J. Schou, H. Sørensen and P. Børgesen, Nucl. Instr. and Meth. B5 (1984) 44.
[14] H.H. Andersen and J.F. Ziegler, Hydrogen Stopping Powers and Ranges in all Elements (Pergamon, Oxford, 1977).
[15] K.B. Winterbon, Ion Implantation Range and Energy Deposition Distributions, Vol. 2, Low Incident Ion Energies (Plenum, New York, 1975).
[16] J. Krim, J.G. Dash and J. Suzanne, Phys. Rev. Lett. 52 (198-) 640; J. Krim, Private communication.
[17] O. Ellegaard, J. Schou, H. Sørensen and P. Børgesen, submitted to Surface Sci.
[18] K. Inoue, H. Sakamoto and H. Kanzaki, Solid St. Commun. 49 (1984) 191.

Surface Science 167 (1986) 474–492
North-Holland, Amsterdam

ELECTRONIC SPUTTERING OF SOLID NITROGEN AND OXYGEN BY keV ELECTRONS

O. ELLEGAARD, J. SCHOU, H. SØRENSEN and P. BØRGESEN *

Physics Department, Association Euratom - Risø National Laboratory, DK-4000 Roskilde, Denmark

Received 29 May 1985; accepted for publication 11 November 1985

Sputtering of solid N_2 and O_2 has been performed with electrons in the keV regime by means of a quartz microbalance technique. Good agreement is found between the sputtering yields obtained with this and the emissivity-change method. O_2 sputters more efficiently than N_2, although these solids are very similar in their physical properties. The yields are almost proportional to the electronic stopping power of the primary electrons. Different models for electronic sputtering of solid condensed gases are discussed and compared with the results. For low excitation densities predictions are attempted on the basis of a simple collision-cascade model where the low-energy cascades are generated by kinetic energy release from electronic deexcitations.

1. Introduction

The sputtering of solidified gases has been investigated by a number of groups. The challenge in this connection has been to identify the mechanism behind the sputtering process [1–3]. Sputtering of surfaces of condensed gases plays an appreciable role in astrophysical problems [4]. In technological problems such as cryopumping in radiation environments the phenomenon has also turned out to be important [5].

A variety of solidified gases has been investigated. These range from the rare gases Ne [6], Ar [2,7], Kr and Xe [8], diatomic gases H_2 [9–11], D_2 [9–12], CO [1,13], N_2 and O_2 [14,15], to polyatomic gases CO_2 [16] and H_2O [1], and organic compounds [3]. Most measurements have been performed with ion bombardment while measurements with electrons as the primaries are more scarce. The investigated energies belong to the keV regime in the case of electrons and vary from keV to MeV energies for ion bombardment.

There is overall agreement that the electronic processes play a major role for

* Present address: Max-Planck-Institut für Plasmaphysik, D-8046 Garching bei München, Fed. Rep. of Germany.

0039-6028/86/$03.50

the large sputtering yield observed for these volatiles [1,3,16–18]. Usually the standard sputtering theory used for metals and semiconductors [19,20] predicts a yield for incident ions that is up to several orders of magnitude too low.

When the density of electronically deposited energy by the primary is very low, one would expect that the sputtering results from electronic and vibrational transitions in mutually distant molecules or atoms. At high densities caused, e.g., by bombardment by medium-mass MeV ions, one has to include the interaction between adjacent ionized or excited target particles. As a matter of fact, such models have been suggested in the literature on a more or less quantitative basis [1,16,21–23]. For keV electron bombardment the energy density created by the incoming particle is low compared to the density from medium-mass MeV ion bombardment.

The irradiation of nitrogen and oxygen at low temperatures by ions, electrons and photons has been studied by several groups, e.g., refs. [24–34]. The sample thickness ranges from monolayers during desorption studies to thick solid targets that have been used, for example, for electron range measurements. The range for keV electrons in solid N_2 and O_2 was determined recently [29,30,34], and turned out to deviate insignificantly from similar measurements on gases [35]. The range of keV hydrogen ions in solid N_2 [25] turned out to be substantially larger than indicated by the corresponding data from gas measurements or theoretical predictions. For solid O_2 no significant deviation was found [32]. The sputtering of solid N_2 and O_2 by MeV ions was investigated by Rook et al. [14], while Brown et al. [15] studied MeV H^+- and He^+-ion bombardment of solid N_2. Rosenberg et al. [27] measured photon-stimulated ion desorption for photon energies around 20 eV. Finally, secondary ion mass spectroscopy was performed by Michl [24] with 0.5–4.0 keV He^+, Ar^+ and Kr^+ ions incident on solid N_2 and O_2.

The present work reports on measurements of sputtering of solid N_2 and O_2 by 0.8–3.0 keV electrons. We have studied the electronic sputtering in the solids of these two homonuclear molecules. The solids have similar physical properties [14,32] (see also table 1), and from an experimental point of view they are not too difficult to handle. The amount of energy deposited electronically in the two solids as well as other parameters important in sputtering theories such as sublimation energy and atomic density are similar. Any difference in sputtering yield may then be related mainly to the way electronically deposited energy is converted into atomic motion.

Whereas Rook et al. [14] and Brown et al. [15] studied the medium to low energy density regime by keV to MeV H^+- and He^+-ion bombardment, our measurements provide information on the low energy density regime. Thus our measurements complement these measurements, and the trends observed in our experiment are found to be in fair agreement with their results. In addition, we have investigated carefully the thickness dependence of the sputtering yield. Special attention is given to thin films of N_2.

2. Experimental

The experimental arrangement and the methods are described in detail by Schou et al. [5] and is shown in fig. 1. The experiment is performed with a He cryostat, below which the target region is suspended. The electrons from an electron gun can either hit the target perpendicular to the surface or be deflected into a Faraday cup for measurements of the true current.

The sputtering yield has been measured by two different methods. For the emissivity-change method a massive gold target is applied, whereas for the frequency-change method, the silver electrode on a quartz-crystal microbalance serves as a substrate. The thickness of the silver electrode exceeds the range of the most energetic electrons. Further discussion of the two methods will follow. A film of condensed gas is made on the target plate or silver electrode when a jet of cooled gas impinges on it. Usually the film growth rate for the gases studied is about 1.5×10^{15} molecules/cm^2 s. Films of N_2 or O_2 can be rapidly removed by heating the substrate with an electrical heater.

The thickness of the film is known from the frequency change of the microbalance. In this way we may also calibrate the gas inlet system when the emissivity-change method is used on a massive substrate. With a cold cryostat the temperature of the target film is close to liquid-helium temperature. A further decrease in temperature may be obtained by pumping on the helium reservoir. Normally, the vacuum pressure is better than 2×10^{-8} Torr with a cold cryostat.

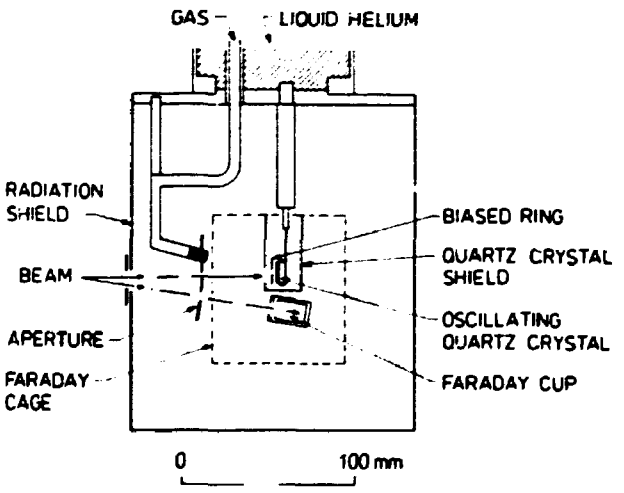

Fig. 1. Experimental arrangement. The target region. When the emissivity-change method is used, the quartz crystal is replaced by a massive target plate.

2.1. The emissivity-change method

This method is based on the following principle: A target irradiated with keV electrons will emit a certain number of secondary electrons. A bias of −45 V applied to a grid in front of the target may suppress the low-energy electron emission. Then only electrons with higher energies (reflected electrons) can escape. We can define an electron reflection coefficient η as follows:

$$i_t^- = (1 - \eta) i_b, \tag{1}$$

where i_b is the true beam current as measured by the Faraday cup and i_t^- is the target current when a negative bias is applied to the grid.

This reflection coefficient varies with primary energy and target material. During irradiation η changes from the N_2 or O_2 value to the substrate value as the film is eroded away. For 2 keV electrons incident on silver we found $\eta_{Ag} = 0.36$, while very thick films of N_2 and O_2 gave the value $\eta_{N_2} \approx \eta_{O_2} = 0.15$ in agreement with previous work [34,36].

It is then possible to estimate the fluence necessary for complete removal of the film and hence the average sputtering yield. The advantage of this method is the good thermal coupling between target material and cryostat bottom. A sufficient coupling has turned out to be very important in sputtering volatile solids. However, the method cannot directly give the eroded area A which must be determined in an alternative way. This is usually done by means of the quartz microbalance [5]. The sputtering yield from a film of thickness x is evaluated from:

$$Y(x) = N\left[\mathrm{d}(Ax)/\mathrm{d}\Phi\right] c. \tag{2}$$

Here N is the number density, Φ the total number of electrons necessary for complete removal and c is a constant (≈ 1) that depends on the geometry and how Φ is estimated [5].

2.2. The frequency-change method

Our measurements are mainly based on this method which directly gives the sputtering yield in terms of the frequency change of a quartz crystal, because this change is directly proportional to the weight loss. In particular, this may of course also be exploited to determine total fluences as mentioned above.

The heat deposited in the target layer by the energetic electrons is conducted away mainly through the small silver electrode on the quartz crystal. However, a comparison of the results for this method with the emissivity-change method ensures that this coupling is sufficiently good. Variation of the temperature by heating the quartz crystal or pumping on the helium reservoir as well as variation of current density on the target is used as a means to check that no significant thermal component is involved in the sputtering process (cf. section 3.1).

The accuracy of the frequency-change method is generally good. The main errors are: (1) Uncertainty in the slope of the linear part of the sputtering curve. (2) Drift of beam currents which could hardly be avoided in this experimental arrangement. Usually, only measurements for which the drift was less than 15% of the initial current were used. A numerical procedure in the data treatment system (based on linear interpolation) may partly compensate this drift. For thick films ($> 3 \times 10^{17}$ molecules/cm^2), for which the bulk level is reached, the standard deviation in the sputtering yield is $\approx 8\%$.

3. Experimental results

3.1. Dependence on temperature, current density and grid bias

Measurements were performed in order to study if the sputtering was partly due to thermal sublimation. If this is the case one would expect to observe temperature and current density effects on the sputtering yield. (The precise temperature of the beam spot is not known, since the thermometer is placed on the crystal holder close to the electrode.) For both N_2 and O_2 the sputtering yield was found to be independent of target temperature between 3 and 14 K. Since these temperatures were measured without beam on target, the actual temperature of the condensed gas is substantially higher. At higher temperatures a significant enhancement of the yield was observed.

A simple test is the dependence on current density. We changed the current density from 1.6 μA/cm^2 to 10 μA/cm^2 but found no influence on the sputtering yield for N_2 and O_2. Thus, in order to avoid temperature and current density effects, all further measurements were performed with ≈ 5 μA/cm^2 at ≈ 5 K. The application of a positive bias (+45 V) did not influence the sputtering yield.

3.2. Results for nitrogen

Fig. 2 shows the thickness dependence for 2 keV electrons on nitrogen. For film thicknesses larger than 2×10^{17} N_2/cm^2 there is virtually no change in the sputtering yield around the mean value 1.15 N_2/electron. We consider this as the bulk value. Below 2×10^{17} N_2/cm^2 there is a very weak increase in yield as well as a more pronounced scattering of the individual points.

A lot of independent measurements have been performed for the thickness 2.5×10^{16} N_2/cm. Here, the results would vary between 0.9 and 1.5 N_2/electron and only the mean value 1.2 N_2/electron is indicated in fig. 2. Further measurements down to 1×10^{16} N_2/cm^2 seem to indicate that the yields are reduced again for very thin films. This phenomenon is discussed further below.

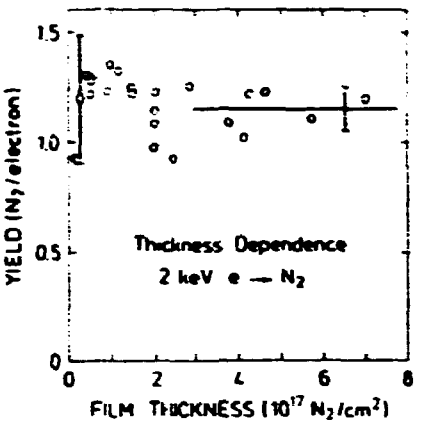

Fig. 2. Thickness dependence for 2 keV electrons incident on nitrogen. The solid line indicates the "bulk" yield 1.15 N_2/electron. The vertical bar indicates the scattering on individual points for the thickness 2.5×10^{16} N_2/cm^2 – only one point is indicated at this thickness.

The total fluences for 2 keV electrons as determined by both the frequency- and emissivity-change method are shown in fig. 3. There is an almost linear relation between total fluence and eroded mass leading to the mean value 1.3 N_2/electron. The good agreement between the two methods confirms that the

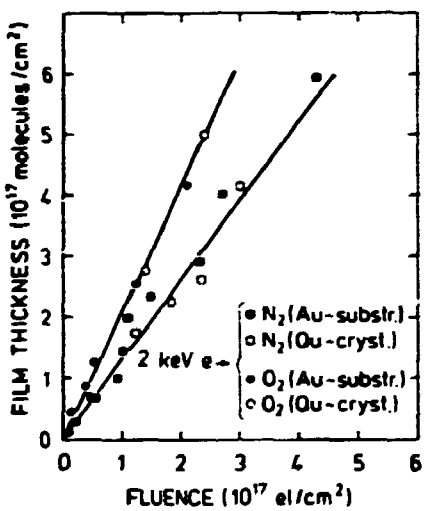

Fig. 3. Comparison of measurements performed with the emissivity-change method for a massive Au substrate and the quartz microbalance method. The initial thickness is plotted versus the fluence (see eq. (2)). The eroded area estimated from the quartz microbalance determined the fluence necessary for complete removal of the film. The slope of the two lines correspond to yields of 1.3 N_2/electron and 2.1 O_2/electron.

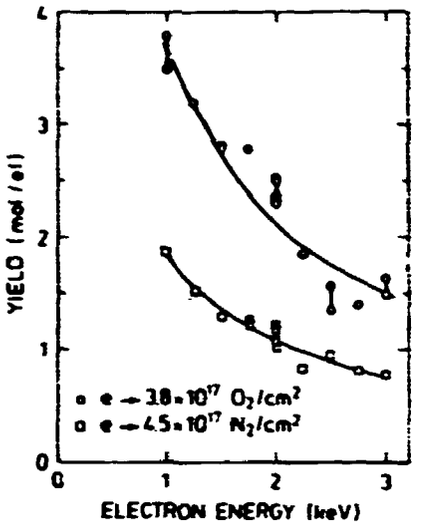

Fig. 4. Energy dependence of the nitrogen and oxygen sputtering yield in the electron energy range 1.0–3.0 keV for the thickness 4.5×10^{17} N_2/cm^2 and 3.8×10^{17} O_2/cm^2. The solid lines indicate the relations $Y(N_2) \propto S_e^{1.15}$ and $Y(O_2) \propto S_e^{1.26}$.

results for the microbalance method are not influenced by the relatively poor thermal coupling of the quartz crystal.

The energy dependence of the nitrogen sputtering yield has been measured in the electron energy range 0.8–3.0 keV. Fig. 4 shows the result for an initial thickness of 4.5×10^{17} N_2/cm^2 for 1 to 3 keV. The sputtering yield is a decreasing function of electron energy in this energy range. In fig. 4 a least-squares fit to the relation $Y = BS_e^q$ is shown as well, where B is some constant and $S_e(E)$ the Bethe stopping cross section for electrons. We found the yields to scale with the electronic stopping cross section or the stopping power $NS_e(E)$ to a power $q = 1.15$.

The pronounced scattering in sputtering yield for thin nitrogen films may be explained by the tendency for nitrogen to grow in clusters or by the crystalline state of the film [37]. It was attempted to investigate this further: After deposition of a film, the target was heated so that a fraction of the film sublimated away. When the average thickness of the film was reduced to $\approx 2.5 \times 10^{16}$ N_2/cm^2, we then returned to normal target temperature. As shown in fig. 5 sputtering of the remaining film leads to a lower yield than sputtering of a film of the same thickness produced directly (without sublimation). When we chose the films to be much thicker after sublimation (2×10^{17} or 4×10^{17} N_2/cm^2) we did not find any reduction in yield. The reason for this could be the tendency for thin nitrogen films to grow in clusters on the silver substrate. In that case we perhaps change this cluster configuration by

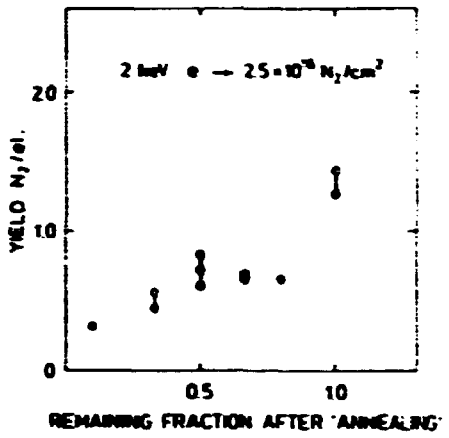

Fig. 5. Same film thickness produced by sublimation from different larger film thicknesses. Yield versus ratio of initial and final film thickness.

heating the quartz crystal: By raising the temperature of the film after the deposition we make the molecules more mobile on the surface. This favours the formation of larger clusters and bare spots on the electrode, and leads to the observed reduction in the sputtering yield. For thicker films ($> 1 \times 10^{17}$ N_2/cm^2) a more homogeneous layer is gradually formed, and this situation is not changed by raising the temperature.

Another possibility is that freshly-deposited films are amorphous, reverting to crystalline form on annealing. The transition might for example enhance the surface binding and lead to smaller sputtering yields. With thicker films, the temperature gradient across the film during deposition is equivalent to raising the temperature of thin films, resulting in crystalline surface regions from the beginning.

3.3. Results for oxygen

The thickness dependence for sputtering of oxygen with 2 keV electrons is shown in fig. 6. The yield decreases from 3.0 O_2/electron for the smallest measured thickness, 1×10^{16} O_2/cm^2, to 2.4 O_2/electron for thicknesses larger than 2×10^{17} O_2/cm^2. We consider this yield as the bulk yield. The oxygen points do not seem to scatter in the same fashion as the nitrogen points, and no decrease in yield for film thicknesses of about 1×10^{16} O_2/cm^2 is observed. This may indicate a more uniform film formation of oxygen than of nitrogen on silver.

The measurements performed by the emissivity-change method (fig. 3) gives $Y \approx 2.1$ O_2/electron. The result is in reasonable agreement with the one obtained from the frequency-change method.

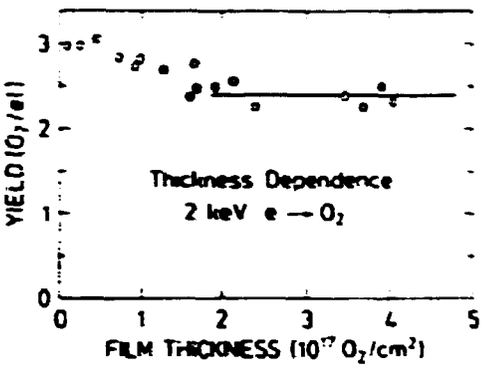

Fig. 6. Thickness dependence for 2 keV electrons incident on oxygen. The solid line indicates the "bulk" yield 2.4 O_2/electron.

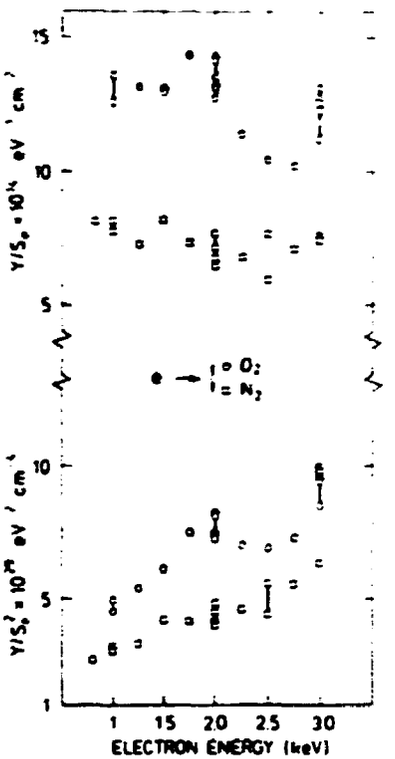

Fig. 7. Upper part: Ratio between yield and electronic stopping cross section as a function of electron energy for N_2 and O_2. Lower part: Ratio between yield and electronic stopping cross section squared as a function of electron energy for N_2 and O_2.

For the energy dependence (fig. 4) measured with a film thickness of 3.8×10^{17} O_2/cm^2 (almost twice the range of 3 keV electrons), we reach the same qualitative conclusions as for N_2: The yield decreases with energy and was found to scale with the electronic stopping cross section to a power $q = 1.20$.

A least-squares fit may not necessarily be the most convincing way of testing whether a single power dependence, with q about 1, applies at all. For both nitrogen and oxygen sputtering we have shown, therefore, the relations Y/S_e and Y/S_e^2 versus electron energy (fig. 7). Fig. 7 indicates an almost linear relation between yield and stopping cross section over the whole energy range while clearly excluding a proportionality with S_e^2. This is an important experimental result and will be a substantial point in the following discussion of the various models proposed for condensed gas sputtering.

3.4. Comparison with other experiments on condensed gases

The majority of the experiments on condensed gas sputtering have been performed with keV to MeV ion bombardment. Only few data are published for sputtering with electrons [5,6,8,9,12,13]. Several groups use Rutherford backscattering [2,8,16] for monitoring target thickness, while the first measurements performed with a quartz microbalance were reported by Schou et al. [5].

A strong dependence of the yield on temperature has been observed for the solid rare gases krypton and xenon [8]. For 750 keV $^4He^+$ ions incident on solid argon [2] the yields were temperature independent below 24 K and rose sharply above this temperature. This enhancement was due to beam-induced evaporation. For temperatures below 14 K it was also demonstrated that the sputtering was apparently not caused by beam-induced evaporation, as no current-density dependence was found between 0.05 and 0.5 $\mu A/cm^2$. Recent measurements performed by Rook et al. [14] on N_2 and O_2 sputtered by 1.5 MeV He^+ ions showed no temperature dependence between 6 and 22 K, and no significant current-density dependence was observed.

The yield dependence on the film thickness has been measured for solid rare gases at MeV ion bombardment [2,7,8] as well. In almost all cases the yield increased with thickness and reached the "bulk" value between 2 and 3×10^{17} atoms/cm^2. The erosion of xenon on a 2000 Å layer of frozen SF_6 resulted in a decreasing yield with increasing film thickness. Such a behaviour has also been observed with the emissivity-change method for the solid hydrogen isotopes [12]. For Ne sputtering with keV electrons the thickness dependence seems to be quite complex [38]. No thickness dependence was observed for N_2 bombarded by MeV light ions [15].

The experimental results for the energy dependence of the sputtering yield by ion bombardment is somewhat more controversial. Reimann et al. [7] suggested that the yield for light MeV ions incident on solid argon was almost

proportional to the electronic stopping power. A square dependence has been found for water, carbon monoxide and sulphur dioxide exposed to MeV ion bombardment [22,39,40].

The data of Brown et al. [15] for light-ion bombardment of N_2 give a linear dependence of the yield on S_e as long as this remained below 200 eV Å^2/molecule. Above this value a transition to a quadratic dependence was observed. According to the authors such a behaviour may be correlated to the average excitation density in the track region. For electron-induced sputtering the data are more scarce. In the case of carbon monoxide Johnson and Brown [22] found a proportionality between a relative electron-induced yield, obtained by use of a quadrupole mass spectrometer, and the stopping power squared. With the frequency-change method Schou et al. [38] have found that for Ne the yield is almost proportional to the electronic stopping power for primary electron energies above 1.5 keV.

4. Discussion

4.1. Models for electronic sputtering

For MeV ion and keV electron bombardment the major part of the energy deposited by the primary particle is expended in electronic excitations and ionizations in the condensed gas, while nuclear stopping plays a vanishing role. Some of this electronically deposited energy must be converted into atomic motion so fast that the translational motion of atoms or molecules is initiated before the energy is lost to the surrounding medium as heat. Atoms or molecules near the surface receiving translational energy can then overcome the small surface binding energy and be sputtered.

A number of different models for the sputtering of solidified gases by particles depositing their energy in the electronic stopping power regime have been suggested in the recent years. One cannot expect to find one "universal" mechanism behind the sputtering process. Besides the basic differences of the irradiated solids, e.g., between water ice, other solid molecular gases and solid rare gases, the magnitude of the excitation density plays a decisive role. When the excitation density becomes sufficiently high, yields nonlinear in the electronic stopping power can be expected [1,16].

We can regard this so-called spike regime in two different ways. One way is the "ion-explosion" model of Brown et al. [39,41]. In this model, the Coulomb repulsion of the ions along the track is considered to be the source of ejection of target particles. This demands low mobility of the electrons in the target material, because the neutralization probability must be low. This is not fulfilled for rare-gas solids but is possible for molecular solids. Another version of the "ion-explosion" model was proposed by Haff [23]. Ions are assumed to

be created at adjacent sites along the track of the primary particle. In their mutual Coulomb repulsion they may acquire enough energy to create a cascade of low-energy secondaries, some of wich may overcome the surface barrier and be sputtered. The yield for both models is expected to be proportional to the electronic stopping power squared.

Let us estimate the effect of such a mechanism in the case of N_2 or O_2. The maximum energy input to a cascade will appear for two adjacent ionized molecules (mean spacing = 3.6 Å). The resulting energy from the Coulomb repulsion E_c = 4 eV is of the same magnitude as the available energy from the dissociative recombination which we regard as the important process for energy release (see section 4.3). The mean spacing between individual ionization events is around 50 Å for 2 keV electrons incident on N_2 or O_2, so normally the energy liberated from repulsion is much less. Thus, this energy estimate and the direct proportionality to the electronic stopping power mean that in our case we do not expect such a mechanism to contribute measurably compared to the mechanism considered below.

Another model is the modified lattice potential model [42], which has successfully explained the erosion of water ice and sulphur dioxide by MeV ions. As this model demands a band gap G to sublimation energy U_0 ratio: $1 \leq G/U_0 \leq 20$, we cannot use this model in the case of N_2 where the G/U_0 ratio is considerably larger than 100 [43]. In the next section we discuss a model, which may explain the electronic sputtering of simple condensed gases.

4.2. *Feasibility of a collision-cascade mechanism*

The applicability of collision-cascade theory for sputtering of solidified gases has become more firmly established. One of the difficulties has been the lack of experimental data for simple homonuclear molecular solids. Furthermore, in many cases the excitation density induced by the incident particle was so high that the mutual interaction between excited or ionized target particles complicated the treatment.

Let us shortly consider some of the recent experimental results. Only very few data are available for sputtering with ions in the low keV regime. Sputtering measurements of frozen Xe have been made by Stevanovic et al. [44] using 20–80 keV heavy ions (N, Ar, Sb and Bi), i.e. in a regime where nuclear stopping is the dominant process. They utilized these results as well as previous ones for light MeV ion bombardment to extract the sputtering yield induced by nuclear collisions. The agreement between this and the estimated yield from ordinary sputtering theory was satisfactory. The sputtering theory could also explain the magnitude as well as the energy dependence of the yield for water ice bombarded by keV Ne^+ ions reported by Bar-Nun et al. [45].

During sputtering or desorption [26,46] the majority of the ejected particles are neutrals. Irradiation of solid CO by keV hydrogen ions demonstrates that

the overwhelming fraction of the sputtered species is neutral CO molecules [47]. Also Brown et al. [15] show that almost only N_2 molecules are ejected from bombardment of solid nitrogen by MeV light ions. Measurements performed by us with a positively biased grid did not show any difference to those with negative bias. This observation indicates that the ejected particles are neutrals in our case as well.

The data for the energy of the sputtered particles are rather scarce. Boring et al. [48] investigated the energy E_0 of sputtered SO_2 and D_2O particles for keV and MeV ion bombardment where nuclear as well as electronic energy losses take place. In both cases an E_0^{-2} dependence for the sputtered particles was found, corresponding to a collision-cascade-like behaviour. Haring et al. [47] indicate that a similar energy distribution for many of the ejected species is observed during light-ion bombardment of solid CO, H_2O and NH_3. In this latter case the energy is primarily deposited in electronic excitations but, nevertheless, this collision-cascade-like behaviour is found here as well. Even during bombardment of frozen SF_6 by 750 eV electrons many of the most energetic, ejected species behave similarly [49]. However, one should emphasize that the maximum of the energy distribution [47–49] is substantially lower than predicted by the collision-cascade theory. On the other hand, we may not exclude a significant energy loss to other channels, e.g. vibrational excitation, which may lead to a slight distortion of the energy spectrum.

From the discussion we suggest that for solid nitrogen and oxygen a collision-cascade mechanism might be involved in the sputtering process even when the incident particle deposits its energy in the electronic stopping power regime. The particles ejected are mainly neutral molecules.

4.3. Evaluation of the yield from the collision-cascade theory

A substantial difference between collision cascades in ordinary non-volatile solids, e.g. metals, and the possible cascades in the condensed gases is the low binding energy of the volatiles. In the latter case, the particles that initiate the low-energy cascades may be created also by non-radiative transitions of molecules or atoms excited by the primary incoming particle. These transitions will typically release a few eV as translational energy of the atoms [1,14,16]. The ratio E_s/U_0 between the liberated energy E_s and the sublimation energy U_0 of the volatile solid is therefore often not much smaller than that for metals bombarded by keV ions. In the latter case sputtering theory [19,20] is successfully applied.

When the atomic motion is created from isotropic sources distributed in the solid we can immediately calculate the yield from a collision-cascade model. The interaction between the low-energy atoms in the cascade is, despite the uncertainty involved, assumed to be given by the normal power approximation

Table 1
Molecular properties

	N_m (Å^{-3})	U_0 (meV)	W (eV)	E_s (eV)	Λ (Å/eV)
N_2	2.21×10^{-2}	78	36.2	3	24.4
O_2	2.88×10^{-2}	90	32.5	7	16.2

N_m, molecular number density [34,54]; U_0, sublimation energy *per molecule* [55]; W, average energy deposited per ion pair produced [56]; E_s, amount of kinetic energy received by the target particles per ion pair produced [14]; Λ, material constant, eq. (3).

to the cross section used in sputtering theory [20]. As shown in appendix A the electronic sputtering yield is given by:

$$Y = \tfrac{1}{4}\Lambda\, E_s\, D_e(0)/W \quad \text{(molecules/primary particle)}. \tag{3}$$

W is the average energy required to make an electron–hole pair, and $D_e(x=0)$ is the surface value of the electronical energy deposited by the primary. The constant $\Lambda = 0.042/(N_m U_0\ [\text{Å}^2])$, see table 1, is determined alone by the properties of the target material, i.e. by U_0 and the molecular density $N_m = \frac{1}{2}N$. A similar approach has been used by Johnson et al. [16] (see appendix A).

The distribution $D_e(x)$ of energy deposited in electronic excitations for electrons incident on air and nitrogen is known from experiments by Grün [50] and Barrett and Hays [51]. The value of $D_e(0)$ is approximately 1.6 $NS_e(E)$ for electrons on N_2 or O_2 in the energy regime under consideration (see, e.g., fig. 3 in ref. [52]).

The prediction (3) can also be compared with existing data on MeV proton bombardment of solid N_2 [15]. For this case the density $D_e(x)$ of electronically deposited energy is constant up to quite large depths and equals the initial stopping power $NS_e(E)$ of the proton.

In order to obtain the yield from eq. (3) we require an estimate of the value of E_s by considering the relaxation processes in the solid. For MeV He^+ ions incident on solid N_2 and O_2 Rook et al. [14] suggested that the dominant process for the energy transfer is dissociative recombination. We assume the energy conversion process to be virtually identical for primary electrons.

According to Rook et al. the important process for solid N_2 is the dissociative recombination $N_2^+(X\,^2\Sigma_g^+) + e \rightarrow N(^4S^\circ) + N(^2D^\circ)$. In the gas phase the liberated energy E_s is about 3 eV. This suggestion is corroborated by electron irradiation experiments that show the presence of N atoms in the ground state as well as the $^2D^\circ$ state in a solid N_2 matrix [28]. The subsequent radiative transitions to the ground state were observed as well. Rook et al. regarded the strong Vegard–Kaplan band $A\,^3\Sigma_u^+ \rightarrow X\,^1\Sigma_g^+$ as unimportant for translational energy release, and indeed, recent experiments indicate that the electronic relaxation of this state takes place in such a manner that the transfer of excess energy to the lattice is minimized [53].

Table 2
Theoretical and measured yields

Bombarding particle	N_2			O_2		
	S_e (eV Å^2)	Y_{cal}	Y_{exp}	S_e (eV Å^2)	Y_{cal}	Y_{exp}
2 keV electrons	14.9	0.5	1.2	16.3	1.3	2.4
0.8 MeV H^+	59.8	1.3	1.2	63.3	3.2	
1.5 MeV H^+	39.8	0.9	0.7	43.9	2.2	
0.03 MeV He^+	130.0	2.9	21	139.8	5.4	74

S_e, electronic stopping cross section of the primary particles; Y_{cal} (molecules/primary particle) is from (3); Y_{exp} (molecules/primary particle) are the experimental sputtering yields. The stopping cross section in the case of electrons is calculated from the Bethe stopping power formula. The stopping cross section and experimental yields in the case of H^+, He^+ ions are from refs. [14,57].

For solid O_2 Rook et al. consider the dissociative recombination $O_2^+(X^2\Pi_g) + e \rightarrow O(^3P) + O(^1D)$ as dominant. The energy release is about 5 eV in the gas phase, and the subsequent quenching of the excited ^1D state results in an additional 2 eV. The total energy release per recombination then becomes $E_x \approx 7$ eV.

For solid N_2 or O_2 there are no indications in the literature of contributions from mobile excitons to the sputtering. Diffusion of excitons has been reported in some cases but without any characteristic diffusion lengths [28]. However, these excitations are different from the ones that we regard as possible sources for the energy release. This is indeed consistent with our observation of the thickness dependence which may be ascribed to the varying intensity of reflected electrons (see below). In contrast an exciton diffusion and decay model would, for example, lead to a sputtering yield increasing with thickness.

The values of the absolute yields calculated from (3) are compared with our electron data and the light MeV ion data of Rook et al. [14] and Brown et al. [15]. The results are summarized in table 2. The agreement with experiment is good for proton bombardment and satisfactory for primary electrons. For He^+ ion bombardment the formula underestimates the yield quite strongly. This is probably caused by the high excitation density. The experimental yield for bombardment by MeV protons is proportional to the electronic stopping power [15], i.e. consistent with our assumption of energy release from mutually distant sources. As mentioned earlier, this proportionality was observed for electron bombardment as well and explained by the dependence on $D_e(0)$, which in turn was proportional to the electronic stopping power.

The cascade model predicts only a thickness dependence of the yield due to changes in $D_e(0)$. In the case of electrons this change is weak and caused by backscattering of primary electrons at the substrate. This can hardly be confirmed in the case of N_2 (fig. 2) due to scattering in experimental points. In the case of O_2 the yield seems to increase for thicknesses below half the electron range (fig. 6).

5. Conclusion

We have investigated the sputtering of two molecular solidified gases with electrons in the energy range 0.8–3 keV. Two different experimental methods are used: Sputtering measured from the weight loss of a quartz crystal or by means of the emissivity-change method. We found agreement between the two methods.

The yield for oxygen is almost a factor of two higher than the yield for nitrogen. These results agree with measurements performed by Rook et al. and are explained by the different amount of kinetic energy available from recombination in the two molecules. We found the yields to scale almost with the electronic stopping power, which means that sputtering may be assumed to take place via ionization events in widely distant molecules for this low energy density regime.

A rather weak thickness dependence of the yields is found, most pronounced for oxygen. In the case of nitrogen strong fluctuations in the yield around a film thickness of $\approx 2.5 \times 10^{16}$ N_2/cm^2 are observed.

Different models for electronic sputtering are discussed. Sputtering from low-energy collision cascades initiated by dissociative recombination can explain our experimental data and existing data for MeV H^+ ion bombardment as well. The model is expected to work only when the density of the electronic excitations as well as their mobility are low.

Acknowledgements

We wish to thank W. Brown and R.E. Johnson for making their unpublished results available to us. We also acknowledge P. Sigmund, R. Pedrys and W. Brown for discussions and valuable comments. We thank as well the technical staff, A. Nordskov, B. Sass and K. Borman for competent assistance.

Appendix A: Derivation of low-energy cascade sputtering yield from isotropic sources (eq. (3))

A straightforward application of sputtering theory to condensed gases is hindered by the lack of knowledge of some of the important parameters that characterize the low-energy cascades (e.g. the sputtering $-\alpha$ [19,20] and the low-energy collision cross section). The former difficulty has been overcome totally by including the *isotropy* of the atoms that initiate the local cascades. For the latter parameter we propose to use the power approximation to the Born–Mayer cross section used in sputtering theory [20]:

$$d\sigma = C_0\, dT/T, \quad C_0 = \tfrac{1}{2}\pi\lambda_0 a^2, \quad \lambda_0 = 24, \quad a = 0.219\ \text{Å}, \tag{A1}$$

where T is the energy transfer between atoms. For the case of a constant source density, e.g. $NS_e(E)/W$, eq. (3) is already derived in ref. [19].

Let us now consider a more general source density $D_e(x)/W$. The average source density is a slowly varying function of depth compared to the atomic dimensions. The density may be a Gaussian distribution, a decreasing linear distribution or a constant one of finite width. The total yield

$$Y = (1/W)\int D_e(x)\, Y(x, \langle R^2\rangle^{1/2})\, dx \tag{A2}$$

is easily found by means of the contribution $Y(x, \langle R^2\rangle^{1/2})$ to the sputtering yield from a plane isotropic source at a distance x (eq. (67a) in ref. [19]). The three-dimensional standard deviation $\langle R^2\rangle^{1/2}$ of the low-energy cascades is very small compared with the characteristic quantities for $D_e(x)$, e.g. the mean value or standard deviation σ_D. We then obtain eq. (3) for the limit $\langle R^2\rangle^{1/2}/\sigma_D \to 0$.

We have considered atomic cascades rather than molecular cascades in order to apply the standard cross section (A1), and to utilize the well-known material constant $\Lambda = (3/4\pi^2)(NC_0/2)^{-1}$ in eq. (3). This assumption implies that the surface barrier for the moving atom is $U_0/2$ (and U_0 for molecules as usual).

If we introduce the diffusion cross section for low-energy collisions, $\bar{\sigma}_d = 2C_0$, the yield formula (3) may be compared with a similar expression given by Johnson et al. [16] (eq. (3b)):

$$Y = \Lambda_1 E_s D_e(0)/W, \quad \Lambda_1 = (3/8\pi^2)(\bar{\sigma}_d N_m U_0)^{-1}. \tag{A3}$$

Our expression differs by a factor 1/4 from the expression given by Johnson et al. This originates from two factors. Firstly, their expression apparently lacks a factor 1/2 due to sputtering from isotropic sources and, secondly, they choose to apply a diffusion cross section $\bar{\sigma}_d \approx 2N_m^{-2/3}$ for the interaction between molecules. For molecular solids such a large cross section will probably underestimate the yield. If we include the missing isotropy factor 1/2 in the expression of Johnson et al., the two expressions will agree completely in the case of atomic solids (i.e. the solid rare gases).

References

[1] R.E. Johnson and W.L. Brown, Nucl. Instr. Methods 209/210 (1983) 469.
[2] F. Besenbacher, J. Bottiger, O. Graversen, J.L. Hansen and H. Sørensen, Nucl. Instr. Methods 191 (1981) 221.
[3] T.A. Tombrello, in: Desorption Induced by Electronic Transitions, DIET 1, Eds. N.H. Tolk, M.M. Traum, J.C. Tully and T.E. Madey (Springer, Berlin, 1983) p. 239.
[4] L.J. Lanzarotti, W.L. Brown, K.J. Marcantonio and R.E. Johnson, Ices in the Solar System, Ed. J. Klinger, in press (1985).

[5] J. Schou, H. Sørensen and P. Børgesen, Nucl. Instr. Methods B5 (1984) 44.
[6] P. Børgesen, J. Schou, H. Sørensen and C. Claussen, Appl. Phys. A29 (1982) 57.
[7] C.T. Reimann, R.E. Johnson and W.L. Brown, Phys. Rev. Letters 53 (1984) 600.
[8] R.W. Ollerhead, J. Bøttiger, J.A. Davies, J. L'Ecuyer, H.K. Haugen and N. Matsunami, Radiation Effects 49 (1980) 203.
[9] S.K. Erents and G.M. McCracken, J. Appl. Phys. 44 (1973) 3139.
[10] P. Børgesen, Risø Report-R-457, Risø National Laboratory, Denmark (1982).
[11] P. Børgesen, J. Schou and H. Sørensen, in: Proc. Symp. on Sputtering, Perchtoldsdorf/Vienna, Austria, April 1980, Eds. P. Varga, G. Betz and F.P. Viehböck (Technische Universität Wien, Vienna, 1980) p. 822.
[12] P. Børgesen and H. Sørensen, Phys. Letters 90A (1982) 319.
[13] J. Schou, O. Ellegaard, P. Børgeser and H. Sørensen, in: Desorption Induced by Electronic Transitions, DIET 2, Eds. W. Brenig and D. Menzel (Springer, Berlin, 1985) p. 170.
[14] F.L. Rook, R.E. Johnson and W.L. Brown, Surface Sci. 164 (1985) 625.
[15] W.L. Brown, L.J. Lanzarotti, K.J. Marcantonio, R.E. Johnson and C.T. Reimann, to be published.
[16] R.E. Johnson and W.L. Brown, Nucl. Instr. Methods 198 (1982) 103.
[17] C. Claussen, Ph.D. thesis, Odense University, Denmark (1982).
[18] R. Pedrys, D.J. Oostra and A.E. de Vries, in: Desorption Induced by Electronic Transitions, DIET 2, Eds. W. Brenig and D. Menzel (Springer, Berlin, 1985) p. 190.
[19] P. Sigmund, Phys. Rev. 184 (1969) 383; 187 (1969) 768.
[20] P. Sigmund, in: Sputtering by Particle Bombardment I, Ed. R. Behrisch (Springer, Berlin, 1981) p. 9.
[21] L.E. Seiberling, J.E. Griffith and T.A. Tombrello, Radiation Effects 52 (1980) 201.
[22] W.L. Brown, W.M. Augustyniak, K.J. Marcantonio, E.H. Simmons, J.W. Boring, R.E. Johnson and C.T. Reimann, Nucl. Instr. Methods B1 (1984) 307.
[23] P.K. Haff, Appl. Phys. Letters 29 (1976) 473.
[24] J. Michl, Intern. J. Mass Spectrom. Ion Phys. 53 (1983) 255.
[25] P. Børgesen, H. Sørensen and Chen-Hao Ming, Nucl. Instr. Methods 212 (1983) 517.
[26] P. Feulner, W. Riedl, and D. Menzel, Phys. Rev. Letters 50 (1983) 986.
[27] R.A. Rosenberg, V. Rehn, A.K. Green, P.R. La Roe and C.C. Parks, Phys. Rev. Letters 51 (1983) 915.
[28] K. Dressler, O. Oehler and D.A. Smith, Phys. Rev. Letters 34 (1975) 1364;
O. Oehler, D.A. Smith and K. Dressler, J. Chem. Phys. 66 (1977) 2097.
[29] M. Øhlenschlæger, H.H. Andersen, J. Schou and H. Sørensen, to be published.
[30] A. Adams and P.K. Hansma, Phys. Rev. B22 (1980) 4258.
[31] F.J. Himpsel, N. Schwentner and E.E. Koch, Phys. Status Solidi (b) 71 (1975) 615.
[32] J. Schou, H. Sørensen, H.H. Andersen, M. Nielsen and J. Rune, Nucl. Instr. Methods B2 (1984) 159.
[33] R.J. Sayer, R.H. Prince and W.W. Duley, Proc. Roy Soc. London A365 (1979) 235.
[34] H. Sørensen and J. Schou, J. Appl. Phys. 49 (1978) 5311.
[35] J.A. La Verne and A. Mozumder, Radiat. Phys. Chem. 23 (1984) 637.
[36] J. Schou, Risø Rapport R-391, Risø National Laboratory, Denmark (1979).
[37] J. Krim, J.G. Dash and J. Suzanne, Phys. Rev. Letters 52 (1984) 640.
[38] J. Schou, P. Børgesen, O. Ellegaard and H. Sørensen, to be published.
[39] W.L. Brown, W.M. Augustyniak, E. Brody, B. Cooper, L.J. Lanzerotti, A. Ramirez, R. Evatt and R.E. Johnson, Nucl. Instr. Methods 170 (1980) 321.
[40] L.J. Lanzerotti, W.L. Brown, W.M. Augustyniak, R.E. Johnson, and T.P. Armstrong, Astrophys. J. 259 (1982) 920.
[41] W.L. Brown, W.M. Augustyniak, L.J. Lanzerotti, R.E. Johnson and R. Evatt, Phys. Rev. Letters 45 (1980) 1632.

[42] C.C. Watson and T.A. Tombrello, Radiation Effects 89 (1985) 263.
[43] H.-J. Lau, J.-H. Fock and E.E. Koch, Chem. Phys. Letters 89 (1982) 281.
[44] D.V. Stevanović, D.A. Thompson and J.A. Davies, Nucl. Instr. Methods B1 (1984) 315.
[45] A. Bar-Nun, G. Herman, M.L. Rappaport and Yu. Mekler, Surface Sci. 150 (1985) 143.
[46] R. Pedrys, private communication.
[47] R.A. Haring, R. Pedrys, D.J. Oostra, A. Haring and A.E. de Vries, Nucl. Instr. Methods B5 (1984) 483.
[48] J.W. Boring, J.W. Garrett, T.A. Cummings, R.E. Johnson and W.L. Brown, Nucl. Instr. Methods B1 (1984) 321;
J.W. Boring, R.E. Johnson, C.T. Reimann, J.W. Garret, W.L. Brown and K.J. Marcantonio, Nucl. Instr. Methods 218 (1983) 707.
[49] R. Pedrys, R.A. Haring, A. Haring and A.E. de Vries, Nucl. Instr. Methods B2 (1984) 573.
[50] A.E. Grün, Z. Naturforsch. 12A (1957) 89.
[51] J.L. Barrett and P.B. Hays, J. Chem. Phys. 64 (1976) 743.
[52] J. Schou, Phys. Rev. B22 (1980) 2141.
[53] H. Kühle, J. Bahrdt, R. Fröhling, N. Schwentner and H. Wilcke, Phys. Rev. B31 (1985) 4854.
[54] K. Kobashi, M.L. Klein and V. Chandrasekharah, J. Chem. Phys. 71 (1979) 843.
[55] M. Bienfait, J.L. Seguin, J. Suzanne, E. Lerner, J. Krim and J.G. Dash, Phys. Rev. B29 (1984) 983.
[56] Average Energy to Produce an Ion Pair, ICRU Report 31, International Commission on Radiation Units and Measurements.
[57] W.L. Brown, private communication.

Nuclear Instruments and Methods in Physics Research B18 (1987) 609-612
North-Holland, Amsterdam

Section VIII. Sputtering of condensed gases

ELECTRONIC SPUTTERING OF SOLID ARGON AND KRYPTON BY keV HYDROGEN IONS

J. SCHOU, R. PEDRYS *, O. ELLEGAARD and H. SØRENSEN

Association Euratom – Risø National Laboratory, Risø National Laboratory, Physics Department, DK-4000 Roskilde, Denmark

Electronic sputtering of solid argon and krypton with the hydrogen ions 6 keV H_2^+ and 9 keV H_3^+ has been studied by means of a quartz microbalance technique. No difference in the yield per atom was found for diatomic or triatomic ions. The thickness dependence of the yield for both argon and krypton is similar to results reported previously for solid argon irradiated by light MeV ions.

1. Introduction

The solid rare gases constitute a particular class of materials with respect to sputtering induced by light particles [1,2]. Several experiments with primary electrons, hydrogen and helium ions on films of solid neon, argon and xenon have demonstrated that the sputtering yield increases with film thickness up to thicknesses above 2×10^{17} atoms/cm^2 [3–9]. Such behaviour is unusual compared with sputtering experiments on other condensed gases or ordinary materials as, for example, metals. The reason is that mobile electronic excitations created along the trajectory of the primary may reach the surface and contribute to the particle emission.

In particular, sputtering of solid argon has been studied frequently [4,5,7,8,10]. The sputtering yield is so large (from 1 to 100 argon atoms per primary) that making the measurements is not too dificult. On the other hand, experiments with solid argon do not necessarily require temperatures close to that of liquid helium. Another feature which made solid argon interesting is the strong luminescence from particle-bombarded argon [5,8]. Since sputtering of argon has mostly been carried out with MeV protons and helium ions [7,8], we have extended the regime of energy with particles below 10 keV as primaries. This work contains results for solid argon irradiated by keV hydrogen ions, whereas a forthcoming publication reports sputtering by keV electrons [4].

In contrast, very few measurements have been carried out for solid krypton [9,10], and no systematic investigation of the thickness dependence of the yield was performed so far. The present work includes a study on the yield from krypton sputtered by keV hydrogen ions as a function of film thickness.

The dominant erosion process at the energies considered in the present work is electronic sputtering, i.e. sputtering via electronic transitions. The contribution from knock-on sputtering may be estimated from linear collision cascade theory [11] to below 10%, mainly because more than 80% of the total energy is deposited in electronic excitations.

2. Experimental

The basic experimental setup as well as the quartz microbalance have been described elsewhere [6,12].

Films from 3×10^{16} up to 1×10^{18} atoms/cm^2 of solidified argon or krypton are produced by letting a jet of cooled gas impinge on an oscillating quartz crystal (fig. 1). The substrate is cooled to a temperature close to that of liquid helium.

Beams of 6 keV H_2^+ or 9 keV H_3^+ are extracted from a duoplasmatron ion source and selected by a 45° magnet. These ions have been utilized, since the beam intensity is sufficient, and since the combination of these two ions allows us to decide whether or not molecular effects are present. The current is measured by deflecting the beam into a Faraday cup. The beam is swept horizontally and vertically over an aperture in front of the target, thus ensuring a homogeneous irradiation of a large part of the target area. As in the case of electron-induced sputtering we apply a negative bias (−90 V) to an open repeller ring in front of the target in order to suppress secondary electron emission.

The current density was below 1 μA/cm^2, where evaporation caused by beam heating has turned out to be insignificant. This current density causes no drift in the oscillator frequency. The sputtering yield is determined from the frequency shift of the microbalance. In a typical sputtering experiment for these solidified gases the frequency change is about 40 Hz. After each run the eroded film is thrown away by heating the quartz crystal.

* Permanent address: Instytut Fizyki, Uniwersytet Jagiellonski, PL 30-059 Krakow, Poland.

0168-583X/87/$03.50

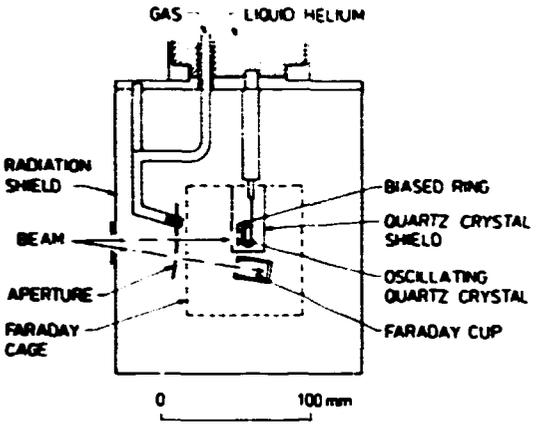

Fig. 1. The experimental setup

No systematic investigations of the temperature dependence of the yield were performed. However, even the much more volatile solid neon showed no dependence on the substrate temperature in the present regime and related measurements indicate that the enhancement of the yield because of sublimation only takes place at temperatures above 23 K [7].

3. Results

The sputtering yield for solid argon is shown as a function of thickness in fig. 2. One notes that the yield

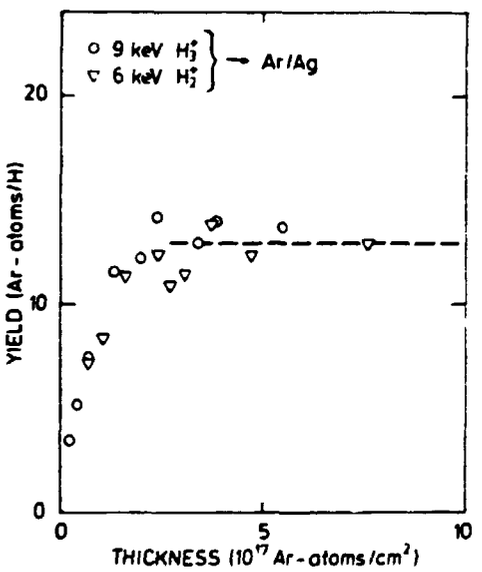

Fig. 2. Thickness dependence of the yield for solid argon. Dashed line: average yield for thick films.

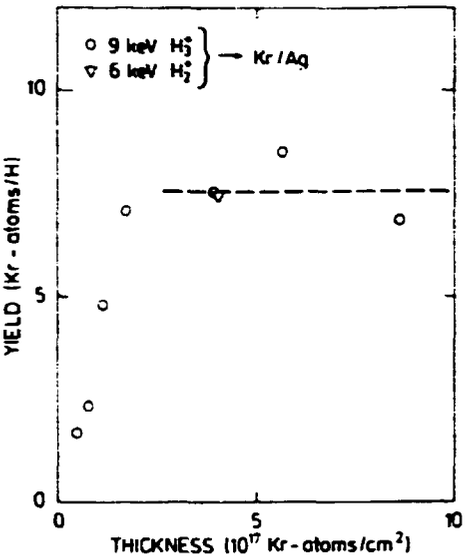

Fig. 3. Thickness dependence of the yield for solid krypton. Dashed line as in fig. 2.

increases with thickness up to a value of about 13 Ar/H.

In addition, fig. 2 demonstrates that there is no significant difference between the experimental yields in

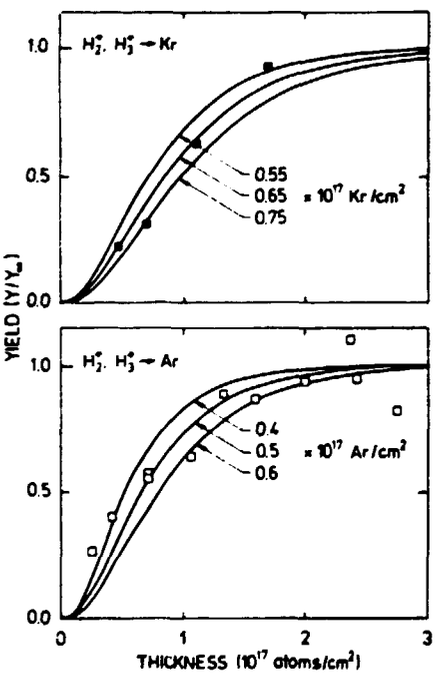

Fig. 4. Comparison between experimental results for argon and krypton, and the yield from eq. (1) for several values of the diffusion length.

argon atoms per hydrogen atom for 9 keV H_3^+ and 6 keV H_3^+. In fig. 3 the dependence on thickness is shown for solid krypton bombarded by these ions. The sputtering yield increases with thickness as well, but the data indicate that the saturation thickness may be slightly larger for krypton than for argon.

4. Discussion

The thickness dependence of the yield demonstrates that electronic excitations created along the track up to quite large depths contribute to the yield. Since these excitations in solid rare gases are largely mobile, and in some cases even have been ascribed a characteristic diffusion length [13], one may expect that a considerable fraction of the excitations deexcite close to the surface. By such a deexcitation sufficient energy (1–2 eV) is released for atomic motion, i.e. for the eventual particle ejection from the solid.

As a fair approximation one may assume that the molecular ions H_3^+ and H_2^+ will dissociate upon impact under an equal sharing of energy. Such a multiple impact could increase the density of excitations locally near the region of impact compared with the incidence of H^+ with equal energy per atom. In a material without mobile excitations such an impact of a molecular ion might lead to an enhancement of the yield per incident atom. However, since excitations from the whole excitation volume may contribute and since these excitations do not interact mutually, no enhancement of the yield per hydrogen atom occurs.

The absence of any molecular effect is in complete agreement with the recent results for solid neon bombarded by hydrogen ions as well [6]. This behaviour reflects the fact that the production of mobile excitations by disintegrated molecular ions takes place at all film thicknesses from the surface up to the complete penetration distance in solid neon. A similar observation has been made by Ollerhead et al. for 1 MeV H_3^+ ions and 500 keV H^+ ions incident on solid xenon [9].

The thickness dependence shown in fig. 2 is completely similar to existing yield curves which have been obtained for MeV He^+ and H^+ ion bombardment of argon with different methods and at slightly different temperatures [7,8]. The behaviour of the yield as a function of thickness for 3 keV primary electrons obtained at the same setup scarcely deviates from the present result [4].

The precise type of the mobile excitation in solid argon and krypton is as yet unestablished. Reimann et al. suggest that the mobile species are atomic holes R^+ [8], but photon irradiation experiments indicate that molecular excitons R_2^* are mobile as well [13]. Another possibility for the mobile carrier is a molecular hole R_2^+ as asserted by Le Comber et al. [14]. The translational energy for the atomic motion is released as the result of a dissociative recombination of R_2^+ or by a radiative transition of the $(n = 1)$-exciton R_2^* to the repulsive ground state [3,8]. The liberated energy is about 1–2 eV in the first case, and 1.6 and 1.3 eV in the latter case for argon and krypton, respectively [15]. Because of the weak binding these deexcitations initiate low-energy cascades which ultimately may lead to particle ejection from the solid [3,8,16,17].

Let us consider a mobile electronic excitation without specifying the precise type. We apply a constant stopping power for the primaries as a straightforward approximation, and assume that the surface is highly reflecting for the excitations, in agreement with the considerations for solid argon in refs. [3] and [8]. The interface between the film and the metal is, as usual, absorbing [3,4,15].

According to the treatment in refs. [4] and [18] the yield for a film of thickness d is determined by

$$Y(d) = (1 - 1/(\cosh(d/l_0)))\,Y_\infty . \qquad (1)$$

Y_∞ is the saturation yield for thick films, and l_0 the diffusion length for the excitations. The yield curve has been calculated for several values of l_0 (fig. 4), and one notes that the overall shape agrees fairly well with the experimental values for $l_0 = 0.5 \times 10^{17}$ Ar/cm^2 and $l_0 = 0.65 \times 10^{17}$ Kr/cm^2. However, the value for krypton is considerably more uncertain because of the relatively few data points. The constant stopping power approximation is questionable for krypton, since the diffusion length is comparable to the projected range of the primaries [19]. Nevertheless, we consider the result as a useful indication of the proper value. For solid argon the projected range is about 2.5 times larger than l_0, and the approximation correspondingly better.

The contribution from hydrogen atoms reflected from the metal substrate has been estimated to be below 15% of the total yield on the basis of the treatment for thin films in ref. [3] and existing data for the energy spectrum of reflected protons [20]. Then the determination of the diffusion length is only very weakly influenced by the contribution of backscattered primaries.

The present value of the diffusion length (~ 190 Å) for solid argon agrees very well with the ones obtained by Reimann et al. for MeV light ion bombardment. These authors determined a similar value, $l_0 = (190 \pm 40)$ Å, whereas the results from Besenbacher et al. [7] indicate a somewhat longer length. The value from electron incidence is in fair agreement with the ones obtained for ion bombardment as well [4,18].

The present value of l_0 is considerably larger than the diffusion length for the $(n = 1)$-exciton determined from photoemission experiments with a value of $l_0 = 120$ Å [13]. However, recent measurements of the luminescence from the decay of this exciton from a vibrational excited state, i.e. the W band, indicate that the diffusion

length may be enhanced up to about 1000 Å for films produced in a particularly careful manner [5].

The values of about 0.5×10^{17} atoms/cm^2 deduced for solid argon and krypton are smaller than that for solid neon which - determined to be approximately 1.0×10^{17} Ne atoms/cm^2 [3,6]. This difference between neon and the other solid rare gases has been established in photoemission experiments as well [13].

5. Conclusion

The thickness dependence of the sputtering yield has been investigated for solid argon and krypton bombarded by molecular hydrogen ions. The diffusion length for argon 0.5×10^{17} atoms/cm^2 agrees well with the length obtained for other primary particles. For solid krypton the diffusion length for the mobile excitations has been estimated to be 0.65×10^{17} atoms/cm^2. However, this value is somewhat uncertain in view of the limited number of data points.

No enhancement in the yield per atom was found for triatomic relative to diatomic ions. This observation confirms the assertion that excitations from the complete excitation volume may contribute to the yield.

R. Pedrys is grateful to Risø National Laboratory for the hospitality he enjoyed during his stay.

References

[1] R. Pedrys, presented at this Conference (Symposium on Sputtering, 1986).
[2] W.L. Brown and R.E. Johnson, Nucl. Instr. and Meth. B13 (1986) 295.
[3] J. Schou, P. Børgesen, O. Ellegaard, H. Sørensen and C. Claussen, Phys. Rev. B34 (1986) 93.
[4] O. Ellegaard, R. Pedrys, J. Schou, H. Sørensen and P. Børgesen, to be published.
[5] F. Coletti, J.M. Debever and G. Zimmerer, J. Phys. Lett. 45 (1984) L-467.
[6] O. Ellegaard, J. Schou and H. Sørensen, Nucl. Instr. and Meth. B13 (1986) 567.
[7] F. Besenbacher, J. Bøttiger, O. Graversen, J.L. Hansen and H. Sørensen, Nucl. Instr. and Meth. 191 (1981) 221.
[8] C.T. Reimann, R.E. Johnson and W.L. Brown, Phys. Rev. Lett. 53 (1984) 600; W.L. Brown, C.T. Reimann and R.E. Johnson, in: Desorption Induced by Electronic Transitions, DIET II, eds., W. Brenig and D. Menzel (Springer, Berlin, 1985) p. 199.
[9] R.W. Ollerhead, J. Bøttiger, J.A. Davies, J. l'Ecuyer, H.K. Haugen and N. Matsunami, Radiat. Eff. 49 (1980) 203.
[10] R. Pedrys, D.J. Oostra and A.E. de Vries, in: Desorption Induced by Electronic Transitions, DIET II, eds., W. Brenig and D. Menzel (Springer, Berlin, 1985) p. 190.
[11] P. Sigmund, in: Sputtering by Particle Bombardment, ed., R. Behrisch (Springer, Berlin, 1981) p. 9.
[12] J. Schou, H. Sørensen and P. Børgesen, Nucl. Instr. and Meth. B5 (1984) 44.
[13] N. Schwentner, E.-E. Koch and J. Jortner, Electronic Excitations in Condensed Rare Gases (Springer, Berlin, 1985).
[14] P.G. Le Comber, R.J. Loveland and W.E. Spear, Phys. Rev. B11 (1975) 3124.
[15] C. Claussen, Thesis, Odense University (1983).
[16] O. Ellegaard, J. Schou, H. Sørensen and P. Børgesen, Surf. Sci. 167 (1986) 474.
[17] R. Pedrys, D.J. Oostra, A. Haring, A.E. de Vries, O. Ellegaard, J. Schou and H. Sørensen, to be published.
[18] O. Ellegaard, Thesis, Risø rep. M-217, to be published.
[19] H.H. Andersen and J.F. Ziegler, Hydrogen Stopping Powers and Ranges in all Elements (Pergamon, Oxford, 1977).
[20] W. Eckstein and H. Verbeck, Nucl. Fus., Special Issue (1984) 12.

Nuclear Instruments and Methods in Physics Research B27 (1987) 188 - 200
North-Holland, Amsterdam

Section VII. Frozen gas sputtering and charge transfer at surfaces

SPUTTERING OF FROZEN GASES

Jørgen SCHOU

Association Euratom - Risø National Laboratory, Risø National Laboratory, Physics Department, DK-4000 Roskilde, Denmark

Particle-induced erosion of frozen gases takes place as beam-induced evaporation as well as sputtering. At sufficiently low temperatures electronic or knock-on sputtering is the dominant mechanism for particle ejection. Knock-on sputtering may largely be compared to ordinary sputtering of metals, although the yields are much higher for ices than for metals because of the low surface binding energy. Electronic sputtering exhibits large differences from the solid rare gases to the solid diatomic homonuclear gases or the solid heteronuclear molecular gases.

1. Introduction

Ten years ago the basic knowledge in the sputtering of frozen gases was scarce. However, the subject has developed rapidly and has been studied systematically in many respects. Whereas several current review articles exist on erosion of condensed gases by energetic particles [1,2], particularly by keV and MeV ions [3–5], only very few measurements of particle sputtering or photon sputtering were carried out before 1978 [6–12]. Nevertheless, condensed gas erosion was recognized as playing an appreciable role in several areas, although reliable laboratory data almost did not exist ten years ago. The improved knowledge of the basic erosion processes has recently been demonstrated in a number of reviews on the erosion of icy surfaces in interplanetary space [13–15]. The erosion of pellets of solid hydrogen and deuterium injected into plasma devices has been summarized by Chang et al. [16] and Milora [17], although the effect of the impinging high-energy particles has not been fully incorporated in these reviews. Finally, one may consider charged-particle or photon impacts on cryopumping surfaces in ultra-high vacuum devices [9,18].

The solidified gases included in the present work are all room-temperature gases apart from water ice. The type of binding ranges from weak Van der Waals for the low-temperature solids to more complicated ones, for example, for water ice. The surface binding energy, characterized by the sublimation energy is as low as 7 to 14 meV for molecules of the hydrogen isotopes [19], 20 to 170 meV for the solid rare gases (table 2), and 80 to 520 meV for the molecular condensed gases from solid nitrogen to water ice [3].

These frozen gases are all electrical insulators with electronic band gaps from a few eV up to approximately 21 eV for solid neon. Because of the lack of the electron contribution to the thermal conductivity these solids are also poor thermal conductors, with the heat deposited by the beam particles conducted away from the impact area comparatively slowly.

Before considering the consequences of these properties let us briefly discuss the different types of erosion (fig. 1). At elevated target temperature or at high beam current densities beam-induced evaporation is the prevailing mechanism. In contrast, at sufficiently low temperatures and current densities the dominant particle erosion mechanism is sputtering, i.e. target particle ejection as a result of single-particle impact events.

The low binding energy means that the erosion yield for both beam-induced evaporation and sputtering is very large compared with yields from metals, for example. The lack of free electrons in the frozen gases means that the energy deposited in electronic excitations may be converted partly to translational energy of the target particles, and will contribute to sputtering. The yield from this component in sputtering, the electronic sputtering (fig. 1), may even exceed the yield from ordinary (knock-on) sputtering by several orders of

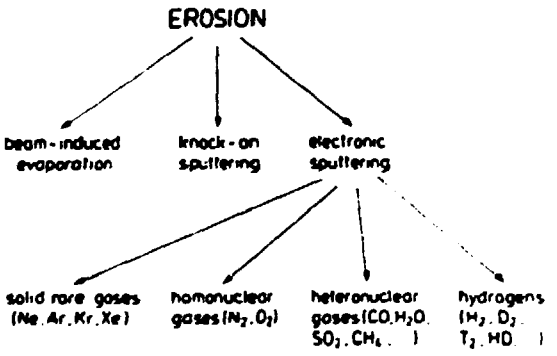

Fig. 1. Schematic survey of the erosion processes.

0168-583X/87/$03.50

magnitude. Finally, these electrical insulators charge up easily during charged-particle irradiation, so that countermeasures frequently have to be taken during the experiments.

In the present work the main emphasis will be given to the general aspects of sputtering as well as the electronic sputtering of solid rare gases and the solid homonuclear, diatomic gases. Sputtering results from the solid hydrogens will not be included, as the mechanism for sputtering is still poorly known.

2. Experimental methods

Most of the experiments have been carried out, so far, with a standard set-up in which a film of the frozen gas has been deposited on a low-temperature substrate. In fig. 2 a schematic survey of the most important measured quantities is shown including a number of parameters which influence the yield. The thickness of the irradiated film ranges from less than 50 Å up to more than 1 mm. The primaries have been electrons of energies from a few eV up to 3.5 keV as well as a number of ions (from H^+ up to Xe^+ and Bi^+) from about 1 keV up to 25 MeV. The temperature of the substrate has been reported to be below 4 K in some experiments with the most volatile ices, but experiments at more than 100 K have also taken place for the least volatile ones.

The overwhelming majority of the emitted particles are neutrals. Usually, the charged fraction is hardly measurable [4,20–22]. So far, the largest ion fraction (~ 0.1) has been reported for ion-bombarded solid hydrogen [23]. Nevertheless, the secondary ions have been well studied, because of the extreme sensitivity with which the ions may be detected [22,24,25]. Also the emission of electronically excited atoms has been observed [26].

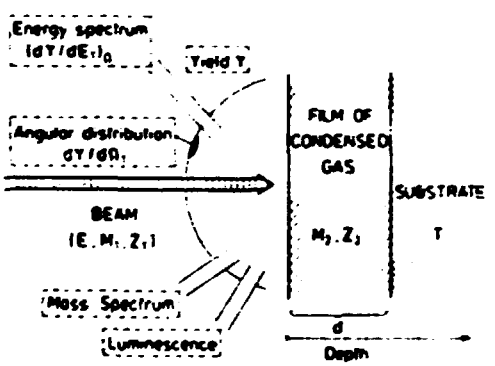

Fig. 2. Schematic survey of the experimentally studied quantities in an erosion experiment.

Up to now the erosion yield Y has been determined in several ways. The two most accurate methods are the Rutherford backscattering analysis (RBS) of the remaining film area density, or measurement of the instantaneous film thickness by the frequency change from a quartz-crystal microbalance. The RBS analysis has been applied by the groups at AT&T Bell Lab. [27,28], in Århus [20], in Chalk River [29], in Hamilton [30], and in Pasadena [31]. The frequency-change method has been used by the groups at Risø [21,32] and in Salt Lake City [22]. Also measurements directly by quadrupole mass spectrometers with a reliable calibration procedure have turned out to be important (at AT&T Bell Lab. [4,28] and in Tel Aviv [33]). Moreover, the remaining film area density has been determined from the energy loss of fast-charged particles from a radioactive source on the substrate surface in Charlottesville [34].

In addition to these measurements of the instantaneous thickness or the number of sputtered particles a variety of methods, in which some signal from the film or substrate is monitored, have been introduced. These methods have been developed to different levels of accuracy, and in general it is very difficult to measure a thickness-dependent yield [32]. At Risø the change in the current of the reflected electrons during the erosion was utilized [32,35], whereas secondary ions were monitored in Tempe [25]. Preliminary results have been obtained by using the mass signals in Amsterdam [36].

The *energy distribution* $(dY/dE_1)_{\Omega_1}$ of the ejected particles at a fixed solid angle Ω_1 has been determined by a time-of-flight method in Amsterdam [37], at AT&T Bell Lab. and in Charlottesville [38]. The angular distribution $(dY/d\Omega_1)$ has apparently not been systematically investigated yet.

Table 1
Comparable data [a]

Primary ion	Target	Yield	Laboratory	Comments
1.5 MeV He^+ [b]	Ar	44	Århus	Ref. [20]
1.5 MeV He^+ [b]	Ar	43	AT&T Bell	Ref. [28]
4 keV Ne^+ [c]	Ar	790	Salt Lake City	Ref. [22]
4 keV Ne^+ [c]	Ar	900	Risø	Ref. [42]
4 keV Ne^+ [d]	H_2O	18.4	Tempe	Ref. [25] $\theta = 45°$
4 keV Ne^+ [c]	H_2O	9.0	Tel Aviv	Ref. [33] $\theta = 60°$
10 keV Ne^+ [f]	D_2O	7.8	Charlottesville	Ref. [43] $\theta = 0°$

[a] Conc. the accuracy consult the references.
[b] RBS method.
[c] Frequency-change method.
[d] SIMS method. θ is the angle of incidence.
[e] Mass spectrometry.
[f] Energy loss measurements.

A large effort has been concentrated on the mass composition of the ejected particles by quadrupole mass spectrometry in Amsterdam [39], at AT&T Bell Lab. and in Charlottesville [38]. The reason is that frequently fragments of polyatomic target molecules are ejected [38,39] and even for the monoatomic solid rare gases not only have single atoms been observed, but also dimers and trimers of the target atoms [40].

Particle-induced luminescence during sputtering has been observed systematically only for the solid rare gases (at AT&T Bell Lab. [28] and in Marseille [41]).

The current status of agreement among data from different laboratories is summarized in table 1. Unfortunately, many of the frozen solids have not been investigated for similar primary energies and particles at the different laboratories. It would be highly desirable to have a larger common data base, in particular having different methods of measurements.

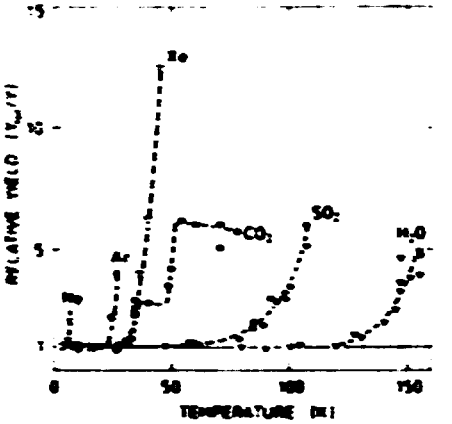

Fig. 3. Beam-induced evaporation caused by external heating. The relative yield Y_{tot}/Y is plotted versus substrate temperature. Y_{tot}, total yield; Y, low-temperature yield. Ne data [46]; Ar data [28]; Xe data [29]; CO_2 data [47]; SO_2 data [44]; H_2O data [45].

3. Beam-induced evaporation

It is well established that the sputtering of frozen gases is independent of temperature below a certain threshold [20,21,44–46]. This is convincingly demonstrated fig. 3, which includes solid rare gases as well as solid heteronuclear gases [47]. Except for carbon dioxide the yield increases sharply above the characteristic threshold temperature. This quantity is clearly correlated with the sublimation energy U_0, which for example is much larger for sulphur dioxide (0.37 eV) than that for xenon (0.164 eV). The behaviour of the yield from solid carbon dioxide has been explained by the formation of two distinct new molecules with low activation energies for diffusion [47].

The general behaviour with the large increase at elevated temperatures is a consequence of the low binding energy and the poor thermal conductivity of these materials. Beam-induced evaporation has been treated by the low-temperature spike model of Sigmund et al. [48,49]. The total yield Y_{tot} is a sum of the ordinary low-temperature yield Y (from electronic sputtering or knock-on sputtering) and a term that accounts for the yield increase by evaporation:

$$Y_{tot} = Y + \frac{1}{J}\left[\phi(T_s + \Delta T_{eff}) - \phi(T_s)\right]. \qquad (1)$$

where J is the current density, T_s the temperature of the ambient target, and ΔT_{eff} the average temperature rise of the target as the result of beam heating. The evaporation rate (number of atoms evaporated per unit time and area) [46,48]

$$\phi(T) = AT^{-1/2}\exp(-U_0/k_B T) \qquad (2)$$

is then enhanced drastically by an increase ΔT_{eff} from the beam because the total temperature $T_s + \Delta T_{eff}$ enters as an argument in the exponential. (A is a constant and k_B Boltzmann's constant).

All of the results shown in fig. 3 have been determined by heating the substrate during particle bombardment by an external heater. However, a very efficient way of heating may be obtained by increasing the current density. Usually, the sputtering experiments are performed below a current density threshold in a regime where the yield is independent of the current density. A strong enhancement for high-current densities was observed by Schou et al. from solid neon [32]. This effect was explained by the increase of ΔT_{eff} in eq. (1) as a result of beam heating.

4. Sputtering: general aspects

Sputtering of insulators may be characterized as knock-on sputtering (collisional sputtering) or electronic sputtering as indicated in fig. 1. Knock-on sputtering is very well known from ion bombardment of metals. It may be described as a sequence of events, in which target particles are set in motion, from the first collision between the primary and a target atom up to an eventual particle ejection as the result of collisions between slow target particles (fig. 4). The main features of knock-on sputtering for sufficiently small energy densities are well predicted by the linear collision-cascade theory [50,51]. The backsputtering yield Y from a plane surface is given by

$$Y = \Lambda F_D(E, 0). \qquad (3)$$

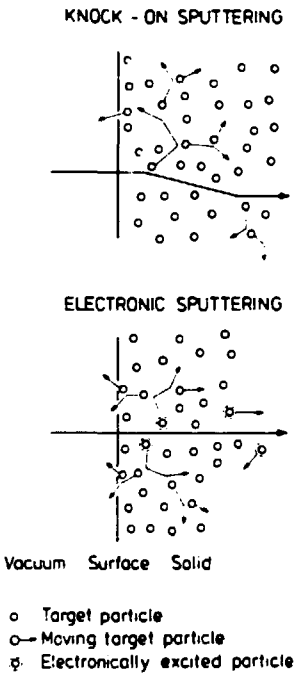

Fig. 4. Schematic survey of knock-on sputtering and electronic sputtering. The cases shown represent low excitation (collisional) densities.

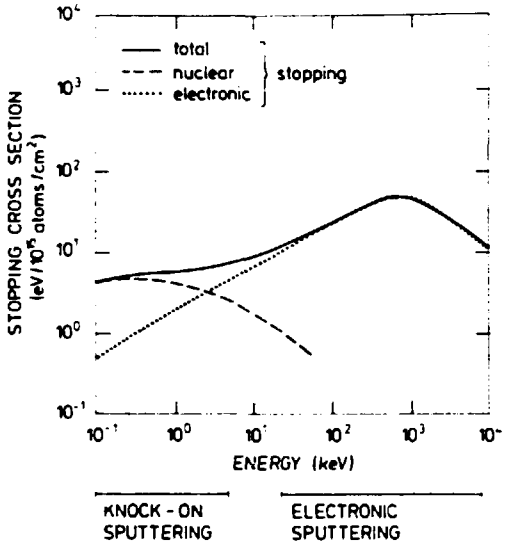

Fig. 5. Stopping cross sections for helium ions in gaseous nitrogen [52,53]. The corresponding sputtering regimes for solid nitrogen are indicated below.

where $F_D(E, x)$ is the spatial distribution of energy deposited into nuclear collisions by the primary of initial energy E. The constant $\Lambda = 3/(4\pi^2 N C_0 U_0)$ depends only on the properties of the target material, the sublimation energy U_0 and the atomic density N ($C_0 = 1.81$ Å^2). The surface value of the deposited energy ($x = 0$) is often expressed by the nuclear stopping power $NS_n(E)$ for the primary particle and a dimensionless parameter α:

$$F_D(E, 0) = \alpha N S_n(E). \tag{4}$$

α is a function of the mass ratio of the beam and target atom mass, and a slowly varying function of the energy. (We consider here and in the following only perpendicular incidence.) The energy distribution of the sputtered particles, which explicitly enters into the evaluation of Λ, is determined by

$$dY/dE_1 = k_s E_1/(E_1 + U_0)^3, \tag{5}$$

where k_s is a constant (see ref. [51]) and E_1 the energy of the emitted particle. For large energies the energy distribution exhibits the well-known E_1^{-2}-tail, and for small energies a maximum at $E_1 = U_0/2$.

Knock-on sputtering is important for the energy regime in which nuclear stopping is dominant. This is shown in fig. 5 for He ions incident on nitrogen. The stopping cross section $S(E) = |dE/dx|/N$ for the gas phase has been utilized [52,53], although the electronic stopping cross section in the solid phase might be somewhat smaller than the one for the gas phase [54,55]. For the large energies the electronic stopping cross section exceeds the nuclear one by more than one order of magnitude. The corresponding sputtering in this regime from insulators [20,27,56,57] turned out to be strongly correlated to the electronic stopping cross section. In fact, this connection has encouraged the use of the phrase "electronic sputtering". Fig. 5 shows that there is a transition regime as well, for which the sputtering yield consists of comparable knock-on and electronic contributions.

The combination, helium ions incident on nitrogen, is a particular example for which the contribution of fast recoils to the electronic sputtering is very small. For many combinations, where this contribution is significant, a convenient starting point is the deposition of the total energy E of the primary into nuclear collisions or electronic excitations:

$$E = \int D(E, x)\,dx + \int D_e(E, x)\,dx = \nu(E) + \eta(E). \tag{6}$$

D_e is the spatial distribution of energy deposited in electronic excitations. ν and η are consequently, the energy which ultimately ends up in atomic motion or electronic excitations, respectively [58]. In eq. (6), ν *represents the energy which is available for knock-on sputtering*, and η *the energy for electronic sputtering*. For

keV electron bombardment ν is negligible, and, therefore, the sputtering is purely electronic.

Let us now return to the question of how well the linear collision-cascade theory works for frozen gases. The surprising experimental result is that practically all spectra show large energy intervals with the characteristic E_1^{-2}-behaviour [36–38,40,45,59–63] except for some components of heteronuclear molecules [36,37,62]. This shows clearly that a fraction of the yield originates from linear collision-cascades. Of course, this is expected for knock-on sputtering. However, this behaviour is observed also for beam-particle/target-material combinations for which the energy deposition evidently is electronic, e.g. 1.5 MeV He^+ ions incident on water ice [60]. A convincing demonstration of similar behaviour has been suggested by Pedrys for 6 keV H^+ ions incident on solid argon [63]. This case is a clear example of electronic sputtering alone [5,64]. In fig. 6. $E_1^{1/3}(dY/dE_1)^{-1/3}$ is depicted as a function of the energy E_1. If eq. (5) holds, then the data points should be positioned on a straight line. Since this actually is the case, one is led to the conclusion that linear collision-cascades under certain circumstances play a very large role for sputtered particles of low-energy during *electronic sputtering* as well.

These experimental results as well as previous considerations on low-energy cascades in frozen gases [65] have demonstrated the feasibility of a collision-cascade model also in these materials. In the model by Ellegaard et al. [21] the electronic sputtering yield Y is determined by an expression in analogy to eq. (3):

$$Y = \tfrac{1}{2}\Lambda D_e(E,0)(E_s/W). \qquad (7)$$

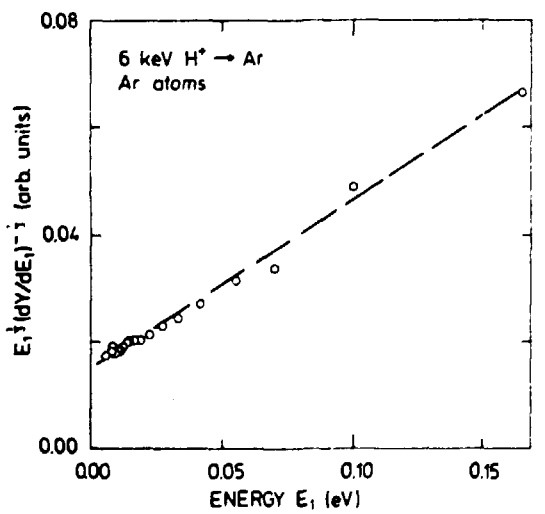

Fig. 6. Energy spectrum of ejected Ar atoms from solid Ar bombarded by 6 keV H^+ ions [63]. $E_1^{1/3}(dY/dE_1)^{-1/3}$ is plotted versus the kinetic energy E_1 of the emitted particles.

E_s is the nonradiative energy release from electronic deexcitations, and W the energy required to make an electron–hole pair. Let us then consider how this sputtering takes place (fig. 4). As a result of the slowing-down of the primary particle atoms or molecules are ionized or electronically excited. When these excitations deexcite, e.g., by dissociative recombination, the liberated energy E_s may be sufficient to initiate a low-energy cascade. Since these nonradiative transitions are completely isotropically distributed (as indicated in fig. 4) in contrast to the knock-on case, one arrives at the factor $\frac{1}{2}$ in eq. (7) [21]. The formula is based on the assumption that the energy E_s is released (in a single event) per electron–hole pair, but extensions of eq. (7) are straightforward.

For the simple case of a light MeV-ion one has as a very good approximation that the surface value $D_e(E,0)$ is equal to the electronic stopping power $NS_e(E)$. For electrons the surface value is somewhat larger than $NS_e(E)$, cf. section 6.

Eq. (7) is very similar to the expression indicated by Brown et al. [2] and Garrison et al. [66]. (These authors do not include the isotropy factor $1/2$ and utilize a different material constant [2,21]). As discussed in section 6 the formulas give a satisfactory prediction of the yield for low excitation densities from for example keV electrons or MeV protons.

Eq. (3) and (7) now enable us to estimate the efficiency of the sputtering, i.e. how well is the energy deposition F_D or D_e exploited for the production of sputtered particles? Electronic sputtering is clearly a factor of $\frac{1}{2}(E_s/W)$ less efficient than knock-on sputtering. For solid nitrogen, for example, this quantity is about 0.04.

The simple formula (7) is inapplicable to materials with mobile excitations, for example, as solid rare gases, but extensions of the formula are available [67]. Generally, for the heteronuclear molecules the energy-releasing processes as well as the value of E_s are not systematically known. For water ice, Chrisey et al. recently pointed out that the efficiency of electronic sputtering might be as large as for the knock-on sputtering [43].

Electronic sputtering has been observed for other insulating materials than frozen gases, e.g. alkali halides [68]. The main reason for the occurrence of this particular type of sputtering is the existence of repulsive states, from which kinetic energy for the ejection process is available. However, this means that the energy conversion strongly depends on the specific material, and that one cannot expect to find a single "universal" mechanism for the electronic sputtering. For metals the beam-induced electronic excitations do not generate any repulsive states for the atoms because of the fast relaxation of the free electrons. Consequently, electronic sputtering does not take place from particle-bombarded metals.

The considerations on collision-cascade sputtering in this section apply to cases in which the energy deposition by the primary particle is relatively small. For high excitation densities one reaches the elastic spike regime for knock-on sputtering [5,51,69–71] and an ionization spike regime for electronic sputtering. These regimes are characterized by the creation of dense cascades, in which the moving particles have a large probability of striking other target particles that already have been set in motion. Examples of ionization spikes have been reported for medium-mass ion bombardment of water ice [72,73], and sulphur dioxide [31] in the MeV regime.

5. Knock-on sputtering of frozen gases

This topic has recently been treated by Pedrys [5] and will only be briefly described. As mentioned in the general survey a majority of the existing spectra show the characteristic E_1^{-2}-behaviour [37,38,40,45,61,62]. This does not mean that all spectra agree consistently with the linear collision-cascade predictions. For example, in many cases the yield exceeds the theoretical value by more than one order of magnitude and, the maximum of the spectrum is far below the expected value at $E_1 = U_0/2$. Nevertheless, it means that a linear collision-cascade is responsible for the particle ejection at an early stage of the sputtering process.

Many of the results obtained for knock-on sputtering have been compared to the sputtering formula for linear collision-cascade theory (eq. (3)). As an overall trend the agreement is satisfactory as long as the (collisional) excitation density is small or the sublimation energy correspondingly large [2,5,25,30,33,34,43,60,61]. (An observation of a very high yield from the solid rare gases for very small fluences leads, however, to a clear disagreement [34,61]).

The high yields and the discrepancy between the observed maximum of the energy spectra and the linear collision-cascade prediction may be explained by the development of elastic spikes in the solid during the late stage of the sputtering process [5]. An alternative model based on a hydrodynamic expansion has been suggested by David et al. [74] and Urbassek et al. [75]. For both models the agreement is satisfactory.

6. Electronic sputtering: solid diatomic homonuclear gases

The class of condensed homonuclear gases includes primarily solid nitrogen and oxygen. So far, no measurements have been performed on solid halides, and it is possible that these reactive materials do not exhibit simple characteristics as do nitrogen and oxygen.

Solid nitrogen and oxygen are particularly simple cases, because the yield is almost independent of the film thickness, and because the energy dependence of the yield may well be described by a linear function of the stopping power for low excitation densities.

Measurements by Rook et al. [76] with light MeV-ions incident on both solids indicate that the yield is practically constant for film thicknesses from 5×10^{16} up to 5×10^{17} molecules/cm^2. For 1–3 keV electron incidence Ellegaard et al. [21] showed that a slight decrease with increasing film thickness for thicknesses less than one-half of the electron range was caused alone by primaries backscattered from the substrate. At large thicknesses the yield was constant. This independence of film thickness demonstrates that no *mobile electronic excitations* are responsible for the sputtering.

The energy dependence of the yield is shown in fig. 7. The proton data from Brown et al. [4] are plotted versus the stopping power, whereas the data for electron incidence from Ellegaard et al. [21] have been plotted versus the surface value of the electronically deposited energy, $D_e(0) = 1.6\ NS_e(E)$. The proton data are directly proportional to the stopping power up to about 10 eV/10^{15} N-atoms/cm^2. The electron data are described by a yield proportional to the stopping power with an exponent q slightly larger than one ($q = 1.15$). For both projectiles this virtually linear relationship indicates that the ejected particles originate from mutually independent ionization events.

For both nitrogen and oxygen the energy conversion from electronic energy to translational energy primarily takes place via dissociative recombination of the molecular ions. For nitrogen the process $N_2^+(X^2\Sigma_g^+) + e^- \rightarrow N(^4S^0) + N(^2D^0)$ leads to an average energy release of $E_s = 3$ eV. In oxygen a more complex process liberates about 7 eV [76]. Since this energy release is almost two orders of magnitude larger than the sublimation energy, low-energy collision cascades are created along the track of the primaries. As usual, cascades close to the surface result in particle ejection.

The calculated yield (eq. (7)) agrees well with the proton data, since the data points are reproduced within 30% (fig. 7). The electron data are about a factor of two larger than the calculated ones for $D_e(0) = 1.6NS_e$ [21]. Nevertheless, the formula indicates that the yield from oxygen should be a factor of two larger than that from nitrogen, since all other parameters, e.g. the sublimation energy, stopping power, and W-value, are practically similar. This is actually the case for the results for primary electrons. (For MeV He-ions with much larger excitation densities the yield from oxygen is greater than that from nitrogen by a factor which varies from 3 to 6.)

Although the predictions from formula (7) or the corresponding one by Johnson et al. [2,76] certainly give the right order of magnitude, the strong molecular binding leads to inavoidable difficulties in the treat-

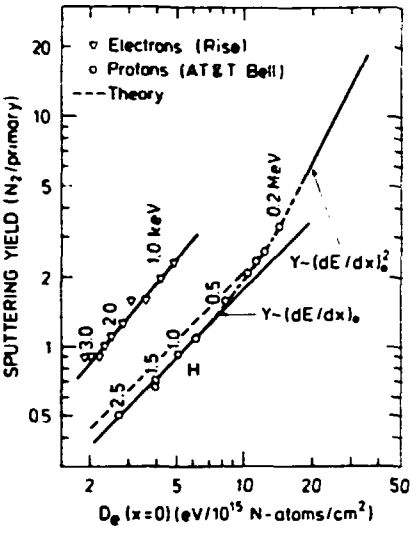

Fig. 7. Electronic sputtering yield for solid nitrogen. The yield is plotted versus the surface value of the electronically deposited energy. Electron data for the film thickness 2×10^{17} N_2/cm^2 [82]; proton data for 3.6×10^{17} N_2/cm^2 [4]. Dashed line, eq. (7).

ment. Ellegaard et al. [21] use the well-known Born–Mayer cross section, but have to consider the cascades as atomic rather than molecular ones in order to obtain a consistent treatment. This is in disagreement with the experimental observation that the emitted particles are mainly molecules [2]. On the other hand, Rook et al. [76] and Brown et al. [2] consider molecular cascades, but they have to introduce a cross section different from Born–Mayer to account for the poorly known slowing-down processes of the low-energy molecules.

None of the formulas are adequate for the high excitation densities, which are produced by MeV He ions or by protons with energies below 0.5 MeV. Brown et al. pointed out that the transition to a sputtering yield proportional to the quadratic stopping power takes place at excitation densities, for which the low-energy cascades start to overlap [4]. By including a correction for the near-surface equilibrium charge state of the incident He ions, Brown et al. [2] managed to get the helium results to coincide with the continuation of the hydrogen curve for high excitation densities.

These latter results demonstrate clearly that it would be desirable to measure sputtering yields from solid nitrogen bombarded by ions heavier than helium. Nitrogen is a feasible basis for all investigations with medium-light MeV ions, because of the clear linear behaviour at small excitation densities and, because the conversion mechanism at these densities is relatively well understood.

It is regrettable that no energy spectra of the ejected particles have been measured for solid nitrogen and oxygen. Such spectra would unambigously confirm the linear collision-cascade nature of the sputtering process.

7. Electronic sputtering: solid rare gases

Among the condensed gases the rare gas solids are particularly interesting, since the electronic excitations in these materials are mobile. The excitations below the band gab, the excitons, have recently been treated by Schwentner et al. [77] and Zimmerer [78], whereas the mobility of the holes and the "free" electrons has been discussed by Spear et al. [79,80].

Before considering the mobile species let us briefly discuss the decay of these electronically excited states. The energy release from these decays may create low-energy collision-cascades in the bulk and at the surface. The sputtered particles originate from the cascades close to the surface, or directly from decaying molecular excitons or holes at the surface.

Although most of the transitions in the rare gas solids are radiative, two transitions are very efficient in converting energy from electronically excited states to translational energy: Dissociative recombination of the molecular hole R_2^+ (i) or a radiative transition of the molecular excitons R_2^* to the repulsive ground state (ii). For argon a simplified scheme is shown in fig. 8. The dominant transition in all heavier rare gas solids is the M-band which originates from a transition from the lowest vibrational state of the molecular exciton R_2^* to the ground state. In argon the subsequent repulsion leads to an average energy release of about 1.6 eV (process (ii)) [28,70,81]. The W-band is the transition from a highly vibrationally excited state of the molecu-

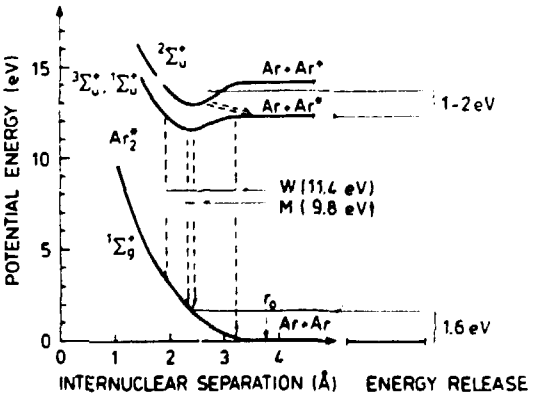

Fig. 8. Schematic representation of the important transitions in solid argon. The energy levels are from the solid. The transitions which may lead to energy release are indicated by dashed arrows.

lar exciton. This deexcitation is important only for solid neon and argon, but the energy release is similar to the M-band except for the infrequent transitions close to the left-hand turning point with a strong ground-state repulsion. The electron capture to the molecular hole R_2^+ leads to a dissociative recombination, which in solid argon liberates about 1–2 eV (process (i)) [28,67]. For both processes (i) and (ii) the energy release is more than one order of magnitude larger than the sublimation energy of both solid neon and argon. For krypton and xenon process (i) may operate in the sputtering process as well.

The behaviour of the sputtering yield from solid argon with increasing film thickness d is shown in fig. 9. One observes that even electronic processes which take place at thicknesses of more than 2×10^{17} atoms/cm^2 contribute to the particle yield. The thickness dependence is very similar for the different primary particles [20,28,64,67] and for the three laboratories. For all cases a characteristic diffusion length of about 0.5×10^{17} Ar/cm^2 (≈ 210 Å) is derived.

The thickness-dependence of the yield for all solid rare gases is shown in fig. 10 [28,29,46,64]. Only neon deviates somewhat from the general trend because of the slow saturation at large film thicknesses and the strong enhancement for thin films. Without considering the specific type of the difussing excitation one may determine a diffusion length l_0 which describes the behaviour quite well for all four solids [46,67,82]. This is made in analogy with the earlier diffusive description of the excitons in the lowest state [78,83,84]. For solid argon, krypton and xenon the diffusion length have been obtained from fig. 10 by a fit to the yield formula

$$Y(d) = [1 - 1/\cosh(d/l_0)]\, Y_\infty . \qquad (8)$$

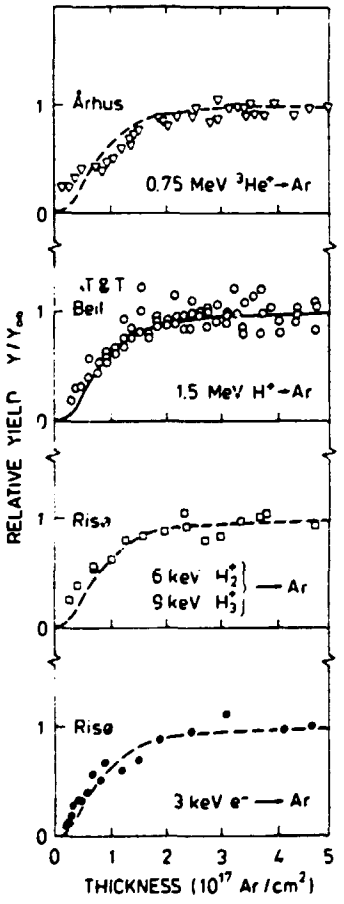

Fig. 9. The thickness-dependence of electronic sputtering from solid argon for different projectiles. The relative yield is plotted versus thickness. All yields have been normalized to the "thick-film" yield $Y_\infty = 1$. Solid and dashed lines, eq. (8), with $l_0 = 210$ Å (1.5 MeV H^+ [28]) as reference. 0.75 MeV $^3He^+$ [20]; 6 keV H_2^+ and 9 keV H_3^+ [64]; 3 keV e^- [67].

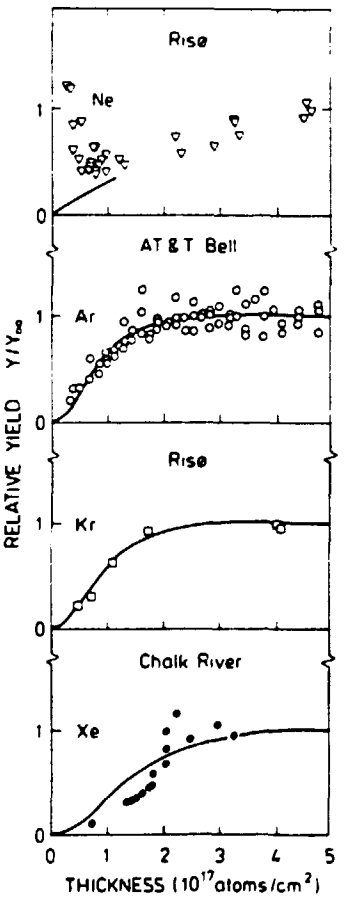

Fig. 10. The thickness-dependence of the electronic sputtering yield for the solid rare gases. The plot is similar to fig. 9. The solid line indicates the best fit to eq. (8). The values of l_0 are given in table 2. References as well as primary particles and energies in table 2.

This expression has been derived from the assumptions that the primary beam produces a uniform excitation density throughout the film, and that the surface acts as a reflecting boundary for the mobile excitations. The first assumption is clearly fulfilled for argon and xenon. The evaluation of l_0 for neon is more complex [46].

The diffusion lengths are indicated in table 2. This thickness, which for all films is known only as area density (atoms/cm^2), is converted to ordinary length unit (Å) from the tabulated number densities . The diffusion length may be compared to the extracted values for the diffusion of the lowest exciton states from measurements of photoluminescence yield spectroscopy or photoelectron emission [77,78]. The films from the optical measurements are of comparable quality, and the results are not too different from the sputtering results apart from the one for neon. However, this agreement might be fortituous. For neon the optically determined diffusion length is evaluated with a large uncertainty [86].

The similar increase in yield with thickness for all four solids might be an indication that the dominant mobile excitations are similar. A number of suggested carriers are listed in table 3. The carrier R_2^* is expected to be mobile only in the highly excited vibrational states and solely in solid neon and argon. The free exciton R^* is extremely mobile. However, the free excitons are important only in the heavy solid rare gases and preferentially in samples of high quality [78,87]. The atomic hole R^+ is a possible candidate in all four solids, even though the total diffusion length is extended by an additional diffusion of free excitons or molecular excitons. The atomic holes carry out the diffusion by electron charge transfer according to Reimann et al. [28] and Brown et al. [88]. The interpretation of the charge mobility in terms of molecular holes is based on experiments performed slightly below the triple point [80]. Since all sputtering experiments have been performed at temperatures close to that of liquid helium, we will disregard this latter carrier in the following.

The drastic enhancement of the yield of neon at small film thickness is probably not a behaviour that is related to the rare-gas properties. This is rather a consequence of the high volatility and the interaction with the substrate, in which most of the electronic energy will be deposited. A similar enhancement has been observed for hydrogen ions incident on neon [89], and for bombardment of the solid hydrogens by electrons and ions [6,35,90,91]. Even for the less volatile solids as argon and nitrogen this behaviour has been observed for film thicknesses less than 10^{16} atoms/cm^2 [7,92].

The dependence on the primary energy for light-ion bombardment in the MeV regime of solid argon and xenon is demonstrated in fig. 11. No systematic data are available for neon and krypton. The data shown indicate clearly that the yield for thick films is proportional to the electronic stopping power rather than the stopping power squared [93]. The model suggested above with diffusion of atomic holes or excitons, which is based on mutually independent excitations, would lead to a constant ratio of yield to electronic stopping power. Since this apparently is not the case, Reimann et al. [28]

Table 2
Diffusion length for solid rare gases

	Ne	Ar	Kr	Xe
Number density [a] (6 K) [10^{22} atoms/cm^2]	4.54	2.67	2.22	1.73
Sublimation energy [b] (0 K) [meV]	19.6	80	116	164
Primary particle	2 keV e^-	1.5 MeV H^+	6 keV H_2^+ 9 keV H_3^+	1 MeV $^4He^+$
Ref.	[46]	[28]	[64]	[29]
Diffusion length l_0 [c] [Å]	230 [d]	210 [e]	300 [e]	580 [e]
Optically determined diffusion length [f] [Å]				
Luminescence	-	40-100	200-250	150-2000
Photoelectr.	2500	120	30-300	75-300

[a] Ref. [85], pp. 770-783.
[b] Ref. [85], p. 689.
[c] Conc. accuracy of the values: consult the references.
[d] Model: absorbing surface.
[e] Model: reflecting surface.
[f] Diffusion of $n = 1$, $n' = 1$ and $n = 2$ excitons. Ref. [77], p. 183 and ref. [78].

Table 3
Mobile electronic excitations in solid rare gases

Mobile electronic excitation	Type	Suggested by	Applied on	Energy releasing process [b]
R_2^*	Vibrationally excited molecular exciton	Borgesen et al. [81] Claussen [70]	Ne. Ar	(ii)
R^*	Free exciton	[a]	Ne. Ar. Kr. Xe	(ii)
R^+	Atomic hole	Reimann et al. [28]	Ar	(i) + (ii)
R_2^+	Molecular hole	Le Comber et al. [80]	Ne. Ar. Kr. Xe	(i) + (ii)

[a] See, e.g., refs. [77,78].
[b] (i) and (ii) refer to notation in section 7.

and Brown et al. [88] have suggested that some interaction between the excitations takes place for high excitation densities. Bombardment by hydrogen ions with energies below 10 keV indicates as well that the yield from solid neon and argon is practically proportional to the electronic stopping power for densities below 20 eV/10^{15} atoms/cm^2 [5,89,94]. For primary electrons with a range comparable to the diffusion length one obtains a more complex dependence [46,67]. At high electron energies one expects that the yield is proportional to the stopping power as well.

The magnitude of the yield, e.g. in fig. 11, is determined primarily by the sublimation energy. Nevertheless, one notes that the yield for 1.5 MeV $^4He^+$-ions incident on solid argon is about 40 Ar/He^+ [20,28] compared to about 8 Xe/He^+ for ions of the same energy on solid xenon [29]. Since the sublimation energy increases only by a factor of 2 (table 2) from argon to xenon, it is clear that the energy release from the electronic deexcitation only is half of the magnitude of that from solid argon. This observation agrees well with the predicted energy release from the ground state repulsion in solid xenon [70].

However, the choice of boundaries for the diffusing excitations determines the magnitude of the yield to a certain extent. Only for a reflecting surface is a satisfactory agreement obtained between the experimental results for argon and the corresponding calculations based on the diffusion model [67,88]. Therefore, a reflecting surface has been assumed as well for the evaluation of the diffusion lengths in krypton and xenon. On the other hand, the corresponding use of an absorbing surface hardly changes the value of the diffusion length by more than 10–15%. For solid neon, the magnitude of the yield is explained, only if one applies an absorbing surface as boundary condition, and assumes that the surface-trapped deexciting molecules induce further sputtering [46,94]. The reason for the different surface conditions is not known.

The knowledge of the energy conversion process has been considerably extended by the threshold experiments performed by Coletti et al. [41,95]. The sputtering of neon and argon by low-energy electrons starts close to the threshold for exciton production, whereas no strong enhancement is observed for energies around the band gap. This is a significant indication that decaying excitons (process (ii)) are the dominant energy source for particle ejection.

Another important point for identifying the energy conversion process is the observation of a pronounced peak at 0.3 eV in the energy spectrum of the ejected particles for solid krypton bombarded by 6 keV hydrogen ions [5,63]. Since a similar structure is not shown by solid argon, this might be as strong indication of the presence of a ground-state repulsion process (ii) operat-

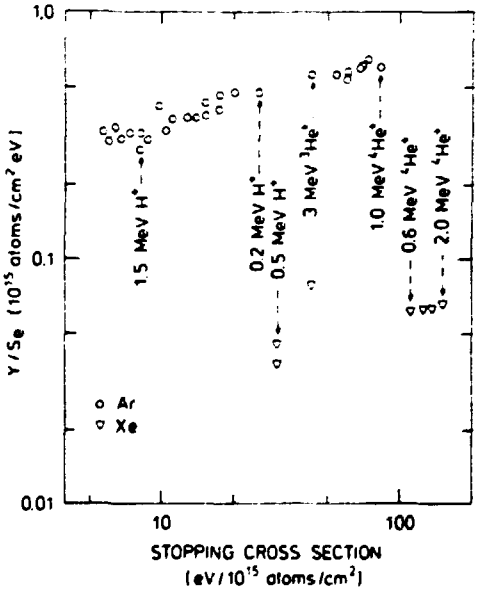

Fig. 11. The yield-dependence on the stopping cross section for solid argon and xenon. The ratio of the electronic sputtering yield to the stopping cross section is plotted versus the stopping cross section. Ar data [86]; Xe data [29].

ing at the surface. This is in agreement with the experimental observation that the decay of molecular excitons in argon at the surface takes place via the W-transition (fig. 8) as well [96].

The latter considerations indicate that it will be important to have energy spectra from solid xenon, where the W-transition is extremely unlikely. In particular electron-induced spectra will be useful for xenon (and for krypton and argon), because one definitely avoids the production of "knock-on damage" in the frozen gas. The resulting imperfections act as traps for the excitons and reduce the rate of excitations arriving at the surface.

In this connection it would be exciting to study the influence of the sample preparation on the magnitude of the yields. Coletti et al. [41] demonstrated that for argon layers deposited at elevated temperatures the fluorescence yield for the W-band saturates for thicknesses larger than 4000 Å. The corresponding large diffusion length compared to the optically determined one is a consequence of the improved sample quality. These authors correlated the intensity of the W-band to the sputtering yield as well, and this has also been observed for argon bombarded by MeV ions. Reimann [92] observed that the intensity of the W-band showed precisely the same thickness behaviour as the sputtering yield. In view of these results one would expect a larger yield from "high-temperature" samples than for the films deposited on substrates with temperatures close to that of liquid helium. In particular, an interesting experiment would be to study the sputtering yield for xenon samples of high quality, because the excitons in this solid are present mainly as free excitons [78,87].

Finally, some experimental results, which may bridge the gap between the threshold experiments at a few tens of eV by Coletti et al. [41,95] and the keV electron results for solid argon by Ellegaard et al. [67], are desirable. Such results would indicate, whether or not the models suggested by Coletti et al. for low-energy sputtering by electrons have any significance at larger energies.

8. Electronic sputtering: solid heteronuclear gases

This class of frozen gases is primarily characterized by the radiation-induced chemical reactions. This means that not only the original constituent, but also fragments of that as well as entirely new molecules are emitted during the sputtering process [33,36,38,39,43, 59,60]. The formation of these new molecules on the substrate means that a nonvolatile residue is left on the substrate after the original film has been removed [31,39,43,97–101]. However, one should emphasize that newly formed molecules also have been observed during keV ion bombardment in the "knock-on" regime [96].

The energy spectra again show an E_1^{-2}-behaviour in many cases [37,38,43,59,60,62]. It means that linear collision-cascades contribute to the sputtering. However, in contrast to the simple molecular gases as, for example, solid nitrogen, the electronic sputtering yield has turned out so far to be proportional to the stopping power squared for water ice [72], sulphur dioxide [103] and carbon monoxide [60]. This demonstrates that the sputtering requires the cooperation of two independent ionizations. Although it is reasonable to expect that excess energy from chemical reactions between fragments in the solid may initiate low-energy collision cascades, there is no systematic pattern of the sputtering mechanism at present in these complicated frozen gases. So far, no thickness dependence of the yield has been reported for these frozen molecules, but a number of transient phenomena have been observed [38].

9. Conclusion

The sputtering of frozen gases may not be explained on the basis of one "universal" mechanism. Although there are similarities between knock-on sputtering of the ices, the individual differences in the electronic deexcitation mechanisms lead to substantial differences in the behaviour of the electronic sputtering yield.

Acknowledgements

Discussions with and support from P. Sigmund, R. Pedrys, O. Ellegaard, P. Gürtler, H. Sørensen, R.E. Johnson and P. Børgesen have been appreciated by the author.

References

[1] T.A. Tombrello, in: Desorption Induced by Electronic Transitions, DIET I, eds. N.H. Tolk, M.M. Traum, J.C. Tully and T.E. Madey (Springer, 1983) p. 239.
[2] W.L. Brown and R.E. Johnson, Nucl. Instr. and Meth. B13 (1986) 295.
[3] W.L. Brown, in: Ion Implantation and Beam Processing, eds. J.M. Poate and J.S. Williams (Academic Press, New York, 1984) p. 99.
[4] W.L. Brown, L.J. Lanzerotti, K.J. Marcantonio, R.E. Johnson and C.T. Reimann, Nucl. Instr. and Meth. B14 (1986) 392.
[5] R. Pedrys, presented at SOS 86, Symp. on Sputtering, Spitz (1986).
[6] S.K. Erents and G.M. McCracken, J. Appl. Phys. 44 (1973) 3139.
[7] S.K. Erents and G.M. McCracken, in: Atomic Collisions in Solids, eds. S. Datz, B.R. Appleton and C.D. Moak (Plenum, New York, 1975) p. 625.
[8] G.M. McCracken, Vacuum 24 (1974) 463.

[9] C. Benvenuti and R.S. Calder, Phys. Lett. A35 (1971) 291.
[10] C. Benvenuti, R.S. Calder and G. Passardi, J. Vac. Sci. Technol. 13 (1976) 1172.
[11] H.H. Farrell, M. Strongin and J.M. Dickey, Phys. Rev. B6 (1972) 4703.
[12] R. Clampitt, Vacuum 34 (1984) 113.
[13] T.A. Tombrello, Rad. Effects 65 (1982) 149.
[14] R.E. Johnson, L.J. Lanzerotti and W.L. Brown, Adv. Space Res. 4 (1984) 41.
[15] L.J. Lanzerotti, W.L. Brown and R.E. Johnson, Nucl. Instr. and Meth. B14 (1986) 373.
[16] C.T. Chang, L.W. Jørgensen, P. Nielsen and L.L. Lengyel, Nucl. Fus. 20 (1980) 859.
[17] S.L. Milora, J. Fus. Energy 1 (1981) 15.
[18] O. Gröbner and R.S. Calder, IEEE-Trans. Nucl. Sci. 20 (1973) 760.
[19] P.C. Souers, Hydrogen Properties for Fusion Energy (University of California Press, London, 1986).
[20] F. Besenbacher, J. Bøttiger, O. Graversen, J.L. Hansen and H. Sørensen, Nucl. Instr. and Meth. 191 (1981) 221.
[21] O. Ellegaard, J. Schou, H. Sørensen and P. Børgesen, Surf. Sci. 167 (1986) 474.
[22] D.E. David, T.F. Magnera, R. Tian, D. Stulik and J. Michl, Nucl. Instr. and Meth. B14 (1986) 378.
[23] P. Børgesen, J. Schou and H. Sørensen, J. Nucl. Mater. 93/94 (1980) 701.
[24] J. Michl, Int. J. Mass Spectrom. Ion Phys. 53 (1983) 255.
[25] J.W. Christiansen, D. Delli Carpini and I.S.T. Tsong, Nucl. Instr. and Meth. B15 (1986) 218.
[26] F. Coletti, J.M. Debever and G. Zimmerer, J. Chem. Phys. 83 (1985) 49.
[27] W.L. Brown, L.J. Lanzerotti, J.M. Poate and W.M. Augustyniak, Phys. Rev. Lett. 40 (1978) 1027.
[28] C.T. Reimann, R.E. Johnson and W.L. Brown, Phys. Rev. Lett. 53 (1984) 600.
[29] R.W. Ollerhead, J. Bøttiger, J.A. Davies, J. L'Ecuyer, H.K. Haugen and N. Matsunami, Rad. Effects 49 (1980) 203.
[30] D.V. Stevanovic, D.A. Thompson and J.A. Davies, Nucl. Instr. and Meth. B1 (1984) 315.
[31] D.J. Lepoire, B.H. Cooper, C.L. Melcher and T.A. Tombrello, Rad. Effects 71 (1983) 245.
[32] J. Schou, H. Sørensen and P. Børgesen, Nucl. Instr. and Meth. B5 (1984) 44.
[33] A. Bar-nun, G. Herman, M.L. Rappaport and Yu. Mekler, Surf. Sci. 150 (1985) 143.
[34] D.J. O'Shaughnessy, J.W. Boring, J.A. Phipps, R.E. Johnson and W.L. Brown, Nucl. Instr. and Meth. B13 (1986) 304.
[35] P. Børgesen and H. Sørensen, Phys. Lett. 90A (1982) 319.
[36] R. Pedrys, R.A. Haring, A. Haring and A.E. de Vries, Nucl. Instr. and Meth. B2 (1984) 573.
[37] R.A. Haring, R. Pedrys, D.J. Oostra, A. Haring and A.E. de Vries, Nucl. Instr. and Meth. B5 (1984) 483.
[38] C.T. Reimann, J.W. Boring, R.E. Johnson, J.W. Garrett, K.R. Farmer, W.L. Brown, K.J. Marcantonio and W.M. Augustyniak, Surf. Sci. 147 (1984) 227.
[39] R.A. Haring, R. Pedrys, D.J. Oostra, A. Haring and A.E. de Vries, Nucl. Instr. and Meth. B5 (1984) 476.
[40] R. Pedrys, R.A. Haring, A. Haring, F.W. Saris and A.E. de Vries, Phys. Lett. 82A (1981) 371.
[41] F. Coletti, J.M. Debever and G. Zimmerer, J. Phys. Lett. 45 (1984) L-467.
[42] R. Pedrys, J. Schou and H. Sørensen, to be published.
[43] D.B. Chrisey, J.W. Boring, J.A. Phipps, R.E. Johnson and W.L. Brown, Nucl. Instr. and Meth. B13 (1986) 360.
[44] W.L. Brown, W.M. Augustyniak, L.J. Lanzerotti, R.E. Johnson and R. Evatt, Phys. Rev. Lett. 45 (1980) 1632.
[45] J.W. Boring, J.W. Garrett, T.A. Cummings, R.E. Johnson and W.L. Brown, Nucl. Instr. and Meth. B1 (1984) 321.
[46] J. Schou, P. Børgesen, O. Ellegaard, H. Sørensen and C. Claussen, Phys. Rev. B34 (1986) 93.
[47] W.L. Brown, L.J. Lanzerotti and R.E. Johnson, Science 218 (1982) 525.
[48] P. Sigmund and M. Szymonsky, Appl. Phys. A33 (1984) 141.
[49] M. Urbassek and P. Sigmund, Appl. Phys. A35 (1984) 19.
[50] P. Sigmund, Phys. Rev. 1984 (1969) 383; 187 (1969) 768.
[51] P. Sigmund, in: Sputtering by Particle Bombardment I, ed. R. Behrisch (Springer, Berlin, 1981) p. 9.
[52] J. Lindhard, V. Nielsen and M. Scharff, Mat. Fys. Med. Dan. Vid. Selsk. 36, No. 10 (1968).
[53] J.F. Ziegler, Helium Stopping Powers and Ranges in All Elemental Matter (Pergamon, New York, 1977).
[54] P. Børgesen, Risø-Report R-457, Risø National Laboratory (1982).
[55] P. Børgesen, Nucl. Instr. and Meth. B12 (1985) 73.
[56] J.E. Griffith, R.A. Weller, L.E. Seiberling and T.A. Tombrello, Rad. Effects 51 (1980) 223.
[57] H. Overeijnder, A. Haring and A.E. de Vries, Rad. Effects 37 (1978) 205.
[58] J. Lindhard, V. Nielsen, M. Scharff and P.V. Thomsen, Mat. Fys. Medd. Dan. Vid. Selsk, 33, No. 10 (1968).
[59] J.W. Boring, R.E. Johnson, C.T. Reimann, J.W. Garret, W.L. Brown and K.J. Marcantonio, Nucl. Instr. and Meth. 218 (1983) 707.
[60] W.L. Brown, W.M. Augustyniak, K.J. Marcantonio, E.H. Simmons, J.W. Boring, R.E. Johnson and C.T. Reimann, Nucl. Instr. and Meth. B1 (1984) 307.
[61] J.W. Boring, D.J. O'Shaughnessy and J.A. Phipps, Nucl. Instr. and Meth. B, to be published.
[62] R. Pedrys, D.J. Oostra and A.E. de Vries, in: Desorption Induced by Electronic Processes, DIET II, eds. W. Brenig and D. Menzel (Springer, Berlin, 1985) p. 190.
[63] R. Pedrys, D.J. Oostra, A. Haring, A.E. de Vries, O. Ellegaard, J. Schou and H. Sørensen, to be published.
[64] J. Schou, R. Pedrys, O. Ellegaard and H. Sørensen, Nucl. Instr. and Meth. B, to be published.
[65] R.E. Johnson and W.L. Brown, Nucl. Instr. and Meth. 198 (1982) 103.
[66] B.J. Garrison and R.E. Johnson, Surf. Sci. 148 (1985) 388.
[67] O. Ellegaard, R. Pedrys, J. Schou, H. Sørensen and P. Børgesen, to be published.
[68] M. Szymonski, J. Ruthowski, A. Poradzisz, Z. Postawa and B. Jørgensen, in: Desorption Induced by Electronic Transitions, DIET-II, eds. W. Brenig and D. Menzel (Springer, Berlin, 1985) p. 160.
[69] P. Sigmund and C. Claussen, J. Appl. Phys. 52 (1981) 990.

[70] C. Claussen, Ph. D. Thesis, University of Odense (1982).
[71] C. Claussen, Nucl. Instr. and Meth. 194 (1982) 567.
[72] W.L. Brown, W.M. Augustyniak, E. Brody, B.H. Cooper, L.J. Lanzerotti, A. Ramirez, R. Evatt and R.E. Johnson, Nucl. Instr. and Meth. 170 (1980) 321.
[73] B.H. Cooper and T.A. Tombrello, Rad. Effects 80 (1984) 203.
[74] D.E. David, T.F. Magnera, R. Tian and J. Michl, Rad. Effects 99 (1986) 247.
[75] H.M. Urbassek and J. Michl, to be published.
[76] F.L. Rook, R.E. Johnson and W.L. Brown, Surf. Sci. 164 (1985) 625.
[77] N. Schwentner, E.-E. Koch and J. Jortner, Electronic Excitations in Condensed Rare Gases (Springer, Berlin, 1985).
[78] G. Zimmerer, in: Excited State Spectroscopy in Solids, ed. M. Manfredi (North-Holland, Amsterdam, 1987).
[79] W.E. Spear, Adv. Phys. 23 (1974) 523.
[80] P.G. Le Comber, R.J. Loveland and W.E. Spear, Phys. Rev. B11 (1975) 3124.
[81] P. Børgesen, J. Schou, H. Sørensen and C. Claussen, Appl. Phys. 29 (1982) 57.
[82] O. Ellegaard, Ph. D. Thesis, Risø National Laboratory (1986).
[83] Z. Ophir, B. Raz, J. Jortner, V. Saile, N. Schwentner, E.-E. Koch, M. Skibowski and W. Steinmann, J. Chem. Phys. 62 (1975) 650.
[84] Ch. Ackermann, R. Brodmann, U. Hahn, A. Suzuki and G. Zimmerer, Phys. Status Solidi B74 (1976) 579.
[85] Rare Gas Solids I–II, eds. M.L. Klein and J.A. Venables (Academic Press, London 1977).
[86] D. Pudewill, F.-J. Himpsel, V. Saile, N. Schwentner, M. Skibowski, E.-E. Koch and J. Jortner, J. Chem. Phys. 65 (1976) 5226.
[87] G. Zimmerer, J. Lumin. 18–19 (1979) 875.
[88] W.L. Brown, C.T. Reimann and R.E. Johnson, in: Desorption Induced by Electronic Transitions, DIET II, eds. W. Brenig and D. Menzel (Springer, Berlin, 1985) p. 199.
[89] O. Ellegaard, J. Schou and H. Sørensen, Nucl. Instr. and Meth. B13 (1986) 567.
[90] P. Børgesen, J. Schou, H. Sørensen and O. Ellegaard, to be published.
[91] P. Børgesen, J. Schou and H. Sørensen, in: Proc. Symp. on Sputtering, eds. P. Varga, G. Betz and F.P. Viehböck (Technische Universität Wien, Austria, 1980) p. 822.
[92] C.T. Reimann, W.L. Brown and R.E. Johnson, to be published.
[93] The hydrogen points obtained for thin films have been corrected for the thickness-dependence. The point for 1 MeV protons is not included.
[94] O. Ellegaard, J. Schou, R. Pedrys and H. Sørensen, to be published.
[95] J.M. Debever and F. Coletti, private communication.
[96] E. Roick, R. Gaethke, P. Gürtler, T.O. Woodruff and G. Zimmerer, J. Phys. C17 (1984) 945.
[97] J. Schou, O. Ellegaard, P. Børgesen and H. Sørensen, in: Desorption Induced by Electronic Transitions, DIET II, eds. W. Brenig and D. Menzel (Springer, Berlin, 1985) p. 170.
[98] A.E. de Vries, R. Pedrys, R.A. Haring, A. Haring and F.W. Saris, Nature 311 (1984) 39.
[99] A.E. de Vries, R.A. Harling, A. Haring, F.S. Klein, A.C. Kummel and F.W. Saris, J. Phys. Chem. 88 (1984) 4510.
[100] R. Pedrys, D.J. Oostra, R.A. Haring, L. Calcagno, A. Haring and A.E. de Vries, Nucl. Instr. and Meth. B17 (1986) 15.
[101] L. Calcagno, G. Foti and G. Strazzulla, Rad. Effects 91 (1985) 79.
[102] R.A. Haring, A. Haring, F.S. Klein, A.C. Kummel and A.E. de Vries, Nucl. Instr. and Meth. 211 (1983) 529.
[103] L.J. Lanzerotti, W.L. Brown, W.M. Augustyniak, R.E. Johnson and T.P. Armstrong, Astrophys. J. 259 (1982) 920.

Appl. Phys. A 46, 305–312 (1988)

Applied Physics A Solids and Surfaces

Sputtering of Solid Argon by keV Electrons

O. Ellegaard, R. Pedrys*, J. Schou**, H. Sørensen, and P. Børgesen***

Association EURATOM-Risø National Laboratory, Physics Department, DK-4000 Roskilde, Denmark

Received 19 March 1988/Accepted 18 April 1988

Abstract. Sputtering of the solid rare gas Ar by 0.8–3.0 keV electrons was studied experimentally and theoretically. The argon films were deposited on a quartz-crystal microbalance kept at liquid-helium temperature. The yield was determined from the mass loss during irradiation. The absolute yield shows a significant dependence on film thickness in accordance with earlier measurements on electronic sputtering of solid argon. The yield shows a maximum of about 3.0 ± 0.4 Ar/elec. at 1.5 keV. The thickness dependence reflects the mobility of electronic excitations created by the primary electrons. The data analysis is based on a theoretical treatment for the diffusive motion of these excitations. From the thickness as well as the energy dependence of the yield we may derive a characteristic diffusion length for the excitations of 200–300 Å.

PACS: 61.80 Fe, 66.30 Lw, 79.20 Kz

Sputtering measurements on condensed rare gases have been carried out for more than a decade. Data are now available for solid Ne [1–3], Ar [4–10], Kr [8–10], and Xe [8, 9, 11, 12]. These results are summarized in recent reviews [13, 14].

The primary particles have spanned the nuclear stopping regime (keV heavy ions) as well as the electronic stopping regime (electrons and MeV light ions). In addition, the composition and energy of the sputtered particle flux [15–17] have been determined in a few cases. In contrast to metals and semiconductors the condensed gases also undergo significant sputtering in the electronic stopping regime. In the nuclear stopping regime the experimental sputtering yields significantly exceed the prediction from ordinary sputtering theory for heavy projectiles [8].

There are many reasons to believe that electronic transitions of excited target atoms or molecules are strongly involved in the sputtering process. Sputtering demands kinetic energy of the atoms or molecules. A repulsive decay may impart kinetic energy to the target particles. Models for the production of etchable tracks in insulators by heavy fast ions [17] as well as for desorption of gases adsorbed on metal surfaces [18] invoke the production of repulsive forces between neighbouring atoms or between moving atoms and the metal.

The rare gas solids constitute a peculiarly interesting class of condensed gases. They serve as a prototype material for the large class of Van der Waals crystals. The atoms are only slightly perturbed in the weakly bound ground state. In an electronically excited state the atoms can be displaced towards each other forming more strongly bound excited dimers (excimers). The electronic excitations are furthermore characterized by the rich exciton structure for energies below the band gap. The band gaps in the rare gas solids are much larger than the binding energies of the atoms (see Table 1 for Ar), and the free electron mobilities are rather high compared to other condensed gases. The physical properties and electronic excitations are extensively discussed in [20–24].

Argon is a simple, well-studied system. The atomic and molecular transitions following energetic particle bombardment are well known, and a close connection

* Permanent address: Instytut Fizyki, Uniwersytet Jagiellonski, PL-30-059 Krakow, Poland
** To whom all correspondance should be sent
*** Present address: Department of Materials Science and Engineering, Cornell, University, Ithaca, NY 14853, USA

Table 1. Properties of solid argon

Density[a] (10^{22} atoms/cm^3)	Sublimation energy (U_0)[a] (meV)	W (eV)	Mean ionization potential (eV)
2.67	80	26.4[b]	207
Band Gap (eV)	**Drift mobility[c]**		
	Electrons (cm^2 V^{-1} s^{-1})		Holes (cm^2 V^{-1} s^{-1})
14.16	10^3		2.3×10^{-2}

[a] [20]
[b] Gas phase value [32]
[c] [41]

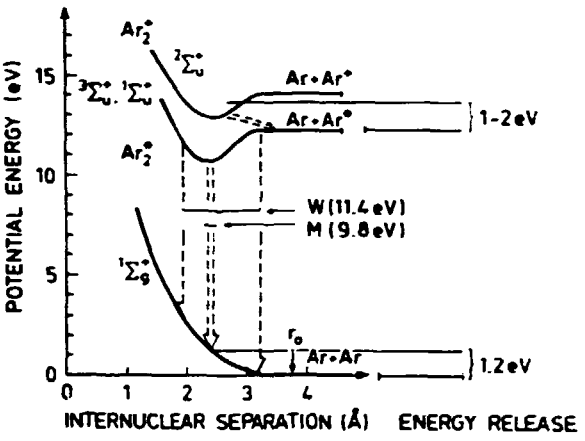

Fig. 1. Schematic representation of the important potential energy curves for molecular Ar_2^* in solid Ar. The transition from the vibrationally relaxed exciton to the ground state (the *M* band) as well as that from the highly vibrationally excited one (the *W* band) are shown

between luminescence and sputtering has been established [5–7, 25–27]. Results in the electronic sputtering regime obtained by light MeV ions indicate that the sputtering yield is more linearly than quadratically proportional to the electronic stopping power [6, 7, 13, 27]. Sputtering by electrons extends the investigated electronic stopping regime down to even lower values.

The release of kinetic energy by electronic deexcitations may produce sputtering, and it has been demonstrated experimentally that both sputtering and luminescence are produced during subsequent sequences of relaxation processes [5–7, 25, 27, 28]. The mobile excitations produced in the rare-gas solid by the excitation and ionization processes may be of different types: an atomic exciton R^*, a molecular exciton R_2^* or an atomic hole R^+. These excitations are produced either directly or during the electronic relaxation process. Energy can be released in several steps either as kinetic energy of the constituent atoms or as photons by luminescence. The dissociative recombination provides 1–2 eV while the decay of Ar_2^* to the repulsive ground state releases about 1.2 eV as kinetic energy [6, 7, 17]. (Fig. 1).

In the present work we shall consider the yield dependence on argon film thickness as well as on primary energy for 0.8–3.0 keV electrons. The results are analyzed on the basis of a diffusion treatment for the mobile excitations.

1. Experimental

The experiment is performed with a liquid helium cryostat, below which the target region is suspended. The details of the experimental setup have been described elsewhere [29, 30].

The sputtering yield has been measured by two different methods. For the emissivity-change method a massive gold target is applied, whereas for the frequency-change method, the silver electrode on a quartz crystal microbalance serves as a substrate.

The emissivity-change method utilizes the dependency of the number of reflected electrons per primary on the thickness of the deposited film. The sputtering yield is obtained directly from the slope of the initial film thickness plotted versus the fluence necessary to erode this film away (see Fig. 2) [30]. It is not possible

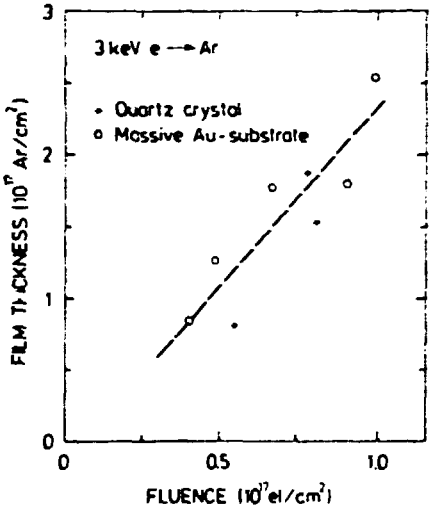

Fig. 2. Comparison of measurements performed at 3 keV with the emissivity change method for a massive Au substrate and the quartz microbalance method. The initial film thickness is plotted versus the fluence necessary to erode the film away. The slope of the dashed line corresponds to $Y_{mean} \approx 2.4$ Ar atoms per electron. (The fluence has been corrected for beam broadening, cf. [30])

to detect any thickness dependence for solid argon by this method, since the reflection coefficient for gold and silver is fairly similar to that for thick argon films. It is well known that the reflection coefficient for a thin argon film deposited on gold is very close to the one for a bare gold substrate [30]. Therefore, the increase in the target current during erosion from the emissivity change has to be significantly larger than the simultaneous beam drift. The points in Fig. 2 have been obtained for film thicknesses larger than 20% of the electron range. The slope of the dashed line indicates an average of the yield for the film thicknesses investigated.

The frequency-change method provides us with the mass loss per incident particle in a straightforward manner. In this case the thickness of the silver electrode exceeds the range of the most energetic electrons. The heat deposited in the solidified gas by the energetic electrons is conducted away mainly through the small silver electrode on the quartz crystal. This is generally expected to work less efficiently than heat conduction through the gold substrate. However, a comparison of the results for this method with the emissivity-change method as in Fig. 2 seems to indicate that this coupling is sufficiently good.

A film of condensed argon is made on the target plate or silver electrode by letting a jet of gas impinge on it through a precooled gas tube. Usually the film growth rate is about 1×10^{15} atoms/cm^2/s. The film can be rapidly removed by heating the substrate with an electrical heater. The thickness of the film is known from the frequency change of the microbalance. For a massive target the film thickness is determined by a calibration procedure. With a cold cryostat the temperature of the target film is close to liquid helium temperature.

A beam of 0.8–3.0 keV electrons can either hit the target perpendicular to the surface or be deflected into a Faraday cup for measurements of the true current. The beam is further swept horizontally and vertically over an aperture in front of the target, thus ensuring a homogeneous irradiation of a large part of the target area. The current density was kept below 10 μA/cm^2, where evaporation caused by beam heating turned out to be insignificant even for the much more volatile solid neon [30].

A negative bias (−90 V) was applied to an open repeller ring in front of the target. In this way secondary electron emission is suppressed, and charge-up problems are reduced substantially.

2. Results

The results obtained on a gold substrate with the emissivity change method have been compared with data from the quartz crystal (Fig. 2). In both cases the fluence necessary to remove the film has been determined either by the increase in the reflection coefficient or by the change in the frequency as described in [3, 30]. Since this comparison requires a complete erosion of the film, only thicknesses up to 2.6×10^{17} Ar-atoms/cm^2 have been included. The fair level of agreement between 0.8 and 2.6×10^{17} Ar-atoms/cm^2 ensures that the thermal coupling of the quartz microbalance actually is sufficient for "pure" electronic sputtering of solid argon. These results have been obtained by long runs in which the influence of beam drift cannot be neglected. Therefore, the points shown below are more reliable.

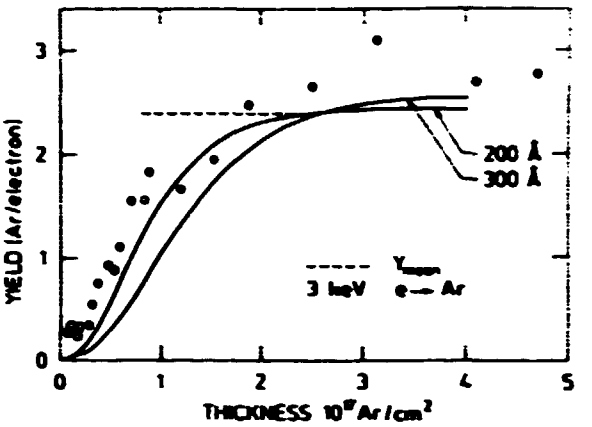

Fig. 3. Sputtering yield of solid Ar versus initial thickness for 3-keV electron bombardment. (O) experimental results. Solid curves: Diffusion model with $L_0 = 200$ Å and 300 Å. [$f = 1$ and $E_s = 2.7$ eV in (2) and (4)]. - - -, Y_{mean} from Fig. 2

The experimental thickness dependence of the sputtering yield for 3-keV electron incidence is shown in Fig. 3. The average yield Y_{mean} from Fig. 2 is indicated as well. The overall trend is very similar to the results for MeV light ions obtained by Besenbacher et al. [4] and Reimann et al. [5–7] as well as for hydrogen ions in the keV regime [10]. The yield saturates at 2 to 3×10^{17} Ar/cm^2 and goes almost to zero at small thicknesses.

The energy dependence in the range 0.8–3.0 keV (Fig. 4) resembles the results obtained on solid neon [3]. The sputtering yield peaks at about 1.5 keV in both cases, but decreases somewhat slower at higher energies in the case of solid argon. The sputtering yield does not follow the electronic stopping power of the electrons, which is a decreasing function of the electron energy in the present regime. This behaviour is very different from that of the molecular gases nitrogen and oxygen for which the sputtering yield was almost proportional to the electronic stopping power [14, 31].

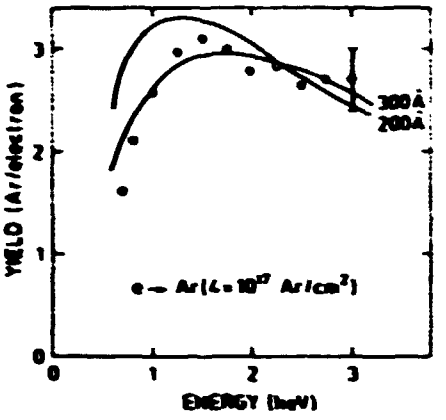

Fig. 4. Sputtering yield of 4×10^{17} Ar/cm^2 thick films versus primary electron energy. (O), experimental results. Solid curves as in Fig. 3

Finally, the impurity effect was investigated by mixing oxygen (~1.0 vol.%) and argon before condensation of the gas. The yield decreased to about 50% of the pure film value. This result is in very good agreement with the data of Brown et al. [27].

3. Discussion

In the analysis of the experimental results obtained with electron incidence we will consider the full deexcitation scheme including the dissociative recombination of the molecular hole as suggested by Johnson and Inokuti [24] and Reimann et al. [5, 6]. In the present work, as in [3], we consider a mobile electronic excitation without specifying the precise type or combination of types. Through self-trapping and decay of a mobile excitation near the surface, kinetic energy becomes available for sputtering. The difference between the results obtained by MeV H^+ and He^+-ion incidence and electron incidence is due mainly to the unequal deposition of energy in the solid.

The important quantity for a model calculation then becomes the density of trapped excitations $E(x)$. If this density changes very little over distances from the surface within which atomic ejection takes place, only the surface value $E(0)$ is needed. The total amount of kinetic energy released during the electronic relaxation processes is $E_s \sim 2.7$ eV per electron-hole pair created (Fig. 1). We include in this value 1.5 eV as an approximation for 1–2 eV from the dissociative recombination as well as 1.2 eV from the ground state repulsion. We consider this energy quantity as available for a low-energy cascade similarly to the value of E_s proposed by Reimann et al. [6].

We propose to apply the formula which gives the sputtering yield Y caused by a low-energy cascade mechanism in solid nitrogen and oxygen as published earlier [31]

$$Y = 1/2\, A(D_d(0)/W) \cdot E_s \text{ (atoms/electron)}. \quad (1)$$

$D_d(0)$ is the surface value of the density of electronically deposited energy $D_d(x)$, and W the mean energy for creation of an electron-hole pair [32]. $A = 3/(4\pi^2 N C_0 U_0)$ is the usual material dependent parameter, determined by the atomic density N, the energy U_0 of the surface barrier, and the standard cross section C_0 for low-energy collisions between argon atoms [33].

We have applied the value $U_0 = 60$ meV which leads to the best agreement with experimental spectra [17], although this value is slightly less than the sublimation energy of 80 meV.

In the case considered here with mobile excitations we substitute the density of trapped excitations at the surface $E(0)$ instead of $D_d(0)/W$ in the formula (1) and obtain:

$$Y = 1/2\, AE(0)E_s \text{ (Ar-atoms/electron)}. \quad (2)$$

This extension of the analytical expression to mobile excitations allows us to calculate the sputtering yield directly, provided $E(0)$ can be determined. The quantity $E(0)$ may be directly determined when the solution to the diffusion problem for the mobile excitations is found.

An alternative expression is obtained from the result of a computer simulation made by Garrison and Johnson [34]. Reimann et al. [5] calculated that a deexcitation releasing a kinetic energy of $E_s \approx 3.6$ eV within a sputter depth Δx of about 10 Å may cause an average of $A_0 \sim 3.2$ ejected Ar atoms. With $E(x) \approx E(0)$ for $x \leq \Delta x$ their yield becomes:

$$Y = \int_0^\infty E(0) A_0 e^{-x/\Delta x}\, dx \text{ (Ar-atoms/primary)}. \quad (3)$$

We have not used this latter expression, but have solved the diffusion equation for an unspecified mobile electronic excitation in the solid (Appendix A). Following the considerations by Schou et al. [3] and Reimann et al. [6, 27] we analyze the case of a reflecting boundary condition. The solution for any initial distribution of electronic excitations $C(x)$ can be found by integration. $C(x)$ is related to the density of electronically deposited energy $D_d(x)$ through:

$$C(x) = f \cdot D_d(x)/W. \quad (4)$$

f is the number of specific excitations per electron-hole pair created in the solid, i.e. $f = 1$ for diffusion of holes [3]. If the surface is not assumed to be perfectly reflecting, the yield will increase relative to the value for a reflecting boundary condition [3, 5, 6].

An experimental energy dissipation profile $D_e(x)$ for electrons in solid argon does not exist, and the scaling of the Gaussian profile for nitrogen [35] applied earlier by us for neon [3] does not hold accurately for heavier targets such as argon. Everhart and Hoff on the other hand gave an analytical expression for electrons ($5 < E < 25$ keV) in solids with a similar atomic number [36]. Their results can then be extrapolated to our energy regime. The distribution of deposited electronic energy (corrected for the energy loss because of backscattered electrons) was given by a polynomial:

$$D_e(x) = a'_0 + a'_1 x + a'_2 x^2 + a'_3 x^3, \tag{5}$$

with

$$a'_0 = 0.54\,E/R_e, \quad a'_1 = 5.6\,E/R_e^2,$$
$$a'_2 = 11.2\,E/R_e^3, \quad a'_3 = 5.12\,E/R_e^4. \tag{6}$$

The penetration depth R_e was deduced from Monte-Carlo calculations of the range profiles of keV electrons in similar materials [37]:

$$R_e = 6.0\,E(\text{keV})^{1.4}\ \mu\text{g/cm}^2. \tag{7}$$

The energy density profiles for 1-, 2-, and 3-keV electrons in solid argon are shown in Fig. 5. The total number of electron-hole pairs created increases with primary energy, but as the penetration depth becomes smaller, a larger fraction of the excitations can reach the surface prior to self-trapping. Hence, we expect the yield to show a maximum as a function of primary energy for energies that are not too large.

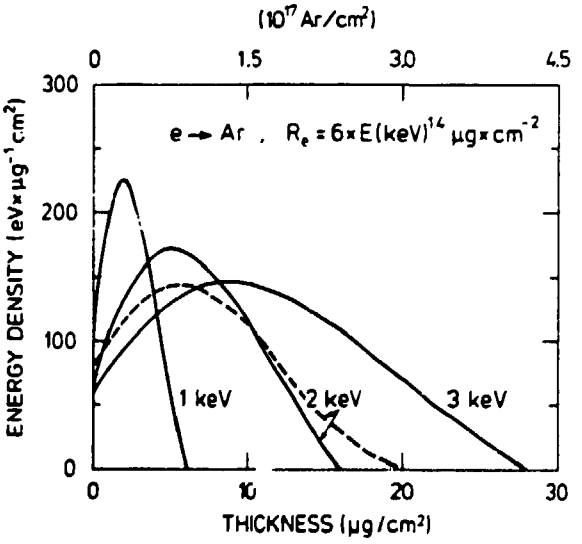

Fig. 5. Electronic energy deposited per unit depth in solid argon by 1–3 keV electrons. Solid lines (5) with $E = 1$, 2, and 3 keV. Dashed line: Gaussian profile (A.9). $r_D \approx 0.375\,R_e$ and $\sigma_D \approx 0.34\,R_e$ for 2-keV electron incidence

The Gaussian profile evaluated similarly to that for neon at 2 keV (Fig. 5) deviates significantly from the Everhart-Hoff profile as expected.

With the profile $D_e(x)$ from (5), we may find $E(0)$ (Appendix A). If we further insert this value together with the parameters in Table 1 and the standard cross-section for low-energy collisions $C_0 \simeq 1.8\,\text{Å}^2$ into (2), the thickness as well as the energy dependence of the yield can be calculated. Two fits with $f = 1$ and different values of the diffusion length l_0 are shown in Fig. 3. The best agreement with the experimental thickness dependence is found by applying the value $l_0 \approx 200$ Å. This fit is even significantly lower than most of the points for the thin films. However, the effect of the substrate-reflected electrons has not been included in the model. These electrons cause sputtering also when they pass the surface in backward direction. Such an enhancement for thin films has been demonstrated previously for electron bombardment of solid oxygen [31]. This contribution increases the experimentally obtained yield relative to the calculated fit for thin films.

The value $l_0 \approx 200$ Å is similar to the result obtained by Reimann et al. ($l_0 \approx 190\,\text{Å} \pm 40\,\text{Å}$) [5], but larger than those obtained earlier in photoemission experiments ($l_0 \approx 120$ Å) [22, 38]. However, the existing data for all rare gas solids indicate that there is a significant difference between the data obtained from charged-particle irradiation and the optically determined diffusion lengths [13]. The temperature and pressure of the gas during condensation and hence the crystal quality of the film might have some influence on the exciton diffusion process (and on the diffusion length) [22, 26, 28, 39]. However, this effect has not been investigated systematically.

The data for the energy dependence are also fitted by curves with different values of l_0. The curve with $l_0 \approx 300$ Å apparently reproduces the maximum of the curve in the best manner, but the agreement is fair above 1.5 keV for the curve with $l_0 \approx 200$ Å as well. We suggest a diffusion length in the interval 200–300 Å. The absolute value of the yields determined by the model seems to agree with the decay scheme of Reimann et al. as well as experiment.

If we instead choose to apply the less accurate Gaussian energy distribution (Appendix A.3) with the range still given by (7) and $l_0 \sim 200$–300 Å, the calculated yield deviates significantly from the experimental yield. This demonstrates clearly that the analysis for solid argon has to be based on the Everhart-Hoff profile rather than the one used for solid neon.

In the analysis the quantities E_s, f, and U_0 have been determined from arguments independent of the

present results. Therefore, it is quite satisfactory that these input values lead to fair agreement between the theoretical predictions and the experimental results if the standard cross section $C_0 \approx 1.8\,\text{Å}^2$ is applied. We have not refined the analysis beyond the present level, e.g. by including the effect of a partially absorbing boundary as in [5, 6]. The present accuracy of the input parameters U_0, C_0, and E_s as well as the Everhart-Hoff profile means that the value of such an analysis is questionable.

4. Conclusion

Results for sputtering of solid argon by 0.8–3.0 keV electrons, were found to agree with similar results for electronic sputtering induced by light MeV ions. The electron data extend the stopping range to even lower values than were obtained by MeV H^+ ions. The thickness dependence turned out to be almost the same for keV-electron and MeV-ion bombardment. The sputtering yield also has a maximum at 1.5 keV electron energy similar to that found for solid neon [3].

Numerous studies of luminescence and photoelectron spectroscopy from pure and impure solid rare gases have provided information about the electronic relaxation process that follows energetic particle bombardment. Only about 10% of the electronic energy deposited in the film becomes available for kinetic energy of atomic motion. The other part is converted to photons (luminescence), phonons and low energy secondary electrons. There is clear evidence from photoelectron spectroscopy, sputtering and luminescence data, that the excitations in solid argon are mobile. The precise type of the mobile species as well as the diffusion process itself are presently not known in detail. We have utilized the decay scheme proposed by Reimann et al. [5] in our calculations, i.e. the energy available for atomic motion is 2.7 eV. The depth distribution of energy deposited into excitations also entered into the calculation. This profile is determined from experimental work on the slowing down of keV electrons in materials with a similar atomic number. These parameters enter into the final simple formula (2).

From the experimental data we could deduce a diffusion length in the range 200–300 Å. This value is somewhat larger than that of Pudewill et al. [39]: 120 Å, but comparable to that of Reimann et al.: 190 Å ± 40 Å [5].

Finally, absolute sputtering yields were calculated according to the low-energy cascade model. Fair agreement is found with experiment when we apply the standard cross section C_0 for low-energy collisions between atoms normally used in sputtering theory.

Acknowledgements. The authors thank A. Nordskov and B. Sass for competent technical assistance.

Appendix

A.1. Diffusion Equation for a Mobile Excitation

In this appendix we will determine the probability $C(x, x', t)dx$ for a mobile excitation to be in a depth interval $[x, x+dx]$ at the time t after the production at x' at the time $t=0$. The subsequent density $E(x, x')$ of trapped excitations at the depth x is found as well. The diffusion equation for mobile excitations will be solved with the boundary conditions: The surface (at $x=0$) is completely reflecting and the metal-substrate interface (at $x=d$) completely absorbing. These conditions are probably the limiting geometry for an actual system, but they provide a convenient frame work for a mathematical description. The equation will be solved for an initial production of a free excitation at a depth x' below the surface by means of the Green's function of the problem. By solving the diffusion equation for a point source, one may find the solution for any general initial distribution of excitations by simple integration [29].

The behaviour of the excitations is described by their diffusion coefficient D and trapping time τ. These two parameters are related to the diffusion length by $l_0=(D\tau)^{1/2}$ as usual. The quantity relevant for sputtering is the density of trapped excitations:

$$E(x,x')=1/\tau \int_0^\infty C(x,x',t)dt. \tag{A1}$$

The diffusion equation to be solved is (only the one-dimensional equation is needed):

$$D\frac{d^2C}{dx^2}=\frac{\partial C}{\partial t}+\frac{C}{\tau} \tag{A2}$$

with boundary conditions:

$$\left.\frac{\partial C(x,x',t)}{\partial x}\right|_{x=0}=0,\ C(d,x',t)=0. \tag{A3a}$$

and the initial condition:

$$C(x,x',0)=\delta(x-x'). \tag{A3b}$$

The solution for the excitation density for a point source becomes in this case [Ref. 40, p. 276]:

$$C(x,x',t)=\frac{\exp(-t/\tau)}{(4\pi D)^{1/2}t^{1/2}} \times\left(\sum_{n=-\infty}^{\infty}(-1)^n\{\exp[-(x-x'-2nd)^2/4Dt] +\exp[-(x+x'-2nd)^2/4Dt]\}\right). \tag{A4}$$

Then we obtain the solution for the density of energy-releasing excitations $E(x, x')$ by applying (A1):

for $0<x'<x$:

$$E(x,x')=\frac{1}{2l_0}\frac{\exp(-x/l_0)-\exp(-2d/l_0)\exp(x/l_0)}{1+\exp(-2d/l_0)} \times[\exp(x'/l_0)+\exp(-x'/l_0)] \tag{A5}$$

and for $x<x'<d$:

$$E(x,x')=\frac{1}{2l_0}\frac{\exp(x'/l_0)+\exp(-x/l_0)}{1+\exp(-2d/l_0)} \times[\exp(-x'/l_0)-\exp(x'/l_0)\exp(-2d/l_0)]. \quad (A6)$$

A.2. Constant Excitation Density $C(x)=n_0$

The case of a constant excitation density $C(x)=n_0$, which applies for MeV light ion bombardment of solid argon, can then be easily solved. This expression has not been used in the present work, but has been utilized by Schou et al. [10], Schou [13] and by Reimann et al. [5, 7]. We include the calculations for completeness. Then we have: $E(x)=\int C(x')E(x,x')dx'$, and obtain

$$E(x)=n_0\left(1-\frac{\exp(x'/l_0)+\exp(-x/l_0)}{\exp(d/l_0)+\exp(-d/l_0)}\right). \quad (A7)$$

The thickness dependence of the sputtering yield will be determined approximately by the value of the trapped excitation density near the surface:

$$E(0)=n_0[1-1/\cosh(d/l_0)]. \quad (A8)$$

This thickness dependence differs only from the case of an absorbing boundary condition at the surface at small thicknesses $d\lesssim l_0$.

A.3. Gaussian Excitation Density

$$C(x)=n'(2\pi\sigma_D^2)^{-1/2}\exp[-(x-r_D)^2/2\sigma_D^2].$$

For the trapped excitation density for infinite thickness one obtains

$$E(0)=\frac{n'}{2l_0}\exp\left(\frac{\sigma_D^2}{2l_0^2}-\frac{r_D}{l_0}\right)\operatorname{erfc}\left(\frac{\sigma_D}{l_0\sqrt{2}}-\frac{r_D}{\sigma_D\sqrt{2}}\right), \quad (A9)$$

where $n'=(fE/W)$ in analogy to (4).

The range r_D and standard deviation σ_D is normally given as a fraction of the range R_e. In atmospheric air the following relations were found to be fair approximations: $r_D\approx 0.375\,R_e$ and $\sigma_D\approx 0.340\,R_e$ [35]. These values were used for the discussion.

A.4. Polynomial Excitation Density:

$$C(x)=a_0+a_1x+a_2x^2+a_3x^3,\ 0<x<R_e$$

An excitation density of this type can be found in materials with medium atomic numbers bombarded by electrons as mentioned in Sect. 3. A simple analytical expression can be found for $E(0)$ in the case $d<R_e$, i.e. the film thickness is less than the penetration depth R_e of the electrons. In the case $d\geqq R_e$ no simple expression can be found, but $E(0)$ may still be determined by applying (A6). We obtain for $d<R_e$:

$$E(0)=a_0+2a_2l_0^2+\tanh(d/l_0)(a_1l_0+6a_3l_0^3) -1/\cosh(d/l_0)(a_0+a_1d+a_2d^2+a_3d^3+2a_2l_0^2+6a_3l_0^2d). \quad (A10)$$

This expression and the one found for $d>R_e$ can then be inserted into (2).

References

1. P. Børgesen, J. Schou, H. Sørensen, C. Claussen: Appl. Phys. A **29**, 57–61 (1982)
2. O. Ellegaard, J. Schou, H. Sørensen: Nucl. Instr. Meth. B **13**, 567–571 (1986)
3. J. Schou, P. Børgesen, O. Ellegaard, H. Sørensen, C. Claussen: Phys. Rev. B **34**, 93–106 (1986)
4. F. Besenbacher, J. Bøttiger, O. Graversen, J.L. Hansen, H. Sørensen: Nucl. Instr. Meth. **191**, 221–234 (1981)
5. C.T. Reimann, R.E. Johnson, W.L. Brown: Phys. Rev. Lett. **53**, 600–603 (1984)
6. W.L. Brown, C.T. Reimann, R.E. Johnson: Nucl. Instr. Meth. B **19–20**, 9–15 (1987)
   C.T. Reimann, W.L. Brown, R.E. Johnson: Phys. Rev. B. **37**, 1455–1473 (1988)
7. J. Schou, O. Ellegaard, H. Sørensen, R. Pedrys: Nucl. Instr. Meth. B (in press)
8. D.J. O'Shaughnessey, J.W. Boring, J.A. Phipps, R.E. Johnson, W.L. Brown: Nucl. Instr. Meth. B **13**, 304–308 (1986)
9. J.W. Boring, D.J. O'Shaughnessy, J.A. Phipps: Nucl. Instr. Meth. B **18**, 613–617 (1987)
10. J. Schou, R. Pedrys, O. Ellegaard, H. Sørensen: Nucl. Instr. Meth. B **18**, 609–612 (1987)
11. R.W. Ollerhead, J. Bøttiger, J.A. Davies, J. L'Ecuyer, H.K. Haugen, N. Matsunami: Radiat. Eff. **49**, 203–212 (1980)
12. D.V. Stevanovic, D.A. Thompson, J.A. Davies: Nucl. Instr. Meth. B **1**, 315–320 (1984)
13. J. Schou: Nucl. Instr. Meth. B **27**, 188–200 (1987)
14. W.L. Brown, R.E. Johnson: Nucl. Instr. Meth. B **13**, 295–303 (1986)
15. D.E. David, T.F. Magnera, R. Tian, D. Stulik, J. Michl: Nucl. Instr. Meth. B **14**, 378–391 (1986)
16. R. Pedrys, D.J. Oostra, A.E. de Vries: In *Desorption Induced by Electronic Transitions, DIET 2*, ed. by W. Brenig, D. Menzel (Springer, Berlin, Heidelberg 1985) pp. 190–198
17. R. Pedrys, D.J. Oostra, A. Haring, A.E. de Vries, J. Schou: Nucl. Instr. Meth. B (in press)
18. R.L. Fleischer, P.B. Price, R.M. Walker: J. Appl. Phys. **36**, 3645–3652 (1965)
19. D. Menzel, R. Gomer: J. Chem. Phys. **41**, 3311–3328 (1964)
20. *Rare Gas Solids*, Vols. 1 and 2, ed. by M.L. Klein, J.A. Venables (Academic, London 1977)
21. N. Schwentner, E.E. Koch, J. Jortner: *Electronic Excitations in Condensed Rare Gases*, Springer Tracts Mod. Phys. **107** (Springer, Berlin, Heidelberg 1985)
22. G. Zimmerer: In *Excited State Spectroscopy in Solids*, ed. by M. Manfredi (XCVI Corso, Soc. Italiana di Fisica, Bologna 1987) pp. 37–110
23. R.E. Johnson, W.L. Brown: Nucl. Instr. Meth. **198**, 103–118 (1982)
24. R.E. Johnson, M. Inokuti: Nucl. Instr. Meth. **206**, 289–297 (1983)
25. F. Coletti, J.M. Debever: Solid State Commun. **47**, 47–50 (1983)
26. F. Coletti, J.M. Debever, G. Zimmerer: J. de Phys. Lett. **45**, L-467–473 (1984)
27. W.L. Brown, C.T. Reimann, R.E. Johnson: *Desorption Induced by Electronic Transitions DIET 2*, ed. by W. Brenig, D. Menzel (Springer, Berlin, Heidelberg 1985) pp. 199–206
28. F. Coletti, J.M. Debever, G. Zimmerer: J. Chem. Phys. **83**, 49–57 (1985)
29. O. Ellegaard: Ph. D. Thesis, Risø-M-2617, Risø National Laboratory, Roskilde, Denmark, pp. 1–175 (1986)

30. J. Schou, H. Sørensen, P. Børgesen: Nucl. Instr. Meth. B5, 44-57 (1984)
31. O. Ellegaard, J. Schou, H. Sørensen, P. Børgesen: Surf. Sci. **167**, 474–492 (1986)
32. Average energy to produce an ion pair. ICRU Report 31. International commission on radiation units and measurements
33. P. Sigmund: Phys. Rev. **184**, 383–416 (1969); **187**, 768 (1969)
34. B.J. Garrison, R.E. Johnson: Surf. Sci. **148**, 388–400 (1984)
35. M.J. Berger, S.M. Seltzer, K. Maeda: J. Atm. Terr. Phys. **32**, 1015–1045 (1970)
36. T.E. Everhart, P.H. Hoff: J. Appl. Phys. **42**, 5837–5846 (1971)
37. S. Valkealahti, R.M. Nieminen: Appl. Phys. A **32**, 95–106 (1983)
38. Z. Ophir, B. Raz, J. Jortner, V. Saile, N. Schwentner, E.E. Koch, M. Skibowski, W. Steinmann: J. Chem. Phys. **62**, 650–665 (1975)
39. D. Pudewill, F.J. Himpsel, V. Saile, N. Schwentner, M. Skibowski, E.-E. Koch, J. Jortner: J. Chem. Phys. **65**, 5226–5238 (1976)
40. H.S. Carslaw, J.C. Jaeger: *Conduction of Heat in Solids* (Clarendon, Oxford 1959)
41. P.G. Le Comber, R.J. Loveland, W.E. Spear: Phys. Rev. **11**, 3124–3130 (1975)

Nuclear Instruments and Methods in Physics Research B33 (1988) 808–814
North-Holland, Amsterdam

Section XI. Desorption induced by electronic transition

ELECTRONIC AND KNOCK-ON SPUTTERING OF SOLID RARE GASES BY LIGHT keV IONS

Jørgen SCHOU, Ole ELLEGAARD, Hans SØRENSEN and Roman PEDRYS *

Association Euratom – Risø National Laboratory, Physics Department, DK-4000 Roskilde, Denmark

Electronic and knock-on sputtering of solid neon, argon and krypton induced by 2–10 keV He^+-ions and hydrogen ions has been studied by means of a quartz microbalance technique. The contributions from the two kinds of sputtering are determined from the thickness dependence of the yield. For He^+-ions incident on solid argon the conversion of the energy from nuclear stopping to particle ejection is about six times as efficient as the corresponding conversion of electronically deposited energy.

1. Introduction

The sputtering and desorption of solid rare gases have been studied more than the erosion of any other condensed gases [1–4]. The electronic excitations as well as the deexcitation channels in the solid rare gases are relatively well known [5,6]. The weak Van der Waal forces lead to binding energies that range from 20 meV for solid neon up to about 160 meV for xenon. These low values mean that the erosion yield is high compared with room temperature solids. The dominant erosion processes at sufficiently low temperatures and current densities of the primary particles are sputtering and desorption. Sputtering of insulators may be the result of direct collisions between the primary and the target atoms (knock-on sputtering) as well as sputtering via electronic transitions (electronic sputtering). The latter process requires the existence of repulsive potentials during the electronic deexcitation. The highly efficient excimer luminescence process in the solid rare gases is the result of a transition that terminates at a strongly repulsive energy curve.

In the present work we have studied sputtering of solid neon, argon and krypton by 3–10 keV hydrogen and helium ions. At these energies it is possible to observe knock-on and electronic sputtering simultaneously. This work is a continuation of previous studies on sputtering of solid neon [7,8], argon [9] by keV electrons, and related work on sputtering by hydrogen ions on solid neon [10], and argon and krypton [11].

2. Knock-on sputtering

In knock-on (collisional) sputtering the energy required for the atomic motion of the target particles is transferred from the fast primary to the target atoms through direct collisions. The struck atoms may initiate collision cascades via secondary and higher order collisions. The direct momentum transfer to the atoms of the material does not depend on whether the material is a metal, a volatile insulator or a gas, since the velocity of the incident particle is much higher than the velocities of the atoms of the material. The state of the material plays a role only in the last stage of the cascade, when the kinetic energy of the moving atoms becomes comparable to the binding energies of the target atoms. Therefore, the standard theory for knock-on sputtering for metals [12,13] may largely be extended to condensed gases. The treatment considers primarily low collision densities, i.e. the struck atoms in the cascade are at rest before the collision. The backsputtering yield Y from a plane surface is given by

$$Y = \Lambda F_D(E, 0), \tag{1}$$

where $F_D(E, x)$ is the spatial distribution of energy deposited into nuclear collisions by the primary of initial energy E. The constant $\Lambda = 3/(4\pi^2 N C_0 U_0)$ depends only on the properties of the target material, the sublimation energy U_0 and the atomic density N ($C_0 = 1.81$ Å^2). The surface value of the deposited energy ($x = 0$) is often expressed by the nuclear stopping power $NS_n(E)$ for the primary particle and a dimensionless parameter α:

$$F_D(E, 0) = \alpha N S_n(E) \tag{2}$$

α is a function of the mass ratio of the beam and target atom mass, and a slowly varying function of the energy. (We consider here and in the following only perpendicular incidence.) The energy distribution of the sputtered particles, which explicitly enters into the evaluation of Λ, is determined by

$$dY/dE_1 = k_s E_1/(E_1 + U_0)^3, \tag{3}$$

where k_s is a constant (see ref. [12]) and E_1 is the energy of the emitted particle. For large values of the

* Permanent address: Instytut Fizyki, Uniwersytet Jagiellonski, PL 30-059 Kraków, Poland.

0168-583X/88/$03.50

energy E_1 the distribution exhibits the well-known E_1^{-2}-tail and for small energies a maximum at $E_1 = U_0/2$.

The characteristic E_1^{-2}-behaviour of the spectrum has been observed in all experiments in which the solid rare gases have been bombarded by primary rare gas ions [14–16]. However, in many cases the maximum of the spectrum is far below the expected value at $E_1 = U_0/2$. Nevertheless, it means that a linear collision-cascade is responsible for the particle ejection at an early stage of the sputtering process.

The results for the yields agree satisfactorily with eq. (1) as long as the (collisional) excitation density is small or the sublimation energy is correspondingly large [16–18]. Deviations from linear sputtering theory occur typically for heavy-ion bombardment [16,17]. The high yields and the discrepancy between the observed maximum and the linear collision-cascade prediction may be explained by the development of elastic spikes in the solid during the late stage of the sputtering process.

3. Electronic sputtering

At energies and beam particle–target combinations for which the nuclear stopping power is small or negligible, the dominant erosion process is electronic sputtering. This kind of sputtering has been observed not only for condensed gases, but also for other materials as, for example, alkali halides [19,20]. A typical case is the bombardment of solid rare gases by keV electrons [7–9] or light MeV-ions [21–26]. The energy that is deposited as electronic excitations in the material is converted to kinetic energy during the electronic deexcitation. Apart from small variations the mechanism is similar for all the solid rare gases.

The electronic sputtering yield is closely correlated to the electronic stopping power. A high stopping power generally leads to a large yield. The electronic sputtering of solid rare gases is characterized in particular by

(i) a pronounced thickness dependence of the yield,
(ii) a strong luminescence during the irradiation, and
(iii) a significant reduction of the sputtering yield in the presence of oxygen impurities.

The thickness dependence has been observed for all four solid rare gases [2]. The yield for films thicker than about 10^{17} atoms/cm^2 increases with film thickness up to a saturation value at $2–3 \times 10^{17}$ atoms/cm^2. This dependence reflects the mobility of the electronic excitations in the solid rare gases. If the excitations reach the surface and deexcite close to the surface, target particles may be ejected.

The luminescence from the rare gas solids represents that part of the excitation energy which is not available for atomic motion. The strongest line for argon, krypton and xenon originates from the decay of the vibrationally relaxed excimer R_2^*. Reimann et al. [22] pointed out that the characteristic diffusion length for the excitations could be determined equally well from the sputtering yield dependence on thickness as from that of the luminescence yield.

The reduction of the yield because of impurities of oxygen or other rare gases has been demonstrated by Brown et al. [23,24], Reimann et al. [25] and Børgesen et al. [8]. The diffusing excitations are apparently trapped, or the energy releasing excimers quenched by the impurities.

The precise type of the mobile excitation is not yet known. The diffusing species may be an atomic hole R^+, a (highly excited) free exciton R^*, a vibrationally excited molecular exciton R_2^*, or a sequence of these species [2,22,35].

The energy releasing process is primarily the radiative transition labeled M from the molecular exciton R_2^* to the *repulsive* ground state. The deexcitation scheme is shown for solid argon in fig. 1. For solid argon the liberated energy at this process is about $E_s = 1.2$ eV [25,27,28]. This energy is so much larger than the sublimation energy of 80 meV for argon that the repulsing rare gas atoms initiate a low-energy cascade [1–2,29]. For krypton and xenon a peak in the energy distribution has been observed at the expected value for the repulsive ground state [27]. In these materials the cascade behaviour is less pronounced than in solid argon because the ratio of the released energy E_s to the sublimation energy is smaller than in argon.

Reimann et al. [22,25] and Brown et al. [23,24] suggest that the energy releasing process may be dissociative recombination of the molecule R_2^+ as well. This process supplies the repulsing atoms with $E_s \approx 1–2$ eV in argon. How important this additional process is, is for the moment unclear. Threshold experiments with

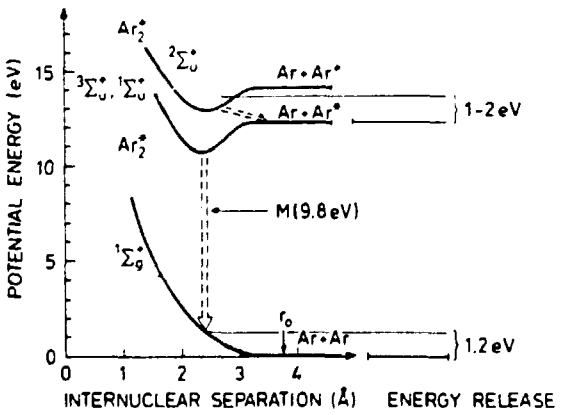

Fig. 1. Schematic representation of the important transitions in solid argon. The energy levels are from the solid. The transitions that may lead to energy release are indicated by dashed arrows.

low-energy photons and electrons on solid argon [4,30] indicate rather that the erosion initiates at the lowest exciton level a few eV below the ionization threshold in the solid rather than at the threshold itself.

A schematic representation of the important transitions are shown for solid argon in fig. 1. The scheme for solid krypton and xenon is similar, but that for solid neon differs significantly [7]. The initial hole Ar^+ becomes self-trapped as Ar_2^+. When this ion captures an electron, the molecular ion recombines into a highly excited atom Ar^* and a ground state atom. The exciton Ar^* becomes self-trapped as a metastable excimer Ar_2^*, which finally deexcites to the repulsive ground state as mentioned above.

Ellegaard et al. [9] derived a simple expression for the electronic sputtering yield Y from a solid rare gas bombarded by a primary particle:

$$Y = \Lambda \tfrac{1}{2} E(0) E_s. \tag{4}$$

Here, $E(0)$ is the surface value ($x = 0$) of the density $E(x)$ of decaying transitions at the depth x. Eq. (4) is based on the assumption that the two repulsing particles with the energy $E_s/2$ initiate a low-energy cascade and that the surface is a reflecting boundary for the excitations. By comparing this equation with eq. (1) for knock-on sputtering one notes that the energy available for sputtering is $\frac{1}{2}E(0)E_s$ instead of $\alpha N S_n$. Since $E(0)E_s$ is much smaller than the corresponding electronic stopping power NS_e, the efficiency of the electronic sputtering is considerably less than that of knock-on sputtering.

There are obvious similarities between electronic sputtering of multilayers and desorption of monolayers [3,31-32]. In the latter experiments the erosion of the monolayers is explained on the basis of the Antoniewicz mechanism [33]. In this model the transfer of energy from electronic excitation to atomic motion occurs by neutralization of the ionized adsorbed atom. In electronic sputtering the parallel case is the dissociative recombination of the trapped molecular ion R_2^+. This process in a multilayer requires a hot electron, which may be a photoelectron, a secondary, or a free substrate electron [1,24]. The cascade multiplication, however, is a clear indicator of a sputtering process rather than desorption of repulsing species.

4. Experimental

The experimental results below were obtained at the setup at Risø. The setup as well as the quartz microbalance have been described elsewhere [10,11,34,35].

Films from 2×10^{16} up to 1×10^{18} atoms/cm^2 of solidified neon, argon or krypton are produced by allowing a jet of cooled gas to impinge on an oscillating quartz crystal (fig. 2). The substrate is cooled to a temperature close to that of liquid helium. Only a few measurements were performed with solid krypton, since it was difficult to transfer the krypton to the quartz crystal without a considerable condensation in the gas tube.

Beams of 2–10 keV helium- and hydrogen-ions are extracted from a duoplasmatron ion source and selected by a 45° magnet. The current is measured by deflecting the beam into a Faraday cup. The beam is swept horizontally and vertically over an aperture in front of the target, thus ensuring a homogeneous irradiation of a large part of the target area. As in the case of electron-induced sputtering we apply a negative bias (−90 V) to an open repeller ring in front of the target in order to suppress secondary electron emission.

The current density was below 1 μA/cm^2, where evaporation caused by beam heating turned out to be insignificant. This current density causes no drift in the oscillator frequency. The sputtering yield is determined from the frequency shift of the microbalance. In a typical sputtering experiment for these solidified gases the frequency change is from 40 to 200 Hz. After each run the eroded film is thrown away by heating the quartz crystal.

No systematic investigations of the temperature dependence of the yield were performed. However, even the most volatile material, solid neon, showed no dependence on the substrate temperature above 7 K [7].

A typical run is shown in fig. 3. A neon film with a thickness of about one-half of the ion range [36] is eroded by 8 keV H_2^+-ions. One notes the linear increase of the frequency with time. The sputtering yield is evaluated directly from the slope ($Y = 66$ Ne/H-atom). The saturation above 1200 s indicates that the neon film is removed. The target current, which was measured simultaneously, increases from a value that is characteristic for solid neon up to one which represents the silver substrate (the electrode of the crystal). The current

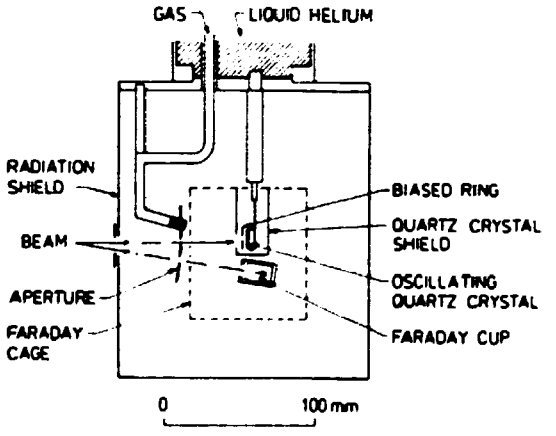

Fig. 2. The experimental setup.

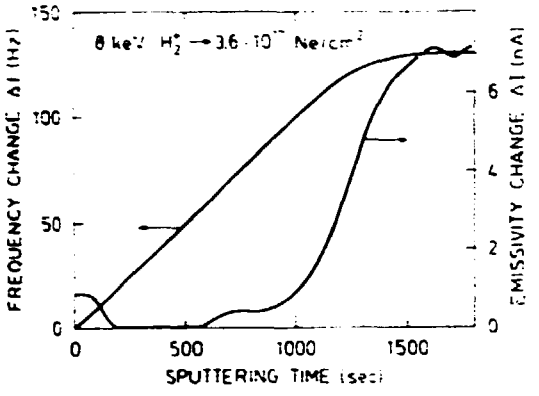

Fig. 3. The erosion of a 3.6×10^{17} Ne-atoms/cm^2 thick film on a Ag-substrate of a quartz crystal by 8 keV H_2^+-ions. The frequency change and the emissivity change are plotted versus time. The average current was 22 nA.

change is caused by the emission of fast ($E_{out} > 90$ eV) reflected protons, since the positive ion emission coefficient is smaller for silver (~ 0.1) than for solid neon (~ 0.5). From the change in emissivity one may also obtain the time necessary to remove the film by sputtering. This method has been utilized on massive substrates in cases for which the results from the quartz crystal were not reliable [7,34,35].

The present energy regime allows us to study knock-on sputtering as well as electronic sputtering with these light ions. However, a comprehensive study of the thickness dependence of the yield was usually possible only for energies from 6 to 10 keV. At low energies the available beam currents were too low for such a series of measurements.

5. Results and discussion

The *thickness* dependence of the yield from solid argon induced by hydrogen and helium-ions is shown in fig. 4. A characteristic diffusion length of about 210 Å was derived previously from the hydrogen points [11]. This value agrees well with other ones determined by the electronic sputtering of argon films that were produced in a similar way [2]. One notes that the yield decreases towards zero with decreasing film thickness. In contrast, the yield for both helium ions decreases with decreasing film thickness to a value of about 0.7 and 0.55 of the bulk yield Y_∞ for the ^{4}He-ions and ^{3}He-ions, respectively. We disregard the sudden increase in yield for thicknesses below 2×10^{16} Ar-atoms cm^2. This enhancement may be ascribed to the previously observed thin-film behaviour which was reported by us for solid neon [7,10] and by Erents and McCracken for solid argon, nitrogen and carbon monoxide [37].

It is tempting to suggest that the constant part of the yield (e.g. $0.55 Y_\infty$ for ^{3}He$^+$-ions) originates from the knock-on sputtering yield and the thickness dependent part from the electronic sputtering yield. The two parts are completely split-up in time, since the development of a linear collision-cascade and a possible elastic spike is terminated after a time of the order 10^{-11} s. The electronic deexcitation starts after the electron capture of the molecular ion Ar_2^+. This may take place in

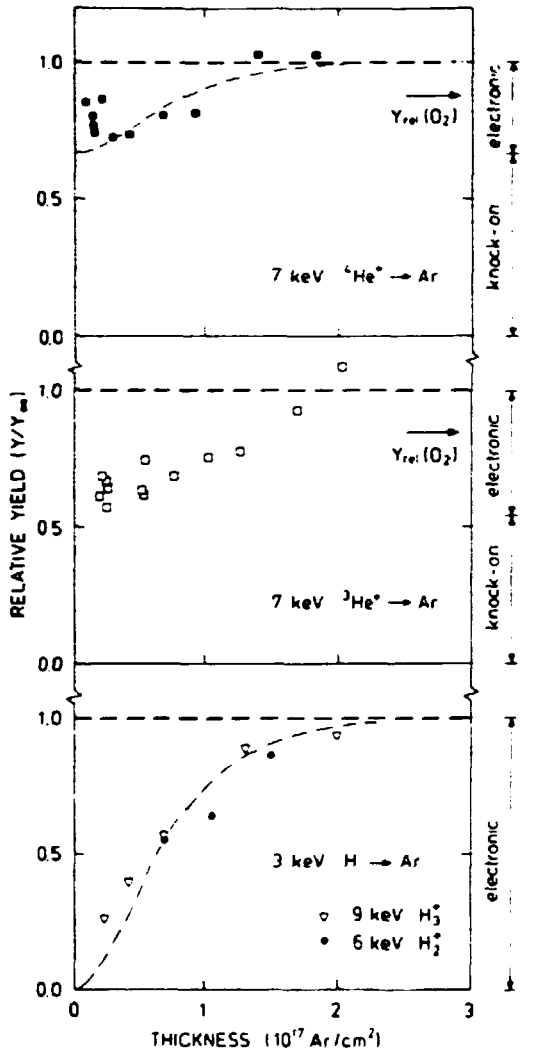

Fig. 4. The thickness-dependence of sputtering from solid argon from helium and hydrogen ions. All yields have been normalized to the "thick-film" yield $Y_\infty = 1$. (·–·–·), the thickness-dependent yield evaluated for a characteristic diffusion length of 210 Å (5×10^{17} Ar-atoms/cm^2) [2,11]. The arrows indicate the yield for thick films doped with about 1% O_2. The contributions of knock-on and electronic sputtering for thick films are indicated at the right-hand side of the figure.

microseconds, if not seconds, after the impact of the primary particle.

This interpretation was corroborated by subsequent experiments with He^+-ions incident on solid argon with a controlled impurity of 1 vol.% O_2 added to the argon gas before film production. It is known from previous experiments that an oxygen contamination of this magnitude reduces the electronic sputtering yield by a factor of 0.5 [9,24]. Since this amount of impurities hardly changes the knock-on sputtering yield for thick films, the decrease agrees well with the suggested values for electronic sputtering.

The knock-on yields evaluated from fig. 4 (24.8 $Ar/^4He^+$ and 18.1 $Ar/^3He^+$) are much larger than that the values predicted by the linear collision-cascade theory ($Y_{cc} \approx 6$ $Ar/^4He^+$ and 4 $Ar/^3He^+$). One notes that the efficiency of the sputtering is surprisingly large and that the ratio (≈ 1.35) of the yields induced by $^4He^+$-ions to that of $^3He^+$-ions is similar to the ratio of the nuclear stopping power (≈ 1.30). The nuclear stopping power was determined from Lindhard et al. [38].

At 7 keV the electronic stopping power is a factor of 3 to 4 larger than the corresponding nuclear one. It means that the energy loss to the electronic excitations is about a factor of 6.5 less efficient in producing ejected atoms that the loss represented by the nuclear stopping power.

The *energy* dependence of the total yield for thick films is determined by the dominant component. For hydrogen ions incident on the rare gas solids the electronic sputtering yield exceeds that from knock-on sputtering significantly. This is clearly demonstrated in fig. 5. The yield curves for solid neon and argon are similar to corresponding curves for the electronic stopping power from Andersen and Ziegler [36]. The nuclear stopping for 7 keV hydrogen ions incident on argon is only a few per cent of the electronic one, and plays, therefore, no role in the sputtering in spite of the high efficiency of the energy conversion.

The high yield from solid neon compared with argon reflects primarily the low binding energy of the neon atoms. The sublimation energy of neon is a factor of 4 smaller than that of argon. Since the energy release E_s according to Fugol [28] is similar for these two materials, actually one expects that the yield from argon is correspondingly small. However, in this comparison we disregarded the possible difference in the stopping power that varies a factor of 3 from neon to argon according to Andersen and Ziegler [36], but only a factor of 1.1 according to Lindhard and Scharff [39]. Indeed, the different values of the stopping power demonstrate that these quantities are not accurately known below 10 keV. On the other hand, it indicates that the yield for neon may be surprisingly large. The krypton points lie a factor 0.6 lower than the argon points. This is consistent with the decrease in sublimation energy by a factor of

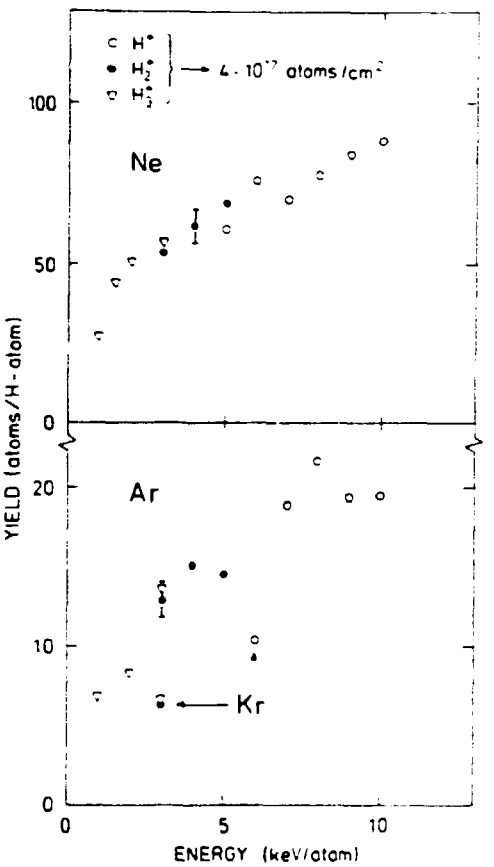

Fig. 5. The energy dependence of the yield from solid Ne [10], Ar and Kr. The yield per incident *atom* is plotted versus primary energy per *atom*. The data shown are usually the average of several points. The standard deviation is indicated.

0.7 from krypton to argon. The two available stopping powers increase only slightly from argon to krypton.

The energy dependence of the yield of thick argon films bombarded by He-ions is shown in fig. 6. One notes that the yield increases with energy, although the contribution from knock-on sputtering is the largest one. This contribution is expected to decrease rather than increase with energy, e.g. according to eq. (2), if the sputtering originates from a linear collision-cascade. Therefore, the electronic sputtering yield rises faster than the decrease of the knock-on sputtering yield.

The results presented in fig. 6 demonstrate, independently of those for the thickness dependence, that knock-on sputtering is important. Without any contribution from knock-on sputtering one would expect that the yield induced by primaries of equal velocity should be similar. Indeed, this is not the case.

However, the energy dependence of the yield does not lead to values of the knock-on and electronic sputtering yield that are consistent with the previously

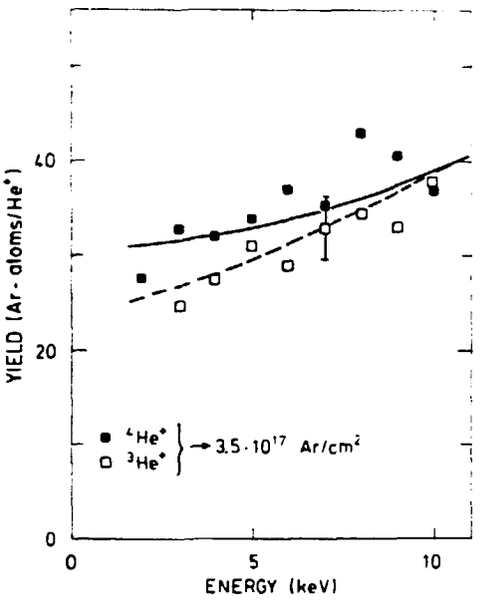

Fig. 6. The energy dependence of the yield from solid Ar induced by 2–10 keV He^+-ions. (———), calculated yield for $^4He^+$-ions on the basis of the efficiencies deduced from fig. 4, but with an electronic stopping power proportional to the energy. (– – –), calculated yield for $^3He^+$-ions. The data shown are the average of several points. The standard deviation is indicated.

evaluated values, if the nuclear and electronic stopping power from Lindhard et al. [38] and Lindhard and Scharff [39] are applied. The resulting yield curves decrease rather than increase with energy. On the other hand, if we apply an electronic stopping power proportional to the energy, we obtain the calculated curves in fig. 6, but with a minor change in the efficiency of the energy loss to the nuclei. The exponent 1 suggested in the stopping power is considerably larger than the value of 0.5 according to the Lindhard–Scharff treatment and that of 0.63 recommended by Ziegler [40].

The present experimental values for helium ions incident on solid argon are considerably smaller than those of (250 ± 75) Ar-atoms/^{4}He-ion obtained by David et al. [41] for 4 keV $^4He^+$-ions. This is surprising since the yields induced by 4 keV Ne^+-ions agree quite well for solid argon [2].

Our *procedure* for *determining the relative contributions* of electronic and knock-on sputtering based on the thickness dependence appears to be superior to other methods, e.g. those suggested by Stevanovic et al. [17] and Chrisey et al. [42]. In both cases it is required that at least one of the contributions should be determined by a theoretical calculation, for example by linear collision-cascade theory.

We are not able to exclude with certainty that the knock-on sputtering yield is proportional to the square of the surface value $F_D(E, 0)$ of the deposited energy. This relationship was observed by Stevanovic et al. [17] for medium-mass ions incident on solid xenon. However, the ratio of the contribution induced by $^3He^+$-ions to that by $^4He^+$-ions favours a linear relationship. This is supported by the estimate in fig. 6, which is based on a linear relationship as well. A comparison with the gas-flow model by Urbassek and Michl [43] has not been made because the model does not include electronic sputtering.

The characteristic diffusion length for solid argon bombarded by helium ions is apparently not reduced by the "knock-on-damage". The curve indicated in fig. 4 for the ^{3}He-ions is the one of 210 Å obtained for hydrogen ions as well. The experimental scattering of the individual points does not allow us to perform a more accurate analysis. However, a value larger than 210 Å is possible. This observation means that the energy loss to the nuclei not only produces damage, but also supplies the track of the primary particle with sufficient heat to improve the local crystal quality.

6. Conclusion

The contributions of electronic and knock-on sputtering to the total yield have been evaluated for keV helium ions incident on solid argon on the basis of the thickness dependence. The knock-on sputtering yield accounts for 0.55–0.7 of the total yield at 7 keV. The efficiency of the energy conversion from the loss to the nuclei to the ejection of argon atoms is about 6 times the efficiency of electronic energy loss. This number is supported by the energy dependence of the total yield, provided that the electronic stopping power is proportional to the energy.

The yield induced by hydrogen ions shows a trend that is similar for solid neon, argon and krypton. In all cases the dominant mechanism is electronic sputtering, and the yield curves resemble those of the electronic stopping power.

The authors have appreciated discussions with H.H. Andersen, W.L. Brown, R.E. Johnson, T. Kloiber, P. Sigmund and A.E. de Vries.

References

[1] W.L. Brown and R.E. Johnson, Nucl. Instr. and Meth. B13 (1986) 295.
[2] J. Schou, Nucl. Instr. and Meth. B27 (1987) 188.
[3] P. Feulner, T. Müller, A. Puschmann and D. Menzel, Phys. Rev. Lett. 59 (1987) 791.

[4] T. Kloiber, W. Laasch, G. Zimmerer, F. Coletti and J.M. Debever, to be published.
[5] G. Zimmerer, in: Excited State Spectroscopy in Solids, ed. M. Manfredi, XCVI Corso, Soc. Italiana di Fisica, Bologna, (1987) p. 37.
[6] N. Schwentner, E.-E. Koch and J. Jortner, Electronic Excitations in Condensed Rare Gases (Springer, Berlin–Heidelberg, 1985).
[7] J. Schou, P. Børgesen, O. Ellegaard, H. Sørensen and C. Claussen, Phys. Rev. B34 (1986) 93.
[8] P. Børgesen, J. Schou, H.Sørensen and C. Claussen, Appl. Phys. A29 (1982) 57.
[9] O. Ellegaard, R. Pedrys, J. Schou, H. Sørensen and P. Børgesen, to be published.
[10] O. Ellegaard, J. Schou and H. Sørensen, Nucl. Instr. and Meth. B13 (1986) 567.
[11] J. Schou, R. Pedrys, O. Ellegaard and H. Sørensen, Nucl. Instr. and Meth. B18 (1987) 609.
[12] P. Sigmund, in: Sputtering by particle bombardment I, ed. R. Behrisch (Springer, Berlin, 1981) p. 9.
[13] P. Sigmund, Nucl. Instr. and Meth. B27 (1987) 1.
[14] R. Pedrys, R.A. Haring, A. Haring, F.W. Saris and A.E. de Vries, Phys. Lett. 82A (1981) 371.
[15] R. Pedrys, D.J. Oostra and A.E. de Vries, in: Desorption Induced by Electronic Transitions, DIET II, eds. W. Brenig and D. Menzel (Springer, Berlin–Heidelberg, 1985) p. 190.
[16] J.W. Boring, D.J. O'Shaughnessy and J.A. Phipps, Nucl. Instr. and Meth. B18 (1987) 613.
[17] D.V. Stevanovic, D.A. Thompson and J.A. Davies, Nucl. Instr. and Meth. B1 (1984) 315.
[18] D.J. O'Shaughnessy, J.W. Boring, J.A. Phipps, R.E. Johnson and W.L. Brown, Nucl. Instr. and Meth. B13 (1986) 304.
[19] P.D. Townsend, in: Sputtering by particle bombardment II, ed. R. Behrisch (Springer, Berlin, 1983) p. 147.
[20] N. Itoh, Nucl. Instr. and Meth. B27 (1987) 155.
[21] F. Besenbacher, J. Bøttiger, O. Graversen, J.L. Hansen and H. Sørensen, Nucl. Instr. and Meth. 191 (1981) 221.
[22] C.T. Reimann, R.E. Johnson and W.L. Brown, Phys. Rev. Lett. 53 (1984) 600.
[23] W.L. Brown, C.T. Reimann, and R.E. Johnson, Nucl. Instr. and Meth. B19/20 (1987) 9.
[24] W.L. Brown, C.T. Reimann and R.E. Johnson, in: Desorption Induced by Electronic Transitions, DIET II, eds. W. Brenig and D. Menzel (Springer, Berlin, 1985) p. 199.
[25] C.T. Reimann, W.L. Brown and R.E. Johnson, to be published.
[26] R.W. Ollerhead, J. Bøttiger, J.A. Davies, J. L'Ecuyer, H.K. Haugen and N. Matsunami, Radiat. Eff. 49 (1980) 203.
[27] R. Pedrys, D. Oostra, A. Haring, A.E. de Vries and J. Schou, these Proceedings (ICACS '87) Nucl. Instr. and Meth. B33 (1988) 840.
[28] I.Ya. Fugol', Adv. Phys. 27 (1978) 1.
[29] B.J. Garrison and R.E. Johnson, Surf. Sci. 148 (1985) 388.
[30] F. Coletti and J.M. Debever, private communication.
[31] Q.-J. Zhang, R. Gomer and D.R. Bowman, Surf. Sci. 129 (1983) 535.
[32] E.R. Moog, J. Unguris and M.B. Webb, Surf. Sci. 134 (1983) 849.
[33] P.R. Antoniewicz, Phys. Rev. B21 (1980) 3811.
[34] J. Schou, H. Sørensen and P. Børgesen, Nucl. Instr. and Meth. B5 (1984) 44.
[35] O. Ellegaard, PhD Thesis, Risø Rep. M-2617, Risø National Laboratory (1986).
[36] H.H. Andersen and J.F. Ziegler, Hydrogen Stopping Powers and Ranges in all Elements (Pergamon, New York, 1977).
[37] S.K. Erents and G.M. McCracken, in: Atomic Collisions in Solids, eds. S. Datz, B.R. Appleton and C.D. Moak (Plenum, New York, 1975) p. 625.
[38] J. Lindhard, V. Nielsen and M. Scharff, K. Dan. Vidensk. Mat. Fys. Med. 36 (1968) no. 10.
[39] J. Lindhard and M. Scharff, Phys. Rev. 124 (1961) 128.
[40] J.F. Ziegler, Helium Stopping Powers and Ranges in All Elements (Pergamon, New York, 1977).
[41] D.E. David, T.F. Magnera, R. Tian, D. Stulik and J. Michl, Nucl. Instr. and Meth. B14 (1986) 378.
[42] D.B. Chrisey, J.W. Boring, J.A. Phipps, R.E. Johnson and W.L. Brown, Nucl. Instr. and Meth. B13 (1986) 360.
[43] H.M. Urbassek and J. Michl, Nucl. Instr. and Meth. B22 (1987) 480.

Radiation Effects and Defects in Solids, 1989, Vol. 109, pp. 235–238
Reprints available directly from the publisher
Photocopying permitted by license only

EROSION AND LUMINESCENCE FROM PURE AND IMPURE SOLID DEUTERIUM

B. STENUM, J. SCHOU and H. SØRENSEN

Association Euratom—Risø National Laboratory, Physics Department, DK-4000 Roskilde, Denmark

and

P. GÜRTLER

Hasylab, DESY, D-2000 Hamburg 52, FRG

(Received September 19, 1988; in final form November 10, 1988)

The first simultaneous measurements of the erosion and luminescence yield from deuterium films bombarded by 2-keV electrons are reported. The luminescence in the region from 200 to 600 nm was measured. A peak at about 275 nm was observed from the solid deuterium. The possible origin of this peak will be discussed. Doping with 0.5% nitrogen changes the luminescence spectrum largely and causes beam-induced evaporation at high current densities.

Key words: erosion, luminescence, solid deuterium, electron bombardment.

INTRODUCTION

Erosion of condensed gases by energetic electrons takes place as beam-induced evaporation and electronic sputtering.[1] Electronic sputtering is a result of the competition between radiative and non-radiative transitions in the irradiated condensed gas. The kinetic energy required for the particle ejection is released by the non-radiative events. For solid rare gases it is well known that the electronic sputtering is caused by radiative transitions to a repulsive ground state.[1,2] In contrast, no luminescence has been observed from irradiated solid hydrogens, and non-radiative transitions may be dominant.

The intention of the present work was to study the luminescence from electron-irradiated solid deuterium simultaneously with sputtering yield measurements. Since the luminescence from deuterium is weak, the studies have to be performed with a relatively high beam current. This means that the erosion yield from this very volatile solid comprises a significant yield of beam-induced evaporation in addition to the ordinary low-temperature yield of electronic sputtering during some of the measurements. Beam-induced evaporation occurred when the solid deuterium target was exposed to external heating because of the heat load from warm parts of the interior of cryogenic setup.[1,3]

EXPERIMENTAL PROCEDURE

The experimental setup used for this study has previously been utilized for other studies of irradiated condensed gases.[3] The cryostat cooled by liquid helium has been described in detail elsewhere.[4] Only a brief description will be given here. A monochromator and a photomultiplier covering the region from 200–600 nm have

been mounted at a side tube of the cryostat. Additional openings in the radiation shields have been made in front of the tube so that light emitted from the electron-irradiated area could be observed. Since the light emission is small the resolution could not be better than 8 nm. The position of the electron gun has been changed in such a way that the electron beam is deflected through an angle of 15° so that light emitted by the filament of the electron gun does not reach the target or enter into the monochromator. The gas is led into the cryostat through a cold tube and solidifies on a cold quartz crystal microbalance. With this setup it is possible to make films of known thickness and to measure the mass loss during the irradiation. The beam current was determined from the target current that is measured simultaneously with the mass loss, and calibrated with the Faraday cup in the standard setup.[5] By a fast beam sweep a limited area of the target was irradiated homogeneously. Cryopumping onto the target was observed before and after irradiation. No corrections were performed since beam heating changes the temperature of the target and hence the cryopumping. By varying the temperature of the gas inlet tube it is possible to vary the purity of the deuterium film. At high gas tube temperatures one may let less volatile impurities through the tube. The concentration of the doped impurities was evaluated from that of the gas mixtures.

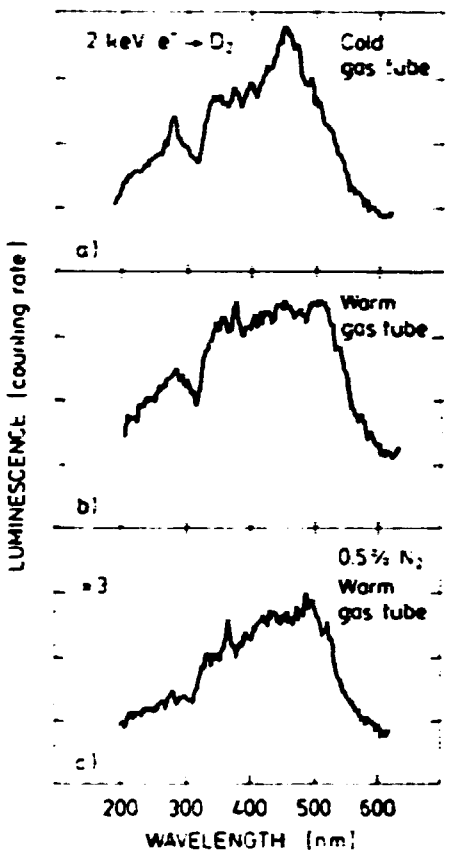

FIGURE 1 Luminescence spectra from (a) purified deuterium, (b) non purified deuterium, and (c) deuterium doped with 0.5% nitrogen.

RESULTS AND DISCUSSION

A luminescence spectrum from partly purified deuterium bombarded with 2 keV electrons is shown in Figure 1a. The peak observed around 450 nm is probably induced by impurities. The yield in this region is enhanced by doping with oxygen and carbon monoxide. This indicates that the peak originates from combinations of oxygen atoms with deuterium atoms. The peak around 275 nm may originate from a transition in the irradiated deuterium since the available dopants all had the effect of reducing rather than increasing the peak. The luminescence from solid deuterium has not been observed previously which means that it is difficult to assign this peak to any known atomic or molecular transition. An emission continuum between 190 and 280 nm from deexciting Rydberg states of D_2 ($N = 3, 4$) to the repulsive ground state $2p\,^3E^+$ has been observed in the gas phase.[7] The formation of D_3^+ and D_5^+ from dissociated and intact molecules is expected to be extremely fast in the solid. The position of the observed peak is somewhat higher than the maximum of the continuum from the gas phase, but it is well known that a red-shift may take placed in a solidified gas.[8] The luminescence yield around 275 nm decreases in less purified deuterium (Figure 1b) because of the quenching from impurities with excited states below the lowest excited state of deuterium.

In Figure 1c a luminescence spectrum from deuterium doped with 0.5% nitrogen is shown. The peak around 365 nm might originate from the atomic transition $N(^2P - ^4S)$ at 347 nm[7] or the $N_2^+(B^2\Sigma_u^+ - X^2\Sigma_g^+)$ transition.[8] At higher nitrogen concentrations the peak becomes more pronounced, and it is also observed in our spectrum from solid nitrogen. However, we cannot exclude that the peak originates from the $ND(A^3\Pi - X^3\Sigma^-)$ transition. The $NH(A^3\Pi - X^3\Sigma^-)$ transition is reported at 336 nm in the gas phase.[8] In the measurements at higher nitrogen concentrations and in our spectra from solid nitrogen the peak from the $N(^2D - ^4S)$ transition at 523 nm in solid deuterium is very intensive.[9] The intensities of most of the observed peaks were found to increase during irradiation.

In Figure 2 the measurements of the erosion yield are shown together with the relative luminescence yield at the most characteristic wavelength. The erosion yields are determined from the saturation yield which is supposed to be less influenced by any cryopumping than the initial yield. The yields have been measured for a film thickness of $3 \cdot 10^{18}$ D_2-molecules/cm^2 which is approximately twice the range of a 2-keV electron. This thickness was chosen because previous results[10,11] have demonstrated that the electronic sputtering yield shows a minimum around this thickness. The reason for the minimum is not known, but apparently the mechanism responsible for the high yield from thin films[1] does not contribute significantly to the yield above this thickness.

The yield from pure deuterium agrees within our accuracy with the previous results obtained without the additional opening for the observation of the luminescence. During the irradiation the deuterium films were colder than those in the present setup. Therefore, the previous results probably represent the low-temperature yield of electronic sputtering without beam-induced evaporation. This assumption is corroborated by the fact that the previous yield results did not show any dependence on the current.

The erosion yield increases with the concentration of the impurities in the deuterium. This enhancement is obviously beam-induced evaporation because of the strong dependence on the current density. The beam-induced evaporation from the impure deuterium films, especially nitrogen-doped, is explained by a reduced heat conductivity of the impure films. The luminescence yield is seen to be

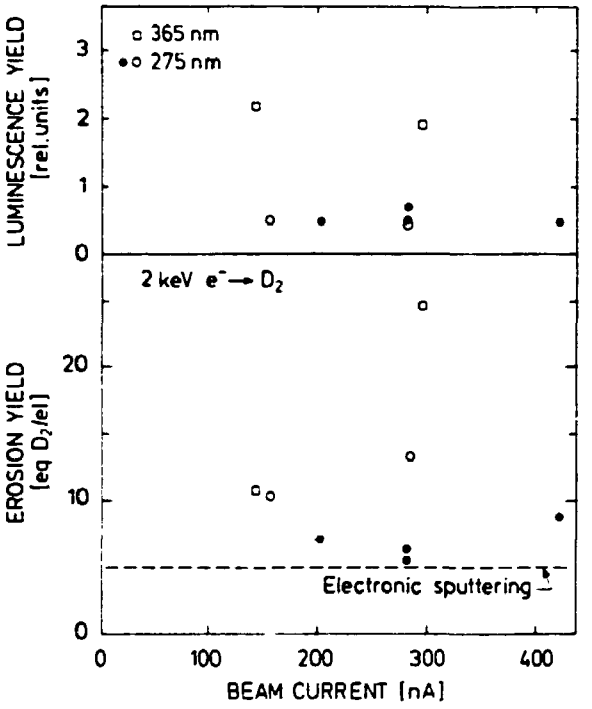

FIGURE 2 Erosion yield and luminescence yield versus beam current.* The absolute erosion yield is given in units of 4 amu, ● cold target and gas tube, ○ warm target and gas tube, □ deuterium doped with 0.5% nitrogen, warm target and gas tube. The electronic sputtering yield is from Ref. 10.

independent of the beam-current, which indicates that the luminescence originates from the solid sample.

REFERENCES

1. J. Schou, *Nucl. Instr. and Meth.* **B27**, 188 (1987).
2. W. L. Brown and R. E. Johnson, *Nucl. Instr. and Meth.* **B13**, 295 (1986); C. T. Reimann, V.. L. Brown, and R. E. Johnson, *Phys. Rev.* **B37**, 1455 (1988).
3. J. Schou, P. Børgesen, O. Ellegaard, and H. Sørensen, *Phys. Rev.* **B34**, 93 (1986).
4. H. Sørensen, *Appl. Phys.* **9**, 321 (1976); J. Schou, H. Sørensen, and P. Børgesen, *Nucl. Instr. and Meth.* **B5**, 44 (1984).
5. A. B. Raksit, R. E. Porter, W. P. Graver, and J. J. Leventhal, *Phys. Rev. Lett.* **55**, 531 (1985).
6. G. Zimmerer, in *Excited State Spectroscopy*, U. M. Grassano and Terzi (Eds.) (North Holland, Amsterdam, 1987) p. 37.
7. R. J. Sayer, R. H. Prince, and H. W. Duley, *Proc. R. Soc. Lond.* **A365**, 235 (1979).
8. R. W. B. Pearse and A. G. Gaydon, *The Indentification of Molecular Spectra* (Chapman and Hall, London, 1976).
9. R. L. Brooks, *J. Chem. Phys.* **85**, 1247 (1986).
10. O. Ellegaard, Risø-M-2617 (1986), Risø National Laboratory, unpublished.
11. P. Børgesen and H. Sørensen, *Phys. Lett.* **90A**, 319 (1982).

*The luminescence yield is given in counting rate per nA.

Nuclear Instruments and Methods in Physics Research B48 (1990) 530-533
North-Holland

THICKNESS DEPENDENCE OF THE SPUTTERING YIELD FROM SOLID DEUTERIUM BY LIGHT keV IONS

B. STENUM, O. ELLEGAARD, J. SCHOU and H. SØRENSEN

Association Euratom - Risø National Laboratory, Physics Department, DK-4000 Roskilde, Denmark

Measurements of the thickness dependence of the sputtering yield from solid deuterium bombarded by 1-10 keV/amu hydrogen ions are reported. For film thicknesses larger than 2×10^{18} D_2/cm^2 the yield is largely independent of the film thickness. A strong enhancement of the yield is observed for thin films. The results for different ion energies demonstrate convincingly that this enhancement is a result of the interaction between the primary ion and the metallic substrate rather than a beam-independent structural interface effect.

1. Introduction

The erosion of condensed gases is a particular area in sputtering and erosion of solids by charged particles [1,2]. It has turned out to be important in interstellar and planetary atmospheric as well as in technological problems such as cryopumping in radiation environments. In particular, the behaviour of the solid hydrogens bombarded by charged particles is important for models on fuel pellet injection into a plasma [3]. However, only few measurements of the neutral erosion and secondary-ion yield from solid hydrogens have been reported in the literature [3-12], and the data base is not yet sufficient for realistic modelling of the ion interaction with solid deuterium.

The major difficulty in producing reliable data for erosion of the solid hydrogens by energetic ions and electrons is the extremely low sublimation energy of the solid. This energy ranges from 7 to 14 meV/molecule from H_2 to T_2 [13]. It means that the sample has to be produced by a cryogenic technique that ensures a temperature below 4 K [3-5].

The analysis of sputtering data from ion-bombarded condensed gases is complicated since the erosion often is caused by two entirely different mechanisms, electronic and knock-on sputtering. Electronic sputtering, i.e. sputtering via electronic transitions, occurs for insulating materials only [1,14], whereas knock-on (ordinary) sputtering takes place for all materials as a result of the collisions between the primary ions and the target atoms [14]. Both types of sputtering processes occur simultaneously during light-ion bombardment of solid rare gases for primary energies about and below 10 keV [15]. The practical separation of the two components of the sputtering yield is difficult, and has been performed in only two cases without assumptions that rely on theoretical predictions [15,16]. In the present study of light-ion bombardment of solid deuterium we were unable to distinguish between the two components.

The present work is a continuation of previous studies on solid hydrogen and deuterium performed at Risø [3-9]. The sputtering yield of deuterium for 2 keV electrons turned out to be strongly dependent on the film thickness and showed a minimum of about 4 D_2/electron at a thickness around 2.5×10^{18} D_2/cm^2 [7,17]. This behaviour which is expected to be a characteristic feature for electron energies of a few keV has made it difficult to estimate the yield dependence on the primary energy. The preliminary investigations for light-ion bombardment of solid deuterium and hydrogen by Børgesen [5] and Børgesen et al. [6] were not so comprehensive that an accurate thickness dependence could be determined. The erosion yield measured by Erents and McCracken [10] shows the same trend as the Risø measurements, i.e. the yield increases with decreasing film thickness. Their measurements on solid deuterium were carried out for films thinner than 2×10^{18} D_2/cm^2 with 5 keV deuterons. For the thickest film these authors [10] obtained a yield of about 200 D_2 per D_2^+ ion.

In this work we present the results of the first systematic study of the target thickness dependence for hydrogen ion bombardment of solid deuterium. It turns out that the behaviour of the ion-induced yield is similar to that of the electron-induced yield for thin films ($< 2 \times 10^{18}$ D_2/cm^2), but very different for thick films. At large thickness the measurements indicate that the yield becomes almost constant, contrary to the strong increase of the electron-induced yield at these thicknesses [7,17]. The observed thin-film enhancement for deuterium partly resembles the trend that we found previously for another volatile condensed gas, solid neon [18,19], and this trend was also observed by Erents

0168-583X/90/$03.50

and McCracken for solid argon, carbon monoxide and nitrogen [20].

2. Experimental

The experimental setup has been described in detail previously [3,15,18]. Only a brief description will be given here.

The deuterium films were produced by letting a jet of gas hit a quartz crystal suspended below a pumped liquid-helium cryostat (fig. 1). With this technique it is possible to make deuterium films of known thickness and to measure the mass loss during irradiation.

Beams of 4–10 keV H^+, H_2^+ and H_3^+ ions are extracted from a duoplasmatron ion source and mass-selected by a 45° magnet. The irradiated area on the target is limited by a 2 mm aperture in front of the target. Only perpendicular beam incidence has been studied in the present work. The beam current was measured before and after irradiation by deflecting the beam into a Faraday cup. In order to ensure a homogeneously irradiated area on the target the beam was swept both horizontally and vertically over the aperture. As in the case of electron-induced sputtering [7], we apply a negative bias (−90 V) to an open repeller ring in front of the target. In this way secondary-electron emission is suppressed, and charge-up problems are reduced substantially.

The current density during the measurement did not exceed 0.5 μA/cm², and the yield turned out to be independent of the beam current at these low currents, so that evaporation by beam-heating is insignificant [3]. This current density causes no drift in the oscillator frequency. The stability of the beam was checked during the sputtering experiment by measuring the target current. 900 subsequent frequency and target current measurements were performed during one run. The sputtering yield was determined from the frequency shift. The total shift varied from 5 Hz for thin films to 50 Hz for thick films. After each run the film was evaporated away by heating the quartz crystal.

We observed a strong initial cryopumping on the target as soon as the beam was deflected into the target chamber. The cyropumping rate was comparable to the beam erosion during the first part of the irradiation time, so that no mass loss was detected. Simultaneously with the cryopumping, a pressure rise in the target chamber was observed. The cryopumping during the measurements was substantially reduced by deflecting the beam into the Faraday cup during film deposition and until the pressure rise dropped down.

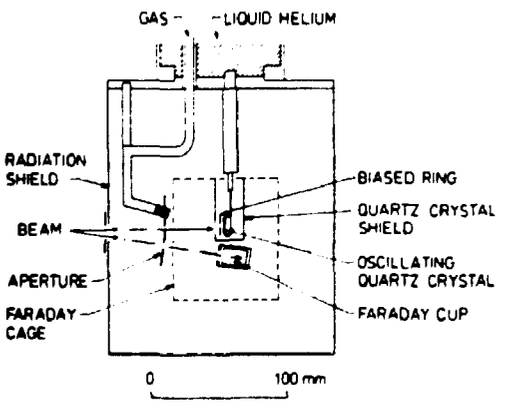

Fig. 1. Schematic drawing of the target region of the experimental setup.

3. Results

The sputtering yield as a function of initial deuterium film thickness was measured for film thicknesses ranging from 0.1 up to 10×10^{18} D_2/cm^2. Results for primary energies from 1.3 up to 10 keV/amu are shown in fig. 2. For all primary energies one notes the very

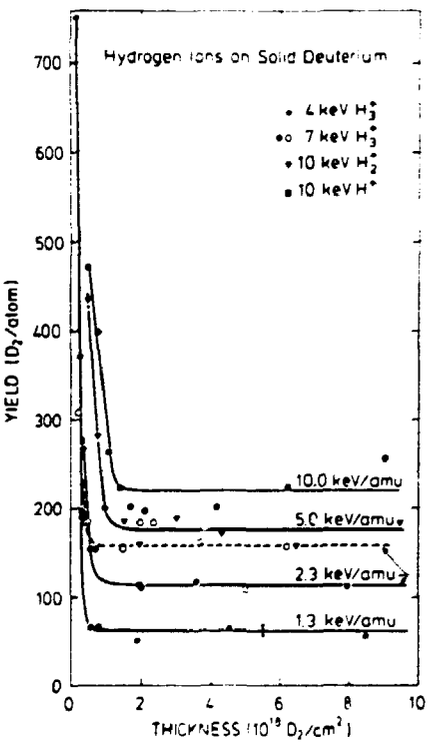

Fig. 2. Thickness dependence of the yield from solid deuterium bombarded by 1.3–10 keV/amu hydrogen ions. The horizontal lines represent the mean values of the field at large thicknesses. The different indications for 7 keV H_3^+ ions represent two independent series. The error bar reflects the standard deviation of the mean value only.

high yield for thin films ($< 1.5 \times 10^{18}$ D_2/cm^2). This thin-film enhancement is apparently larger for the high-energy primaries than for the lowest energies so that the fall-off to the thick-film values occurs at higher thicknesses for the highest ion energies. For thick films the yield may be approximated by a constant value. There is a slight increase with thickness for thick films bombarded by 10 keV H^+ ions, but this tendency has not been confirmed for energies lower than that. The two series at 7 keV H_3^+ ions were performed with a time separation of several years. This shows that the absolute uncertainty is about 40%. However, the reproducibility in subsequent runs was usually better than 10%.

Preliminary results for different hydrogen ions of the same velocity indicate that the polyatomic ions are the most efficient ones in producing sputtering. This molecular effect will be studied in greater detail in the near future.

The thin-film enhancement is not caused by beam-induced evaporation since it turned out that the yield was constant for current densities from 0.05 to 0.5 $\mu A/cm^2$. Only for current densities close to 1 $\mu A/cm^2$ did we observe a significant increase in the yield.

4. Discussion

4.1. Thick films

The yield for thick films increases with energy per mass unit from about 60 D_2/atom at 1.33 keV/amu up to 220 D_2/atom at 10 keV/amu. This behaviour may indicate a significant electronic sputtering yield, since the electronic stopping power largely shows a similar trend. However, in this energy regime, in particular for the low energies, there might as well be an appreciable contribution of knock-on sputtering to the yield. Although the nuclear stopping power is one to two orders of magnitude smaller than the electronic stopping power in this energy regime, it is known from other highly volatile ices that nuclear stopping is much more efficient in producing a high sputtering yield than an electronic stopping of the same magnitude [15,21]. Presently, the number of data points is insufficient to allow us to perform an accurate analysis of results on the basis of the existing models of elastic or electronic spikes and their extensions. [21–24]. A significant increase of the yield for thick films was not observed. For solid rare gases this increase for thick films is a consequence of the mobile excitations in these solids [1,2].

4.2. Thin films

The strong enhancement of the yield for thin films is caused primarily by the interaction between the ion and the metallic substrate, i.e. the silver electrode of the quartz crystals. Erents and McCracken [10] suggested that the electronic energy deposition in the metallic substrate from the ions was extremely efficient in producing sputtering from thin films. This thin-film enhancement is not caused by backscattered ions since this process would lead to only a slight enhancement of the yield of about 15–30% [25].

Since the constant (bulk) yield is obtained from film thicknesses larger than the ion range, one may determine the thickness R_s for which the sputtering yield is no longer influenced by the silver substrate. The quantity R_s is determined from the cross-over between the best straight line that approximates the yield for the thin film and the bulk yield. (For 10 keV H^+ ions the minimum value between 2×10^{18} and 4×10^{18} D_2/cm^2 has been used.) In fig. 3 this sputtering range R_s is compared to the existing range measurements [26] and calculations of Winterbon [27] with Lindhard–Scharff electronic stopping [28]. Obviously R_s is clearly correlated to the range of the ion, although the former increases more slowly for the highest energies.

This correlation between R_s and the range is the first evidence that the energy dissipation in the metallic substrate is responsible for the thin-film enhancement of the sputtering yield. Then the high yield for the thin films is not caused by inhomogeneities of the films, i.e.

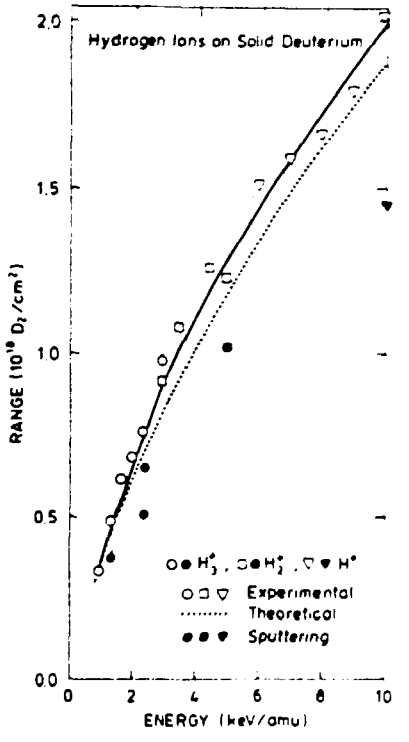

Fig. 3. The sputtering range (see text) of hydrogen ions in solid deuterium compared with previously obtained ranges, experimental and theoretical.

clustering of the deuterium molecules on the silver surface, since this effect would lead to an energy-independent R_s. It is reasonable to expect that the sputtering depth R_s is smaller than the range. The ions cause an enhanced yield only, if the ions reach the film–metal interface before complete slowing-down. The mechanism that leads to this thin-film enhancement has not yet been identified.

The comparatively large extension of the sputtering range for deuterium films is probably connected to the high volatility of solid deuterium. The thin-film enhancement for solid neon disappears for film thicknesses smaller than 1×10^{17} Ne/cm^2 [19], which is much less than the mean penetration depth of the primary electrons [29]. The extension of the thin-film enhancement observed by Erents and McCracken [20] corresponds to a sputtering range of about 1×10^{16} atoms/cm^2 for solid argon, nitrogen and carbon monoxide. Since these authors did not measure any yields for film thicknesses larger than 5×10^{16} atoms, a precise determination of the corresponding sputtering range is impossible. However, the small value of the range to be expected is in complete agreement with the relatively low volatility of these three solidified gases.

5. Conclusion

The thickness dependence of the sputtering yield from solid deuterium bombarded by keV hydrogen ions shows the same trend for all primary energies. For film thicknesses larger than 2×10^{18} D_2/cm^2 the yield is almost constant. The high yield for small film thicknesses is the result of an efficient energy transfer mechanism from the silver substrate to the outermost layers of the deuterium film. This origin of the thin-film enhancement follows from the close correlation between the ion range and the thickness that corresponds to the transition from the thin films to the thick-film regime (bulk). The thin-film enhancement for deuterium as well as other volatile gases deposited on metallic substrates is apparently not a structural interface effect, but a clear beam-induced feature.

References

[1] J. Schou, Nucl. Instr. and Meth. B27 (1987) 188.
[2] W.L. Brown and R.E. Johnson, Nucl. Instr. and Meth B13 (1986) 295.
[3] J. Schou, H. Sørensen and P. Børgesen, Nucl. Instr. and Meth. B5 (1984) 44.
[4] P. Børgesen and H. Sørensen, Phys. Lett. A90 (1982) 319.
[5] P. Børgesen, Risø-Report R-457 (Risø National Laboratory, 1982).
[6] P. Børgesen, J. Schou and H. Sørensen, Proc. Symp. on Sputtering, eds. P. Varga, G. Betz and F.P. Viehböck (Technische Universität, Wien, Austria, 1980) p. 822.
[7] O. Ellegaard, Risø-Report M-2617 (Risø National Laboratory, 1986).
[8] B. Stenum, J. Schou, H. Sørensen and P. Gürtler, Radiat. Eff. Defects in Solids 109 (1989) 235.
[9] H. Sørensen, Appl. Phys. 9 (1976) 321.
[10] S.K. Erents and G.M. McCracken, J. Appl. Phys. 44 (1973) 3139.
[11] R.H. Stulen, in: DIET III, Desorption Induced by Electronic Transitions III, eds. R.H. Stulen and M.L. Knotek (Springer, Berlin, 1988) p. 39.
[12] R. Clampitt, Vacuum 34 (1984) 113.
[13] P.C. Souers, Hydrogen Properties for Fusion Energy (University of California Press, Berkeley, 1986).
[14] J. Schou, in: Structure–Property Relationships in Surface-Modified Ceramics, eds. C.J. McHargue, R. Kossowsky and W.O. Hofer (Kluwer Academic, Dordrecht, The Netherlands, 1989) p. 61.
[15] J. Schou, O. Ellegaard, H. Sørensen and R. Pedrys, Nucl. Instr. and Meth. B33 (1988) 808.
[16] J.W. Boring, R.E. Johnson and S.T. Cui, Radiat. Eff. Defects in Solids 109 (1989) 229.
[17] P. Børgesen, J. Schou, H. Sørensen, O. Ellegaard and B. Stenum, to be published.
[18] O. Ellegaard, J. Schou and H. Sørensen, Nucl. Instr. and Meth. B13 (1986) 567.
[19] J. Schou, P. Børgesen, O. Ellegaard, H. Sørensen and C. Claussen, Phys. Rev. B34 (1986) 93.
[20] S.K. Erents and G.M. McCracken, in: Atomic Collisions in Solids, eds. S. Datz, B.R. Appleton and C.D. Moak (Plenum, New York, 1975) p. 625.
[21] O. Ellegaard, J. Schou and H. Sørensen, to be published.
[22] P. Sigmund and C. Claussen, J. Appl. Phys. 52 (1981) 990. C. Claussen, Nucl. Instr. and Meth. 194 (1982) 567.
[23] R.E. Johnson, J. Phys. (Paris) C2 (1989) 251; K.M. Gibbs, W.L. Brown and R.E. Johnson, Phys. Rev. B38 (1988) 1101.
[24] H.M. Urbassek and J. Michl, Nucl. Instr. and Meth. B22 (1987) 480.
[25] J. Schou, R. Pedrys, O. Ellegaard and H. Sørensen, Nucl. Instr. and Meth. B18 (1987) 609.
[26] P. Børgesen and H. Sørensen, Nucl. Instr. and Meth. 200 (1982) 571.
[27] K.B. Winterbon, in: Ion Implantation Range and Energy Distributions, vol. 2, ed. D.K. Brice (Plenum, New York, 1975).
[28] J. Lindhard and M. Scharff, Phys. Rev. 124 (1961) 128.
[29] S. Valkealahti, J. Schou and R.M. Nieminen, J. Appl. Phys. 65 (1989) 2258.

EUROPHYSICS LETTERS 1 July 1990

Europhys. Lett., 12 (5), pp. 459-464 (1990)

Sputtering of Volatile Solids from Nonoverlapping Subspikes.

O. ELLEGAARD(*), J. SCHOU and H. SØRENSEN

Association EURATOM, Risø National Laboratory, Physics Department DK-4000 Roskilde, Denmark

(received 14 March 1990; accepted in final form 2 May 1990)

PACS. 79.20N – Atom, molecule, and ion impact.

Abstract. – Elastic low-energy spikes can be produced in volatile materials such as condensed gases even for primary particles with comparatively low nuclear stopping power. The sputtering yield from solid neon bombarded by (5 ÷ 10) keV He^+-ions has been measured. Model calculations demonstrate that nonoverlapping subspikes are responsible for particle ejection from this volatile solid.

Introduction. – Light-ion sputtering of condensed gases is characterized not only by a pronounced contribution via electronic transitions (electronic sputtering), but also by the ordinary contribution from direct collisions between the primary and the target atoms (knock-on sputtering) [1, 2]. The sputtering from knock-on processes for nonvolatile targets depends linearly on the nuclear stopping power according to linear collision-cascade theory except for systems with very high nuclear stopping powers [3-5].

In the present work on He-ion sputtering of solid neon, we have studied a projectile-target system for which the total sputtering yield turned out to be approximately proportional to the nuclear stopping power for $^4He^+$- as well as $^3He^+$-ions. Since the electronic stopping power is comparatively low for this system and would lead to a completely different dependence on the primary energy, it means that knock-on sputtering is responsible for this erosion. However, the yield predicted by linear collision-cascade theory is more than one order of magnitude too low. In fact, this behaviour has encouraged us to introduce a model that involves nonoverlapping subspikes (fig. 1). Solid neon is so volatile that one may expect that every collision between the primary light ion and a target atom generates a cascade that develops into a subspike. In this small spike volume all atoms strike other atoms that have already been set into motion. While individual cascades have been observed experimentally for metals [6], no systematic treatment of subspikes has been applied previously to any system. The existing spike models or their extensions for solidified gases are based on the assumption that many collisions between the primary particle and the target atoms contribute to one common spike [7-12]. These models lead to a strong nonlinear dependence of the yield on nuclear stopping power.

(*) Permanent address: University of Odense, DK-5230 Odense, Denmark.

The present system is characterized by a weak interaction, *i.e.* low nuclear stopping power, between the primary He^+-ion and the target atoms. This means that the average distance from one collision to the next between the primary and a target atom usually is so large that the subspikes do not overlap. On the other hand, the nuclear stopping power for the recoils is at least one order of magnitude larger than that of the primaries. As a consequence, the recoils are efficient in generating spikes in this very volatile solid (with a sublimation energy $U_0 = 20$ meV).

The present model describing sputtering via these nonoverlapping subspikes does not include any fitting parameters. In all cases we have utilized the standard values indicated in the references. The predicted yield shows a dependence on the nuclear stopping power similar to our experimental ones, and agrees surprisingly well in absolute magnitude for this system.

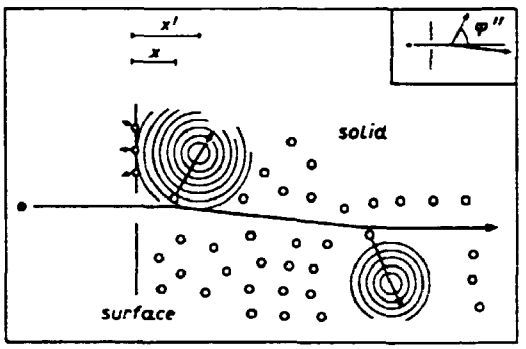

Fig. 1.

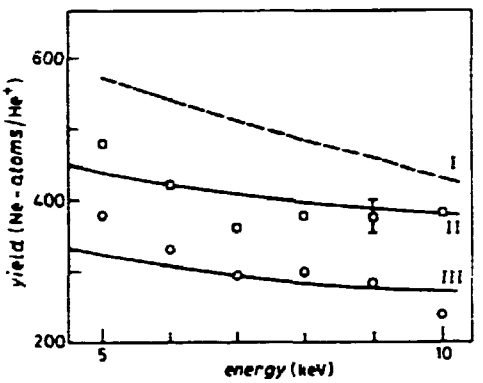

Fig. 2.

Fig. 1. – Geometry of the subspikes. The path of the primary ion is shown. A collision takes place at depth x, but the centre of the subspike develops from x'. The recoil angle φ'' is shown as well.

Fig. 2. – Sputtering yield for □ $^4He^+$ and ○ $^3He^+$ incident on $9 \cdot 10^{17}$ Ne/cm^2. I) $^4He^+ \rightarrow$ Ne, theory, eq. (4), power cross-section $m = 2/3$, $m_1 = 1/2$ (recoils), $\hat{c} = 0.76$ evaluated from [18]. II) $^4He^+ \rightarrow Ne^1$, theory, eq. (4), general cross-section derived from [20]. $\hat{c} = 0.66$. III) $^3He^+ \rightarrow$ Ne, theory, eq. (4), general cross-section from [20], $\hat{c} = 0.66$. A typical standard deviation is indicated.

Experimental. – The films were produced by letting a jet of precooled Ne-gas impinge on an oscillating quartz crystal covered with a silver substrate. Beams of (5 ÷ 10) keV $^4He^+$- and $^3He^+$-ions with current densities below 1 μA/cm^2 were extracted from a duoplasmatron ion-source system equipped with a mass-analysing magnet. The sputtering yields were determined from the frequency shift of the microbalance. This experimental method for sputtering condensed gases has been utilized by our group for several investigations [13-15] and recently by Balaji *et al.* for noble gas ions below 5 keV incident on solid rare gases as well [16].

The results of these studies are shown in fig. 2. Our measured yield is usually an average of at least three independent measurements. They have been performed for such thick films that the electronic sputtering yield would have reached its asymptotic value corresponding to the bulk yield [17]. In fact, no dependence of the yield on thickness was observed up to the standard thickness of $9 \cdot 10^{17}$ Ne-atoms/cm^2.

Model. – The yield evaluation via subspike formation is based on the idea (fig. 1) that

i) the primary particles move along a straight path into the solid from the point of impact at the surface,

ii) every recoil generates a subspike, and

iii) the subspike is treated as a spherical elastic spike.

The starting point for the yield evaluation is the spherical elastic-collision spike model developed by Claussen [9]. From this the yield from a spherical spike located at the depth x below the surface is given by a comparatively simple formula without adjustable parameters. The main problem of Claussen's model is to identify an appropriate spike centre for a given beam-ion target-atom system. Claussen chose to let this centre develop from a depth close to the well-defined damage depth [18]. For other systems this treatment gives a yield that disagrees completely with the experimentally determined one in absolute magnitude and dependence on primary energy. For the present system of He-ions incident on neon the yield estimated in this way is practically zero. The damage volume for neon becomes so large that the energy density of the spike is too low to induce any particle ejection at the surface.

For a subspike with an energy release T at a point located at depth x' we adopt Claussen's expression for the spherical spike

$$Y_s(x', T) = 0.1496\lambda_0 a_{BM}^2 N^{2/3}(T/U_0)^{4/3} g_s(\xi), \qquad \xi = 7.838(x')^3 N U_0/T, \tag{1}$$

where we have used the notation of ref. [3]. N is the atomic density, U_0 the surface binding energy, $\lambda_0 = 24$ and $a_{BM} = 0.219$ Å. The geometric function given by Claussen, $g_s(\xi)$ will be approximated by $\exp[-\alpha\xi]$, where the choice $\alpha = 1.2$ will cover the regime relevant for our system [9].

As cross-section $d\sigma(E, T)/dT$ for producing a recoil atom of energy T by the impact of the primary ion of energy E we have utilized Lindhard's power cross-section [19]

$$d\sigma = C_m E^{-m} T^{-1-m} dT, \tag{2}$$

where C_m is a constant that depends on the parameter m. The advantage of using this cross-section is the clear appearance of the important parameters. Alternatively, we have derived $d\sigma/dT$ from the Kr-C potential given by Wilson *et al.* [20] with Lindhard's screening length (see ref. [3, 4]). The corresponding nuclear stopping power from Wilson *et al.* has been used in both cases.

We assume that the primary ion (atomic number Z_1, mass M_1) moves along a straight path without any energy loss until the first collision with an atom at depth x (fig. 1). Then the total yield can be determined by the probability of energy transfer T times the yield of an individual spherical spike:

$$Y = N \int_0^\infty \int_0^{\gamma E} \frac{d\sigma(E, T)}{dT} Y_s(x', T) dT\, dx, \tag{3}$$

γE is the maximum energy transfer from the primary atom to a target atom at rest ($\gamma = 4M_1M_2/(M_1 + M_2)^2$).

In our model the kinetic energy T is not released in the primary track, but is displaced to the corresponding damage depth for the recoil. Then, the centre of the spike is relocated from depth x of the initial energy transfer to $x' = x + \langle R \rangle \hat{s} \cos\varphi''$ (fig. 1). The scattering

angle φ'' of the recoil atom is expressed as $\cos\varphi'' = (T/\gamma E)^{1/2}$ [3]. $\langle R \rangle$ is the path length of neon atoms with energy T in neon and $\hat{c}$ is a parameter which includes the ratio of damage depth to path length as well as the average over the damage depth. According to the discussion by Claussen [9], we have included the standard deviation of the damage distribution in order to obtain the most realistic value of $\hat{c}$. For the motion of neon atoms in neon it turns out that $\hat{c}$ varies very little for energies in the recoil energy interval, and one finds $\hat{c} = 0.66$ to be a fair approximation [21].

Combining eqs. (1)-(3) and the expression for the depth x', one obtains the yield

$$Y = Y(0)\left[1 - \left(\int_0^{\hat{c}} t^{1/6} h_1(t, \gamma)\Gamma_{in}(1/3, w)\,dt\right)\Big/\Gamma(1/3)\right], \tag{4}$$

$$h_1(t, \gamma) = t^{1/2-m}(5/3 - m)/(\gamma^{5/3-m}) \tag{5}$$

for the power cross-section (2).

In eq. (4) we have applied $t = T/E$. The incomplete gamma-function is determined by the argument

$$w = 7.838\hat{c}^3 \alpha N U_0 \langle R \rangle^3 t^{1/2}/(\gamma^{3/2} E)\,. \tag{6}$$

The yield $Y(0)$ for $\hat{c} = 0$ represents the case for which the centre of the subspike remains in the track of the primary particle:

$$Y(0) = N S_n(E) E^{2/3} \frac{2.51 \cdot 10^{-2} \cdot \Gamma(1/3) N^{1/3} \lambda_0 a_{BM}^2}{U_0^{5/3} \alpha^{1/3}} \cdot h(\gamma)\,, \tag{7}$$

where $h(\gamma) = (1 - m)\gamma^{2/3}/(5/3 - m)$ for the power cross-section. The calculated yields (eq. (4)) are shown in fig. 2 for $^4He^+$-ion incidence for a relevant choice of the parameter m and the corresponding one m_1 for the cross-section of the recoils. The yield evaluated from the general cross-section from Wilson *et al.* has been included as well for both primary ions.

Discussion. – The agreement between the experimental and calculated yield values for the general cross-section in both absolute magnitude and energy dependence is fairly good. The curve for the power cross-section is the one that shows the best agreement among the possible choices ($m = 1/2, 2/3$, $m_1 = 1/2, 1/3$). However, as mentioned previously, one should add the linear collision-cascade yield [9] and the electronic sputtering yield [1] to the curves shown in fig. 3. The former yield is at most 15 Ne/He^+ at the energies considered, while the latter may be estimated from the results for hydrogen ion bombardment in solid neon [13]. The electronic yield is expected to increase linearly with the electronic stopping power up to a yield of about 40 Ne/He^+ at the highest energy considered, $E = 10$ keV. These two contributions do not change the conclusion about the good agreement between the experimental results and the model for sputtering from subspikes.

The contribution from reflected primaries can be estimated to be less than the linear collision-cascade yield for the energies under consideration [21]. The main reason for this is the small number of reflected primaries (< 0.1) [22].

The model can also be employed for He-ions incident on solid argon. For this system the electronic sputtering yield is an appreciable fraction of the total yield. For the single energy $E = 7$ keV, the knock-on sputtering yield has been determined from the thickness dependence of the yield as 25 Ar/$^4He^+$ [15]. This yield is about a factor of 4 larger than that

predicted by the linear collision-cascade theory, but only a factor of 2 larger than the value $Y = 11$ Ar/^{4}He$^+$ obtained from eq. (4).

For hydrogen ions incident on solid neon the subspike model gives an almost constant value of about 25 Ne/H in the energy region from 4 to 10 keV. This is much less than the measured yield that is determined primarily by electronic sputtering [13].

The inclusion of the motion of the recoils is a substantial feature of the model. One arrives at the result that nonoverlapping subspikes centred in the ion track may lead to a yield that is not characterized by a strict proportionality with the nuclear stopping power. However, the factor $E^{2/3}$ is partly cancelled out by the factor in the squared brackets in eq. (4), and the resulting dependence on primary energy E actually leads to similar relationships between the calculated and experimental yields and nuclear stopping power. For values of ε larger than 0.66, the yield decreases with ε.

The condition of nonoverlapping subspikes means that the mean-free distance between two collisions exceeds twice the average radius of the spherical subspike [21]. This turns out to be fulfilled for all values of energy transfer T that are efficient in generating subspikes for primary energies above $(5 \div 6)$ keV in the case of He-ions incident on neon. At energies below this limit, there is a contribution from overlapping subspikes that have been generated by two or more subspikes, in addition to the contribution from the effect of individual ones. Then the geometry of the spike approaches other models or their extensions [7-9, 11, 12, 23].

The effect of heat loss through evaporation from the surface [24] has not been included in the model. This effect tends to reduce the yield compared with eq. (4) [9]. Recently, Vicanek *et al.* [25] pointed out that the value of λ_0 should be approximately one-half of that utilized by Claussen. This would reduce the calculated yield compared with that found experimentally.

Energy spectra of the ejected neutrals induced by light-ion bombardment may be evaluated as well on the basis of the model for nonoverlapping subspikes. The result will be presented by us in a forthcoming publication [21].

In summary, we have demonstrated that a sputtering model based on nonoverlapping subspikes leads to calculated yields that agree well with experimental ones for He$^+$-ion bombardment of the most volatile condensed gases.

* * *

The authors thank P. SIGMUND for valuable comments on the manuscript and R. PEDRYS for useful discussions.

REFERENCES

[1] SCHOU J., *Nucl. Instrum. Meth. B*, 27 (1987) 188.
[2] BROWN W. L. and JOHNSON R. E., *Nucl. Instrum. Meth. B*, 13 (1986) 295.
[3] SIGMUND P., in *Sputtering by Particle Bombardment I*, edited by R. BEHRISCH (Springer, Berlin-Heidelberg) 1981, p. 9; *Nucl. Instrum. Meth. B*, 27 (1987) 1.
[4] SCHOU J., in *Structure-Property Relationships in Surface-Modified Ceramics*, edited by C. J. MCHARGUE, R. KOSSOWSKY and W. O. HOFER (Kluwer Academic, Dordrecht, The Netherlands) 1989, p. 61.
[5] LAM N. Q., in *Fundamental Electron and Ion Beam Interaction with Solids for Microscopy, Microanalysis and Microlithography*, edited by J. SCHOU, P. KRUIT and D. NEWBURY (Scanning Microscopy Suppl., Chicago-AMFO'Hare, IL 60666-0507, USA) in press.
[6] HAGA K., KING W. E., MERKLE K. L. and MESHII M., *Nucl. Instrum. Meth. B*, 16 (1986) 134.
[7] SIGMUND P. and CLAUSSEN C., *J. Appl. Phys.*, 52 (1981) 990.

[8] SZYMONSKI M. and PORADZISZ A., *Appl. Phys. A*, 28 (1982) 175.
[9] CLAUSSEN C., *Nucl. Instrum. Meth.*, 194 (1982) 567; Thesis, University of Odense (unpublished) (1982).
[10] PEDRYS R., *Nucl. Instrum. Meth. B*, in press; OOSTRA D. J., VAN INGEN R. P., HARING A., DE VRIES A. E. and SARIS F. W., *Phys. Rev. Lett.*, 61 (1988) 1392.
[11] JOHNSON R. E., *J. Phys. (Paris)*, 2 (1989) 251; GIBBS K. M., BROWN W. L. and JOHNSON R. E., *Phys. Rev. B*, 38 (1988) 1101.
[12] URBASSEK H. M. and MICHL J., *Nucl. Instrum. Meth. B*, 22 (1987) 480.
[13] ELLEGAARD O., SCHOU J. and SØRENSEN H., *Nucl. Instrum. Meth. B*, 13 (1986) 567.
[14] SCHOU J., SØRENSEN H. and BØRGESEN P., *Nucl. Instrum. Meth. B*, 5 (1984) 44.
[15] SCHOU J., ELLEGAARD O., SØRENSEN H. and PEDRYS R., *Nucl. Instrum. Meth. B*, 33 (1988) 808.
[16] BALAJI V., DAVID D. E., MAGNERA T. F., MICHL J. and URBASSEK H. M., *Nucl. Instrum. Meth. B*, in press.
[17] SCHOU J., BØRGESEN P., ELLEGAARD O., SØRENSEN H. and CLAUSSEN C., *Phys. Rev. B*, 34 (1986) 93.
[18] WINTERBON K. B., SIGMUND P. and SANDERS J. B., *Mat. Fys. Medd. Dan. Vid. Selsk.*, 37 (1970) No. 14.
[19] LINDHARD J., NIELSEN V. and SCHARFF M., *Mat. Fys. Medd. Dan. Vid. Selsk.*, 36 (1968) No. 10.
[20] WILSON W. D., HAGGMARK L. G. and BIERSACK J. P., *Phys. Rev. B*, 15 (1977) 2458.
[21] ELLEGAARD O., SCHOU J., STENUM B. and SØRENSEN H., to be published.
[22] ECKSTEIN W. and VERBEEK H., *Nucl. Fusion, Special Issue* (1984) 12.
[23] SIGMUND P. and SZYMONSKI M., *Appl. Phys. A*, 33 (1984) 141.
[24] URBASSEK M. and SIGMUND P., *Appl. Phys. A*, 35 (1984) 19.
[25] VICANEK M., JIMENEZ RODRIGUEZ J. J. and SIGMUND P., *Nucl. Instrum. Meth. B*, 36 (1989) 124.

Bibliographic Data Sheet **Risø-R-591(EN)**

Title and author(s)

Erosion of Volatile Elemental Condensed Gases by keV Electron and Light-Ion Bombardment

Jørgen Schou

ISBN	ISSN
87-550-1737-I	0106-2840

Dept. or group	Date
Physics Department	November 1991

Groups own reg. number(s)	Project/contract no.

Pages	Tables	Illustrations	References
159	3	12	159

Abstract (Max. 2000 characters)

Erosion of the most volatile elemental gases by keV electron and light-ion bombardment has been studied at the experimental setup at Risø. The present work includes frozen neon, argon, krypton, nitrogen, oxygen and three hydrogen isotopes, deuterium, hydrogen deuteride and hydrogen. The yield of these condensed gases has been measured as a function of film thickness and primary energy for almost all combinations of primary particles (1-3 keV electrons, 5-10 keV hydrogen- and helium ions) and ices. These and other existing results show that there are substantial common features for the sputtering of frozen elemental gases. Within the two groups, the solid rare gases and the solid molecular gases, the similarity is striking. The hydrogenic solids deviate in some respects from the other elements. The processes that liberate kinetic energy for the particle ejection in sputtering are characteristic of the specific gas.

Descriptors INIS/EDB

ARGON; ELECTRON BEAMS; EROSION; EVAPORATION; HYDROGEN ISOTOPES; ICE; KEV RANGE; KRYPTON; LIGHT IONS; LUMINESCENCE; MICROBALANCES; NEON; NITROGEN; OXYGEN; SOLIDS; SPUTTERING; THIN FILMS; VOLATILITY

Available on request from Risø Library, Risø National Laboratory, (Risø Bibliotek, Forskningscenter Risø), P.O.Box 49, DK-4000 Roskilde, Denmark.
Telephone +45 42 37 12 12, ext. 2268/2269
Telex 43 116. Telefax +45 42 36 06 09.

Available on exchange from:
Risø Library,
Risø National Laboratory,
P.O. Box 49, DK-4000 Roskilde, Denmark
Phone 42 37 12 12, ext. 2268/2269
Telex 43 116, Telefax 46 75 56 27

ISBN 87-550-1737-1
ISSN 0106-2840